UC San Diego

UC San Diego Electronic Theses and Dissertations

Title

Development and Reactivity Studies of Highly Ambiphilic Carbenes

Permalink

https://escholarship.org/uc/item/57t561ss

Author

Weinstein, Cory

Publication Date

2018

Peer reviewed|Thesis/dissertation

eScholarship.org Powered by the California Digital Library
University of California

UNIVERSITY OF CALIFORNIA, SAN DIEGO

Development and Reactivity Studies of Highly Ambiphilic Carbenes

A dissertation submitted in partial satisfaction of the requirements for the degree of
Doctor of Philosophy

in

Chemistry

by

Cory Michael Weinstein

Committee in charge:

Guy Bertrand, Chair
Michael K. Gilson
Joseph M. O'Connor
Arnold L. Rheingold
Haim Weizman

2018

Copyright

Cory Michael Weinstein, 2018

All rights reserved

The dissertation of Cory Michael Weinstein is approved, and it is acceptable in quality and form for publication on microfilm and electronically:

Chair

University of California, San Diego

2018

DEDICATION

This dissertation is dedicated to my mom

Without her endless sacrifices and unconditional love and support

Nothing I have ever done would have been possible

EPIGRAPH

"*luck is always better than skill at things*"

-James Murphy

but

"*chance favors the prepared mind*"

-Louis Pasteur

TABLE OF CONTENTS

Signature Page iii

Dedication iv

Epigraph v

Table of Contents vi

List of Abbreviations viii

List of Figures xii

List of Schemes xvii

List of Tables xxi

Acknowledgments xxii

Vita xxix

Abstract of the Dissertation xxxi

Chapter 1 : General Introduction 1
1.1 Molecular and Electronic Description of a Carbene 1
1.2 A Brief History of Carbenes 5
1.3 Measuring the Steric, Donor, and Acceptor Properties of Carbenes 13
1.3.1 Measuring the Sterics of Carbenes 13
1.3.2 Measuring the Donor Properties of Carbenes 17
1.3.3 Measuring the Accepting Properties of Carbenes 22
1.4 Supporting Info 27
1.5 Acknowledgements 29
1.6 References 29

Chapter 2 : Exploring the Reactivity of White Phosphorus with Electrophilic Carbenes 35
2.1 Introduction 35
2.1.1 Elemental Phosphorus: Production and Uses 35
2.1.2 P_4 Reactivity with Carbenes 36
2.2 Synthesis of a P_4 Cage, P_8 Clusters and Other Carbene-P_4 Reactivity Studies 42
2.3 Conclusion 51
2.4 Experimental 52
2.4.1 General Considerations 52
2.4.2 Synthetic Procedures 52
2.4.3 Crystallographic Data 54
2.5 Acknowledgments 57
2.6 References 57

Chapter 3 : Cross-coupling Reactions between Stable Carbenes 60
3.1 Introduction 60

3.2 Synthesis of Carbene Heterodimers and Subsequent Rearrangement Reactions 64
3.3 Computational Calculations 70
3.4 Conclusion 74
3.5 Experimental 75
3.5.1 General Considerations 75
3.5.2 Synthetic Procedures 76
3.5.3 Crystallographic Data 77
3.5.4 Computational Details 81
3.6 Acknowledgements 100
3.7 References 100

Chapter 4 : Development and Reactivity Studies of Cyclic (Alkyl)(amino)carbenes with Expanded Ring Sizes 105
4.1 Introduction 105
4.2 Highly Ambiphilic Room Temperature Stable Six-Membered Cyclic (Alkyl)(amino)carbenes 123
4.2.1 Synthesis 123
4.2.2 Quantum Mechanical, Spectroscopic, and Reactivity Studies of CAAC-6 Derivatives 134
4.3 Development of All-alkyl Substituted Six-membered Cyclic(alkyl)(amino) Carbenes 146
4.3.1 Synthesis 146
4.3.2 Coordination Complexes Featuring Monomethylated CAAC-6 Derivatives 149
4.3.3 All-alkyl CAAC-6-Selenium Adducts Reveal Novel Examples of Non-Classical Hydrogen Bonding 160
4.4 Conclusion 167
4.5 Experimental 167
4.5.1 General Considerations 167
4.5.2 Synthetic Procedures 169
4.5.3 Crystallographic Data 186
4.5.4 Computational Details 200
4.6 Acknowledgements 213
4.7 References 214

Chapter 5 : Investigation of *α,α,γ,γ*-Tetrasubstitued-2-Allenyl Ketimines as “Masked” Remote *N*-Heterocyclic Carbene Sources 221
5.1 Introduction 221
5.2 Pursuit of a Pyrrolidinylidene *r*NHC 227
5.3 Conclusion 239
5.4 Experimental 240
5.4.1 General Considerations 240
5.4.2 Synthetic Procedure 241
5.4.3 Crystallographic Data 244
5.4.4 Computational Details 246
5.5 Acknowledgements 246
5.6 References 247

LIST OF ABBREVIATIONS

Å: Angstrom

AAAC: Acyclic (alkyl)(amino)carbene

Ad: 1-adamantyl

*a*NHC: Abnormal *N*-heterocyclic carbene

Ar: Aryl

BAC: Bis(amino)cyclopropenylidene

BCF: Tris(pentafluorophenyl)borane

BICAAC: Bicyclic alkyl(amino)carbene

CAAC: Cyclic (alkyl)(amino)carbene

CAAGe: Cyclic (alkyl)(amino)germylene

CAArC: Cyclic (amino)(aryl)carbene

CAASi: Cyclic (alkyl)(amino)silylene

CBA: Cyclic bent allene

CH_2: Methylene

cm^{-1}: Wave numbers

Cod: 1,5-cyclooctadiene

CTP: Cyclotriphospirene

Cy: Cyclohexyl

Cz: Carbazole

DAC: *N*,*N*'-diamidocarbene

Dba: Dibenzylideneacetone

DCM: Dichloromethane

ΔE_{ST}: Singlet-triplet gap energy

ΔG: Change in Gibbs free energy

DEPT: Distortionless enhancement by polarization transfer

DFT: Density functional theory

Dipp: 2,6-diisopropylphenyl

DippNH_2: 2,6-diisopropylaniline

DMB: 2,3-dimethylbutadiene

DMF: Dimethylformamide

DMSO: Dimethyl sulfoxide

E: Main-group functionality

E_A: Activation energy

E_{CC}: Energy of a carbon-carbon double bond

EPR: Electron paramagnetic resonance

ESI-MS: Electrospray ionization mass spectrometry

Et: Ethyl

Et_2O: Diethyl ether

eV: Electron Volt

Fc/Fc^+: Ferrocene vs Ferrocenium

HMDS: Hexamethyldisilazide

HOMO: Highest occupied molecular orbital

HOTf: Trifluoromethansulfonic acid

HRMS: High resolution mass spectrometry

Hz: Hertz

^{i}Pr: Isopropyl

IR: Infrared

kcal mol^{-1}: Kilocalories per mole

KO^{t}Bu: Potassium tert-butoxide

LDA: Lithium diisopropylamide

LUMO: Lowest unoccupied molecular orbital

Me: Methyl

Mes: Mesityl, 2,4,6-trimethylphenyl

MgA: Magnesium anthracene

MIC: Mesoionic carbene

MP: Melting point

MS: Molecular sieves

NBO: Natural bond order

n-Bu: Normal butyl

NCHB: Non-classical hydrogen bonding

NHC: *N*-heterocyclic carbene

NICS: Nuclear independent chemical shift

NMR: Nuclear Magnetic Resonance

Np: Neopentyl

OAc: Acetate

OLED: Organic light-emitting diode

p-TsOH: Tosylic acid

$\%V_{bur}$: Percent buried volume

Ph: Phenyl

Ppm: Parts per million

Psi: Pounds per square inch

R: Organic-group functionality

*r*NHC: Remote *N*-heterocyclic carbene

RT: Room temperature

SiNp: Silicon nanoparticle

SOMO: Singly occupied molecular orbital

^{t}Bu: Tertbutyl

TEP: Tolman electronic parameter

TfOTf: Trifluoromethansulfonic acid anhydride

THF: Tetrahydrofurane

Tht: Tetrahydrothiophene

TM: Transition-metal

TMS: Trimethylsilyl

TOF: Turnover frequency

TON: Turnover number

Tp: Trispyrazolborate

Ts: *p*-Toluenesulfonate

UV-Vis: Ultraviolet-visible

VT: Variable temperature

X: Halogen

LIST OF FIGURES

Figure 1.1: Neutral molecular carbon species. 2

Figure 1.2: Gomberg's radical and the first TM vinylidene complex. 2

Figure 1.3: Influences of hybridization on the electronic state of a carbene. 3

Figure 1.4: Influence of mesomeric effects on the electronic state of a carbene (Y = NR_2, OR, F, etc.). 4

Figure 1.5: First reported NHC TM complex. 6

Figure 1.6: Major achievements in NHC TM mediated catalysis (Mes = 2,4,6-trimethylphenyl). 9

Figure 1.7: A free *a*NHC and its most relevant mesoionic resonance forms. 11

Figure 1.8: Calculated HOMO-LUMO gaps (eV) and ΔE_{ST} (kcal mol^{-1}) of an NHC and CAAC at the B3LYP/def2-TZVPP level of theory (left), persistent and isolable carbenes with reduced heteroatom stabilization (middle), and non-exhaustive examples of unknown *r*NHCs (right). 12

Figure 1.9: Stable 5-, 6- and 7-membered DACs (left) and an example of the common resonance form giving rise to the carbenes' high electrophilicity (right). 13

Figure 1.10: Pictorial representation demonstrating only a limited set of examples how different carbenes can have varying steric properties. 14

Figure 1.11: $\%V_{bur}$ is the percentage of the given sphere occupied by the ligand, in this case a carbene. 15

Figure 1.12: Examples of 3D steric mapping of (carbene)AuCl complexes. 17

Figure 1.13: Transitive conclusion from the Tolman electronic parameter. 18

Figure 1.14: Representation of orbitals involved in TM-carbene multiple bonding (left) and its effect on the comparison of TEP values (right). 21

Figure 1.15: Comparing σ-donor character of carbenes through $^{1}J_{Pt-C}$ coupling constants. 22

Figure 1.16: Two extreme resonance forms of carbene-phenylphosphinidene adducts giving rise to a ^{31}P NMR scale. 23

Figure 1.17: Two extreme resonance forms of carbene-selenium adducts giving rise to a ^{77}Se NMR scale. 25

Figure 2.1: Calculated reaction pathway of P_4 with singlet (left) and triplet (right) methylene. Energies given in kcal mol^{-1}. 37

Figure 2.2: $^{31}P\{^{1}H\}$ NMR spectrum of the crude reaction of 2.3 with P_4 (left) and isolated 2.4 (right). 44

Figure 2.3: Solid state structure of 2.4 viewed from a top-down perspective (left) and along the P_4 ring (right). All hydrogen atoms, solvates, and methyl groups on the phenyl substituents (left) are omitted for clarity. 45

Figure 2.4: $^{31}P\{^{1}H\}$ NMR spectrum of 2.5. 46

Figure 2.5: Solid state structure of 2.5 viewed from a top-down perspective (left) and along the P_4 ring (right). All hydrogen atoms, solvates, and isopropyl groups on the phenyl substituents (left) are omitted for clarity. 47

Figure 2.6: $^{31}P\{^{1}H\}$ NMR spectrum of 2.7 (left) and magnified sections AB (middle) and X_2 (right). 48

Figure 2.7: Solid state structure of 2.7 viewed from top-down (left) and side-on (right) perspectives. All hydrogen atoms (both) and the Mes groups (right) are omitted for clarity. Selected bond lengths (Å): P1-C1 1.916(3), P2-C1 1.917(3), P1-P4 2.214(1), P1-P3 2.225(1), P2-P3 2.215(1), P2-P4 2.237(1), P3-P4 2.178(1). 49

Figure 2.8: X-ray structure of decomposition product 2.10. Methyl groups and all hydrogen atoms, except on C1, removed for clarity. Selected bond lengths (Å): C1-C2 1.415(3), C2-C3 1.397(3). 51

Figure 3.1: Reaction pathway for the dimerization of singlet carbenes. 63

Figure 3.2: Nucleophilic carbenes with minimal steric hindrance. 64

Figure 3.3: Highly electrophilic CAAC 3.4, 6-DAC 3.5 and 7-DAC 3.6. 64

Figure 3.4: X-ray structure of rearrangement product 3.7. One molecule in the asymmetric unit is depicted and hydrogen atoms, except on N4, have been removed for clarity. 66

Figure 3.5: X-ray structures of bent allene 3.8 (left) and diene 3.9 (right). Hydrogen atoms, except on C2 in 3.9, removed for clarity. 68

Figure 3.6: X-ray structure of 3.10 with hydrogen atoms, except on C4, removed for clarity. 69

Figure 3.7: X-ray structure of 3.12 in two separate orientations. CH_3 groups of Mes and all hydrogen atoms have been removed for clarity. 70

Figure 3.8: HOMO of 3.12 (isovalue = 0.04). Hydrogen atoms removed for clarity. 74

Figure 4.1: Calculated HOMO-LUMO gaps (eV) and ΔE_{ST} (kcal mol^{-1}) of a CAAC and NHC. 105

Figure 4.2: Bis($CAAC^{Me}$) stabilized Be^0 atom 4.J (left) and its major electronic description (right). 111

Figure 4.3: CAAC-supported main-group radicals and radical cations. 112

Figure 4.4: Mono, bis, and tris(amino)(carboxy) radicals derived from CAACs. 114

Figure 4.5: A stable, monomeric allenyl radical derived from a CAAC, and the calculated Muliken spin densities of the SOMO at the UB3LYP/def2-TZVP level of theory. 115

Figure 4.6: CAAC-supported TM complexes in unique coordination environments. 116

Figure 4.7: Low valent L_2 TM complexes featuring CAAC ligands (R = ($C_6H_3(CF_3)_2$)). 117

Figure 4.8: Photoluminescent coinage metal complexes featuring a CAAC ligand. 118

Figure 4.9: Closely related species to CAACs (Ad = adamantyl; TMS = trimethylsilyl). 122

Figure 4.10: Calculated HOMO-LUMO gap (eV) and ΔE_{ST} (kcal mol^{-1}) of representative carbenes at the B3LYP/def2-TZVPP level of theory. 123

Figure 4.11: Solid state structure of the cationic part of 4.4e. H-atoms, except for H1, and the I_3^- anion have been removed for clarity. Selected bond lengths (Å) and angles (º): N-C1 1.289(1), C1-C2 1.496(1), N-C1-C2 127.0(1). 129

Figure 4.12: Crude $^{13}C\{^1H\}$ NMR spectra of deprotonation reaction forming 4.11a (C_6D_6, 126 MHz).. 131

Figure 4.13: Crude $^{13}C\{^1H\}$ NMR spectra of deprotonation reaction forming 4.11b (C_6D_6, 126 MHz).. 132

Figure 4.14: ^1H NMR of deprotonation reaction forming 4.11c and 4.10c showing ~5:1 mixture (C_6D_6, 500 MHz). 132

Figure 4.15: $^{13}C\{^1H\}$ NMR of deprotonation reaction showing mixture of 4.11c and 4.10c (C_6D_6, 126 MHz). 133

Figure 4.16: Solid state structures of 4.11c (left) and analogous CAAC-5 derivative (right). H-atoms are omitted for clarity. Selected bond lengths (Å) and angles (º): 4.11c N-C1 1.3101(14), C1-C2 1.5252(13), N-C1-C2 117.88(9); CAAC-5 N-C1 1.312(1), C1-C2 1.531(1), N-C1-C2 106.36(1). 134

Figure 4.17: Front view of the calculated singlet (left) and triplet (right) geometries of 4.11c at the B3LYP/def2-TZVPP level of theory (N-C1-C2 is front-facing). 135

Figure 4.18: Experimental versus simulated UV-Vis spectra (left), and MOs and corresponding electronic transitions for 4.11c (right). Degenerate states and hydrogen atoms removed for clarity. 136

Figure 4.19: LUMO of carbene 4.11c (isovalue = 0.03). H-atoms removed for clarity. 136

Figure 4.20: Solid-state structure of 4.13c. H-atoms are omitted for clarity. Selected bond lengths (Å) and angles (°): C1-Au 1.990(5), N-C1 1.323(6), C1-C2 1.533(6), N-C1-C2 117.5(4), C1-Au-Cl 178.7(1). 137

Figure 4.21: Solid state structure of 4.14a. H-atoms are omitted for clarity. Selected bond lengths (Å) and angles (°): N-C1 1.427(2), C1-C3 1.319(2), C1-C2 1.540(2), C3-O 1.179(2), C1-C3-O 173.3(1). 139

Figure 4.22: Solid-state structure of 4.15c. H-atoms are omitted for clarity. Selected bond lengths (Å) and angles (°): C1-Rh 2.087(3), N-C1 1.327(5), C1-C2 1.555(6), C3-O1 1.098(5), C4-O2 1.139(5), Rh-Cl 2.408(1), N-C1-C2 119.7(3), C1-Rh-C3 169.9(2), C1-Rh-C4 97.3(2). 141

Figure 4.23: ^1H NMR of crude mixture 4.18 and 4.10e showing ~10:1 mixture (C_6D_6, 500 MHz)..... 142

Figure 4.24: $^{13}C\{^1H\}$ NMR of crude mixture 4.18 and 4.10e showing ~10:1 mixture (C_6D_6, 126 MHz). 142

Figure 4.25: DEPT-90 NMR of 4.18 showing ten total CH and CH_3 groups ($CDCl_3$, 75 MHz). 143

Figure 4.26: DEPT-135 NMR of 4.18 showing four CH_2 groups ($CDCl_3$, 75 MHz). 143

Figure 4.27: Solid-state structure of 4.18. H-atoms except H1 were removed for clarity. Selected bond lengths (Å) and angles (°): N-C1 1.4378(18), C1-C2 1.508(2), C1-C3 1.524(2), N-C1-C2 120.85(13), N-C1-C3 121.53(13) C2-C1-C3 60.19(10). 144

Figure 4.28: ^{13}C VT-NMR of 4.22e at -80 °C (75 MHz, THF)..... 148

Figure 4.29: X-ray structure of 4.25d. Only a single diastereomer is depicted and H-atoms have been removed for clarity. Selected bond lengths (Å) and angles (°): C1-Rh 2.025(3), C1-N 1.338(5), C1-C2 1.549(5), N-C1-C2 115.7(3)..... 150

Figure 4.30: Average CO stretching frequencies of *cis*-[(CAAC-6)Rh(CO)$_2$Cl] complexes 4.26a-e. 151

Figure 4.31: X-ray structures of (4.27b)$_2$ (left) and 4.27e (right). H-atoms have been removed for clarity. Selected bond lengths (Å) and angles (°): (4.27b)$_2$ C1-Rh1 1.998(3), C3-Rh2 1.991(3), C1-N1 1.301(4), C3-N2 1.311(5), N1-C1-C2 120.1(3), N2-C3-C4 120.1(3); 4.27e C1-Rh 1.957(3), C1-N1 1.317(4), C3-Rh 2.368(2), N-C1-C2 119.8(3), N-C3-Rh 82.7(2)..... 152

Figure 4.32: X-ray structure of 4.28. H-atoms, solvent, and the BF_4^- anion have been removed for clarity. Selected bond lengths (Å) and angles (°): C1-Rh 2.048(4), C1-N 1.304(5), C3-Rh 2.316(3), C3-C4 1.420(5), C3-C5 1.423(6), N-C1-C2 119.2(3), N-C3-Rh 85.5(2). 154

Figure 4.33: X-ray structure of 4.30. H-atoms, solvent, and the $[CuCl_2]^-$ anion have been removed for clarity. Selected bond lengths (Å) and angles (°) are not given because of the low data quality of the structure..... 155

Figure 4.34: X-ray structures of 4.32b-e (sequential left to right). H-atoms have been removed for clarity. Selected bond lengths (Å) and angles (°): 4.32b C1-Au 2.012(1), C1-N 1.304(1), N-C1-C2 121.6(2); 4.32c C1-Au 2.031(7), C1-N 1.296(7), N-C1-C2 123.2(9); 4.32d C1-Au 2.01(2), C1-N 1.31(3), N-C1-C2 121(2); 4.32e C1-Au 2.00(1), C1-N 1.280(4), N-C1-C2 120.5(4). 157

Figure 4.35: X-ray structures of 4.33e. H-atoms and $GaCl_4^-$ anion have been removed for clarity. Selected bond lengths (Å) and angles (°) are not given as the structure could not be fully refined. 158

Figure 4.36: ^{77}Se NMR signals of every CAAC-6-Se adduct..... 161

Figure 4.37 X-ray structures of 4.37a-e and 4.17c (top left to bottom right). H-atoms, except for those closest to Se, have been removed for clarity. Selected bond lengths (Å): 4.37a Se-H 2.497; 4.37b Se-H 2.464; 4.37c Se-H1 2.548, Se-H2 2.609; 4.37d Se-H1 2.531, Se-H2 2.662; 4.37e Se-H1 3.070, Se-H2 3.245, Se-H3 2.850, Se-H4 2.893; 4.17c Se-H 2.548. 162

Figure 4.38: Short intramolecular Se-H distances observed in oxazolylidene-selenium adducts with carbonyls..... 162

Figure 4.39: Reported ^{77}Se NMR signals of unsaturated NHC-selenium adducts showing large discrepancies in the signals (top) and shortest Se-H distances for examples with reported structures (bottom). *NMR in DMSO. 164

Figure 4.40: ^1H NMRs of 4.21a and 4.37a showing C-H···Se NCHB (500MHz, $CDCl_3$)..... 165

Figure 4.41: ^1H NMRs of 4.21b and 4.37b showing C-H···Se NCHB (500MHz, $CDCl_3$). 165

Figure 4.42: ^{77}Se NMR signals of every CAAC-6-Se adduct with correction factor applied when needed. 167

Figure 4.43: Structure of model M..... 209

Figure 4.44: Comparison of computational methods on model compound M (geometry specified above). 210

Figure 4.45: Calculated MOs and corresponding electronic transitions for 4.11c..... 212

Figure 5.1: The only example of a stable singlet carbene in which no heteroatoms are α to the carbene center..... 222

Figure 5.2: Carbeneic character in pyridinylidene *r*NHCs requires the heteroatom to be 2n+1 bonds from the carbene. 222

Figure 5.3: Remote carbenes stabilized by extended enamine π-systems..... 224

Figure 5.4: Comparing *r*NHC and "normal" NHC catalysts. 225

Figure 5.5: Calculated HOMO-LUMO gaps (eV) and ΔE_{ST} (kcal mol^{-1}) of CAAC derivatives and *r*NHC 5.W..... 227

Figure 5.6: Solid state structure of 5.4a. H-atoms, except on oxygen, and the Br^- anion have been omitted for clarity. Selected bond lengths (Å) and angles (º): C1-O 1.329(1), C1-C2 1.505(1), C1-C4 1.373(1), C2-N 1.496(1), C3-N 1.318(1), C3-C4 1.430(1), C4-C1-C2 112.2(1). 230

Figure 5.7: Cyclic voltammogram of chloro pyrrolidinium salt 5.3a. (*n*Bu_4NPF_6 0.1 M in THF vs Fc/Fc^+). 230

Figure 5.8: Experimental and simulated EPR spectra of the neutral product from a one electron reduction of 5.3a 232

Figure 5.9 Crude $^{13}C\{^1H\}$ of the reduction of 5.3a with Mg-anthracene giving allene 5.6a as the major product. 233

Figure 5.10: Solid state structure of 5.3c. H-atoms, HCl_2^- anion, and residual solvent have been omitted for clarity. Selected bond lengths (Å) and angles (º): C1-Cl 1.707(2), C1-C2 1.503(2), C1-C4 1.348(2), C2-N 1.486(2), C3-N 1.317(2), C3-C4 1.461(2), C4-C1-C2 112.7(1). 235

Figure 5.11: ^{31}P NMR π-accepting scale demonstrating that pyrrolidinylidene *r*NHCs are highly electrophilic. 239

LIST OF SCHEMES

Scheme 1.1: Early organic transformations involving carbene intermediates. 5

Scheme 1.2: First attempt at synthesizing an NHC. 6

Scheme 1.3: Pioneering studies in the field of carbene TM complexes (Np = neopentyl). 7

Scheme 1.4: The first isolable carbene featuring stabilization from a "push-pull" resonance form. 8

Scheme 1.5: The first crystalline, isolable carbene. 8

Scheme 1.6: First report of an "abnormal" binding mode for NHCs. 10

Scheme 1.7: Trapping experiments with Se (black) to give carbene-selenium adducts of cyclic (amino)(aryl)carbenes (left) and cyclic (alkyl)(amido)carbenes (right) and their highly downfield ^{77}Se NMR chemical shifts (ppm). 26

Scheme 2.1: Carbene activation of white phosphorus giving a linear P_4 chain 2.C and subsequent derivatization. 38

Scheme 2.2: Carbene activation of P_4 yielding trapped intermediate 2.H, tris(carbene) P_4 adduct 2.F, and bis(carbene) P_1 and P_2 species, 2.I and 2.G, respectively. 39

Scheme 2.3: NHC activation of white phosphorus giving P_{12} isomer 2.J and proposed intermediates. 40

Scheme 2.4: *In situ* reaction of P_4 with imidazolium salts 2.Ka-d. (2.Ka[X]-2.Ma: X = I, R = Me, R' = H; 2.Kb[X]-2.Mb: X = I, R = Me, R' = Me; 2.Kc[X]-2.Mc: X = Cl, R = Mes, R' = H; 2.Kd[X]-2.Md: X = Cl, R = Dipp, R' = H) 41

Scheme 2.5: Lewis acid trapped P_4 butterfly 2.O^{Int1} and subsequent rearrangement product 2.O. ΔG is given in parenthesis in kcal mol^{-1}. 42

Scheme 2.6: Reaction of a highly sterically encumbering NHC with P_4. 43

Scheme 2.7: Dimerization of the P_4 chain diphosphene giving the tetra(carbene)P_8 cluster 2.4. 43

Scheme 2.8: Formation of tetra(carbene) P_8 cluster 2.5. 46

Scheme 2.9: Reaction of P_4 with seven-member DAC 2.6 yielding insertion product 2.7. 48

Scheme 2.10: Reaction of CBA 2.8 with P_4 yielding proposed 2.9[X$^-$] and 2.10. 50

Scheme 3.1: Hypothetical "Wanzlick equilibrium". 60

Scheme 3.2: Carbene dimerization proceeding by electrophilic catalysis. Dipp = 2,6-^{i}Pr$_2$C$_6$H$_3$ 61

Scheme 3.3: Intermediate in acid-induced carbene dimerization (top) and prevention of dimerization by reduction (bottom). Mes = 2,4,6-Me$_3$C$_6$H$_2$ 62

Scheme 3.4: Carbene cross-coupling with NHC 3.1 as the nucleophilic partner. 65

Scheme 3.5: Cross-coupling reaction between 3.3 and 3.4 leading to bent allene 3.8 and intramolecular deprotonation product 3.9. 67

Scheme 3.6: Cross-coupling reaction between 3.3 and 3.5 leading to bent allene 3.10. 69

Scheme 3.7: Cross-coupling reaction between 3.3 and 3.6 leading to carbene heterodimer 3.12. 70

Scheme 3.8: Calculated reaction mechanism for the formation of bent allene 3.8. Energies are given in kcal mol^{-1}. 71

Scheme 3.9: Calculated reaction mechanism for the formation of bent allene 3.10. Energies are given in kcal mol^{-1}. 72

Scheme 3.10: Intramolecular deprotonation reactions to form dienes 3.9 (left) and 3.11 (right). Relative energies are given in kcal mol^{-1} and are arbitrarily set to 0 for both 3.8 and 3.10. 73

Scheme 3.11: Calculated Gibbs free energy for carbene-carbene heterodimer 3.12, and reaction pathway for the non-observed allene 3.13. Energies are given in kcal mol^{-1}. 73

Scheme 4.1: Synthetic routes for CAACs (LDA = lithium diisopropylamide, KHMDS = potassium hexamethyldisilylamide, TfOTf = trifluoromethansulfonic acid anhydride). 107

Scheme 4.2: Examples of inter- and intramolecular CH-insertion reactions with CAACs. 108

Scheme 4.3: Insertion of CAACs into a variety of E-H bonds, with the exception of BH_3. 109

Scheme 4.4: CAAC E-H insertion reactions proceed through a three-membered transition state. 109

Scheme 4.5: Strong donor properties of CAACs translate to a nucleophilic boron center (HOTf = trifluoromethanesulfonic acid). 110

Scheme 4.6: Reduction of $(CAAC^{Me})B(CN)Br_2$ with and without the presence of Lewis external base. 111

Scheme 4.7: Four different oxidation states of antimony stabilized by CAACs. 113

Scheme 4.8: Organic capacitors derived from CAACs. 115

Scheme 4.9: Synthesis of a trinuclear gold cluster in the +1 oxidation state stabilized by three CAACs. 118

Scheme 4.10: Preparation of the active $[(CAAC)Au]^+$ gold catalyst (top left) in the coupling reactions of enamines and alkynes (top right), as well as the hydroamination of alkynes or allenes using ammonia or hydrazine as the nitrogen source (bottom). 119

Scheme 4.11: (CAAC)Rh(cod)Cl catalyst (top left) active in the hydrogenation of aryl groups in phenyl ketones and alcohols (top right), as well as the *cis*-hydrogenation of (multi)fluorinated arenes (MS = molecular sieves). 120

Scheme 4.12: Synthesis of Hoveyda-Grubbs type ruthenium catalysts supported by CAAC ligands (top) which are highly active for the ethenolysis of methyl oleate (bottom). 121

Scheme 4.13: Synthesis of an internal alkenyl imine precursor for a CAAC-6 species. 124

Scheme 4.14: Failed cyclization methods for making a CAAC-6 precursor. 125

Scheme 4.15: Synthesis of a terminal alkenyl imine. Percentages given were determined from crude NMR spectra. 126

Scheme 4.16: Perplexing mixture of two iminium salts. 127

Scheme 4.17: Parallel substoichiometric reactions providing evidence that adventitious I_2 was the root cause of the mixture of iminium salts. 128

Scheme 4.18: General synthesis of CAAC-6 iminium salts 4.4a-e. Isolated yields were calculated with respect to the imines 4.2: 4.4a (11%), 4.4b (14%), 4.4c (19%), 4.4d (not isolated), 4.4e (15%). 129

Scheme 4.19: Deprotonation of 4.4a-c giving CAAC-6 4.11a,b or mixture of CAAC-6 4.11c and alkenyl imine 4.10c, respectively. 130

Scheme 4.20: Proposed decomposition products upon mild heating of carbene 4.11c. 134

Scheme 4.21: Probing the sterics of a CAAC-6. 137

Scheme 4.22: Sterics influencing the stability of amino ketenes derived from CAAC-5 (top) and CAAC-6 (bottom). 138

Scheme 4.23: Probing the electronics of CAAC-6: (ia) 0.4 eq. $[Rh(cod)Cl]_2$, THF, RT, (ib) CO, THF, RT; (ii) $(PhP)_5$, C_6D_6, 60 ºC; (iii) Se, THF, RT. 140

Scheme 4.24: Formation of the carbene C-H insertion product 4.18 is nonreversible. Alkenyl imine 4.10e was also a minor product of the deprotonation reaction. 141

Scheme 4.25: Failed reactions with carbene 4.11c. 144

Scheme 4.26: Reactions of CAAC-6 and P_4 give red phosphorus. 145

Scheme 4.27: Synthesis of CAAC-6 iminium precursors 4.21a-e with monomethylated backbones. Isolated yields were calculated with respect to the imines 4.20a-d or 4.2a, respectively: 4.21a (15%), 4.21b (55%), 4.21c (43%), 4.21d (38%), 4.21e (72%). 147

Scheme 4.28: CAAC-6 4.22e with a monomethylated backbone rearranges to enamine 4.23 above -60 ºC. 147

Scheme 4.29: Formation of a seven-membered CAAC iminium precursor by S_N2 is low yielding. 148

Scheme 4.30: Synthesis of (CAAC-6)Rh(cod)Cl complexes 4.25a-e via *in situ* deprotonation (left) and representation of diastereomer mixture (right). 149

Scheme 4.31: *cis*-[(CAAC-6)$Rh(CO)_2Cl$] complexes 4.26a-e spontaneously lose CO overtime. 151

Scheme 4.32: Halide abstraction reactions yield the cationic C_{ipso} stabilized rhodium center (top) or mixtures of products for all-alkyl CAAC-6 species (bottom). 154

Scheme 4.33: *In situ* deprotonation yields both mono- and bis-(CAAC-6) copper complexes. 155

Scheme 4.34: Synthesis of (CAAC-6)AuCl complexes 4.32a-e via a proto-demetalation procedure. 156

Scheme 4.35: Halide abstraction reactions on 4.32e do not give a “naked” gold atom at room temperature. 158

Scheme 4.36: Synthesis of [(CAAC-6)Au]$_3$[BF_4] complexes 4.36a,b which decompose into [(CAAC-6)$_2$Au][BF_4] complexes 4.35a,b, respectively. 159

Scheme 4.37: Trapping experiments giving CAAC-6 Se adducts 4.37a-e. 160

Scheme 5.1: Oxidative addition to palladium is the only known synthetic route for pyrazolylidene complexes. 223

Scheme 5.2: Synthesis of *r*NHC TM complexes via Au induced cyclization. 226

Scheme 5.3: Retrosynthetic analysis for *r*NHC 5.W. 227

Scheme 5.4: Synthesis of five-membered rings 5.2a,b (left) with diagnostic ^{13}C NMR signals in ppm (right). 228

Scheme 5.5: Attempted deoxygenation reactions of 5.2a (left) and diagnostic ^{13}C NMR signals in ppm of chloro pyrrolidinium salt 5.3a (right). Ar = *p*-OMe(C_6H_5). 229

Scheme 5.6: Reduction of 5.3a with cobaltocene gives proposed C-H insertion product 5.5. 231

Scheme 5.7: Mechanism of allene 5.6a formation (top) and analogous ring opening mechanism of a “normal” pyrazolylidene (bottom). Energies are given in kcal mol^{-1}. 234

Scheme 5.8 Synthesis of tethered compounds 5.2c and 5.3c (top) with diagnostic ^{13}C NMR signals (ppm) on the left and right, respectively (bottom). 235

Scheme 5.9: Reduction of tethered system 5.3c at RT gives the 1,2-methyl migration pyrrole product 5.9. 236

Scheme 5.10: Electrophiles induce the cyclization of allene 5.6a giving *r*NHC TM complexes or an HCl adduct (left) with their respective characteristic ^{13}C and ^{1}H NMR signals (right). Ad = adamantyl, tht = tetrahydrothiopene. 238

Scheme 5.11: Synthesis of the *r*NHC-phenylphosphinidene adduct 5.13 (left) with diagnostic ^{13}C NMR signals in ppm (right). 238

LIST OF TABLES

Table 1.1: Representative examples of changes in $\%V_{bur}$ for some (carbene)AuCl complexes (Au-C bond fixed at 2.00 Å). 16

Table 1.2: Selected carbenes from *cis*-[(L)IrCl(CO)$_2$] and their calculated TEP values (cm^{-1}). 19

Table 1.3: ^{31}P NMR chemical shifts (ppm) and TEP values (cm^{-1}) of carbene-phenylphosphinidene adducts. 25

Table 3.1: Energies of Intermediates and Transition States 82

Table 4.1: Calculated transitions involved in simulated spectrum with respective energies and oscillator strengths. Major Kohn-Sham orbitals involved in the transitions are noted. 213

ACKNOWLEDGMENTS

First I need to thank Prof. Michael Gilson, Prof. Arnold Rheingold, Prof. Joseph O'Connor, and Prof. Haim Weizman for taking time out of your busy schedules to read and review this dissertation.

As for the boss, Prof. Guy Bertrand I am eternally grateful for having the opportunity to work in your lab over the past five years. Your patience with struggling students is unrivaled and your encouragement motivational. The longer my time in graduate school, the more I appreciated the special kind of advisor I had. Your door was always open and you were eager to talk about science at any time. You took great interest in your students as well as their projects and made sure to walk through the lab at least once a day to check up on how we were doing. Beyond anything else, no one can ever call you lazy. If results were ready to be published for a paper, you would sit with us for hours on end refining and editing and refining and editing and editing and refining until the absolute best draft was made. That style of mentorship is hardly found in such a demanding academic era, and I thank you immensely for those one-on-one learning hours.

The decision to pursue a PhD does not happen in a vacuum, and I am equally indebted to my undergraduate advisor at UC Davis Prof. Phil Power. My experience working is his lab set me up to start fast on my own projects in graduate school. Thank you so much Prof. Christine Caputo and Dr. Caroline Knapp for the best post-doc mentors a green but willing undergraduate student could hope for. Also, to my fellow undergraduate researcher (so long ago) and friend Alan Gamage for sharing those late nights studying, discussing classes and lab, and very frequently venting about the status of chemical education in the university system with me.

My first six months of graduate school would have been completely lost had it not been for Prof. Caleb Martin standing by my side. He is a fantastic person and an even better chemist. He would always be "lurking" around interested in everything I was doing. We still text to this day and I wish him the best in his independent career at Baylor.

To the CNRS members Michelle, Mo, Rudy, and David M., you are the gears that keep the Bertrand group moving. From ordering chemicals, finishing up projects, and simply being helpful people to bounce ideas off of, your hard work is underappreciated and what I say here simply does not thank it enough. Nevertheless, thank you for everything.

Staying for five years in a lab with a boss as accomplished as Guy has the inevitable side effect of being introduced to the most amazing and intelligent post-docs from around the world. Seriously, these people make imposter syndrome an absolute reality because they were all so awesome. In no particular order I want to acknowledge these people for being so helpful towards a growing graduate student. Fabian – It was amazing to meet such a brilliant and successful scientist that was also an amazing parent to his young growing children. Robert – Wow. What a person. What lively person. It was impossible not to smile when he was around and the name Jimmy has so much more meaning now. Liqun – I have never seen someone move so fast in the lab without ever making a single mistake. You accomplished so much in your short time here, and I never heard you complain about a single thing. Jiaxang – You had by far the best presentation clothes I have ever seen. So stylish and flashy it was amazing. Maël – I don't think I have eaten more Mexican food than the year that you were in the Bertrand group. Our lunchtime excursions left us incapacitated for hours and waistlines a little larger. Thanks so much for the smiles you brought to my face being my lab neighbor. Fatme – Thank you so much for planning BBQs, beach visits, and night outs for the lab. Without you around to ground us in the real world it's easy to get lost in the world of Pacific Hall. Ryo – I am really glad I had you sitting next to me as a wealth of synthetic knowledge to pick at towards to later part of my graduate years. Max – I thought I had already met the most accomplished post-docs ever and then you showed up in the lab. You truly had a grasp on chemistry that I had never seen before and a way to capitalize on those thoughts and produce results unrivaled by anyone else I have ever met. Dominik – You were such a great mentor and friend for the two years you spent with us. It was so great discussing music and underground Berlin venues with you. Eder – It isn't often in life that you meet people like Eder who can immediately attract so many people around them due to their great personality. Collaborating with you in lab was a treat and I will make sure to only make new

carbenes on Friday now thanks to you. Also I need to give a special thanks to Prof. Takajoshi Fujii, Prof. Xingbang Hu, and Prof. Shengmei Guo for spending time away from groups to help teach us something about chemistry and your home countries.

I also need to thank my fellow in house and visiting graduate students from the Bertrand group: David W., Gaël, Steffen, Martin, Liu, Big Dom, Lilja, Vianney, Connor, Desiree, Johanna, Erik, Pauline, Adam, François, Sima, Melinda, and Victor. Thanks for being amazing people always willing to help and joke around making the long hours well worth it.

To my undergraduate students Yi Rui and Glen, thanks for teaching me how to be a better mentor. Yi Rui, I wish you the best at Columbia University and onwards in your professional career. Glen, I don't need wish the best because you are already one of the best. I am so happy that you decided to continue your graduate career at UCSD. You have a level of excitement about science and academia that you hardly see anymore and it has been awesome to have a person like you around to collaborate with.

A special thanks needs to go a couple of other graduate students. Janell – we entered the lab together and you succeeded in graduating a year earlier than me. It was really great to simply talk about how similar experiences were affecting us at the same time. To Dr. David Ruiz – When you graduated the lab lost truly an amazing individual. It seemed like you organized everything and made sure everyone around you was happy. We certainly had some amazing times both in and especially outside of lab. To Jesse and Daniel, thank you so much for reading and giving comments and this dissertation. Beyond that, these two are one-of-a-kind characters that have incredible personalities. Jesse – keep fighting the fight and as long as you believe Bernie still has a chance. Daniel – you have been one of my closest friends throughout graduate school. I think at this point I have spent more hours around you than any other person over the past five years. Thanks for being such an uplifting and witty person, and keep on dancing into the AM for the rest of us.

None of the work I did would have been possible without the people behind the scenes that run the facilities. Dr. Anthony Mrse – If I needed a long, complicated NMR experiment to work you were

more than willing to sit by my side and make sure everything was operating correctly. To Dr. Curtis Moore and Dr. Milan Gembicky, the UCSD chemistry department would be so much worse without you. I would not have learned half of the crystallographic techniques in twice the time if I went to any other institution. Special thanks also have to also go to the late night janitor Aaron Watkins. You went above and beyond your job description to learn a little something about every person you met. I will always treasure our daily 6 PM conversations making me feel guilty if I didn't go to the gym that day.

I also need to thank Prof. Stacey Brydges, Mark, Kara, and Riley for our collaborations on improving chemical education at UCSD. It was amazing to be a part of such a talented team of individuals that were also so passionate about teaching. Working with you was a fantastic constant reminder that being at UCSD was so much more than just the next experiment.

I would not have remained sane in graduate school if I didn't have the fantastic friend support group around me. First, to my UTC roommates Jon, Kenneth, Josh, Chris, Danielle, David, Andrew, Sam, and Ed, we lived one crazy experience in that two bedroom apartment. All of you are inspiring, thoughtful, talented, and spectacular individuals and there is no way that living situation could have worked with anyone else. To David and Tony, thanks for picking me, a Craigslist stranger, to fill that third room in such a sweet North Park apartment. Who would have predicted how the first 24 hours of us living together would have been so eventful. Listening to you two make music while I typed away at work was such a cool part of living with you and I am excited to watch you two continue growing in your musical careers.

To my roommate and friend Jonathan – from Salinas card shops to college parties to music festivals to graduations to travelling the world, you have always been there. Our conversations have been reduced to gibberish of inside humor reflecting on the wealth of experiences we have shared, and yet we continue to have more. Evolving through life with you always around has been one of the most important things to my development as a human being.

Thanks to Luis for being a world travel partner and a music recommender. Thanks to my friends Justin, Josh, and Blake for the weekends that Owen Wilson would be proud of. Thanks to Matt and Laurie

and Kaye and David for sharing late night beers, dinners, Christmas parties, jazz nights and even inviting me to be being a part of the most important days of their lives. Thanks to Alex “Snus” Carolino for some hilarious experiences on the other side of the world. Thanks to Zyra for making sure to remind me where the bruises in my shins are. Thanks to Athena, Jamie, and Jhelen for planning birthday parties and bringing me cakes when I least expected it. Thanks to Andrew, Tina, Zach, Brian and Paola for being such great neighbors. Thanks to my lifelong college friends RJ and Penny for simply being the best people to visit/have visit period, and for never being able to make it five seconds into a conversation without one of us saying something stupid. Thanks to the hometown “brigadian” heroes Cody, Moose, Bryan, Andrew, Jesse, Tony, Butters, Whitey and Demi for being the most ridiculous collection of friends one could ask for.

I also need to highlight special thanks for another special group of friends. Cameron and Melissa – your kindness, hospitality, cooking abilities, and GOT nights were truly the glue that brought so many of us together. You two are single handedly responsible for nurturing my great friendships with yourselves, Mike, Lewis, Vivi, Charles, Doug, Brandon, Jessie, Rohit, and Jake. I will always treasure those Sunday night group hang outs in your living room.

To Sarah – you have given me one smile after another after another for the past five years of friendship and more. From Chem 6A helproom to late nights playing Overcooked in our PJs, I could not have asked for a more special person to share any day of the week with. You have already taught me so much about life, food, and stupid puns, shared so many internet bird memes, and are by far the wittiest person I have ever met. Thank you so much for being who you are and letting me be a part of your life.

Finally, I need to thank my family. Mom – you were there with me every day of every week of every year as I grew from someone that would throw tantrums for having to write two sentences to “almost” a PhD graduate. Your support and love is never ending and I am eternally grateful for everything you have done. Dad – if I had a rough day at work I could rely on you to be an ear to vent to. I appreciate our late night and early morning commuting phone calls. It has been amazing to have someone always there interested in the everyday goings of my life. To my sister – you continue to amaze me every

day with your free loving personality and musical talents. I brag about you all the time to my friends and that won't stop as we both grow in our lives. To Grandpa Dean and Grandma Norma – thank you so much for sending postcards and news clippings and always being so attentive to my progress in school and as a human being. To Grandpa Jim and Grandma Marylyn – no one could ask for such a kind and hospitable pair of grandparents. If I or my friends needed a couch to sleep on not only would you open your doors but you would also treat us like honored guests just for being there. Thank you so much for the support through the years.

Last but not least, I need to thank the coffee shop baristas and Mexican food cooks for keeping me alive in the early mornings and late nights of graduate school. Without sustenance, this dissertation would not have been possible.

Chapter 2, in part, has been adapted from materials published in Chapter 2 is adapted, in part, from Caleb D. Martin, Cory M. Weinstein, Curtis E. Moore, Arnold L. Rheingold, and Guy Bertrand "Exploring the reactivity of white phosphorus with electrophilic carbenes: synthesis of a P_4 cage and P_8 clusters," *Chemical Communications*, 2013, **49**, 4486-4488. The dissertation author was a co-primary investigator and co-author of this paper.

Chapter 3, in part, has been adapted from Cory M. Weinstein, Caleb D. Martin, Liu Liu, and Guy Bertrand "Cross-Coupling Reactions between Stable Carbenes," *Angewandte Chemie International Edition*, 2014, **53**, 6550-6553. The dissertation author was the primary investigator and author of this paper.

Chapter 4, in part, is adapted from Eder Tomás-Mendivil, Max M. Hansmann, Cory M. Weinstein, Rodolphe Jazzar, Mohand Melaimi and Guy Bertrand "Bicyclic (Alkyl)(amino)carbenes (BICAACs): Stable Carbenes More Ambiphilic than CAACs," *Journal of the American Chemical Society*, 2017, **139**, 7753-7756. The dissertation author was the third author of the manuscripts. Chapter 4 is also in part currently being prepared for submission for publication of the material. Cory M. Weinstein, Glen P. Junor, Daniel R. Tolentino, Rodolphe Jazzar, Mohand Melaimi and Guy Bertrand "Highly Ambilphilic Room Temperature Stable Six-Membered Cyclic (Alkyl)(amino)carbenes," and Cory M.

Weinstein, Glen P. Junor, Rodolphe Jazzar, Mohand Melaimi and Guy Bertrand "All-alkyl Six-Membered Cyclic (Alkyl)(amino)carbenes Reveal a New Form of Non Classical Hydrogen Bonding." The dissertation author was the primary investigator and author of this material.

Chapter 5, in part, is currently being prepared for submission for publication of the material. Cory M. Weinstein, Mohand Melaimi, and Guy Bertrand "Allenyl Ketimines are Masked Remote *N*-Heterocyclic Carbenes." The dissertation author was the primary investigator and author of this material.

VITA

EDUCATION

PhD, Chemistry 2014-2018
University of California, San Diego (Advisor: Prof. Guy Bertrand)

Masters, Chemistry 2012-2014
University of California, San Diego (Advisor: Prof. Guy Bertrand)

Bachelor of Science, Chemical Physics 2008-2012
University of California, Davis (Advisor: Prof. Phil Power)

AWARDS AND HONORS

- John Paine Scholarship, Sigma Alpha Mu Foundation (UCSD) 2017
- Distinguished Graduate Student Fellowship (UCSD) 2016
- Teaching Assistant Excellence Award (UCSD) 2014
- ACS Travel Award (UCSD) 2014
- NSF Graduate Research Fellowship – Honorable Mention (UCSD) 2014
- Richard Larock Undergraduate Research Conference First Prize (UCD) 2012
- L. Mark Newman Family Scholarship, Sigma Alpha Mu Foundation (UCD) 2011
- Deans' Honors List (UCD) 2010

PUBLICATIONS

6. E. Tomás-Mendivil, M. H. Hansmann, **C. M. Weinstein**, R. Jazzar, M. Melaïmi, G. Bertrand "Bicyclic (alkyl)(amino)carbenes (BICAACs): Stable carbenes more ambiphilic than CAACs" *J. Am. Chem. Soc.*, **2017**, *139*, 7753-7756.
5. S. Wang, M. L. McCrea-Hendrick, **C. M. Weinstein**, C. A. Caputo, E. Hoppe, J . C. Fettinger, M. M. Olmstead, P. P. Power, "Tin(II) hydrides as intermediates in rearrangements of tin(II) alkyl derivatives" *J. Am. Chem. Soc.*, **2017**, *139*, 6596-6604.
4. S. Wang, M. L. McCrea-Hendrick, **C. M. Weinstein**, C. A. Caputo, E. Hoppe, J . C. Fettinger, M. M. Olmstead, P. P. Power, "Dynamic behavior and isomerization equilibria of distannenes synthesized by tin hydride/olefin insertions: Characterization of the elusive monohydrido bridged isomer" *J. Am. Chem. Soc.*, **2017**, *139*, 6586-6595.
3. M. L. Mcrea-Hendrick, C. A. Caputo, J. Linnera, P. Vasko, **C. M. Weinstein**, J. C. Fettinger, H. M. Tuononen, P. P. Power, "Cleavage of Ge-Ge and Sn-Sn triple bonds in heavy group 14 element alkyne analogues $(EAr^{iPr4})_2$ (E = Ge, Sn; Ar^{iPr4} = C_6H_3-2,6(C_6H_3-2,6-$^iPr_2$)$_2$) by reaction with group 6 carbonyls" *Organometallics*, **2016**, *35*, 2759-2767.
2. **C. M. Weinstein**, C. D. Martin, L. Liu, G. Bertrand, "Cross-coupling reactions between stable carbenes" *Angew. Chem. Int. Ed.*, **2014**, *53*, 6550-6553.
1. C. D. Martin, **C. M. Weinstein**, C. E. Moore, A. L. Rheingold, G. Bertrand, "Exploring the reactivity of white phosphorus with electrophilic carbenes: synthesis of a P_4 cage and a P_8 cluster" *Chem. Commun.*, **2013**, *49*, 4486-4488.

ORAL PRESENTATIONS

4. Journées de Chimie Organique; Paris, France, "Development of 6-membered cyclic (alkyl)(amino) carbenes as strong donor ligands for organometallic catalysis," 2016.
3. ACS 251st National Meeting; San Diego, CA, "6-membered cyclic (alkyl)(amino)carbenes as strong donor ligands for transition metals in catalysis," 2016.
2. ACS 248th National Meeting; San Francisco, CA, "Stable carbene cross-coupling reactions," 2014.
1. Richard Larock Undergraduate Research Conference; Davis, CA, "Investigation of main-group metal, transition-metal carbonyl complexes," 2012.

TEACHING EXPERIENCE

Senior Graduate Teaching Assistant (UCSD) 2016-2017

- Designed and implemented course modules directed at molding the pedagogical practices of new departmental teaching assistants alongside Professor Stacey Brydges (Chemical Education).

Chemistry Department Teaching Assistant (UCSD) 2012-2017

- General chemistry (8 courses), Introductory Laboratory Techniques (2 courses), Organic Chemistry (3 courses).
- Average overall rating: 4.74/5.00 (555 responses).

National Teaching Assistant Workshop, Invited Participant (Georgia Tech) 2015

- Workshop focused on preparing teaching assistants for leadership in STEM education.

Teaching + Learning at the College Level (formally titled The College Classroom) (UCSD) 2014

- A seminar style course that aims to give a strong foundation in the constructive theory of learning and how to integrate that pedagogy into an active, student-centered class.

Chemistry Tutor, Student Academic Success Center, (UCD) 2010-2012

- Led general chemistry one-on-one and group tutoring workshops for undergraduate students.

PHILANTHROPIC ORGANIZATIONS

Founder, Reviews for Charity (UCSD) 2013-2014

- Led chemistry reviews and workshops for students of general chemistry courses. Students optionally donated money for the review, which was then donated to a non-profit of our choosing. Raised $1047.

Chemistry Tutor, Tutors for Japan Relief (UCD) 2011

- Tutored individual students in general chemistry. In return students gave an optional monetary donation which was sent to help with disaster relief in Japan. Raised $200.

ABSTRACT OF THE DISSERTATION

Development and Reactivity Studies of Highly Ambiphilic Carbenes

by

Cory Michael Weinstein

Doctor of Philosophy in Chemistry

University of California, San Diego, 2018

Professor Guy Bertrand, Chair

Since their seminal isolation as stable species in 1988, carbenes have become indispensable ligands across a myriad of fields within chemistry. The origin of their exceedingly wide ranging popularity is the energetic accessibility of these purely organic molecules' frontier orbitals. In this dissertation, these energetic boundaries will be pushed to new limits giving reactivity not previously observed for stable carbenes. Indeed, by utilizing highly electrophilic carbenes, the isolation of P_8 clusters and a novel type of carbene P_4 adduct was achieved. Additionally, coupling reactions of electrophilic carbenes with a nucleophilic partner resulted in the formation of two rare examples of bent allenes, as

well as the isolation of the first carbene-carbene heterodimer. Furthermore, the synthetic development and isolation of six-membered cyclic (alkyl)(amino)carbenes is discussed in detail. These highly ambiphilic carbenes allow for the stabilization of a rare amino ketene, intramolecular C-H activation of an unactivated methylene group, and have even provided evidence towards the description of novel C-H···Se non-classical hydrogen bonding. Finally, the stability and electronic properties of a pyrrolidinylidene derived remote *N*-heterocyclic carbene was investigated. This unique ligand opened into an $\alpha,\alpha,\gamma,\gamma$-tetrasubstitued-2-allenyl ketimine in its free state, however the resulting allene was shown to react as a carbene in the presence of electrophiles.

Chapter 1 : General Introduction

1.1 Molecular and Electronic Description of a Carbene

In accordance with the paradigm shifting observation by Lewis,[1] molecular species that feature a neutral carbon atom must fall into one of four categories (Figure 1.1). The most common and widely observed is category **I**, in which carbon satisfies the octet rule and is involved with exactly four bonds of σ and/or π character, with C_2 having been the subject of considerable debate.[2-9] The defining character for Category **II** is a carbon atom featuring a single non-bonded electron, namely carboradicals. Without a doubt, this category is highlighted by the report of Gomberg on the isolation of the triphenylmethyl radical (Figure 1.2, left).[10] This seminal discovery demonstrated that carbon could defy the octet rule and remain persistent in this highly reactive electronic state, when given proper mesomeric and kinetic stabilization. Indeed, although carbynes (category **IV**) are still only stable as free species in interstellar space,[11-12] carbenes (category **III**) have been transformed from laboratory curiosities to chemical workhorses over the last 180 years.[13-19]

Carbenes are defined as neutral, divalent carbon species that can exist in either a singlet (S =1) or triplet (S = 3) spin state. Furthermore, there are two possible forms of carbenes. In the less frequently studied version, the carbene carbon is bonded to only one other atom in its free state with a bond order ≥ 2 (category **III**, bottom). The parent form, namely a vinylidene, was first structurally characterized by Mills and Redhouse in 1966 as a transition-metal (TM) complex. They demonstrated that upon irradiating a benzene solution of diphenylketene and $Fe_2(CO)_9$, the respective bimetallic vinylidene complex could be isolated **(**Figure 1.2, right).[20-21] Although many vinylidene TM complexes have been made since this first report, the free species still needs to be structurally characterized.

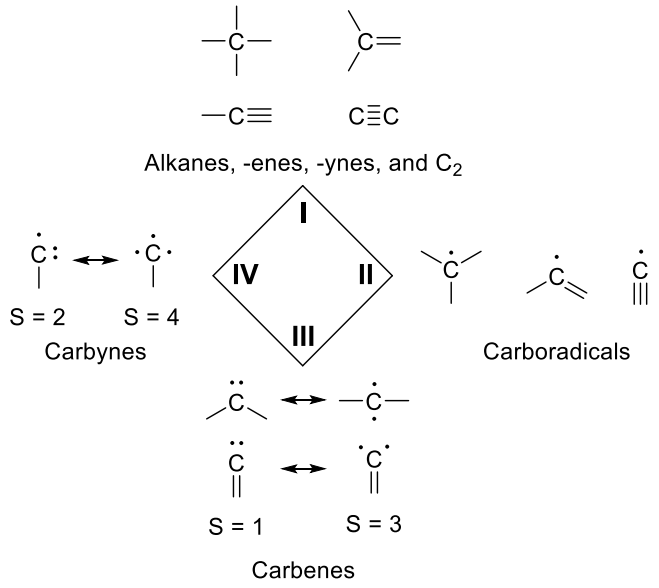

Figure 1.1: Neutral molecular carbon species.

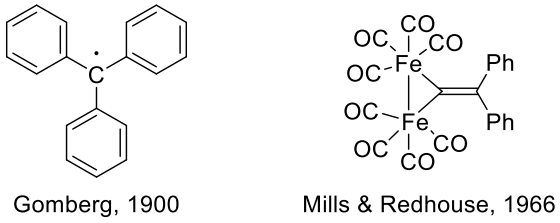

Figure 1.2: Gomberg's radical and the first TM vinylidene complex.

The far more common and heavily researched carbene form, and the focus of this dissertation, features a central carbon atom bonded to exactly two other elements ($1 \leq$ bond order ≤ 2) (category **III**, top). Given this description, two extreme geometric states can be envisioned (Figure 1.3). In one case, the geometry about the carbene center is completely linear resulting from sp hybridization of two of the carbene orbitals. The remaining two p-orbitals (formally p_x and p_y) are therefore energetically degenerate and nonbonding in character. This causes the two remaining electrons to fill the orbitals with parallel spin, giving an electronic triplet state. To be clear however, no carbene can be described as purely sp hybridized as most carbenes have significant bending at the carbene center. The bending is achieved by greater sp^2 hybridization of the carbene center which causes the former p_x-orbital to significantly mix with

an s-orbital lowering its energy. The now in plane orbital is more commonly referred to as the carbene σ-orbital. Since the p_y-orbital is orthogonal to the sp^2 plane, its energy is largely unchanged with respect to the extreme linear description, and will furthermore be referred to as the p_π or π-orbital. Without any additional mesomeric stabilization, the bent carbene is still a triplet in the ground state. Indeed, spectroscopic experiments corroborated by quantum mechanical calculations have determined that the parent carbene methylene (CH_2) has a triplet ground state with an internal bond angle of ~134°.[22] Calculations have shown however, that restricting methylene to a more acute angle of 102° results in additional stabilization of the σ-orbital.[23] This fundamentally changes the spin state of the carbene to a singlet as the two electrons fill exclusively into the σ-orbital leaving the π-orbital empty. The difference in energy between the triplet and singlet states of a carbene is known as the singlet-triplet gap (ΔE_{ST}) and is commonly used to help evaluate the stability of a singlet carbene. For CH_2, the ΔE_{ST} has been calculated to be -9.1 kcal mol^{-1} making the triplet state slightly more stable than the singlet.[24]

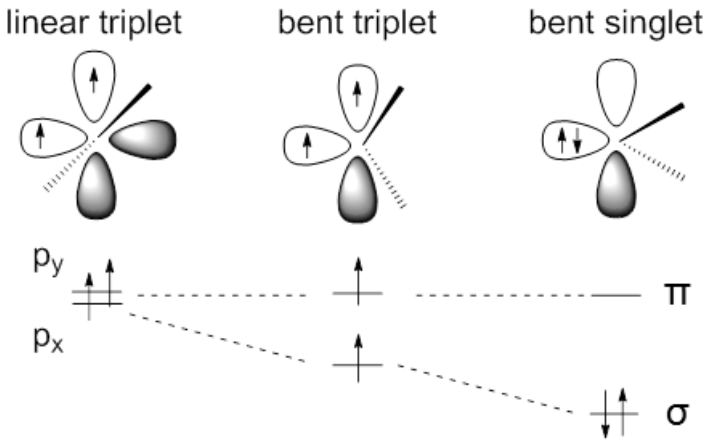

Figure 1.3: Influences of hybridization on the electronic state of a carbene.

The distinction between triplet and singlet carbenes is crucial as they undergo largely different reactivity pathways. Triplet carbenes are diradicals and are highly reactive with limited experimental lifetimes in the laboratory.[25] On the other hand, singlet carbenes are easier to handle, and can even show ambiphilic behavior as they contain both a filled and empty orbital at a singular atom. Although

restricting the internal bond angle is one way to favor the singlet over triplet state, a more effective strategy is through utilizing mesomeric effects of the neighboring atoms to the carbene carbon.

Given the wide variety of possible elements to choose from, many different permutations of α-substituents adjacent to the carbene center could be envisioned, and several of the more historically significant forms will be highlighted later in this chapter. For now, simply consider the cases in which the neighboring atoms are π-donors and σ-acceptors (Figure 1.4). Here, the neighboring atoms harbor a lone pair of electrons which can donate into the empty π-orbital of the carbene. This results in the formation of a three-centered four-electron bond with some multiple bond character. By extension, the formally empty π-orbital of the carbene is now anitbonding in character with respect to this new bond, therefore destabilizing it and giving a higher energy lowest unoccupied molecular orbital (LUMO). Furthermore, the relatively large electronegative character of these elements inductively stabilizes the carbene σ-orbital lone pair, thus lowering the energy of the highest occupied molecular orbital (HOMO). The overall effect is an increased HOMO-LUMO gap which induces a singlet ground state.

Given the peculiar electronic environment about the carbene center, many chemists became interested in the preparation and isolation of this unique class of ligand. With the principle idea that mesomeric effects should stabilize the singlet state of a carbene, the race was on to find ways to synthesize the free species in a laboratory.

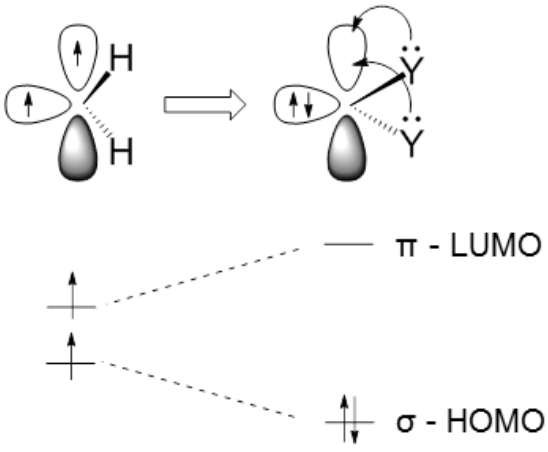

Figure 1.4: Influence of mesomeric effects on the electronic state of a carbene (Y = NR_2, OR, F, etc.).

1.2 A Brief History of Carbenes

In 1835, long before there was any understanding of atomic and molecular orbitals, Dumas attempted to generate methylene through the dehydration of methanol.[26] Following in his steps, Nef aimed to generalize this reaction from CH_2 to CX_2 (X = halogen).[27] Disappointingly for both, the proposed carbene intermediate was determined to be too unstable for isolation or viable use. It wasn't until the turn of the next century before Staudinger could confirm the first "carbene like" reactivity of CH_2.[28] In this seminal experiment, diazomethane was irradiated in the presence of hydrazine giving a transient methylene intermediate which inserted into an N-H bond forming methylhydrazine (Scheme 1.1). Similar to how Nef followed Dumas, Doering followed Staudinger in 1954 attempting to generate the dihalocarbene CCl_2 by deprotonating chloroform.[29] When this reaction was done in the presence of olefins, a cyclopropanation reaction was observed which solidified the potential usefulness of carbenes as building blocks in organic synthesis.

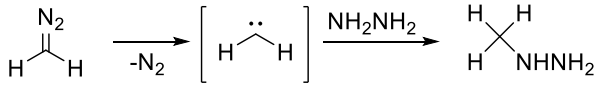

Staudinger, 1912

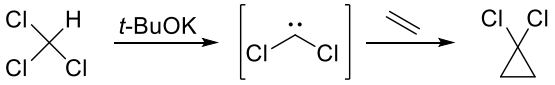

Doering, 1954

Scheme 1.1: Early organic transformations involving carbene intermediates.

It wasn't until the early 1960s that groups first started to investigate how mesomeric effects might stabilize a carbene enough for isolation. In one of the most seminal reports from the field, Wanzlick attempted to isolate the first *N*-heterocyclic carbene (NHC) by eliminating a molecule of chloroform through thermolysis of the respective precursor (Scheme 1.2).[30-31] The reaction gave a tetraazafulvalene, presumably resulting from the dimerization of two NHC intermediates. This experiment was the first

indication that utilizing mesomeric stabilization, in addition to preventing dimerization through kinetic protection, might lead to isolable carbenes as free species. Note that carbene dimerization is covered in much greater detail in Chapter 3 of this thesis.

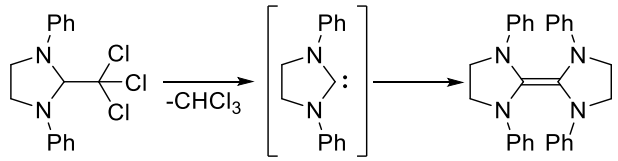

Wanzlick, 1962

Scheme 1.2: First attempt at synthesizing an NHC.

Concurrent with the investigation of carbenes as free species, many groups showed that these ligands could be trapped as complexes with a wide range of TMs. Without realizing it at the time, the first reported NHC complex was made by Tschugajeff in 1925 when he reported the formation of a yellow salt.[32] It wasn't until 1970 however, that Tschugajeff's "yellow salt" was structurally identified to be the chelating $PtCl_2(NHC)_2$ complex (Figure 1.5).[33-34]

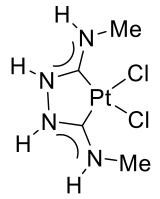

Tschugajeff, 1925

Figure 1.5: First reported NHC TM complex.

The first unambiguously structurally identified carbene complex was made by Fischer in 1964. The major advancement was achieved by nucleophilic attack of phenyl lithium onto a carbonyl group of a tungsten hexacarbonyl complex, followed by O-alkylation (Scheme 1.3). Because of his significant achievement, TM complexes featuring carbenes with singlet character are known as "Fischer carbenes" to this day. Only four years after Fischer, both Öfele and Wanzlick independently showed that NHC TM complexes could be directly synthesized via intermolecular deprotonation of the corresponding iminium

precursors if a TM complex was preloaded with the appropriate Brønsted base. Lappert followed suit in 1971 with a clever experiment.[35] Here, his group used an electron rich olefin similar to Wanzlick's dimer and showed that when refluxed in a xylene solution of $[PtCl(\mu\text{-}Cl)(PEt_3)]_2$, it could split into two molar equivalents of $PtCl_2(NHC)(PEt_3)$. This result suggested that TM complexes with accessible LUMOs could be capable "carbene traps." The last major early achievement in carbene TM chemistry came from the DuPont research facilities in 1974 by Richard Schrock. In this report, he offered evidence that an all-alkyl carbene complex was formed by α-hydride elimination when neopentyl (Np) lithium was added to $TaCl_2(Np)_3$.[36] Like Fischer, this pioneering achievement by Schrock still lives on colloquially as carbenes coordinated to TMs featuring triplet ground states are called "Schrock" carbenes.

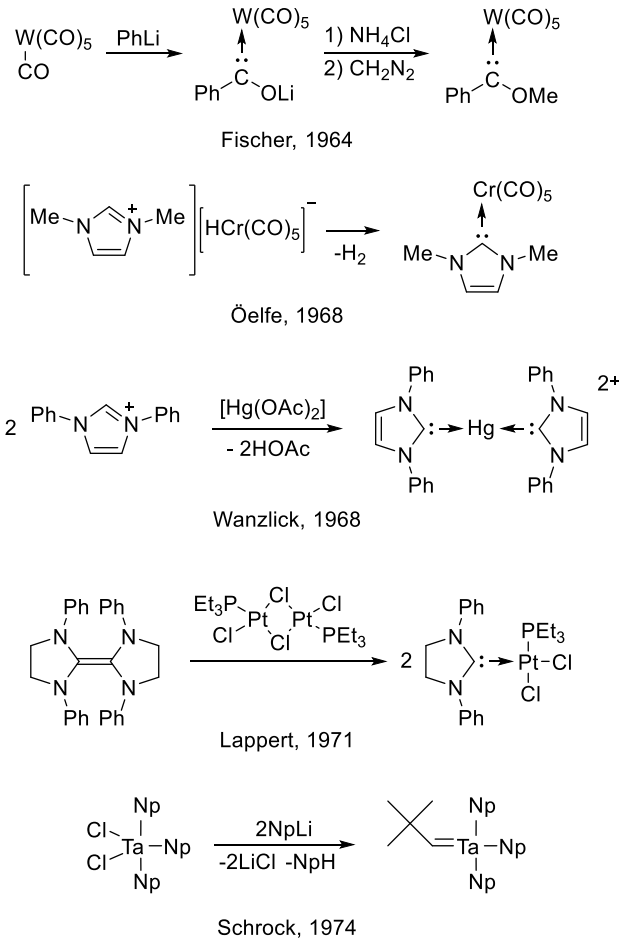

Scheme 1.3: Pioneering studies in the field of carbene TM complexes (Np = neopentyl).

Although many attempts followed, it wasn't until 1988 that the first isolable carbene was synthesized by the group of Bertrand.[37] In this report, a (phosphino)(silyl)carbene was generated by irradiation of the respective diazo precursor (Scheme 1.4). The oily, singlet carbene is electronically stabilized from the "push-pull" design of the α-substituents. More specifically, the phosphino group "pushes" its lone pair of electrons into the formally unoccupied π-orbital of the carbene. Furthermore, the σ lone pair of electrons on the carbon atom is "pulled" away from the carbene center via a symmetry overlap of the low-lying σ*-orbital on the silyl group. The result is that this carbene can be drawn in a zwitterionic, alleneic resonance form. Nonetheless, it has been demonstrated to react like a carbene.[38]

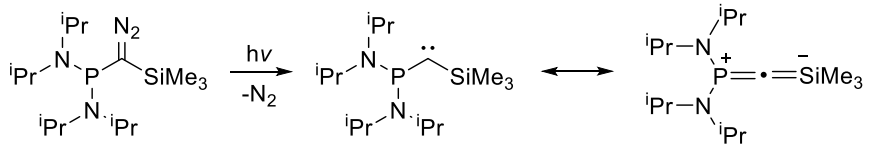

Scheme 1.4: The first isolable carbene featuring stabilization from a "push-pull" resonance form.

The first crystalline carbene was not discovered until three years later when Arduengo, building off the years of research by Wanzlick, Öelfe and Lappet, reported the synthesis of the first free NHC (Scheme 1.5).[39] The key difference between Arduengo's and Wanlick's NHC was the incorporation of adamantyl substituents onto the nitrogen atoms. The increased bulk kinetically prevented dimerization of the carbene. Indeed, Arduengo's NHC is indefinitely stable at room temperature in the absence of air or moisture. This monumental achievement now made NHCs viable ligands for many fields of chemistry.[13, 40-42]

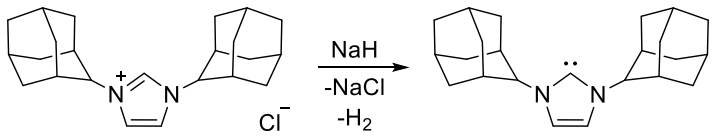

Scheme 1.5: The first crystalline, isolable carbene.

Since 1991, the number of NHC related publications has grown exponentially every year. The peculiar properties of NHCs have led to new discoveries in many a wide range of fields from material science[43] to medicinal applications.[44] Without a doubt however, the field that has benefited the most from the accessibility of these ligands has been TM mediated catalysis.[15, 45-46] The first report of NHCs being used as a ligand in TM catalysis came from Hermann in 1995.[47] Here, his group demonstrated a $PdI_2(NHC)_2$ catalyst was highly efficient (TOF = 15000) at Heck coupling reactions in addition to exhibiting high thermal stability due to the strong nature of the M-C bond (Figure 1.6). This paradigm shifting paper paved ways for NHCs to all but replace phosphines as traditional ligands for TMs as they are much stronger donors and make highly robust catalysts. One of the key examples of this change came from the evolution of Grubbs' catalyst in 1999.[48] Indeed, by moving from the bis(phosphine) 1st generation, to the mixed phosphine-NHC 2nd generation catalyst, this extremely potent olefin metathesis catalyst has made possible a myriad of new polymer research fields. Note that this ruthenium catalyst features both a "Fischer" and "Schrock" type carbenes as ligands. Grubbs was recognized for this major accomplishment in 2005 upon being awarded a share of the Nobel Prize in Chemistry.

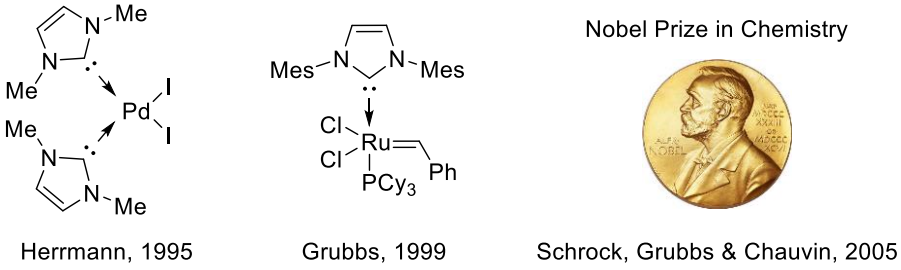

Figure 1.6: Major achievements in NHC TM mediated catalysis (Mes = 2,4,6-trimethylphenyl).

There is little question that after Arduengo's seminal discovery, the field of carbene chemistry has been dominated by "classical" NHCs. In 2002 however, the group of Crabtree reported the serendipitous discovery of a new bonding mode for an NHC.[49] When $IrH_5(PPh_3)_2$ was subjected to an iminium salt featuring a pendant pyridine moiety, two complexes were isolated in which the NHC coordinated to the iridium center via either the C2 or C4 carbon (Scheme 1.6). The variation in coordination mode of the

NHC was quite remarkable considering that the calculated pK_a of the protons on the C2 and C4 positions were 24 and 33, respectively.[50-51] It was hypothesized that formation of the "abnormal" NHC (*a*NHC) binding mode proceeded through oxidative addition of the former C4-H bond to form an iridium(V) intermediate which quickly reductively eliminates H_2. Evidence for this hypothesis came from the observed difference in reactivity when varying the anion of the iminium precursor. Indeed, halides, which form favorable hydrogen bonds, promoted deprotonation at the C2 position, whereas weakly coordinating anions (BF_4^-, PF_6^- and SbF_6^-) instead favored the oxidative addition pathway.[52] The greater importance of this result however, was that there was a renewed interest in carbenes featuring limited heteroatom stability: A condition that Wanzlick would have never dreamed.[53-55]

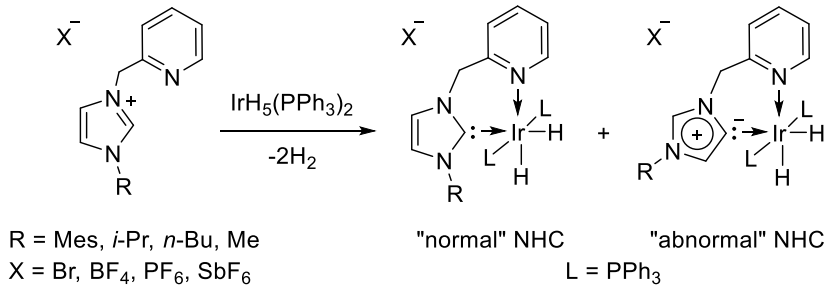

Crabtree, 2002

Scheme 1.6: First report of an "abnormal" binding mode for NHCs.

Crabtree's seminal report was highlighted again seven years later when the group of Bertrand isolated a crystalline *a*NHC.[56] This was accomplished by cleverly synthesizing an appropriate precursor which featured a phenyl substituent at the C2 and C4 positions, therefore blocking the classical deprotonation pathway (Figure 1.7). The so-called mesoionic carbene (MIC) was named as such because canonical resonance structures of the carbene cannot be drawn without formal charges. Although sensitive to rearrangement at 50 ºC, the MIC is stable at room temperature for several days in the absence of air and moisture.

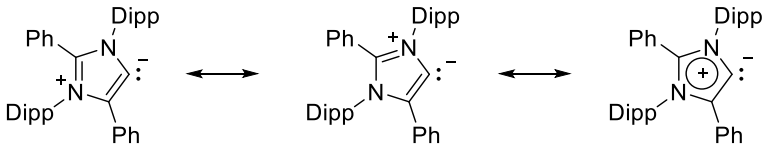

Figure 1.7: A free *a*NHC and its most relevant mesoionic resonance forms.

In addition to MICs, the group of Bertrand has been highly influential in developing and isolating carbenes with limited heteroatom stabilization (Figure 1.8).[57-58] Persistent acyclic (alkyl)(amino)carbenes (AAACs) and cyclic (alkyl)(amino)carbenes (CAACs) were first reported in 2004 and 2005, respectively.[59-60] Although AAACs decompose at room temperature after three days in solution, CAACs are indefinitely stable in solution and the solid-state, thus making them more practically useful. CAACs feature a saturated five-membered heterocycle with only one nitrogen atom α to the carbene center. With respect to analogous five-membered saturated NHCs, CAACs differ by only one quaternary carbon group, and therefore have only one π-donor/σ-acceptor adjacent to the carbene center. This chemical environment causes a CAAC to have a lower LUMO (0.06 vs. 0.70 eV), higher HOMO (-5.20 vs. -5.62 eV), and smaller ΔE_{ST} (48.3 vs. 72.7 kcal mol^{-1}) than an analogous NHC.[58, 61] Altogether, this means that CAACs are in general both more nucleophilic and electrophilic than NHCs (see chapter 4 for a more detailed description and history of CAACs).

Just one year later, the Bertrand group was also able to synthesize and isolate a bis(amino)cyclopropenylidene (BAC).[62] Remarkably, this carbene has no direct heteroatom stabilization as the nitrogen atoms are instead γ to the carbene center. The stability of BAC is instead attributed to a conjugated π system, in addition to the aromaticity of the three-membered ring. Nonetheless, BAC still remains as the only stable carbene with no heteroatoms adjacent to the carbene center. That being said, many groups have developed methods to access TM-NHC complexes in which the heteroatoms are "remote" (at least two bonds away) from the NHC center (*r*NHC); leaving the field of stable *r*NHCs wide open for investigation (see chapter 5).[53, 63-65]

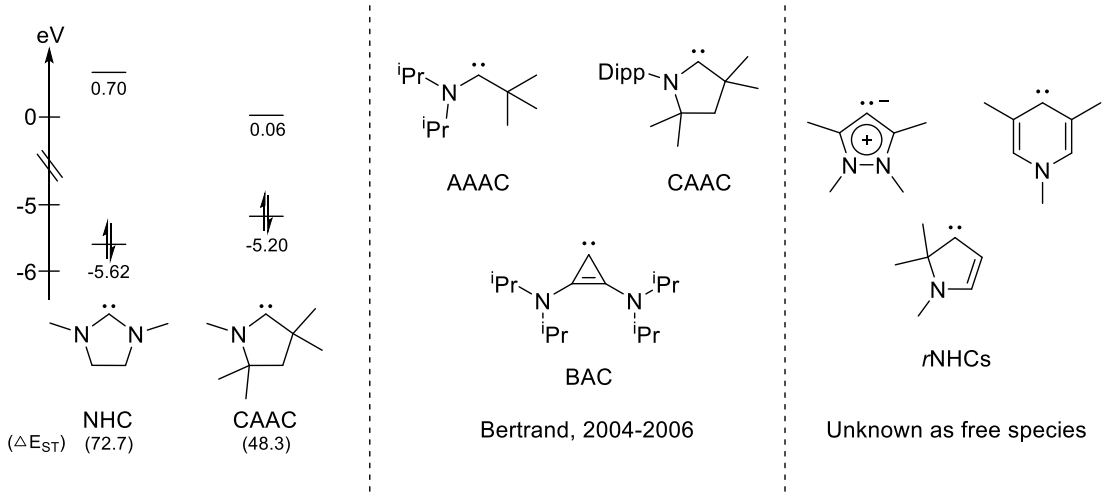

Figure 1.8: Calculated HOMO-LUMO gaps (eV) and ΔE_{ST} (kcal mol^{-1}) of an NHC and CAAC at the B3LYP/def2-TZVPP level of theory (left), persistent and isolable carbenes with reduced heteroatom stabilization (middle), and non-exhaustive examples of unknown *r*NHCs (right).

The last modern, significant advancement in the field of stable carbene chemistry has been the development of *N*,*N*'-diamidocarbenes (DACs) by the group of Bielawski (Figure 1.9).[66-69] Although appearing to be strikingly similar to classical NHCs, the carbene center of a DAC benefits from far less π-stabilization of the adjacent nitrogen atoms due to the large contribution of an amido resonance form. As an effect, DACs are among the most electrophilic stable carbenes known, and have even recently been shown capable of reacting as an excited state triplet carbene.[70] The unique π-acidity of DACs was capitalized by the author of this thesis, and is highlighted by the results reported in chapters 2 and 3.

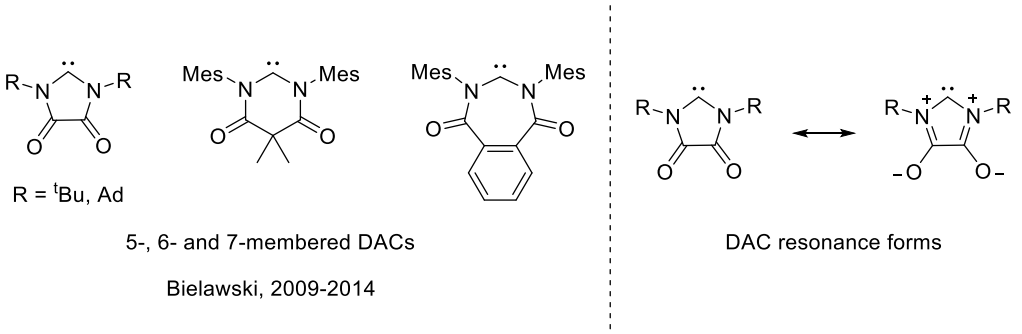

Figure 1.9: Stable 5-, 6- and 7-membered DACs (left) and an example of the common resonance form giving rise to the carbenes' high electrophilicity (right).

1.3 Measuring the Steric, Donor, and Acceptor Properties of Carbenes

1.3.1 Measuring the Sterics of Carbenes

Given the immense library of carbenes that have been synthesized since 1988, it is easy to imagine that the steric environment around a carbene center can vary drastically. Much of the steric bulk important in dictating the kinetic protection of a carbene, and by extension its reactivity, comes from the groups adjacent to the carbene. For example, NHCs have two NR groups which protrude outward in the plane of the carbene lone pair (Figure 1.10). Simply designing NHCs with different R groups would naturally give rise to different environments. Beyond this, changing one of the nitrogen atoms to any sp^3 hybridized oxygen (oxazolylidene) or carbon (CAAC) changes the steric environment immensely as the number of substituents protruding towards the front of the ring changes both in number and 3D positioning. On the other hand, even NHCs with identical functional groups can vary greatly with respect to their steric hindrance if the size of the NHC ring is changed (e.g. 5-, 6-, 7-membered, etc.). Adding even more complexity, all of these scenarios are interchangeable, thus leading to even more possibilities. Considering that certain steric environments might favor some reactions over others, especially with respect to the fields of organo- and TM-catalysis,[45, 71] a method to evaluate, compare, and understand differences in steric parameters among carbenes is indeed desirable. Luckily, the group of Nolan tackled this specific problem by introducing a parameter called percent buried volume ($\%V_{bur}$).[72]

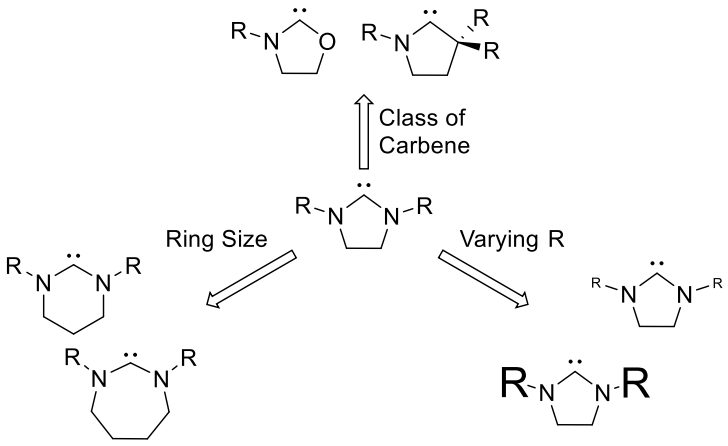

Figure 1.10: Pictorial representation demonstrating only a limited set of examples how different carbenes can have varying steric properties.

As described by Nolan et al., "$\%V_{bur}$ is defined as the percentage of a sphere (r = 3.5 Å) around the metal center that is occupied by a given ligand" (Figure 1.11).[73] In layman's terms, the bigger a ligand's substituents are in the direction of ligation, the greater amount of space occupied, and thus the $\%V_{bur}$ will be higher. There are two main limitations to this measurement. First, the relative position of substituents on a carbene can be greatly affected by electrostatic and/or Van der Waals forces of neighboring ligands. It has therefore been convention to compare the $\%V_{bur}$ of LAuCl complexes. Here, the only other ligand is a chlorine atom that is *trans* to the ligand being analyzed, and thus has relatively zero effect on the positioning of the ligand's substituents. The other limitation of a $\%V_{bur}$ measurement is that it is reliant on the quality of either X-ray or quantum chemical calculation data. Crystal packing and solvent effects can greatly change the lowest energy position of atoms in a structure, which would further change the $\%V_{bur}$. Additionally, X-ray data represents only a static measurement of atomic positioning, thus $\%V_{bur}$ might not give an adequate representation of how bulk would be distributed in homogenous solutions. The same argument can be made with respect to atomic positioning derived from chemical calculations as this accounts for the lowest energy positions in the gaseous state. It is therefore important that chemists use $\%V_{bur}$ comparisons with some discretion, and not draw conclusions on steric differences

when two ligands vary in $\%V_{bur}$ by less than ~0.5% or ~1.2% when containing rigid or flexible substituents, respectively.[73]

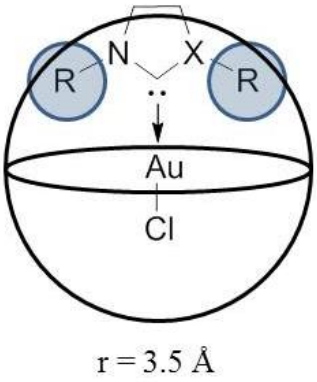

Figure 1.11: $\%V_{bur}$ is the percentage of the given sphere occupied by the ligand, in this case a carbene.

Nonetheless, $\%V_{bur}$ is still a useful measurement for comparing kinetic protection. Furthermore, given a quality CIF or XYZ file, a value for the buried volume can be easily obtained by using the free SambVca tool available online.[74] Some examples are shown below comparing different carbenes and their respective $\%V_{bur}$ (Table 1.1).[73, 75] Note that by convention, hydrogen atoms are removed from molecules and the M-C bond length is fixed at a certain value before a buried volume value is calcualted. As is evident from entries **1**-**3**, the $\%V_{bur}$ changes immensely by simply substituting for different NR groups on the NHC. When comparing NHCs with similar substituents on the nitrogen atoms, an increase in ring size results in an increase in $\%V_{bur}$. This can be seen by comparing entries **1**, **5** and **6** which have successive increasing ring sizes, and thus increasing $\%V_{bur}$ of 45.4, 50.9 and 52.7%, respectively. Of note is also the comparison between six-membered NHCs **4** and **5**. Although both feature similar ring sizes and Dipp substituents on nitrogen, the second nitrogen substituent in entry **4** is a piperidine group locked behind the carbene, therefore greatly reducing the $\%V_{bur}$ by 12.4%. Finally, two CAACs are given as examples in entries **7** and **8** showing how the change in hybridization to an sp^3 carbon atom can also affect the buried volume. Comparing **7** to **8** also highlights how directional bulk is more significant to the steric hindrance around the carbene than simply having a bulky substituent. Indeed, although adamantyl is

a bigger group than menthyl by volume, the rigidity of the menthyl substituent in **8** causes the $\%V_{bur}$ to be 3.1% bigger than **7**.

Table 1.1: Representative examples of changes in $\%V_{bur}$ for some (carbene)AuCl complexes (Au-C bond fixed at 2.00 Å).

Entry	Carbene	$\%V_{bur}$	Entry	Carbene	$\%V_{bur}$
1	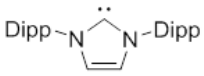	**45.4**	**5**	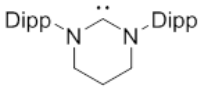	**50.9**
2	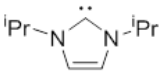	**27.5**	**6**	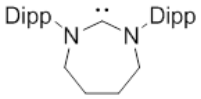	**52.7**
3	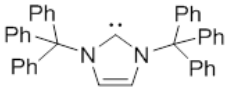	**57.3**	**7**	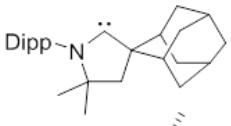	**47.9**
4	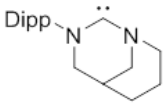	**38.5**	**8**	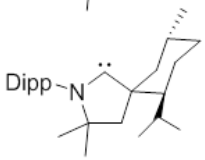	**51.0**

It is worth mentioning that the group of Cavallo recently released an updated version of the online SambVca program titled SambVca2.[76] This version includes a new steric mapping feature that gives information on the relative steric crowding of a ligand's substituents dissected into four quadrants (Figure 1.12). The redder the shading of a region in the output image file, the more steric impact a ligand has on that region of space. The visual provides additional information that enables clear differentiation of the steric impact in 3D space between carbenes. For example, most of the steric crowding for the NHC (left) comes from one of the isopropyl groups of the Dipp substituent. This is visualized by the heavy red shading of the southwest quadrant on the steric map. On the other hand, the steric bulk of the CAAC (right) is more homogeneously distributed across all four quadrants as visualized from the fairly uniform yellow color.

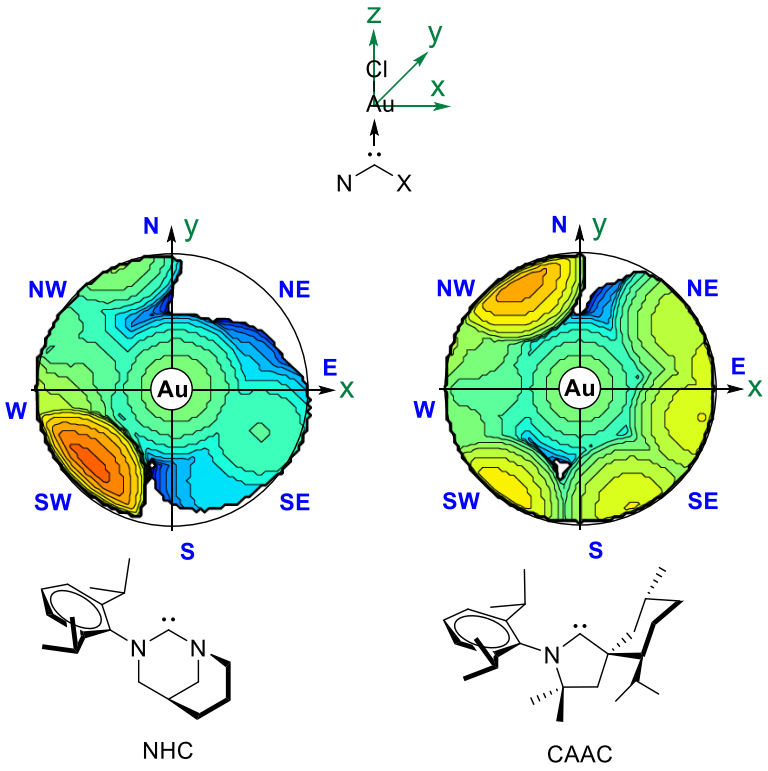

Figure 1.12: Examples of 3D steric mapping of (carbene)AuCl complexes.

1.3.2 Measuring the Donor Properties of Carbenes

Carbenes are most commonly employed as ligands due to their strong σ-donor properties (*vide supra*). Like the case of sterics in section 1.3.1, there are a wide range of possible stable carbenes with a myriad of possible donor strengths. It is therefore important to have a uniform, reliable metric that can compare the relative donor strengths of all carbenes.

In the late 1970s, Tolman developed a method by which a similar comparison of donor strengths could be made between phosphines.[77] By mixing a 1:1 solution of phosphine and $Ni(CO)_4$, a simple ligand substitution took place yielding the respective tetrahedral (phosphine)$Ni(CO)_3$ complex. Since carbonyl ligands have π* orbitals that can participate in strong backbonding with the filled Ni d-orbitals, as the donor strength of a phosphine increases, the more electron rich the Ni center becomes which results in a greater percentage of d-orbital electron density overlapping with the carbonyl LUMO. This effectively weakens the CO triple bond as it acquires more anitbonding character. Tolman recognized that

the overall transitive effect of phosphine donor strength could be easily ranked by simply measuring the IR spectrum of each respective (phosphine)$Ni(CO)_3$ molecule. For strongly donating phosphines, the A_1 carbonyl stretching frequency is red shifted due to the effective weaker bond order of the carbonyl groups. Conversely, the weaker the phosphine donor, the more the stretching frequency would be blue shifted. This measurement could be further generalized to comparing other neutral, two electron donors (e.g. amines) and became colloquially known as the Tolman electronic parameter (TEP) (Figure 1.13).

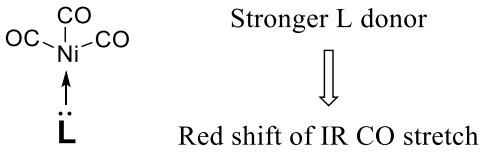

Figure 1.13: Transitive conclusion from the Tolman electronic parameter.

Given that carbenes are also neutral, two electron donors, it's not a surprise that TEP values were extended to carbenes. Although Tolman conducted his original experiments with $Ni(CO)_4$, the field has moved towards using $[M(cod)Cl]_2$ (cod = 1,5-cyclooctadiene; M = Rh, Ir) starting materials to avoid the highly toxic nickel complex. In these cases, the carbene of choice is first reacted with the group IX dimer yielding the respective (carbene)MCl(cod) complex. Simply bubbling CO into a solution of this species displaces the cod and cleanly gives *cis*-[(carbene)$MCl(CO)_2$]. Since this complex contains both *cis*- and *trans*-carbonyl ligands to the carbene, the symmetric and asymmetric CO stretching frequencies in the IR spectrum need to be averaged, and the resulting value applied to one of the following equations (Equation 1.1-1.4) depending on which comparison is desired.[40, 78-79] It is important that the IR spectrum of the molecule of interest be recorded in DCM when possible, as different solvents will give rise to misleading TEP values.[80]

Rh to Ni: TEP $[cm^{-1}] = 0.8001\nu_{CO}^{avg/Rh}[cm^{-1}] + 420\ [cm^{-1}]$ (1.1)

Ir to Ni: TEP $[cm^{-1}] = 0.8475\nu_{CO}^{avg/Ir}[cm^{-1}] + 336\ [cm^{-1}]$ (1.2)

Rh to Ir: $\nu_{CO}^{avg/Ir}[cm^{-1}] = 0.9441\nu_{CO}^{avg/Rh}[cm^{-1}] + 98.9\ [cm^{-1}]$ (1.3)

Ir to Rh: $\nu_{CO}^{avg/Rh}\,[cm^{-1}] = 1.0356\nu_{CO}^{avg/Ir}\,[cm^{-1}] - 56.9\,[cm^{-1}]$ (1.4)

For a quick introductory comparison of this technique, a series of *cis*-[(L)IrCl(CO)$_2$] complexes and their respective calculated TEP values are given below (Table 1.2).[40, 81] These carbenes show a wide range of donor properties as their respective TEP values vary from 2038.4 to 2055.8 cm^{-1}. Comparing entry **1** to **3**, changing the substituents on the nitrogen atom from an aryl to an alkyl group has only a small effect on the overall donor properties of the carbene as the TEP value changes by only 0.1 cm^{-1}. When entry **2** is considered for comparison as well, it appears that the bigger the group on the nitrogen atom, the higher the TEP value (Dipp > Mes > Cy). This highlights a small drawback in comparing TEP values of ligands with varying bulk. The bulkier the ligand, the more it might perturb the *cis*-CO bonding geometry, decreasing the allowed symmetry overlap of TM-d and CO-π* orbitals, and therefore giving a slightly higher TEP value. Luckily however, the affect usually only accounts for <1 cm^{-1} of error which makes TEP values still a broadly useful comparison measurement.

Table 1.2: Selected carbenes from *cis*-[(L)IrCl(CO)$_2$] and their calculated TEP values (cm^{-1}).

Entry	L	TEP	Entry	L	TEP
1	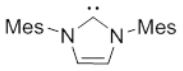	**2049.6**	**5**	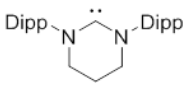	**2045.5**
2	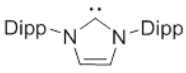	**2050.2**	**6**	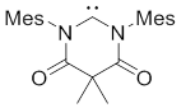	**2055.8**
3	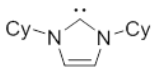	**2049.5**	**7**	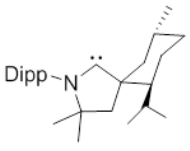	**2041.0**
4	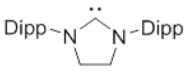	**2051.1**	**8**	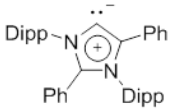	**2038.4**

Continuing with comparisons, entry **4** has a slightly higher TEP value than entry **2** by 0.9 cm^{-1}. The only difference between the two carbenes is that in entry **2**, the heterocycle is aromatic whereas in **4** it is completely saturated. Effectively, this translates into the aromatic species having more electron density on the carbene carbon than the saturated version, thus making it an overall better donor. For completely saturated NHCs entries **4** and **5**, a large decrease in TEP value is observed when expanding from a five- to six-membered ring. Using arguments discussed in section 1.1, as the internal bond angle of a carbene is increased, the energy level of the HOMO is raised due to increased p-character of the orbital. Therefore, expanding the ring size of a carbene results in a higher HOMO, and thus makes the carbene a stronger overall donor.

The lowest TEP values recorded in Table 1.2 belong to carbenes **7** and **8**, a CAAC and MIC, respectively. Both carbenes feature reduced heteroatom stabilization having only one nitrogen atom adjacent to the carbene center. Removing the inductive stabilization of a nitrogen atom α to the carbene center greatly increases the HOMO energy level of the carbene. This translates to much better overall donating properties, and subsequently the very low recorded TEP values. Between **7** and **8**, the lower TEP value belongs to the MIC due to it having an aromatic ring, whereas the CAAC is completely saturated. The data fits a qualitative argument that a MIC should be a stronger donor as the carbene is depicted as a carbanion in its major resonance form. Overall, these extremely low TEP values highlight how carbenes with reduced heteroatom stabilization adjacent to the carbene should be the ligand of choice when strong donors are desired.

The final carbene not yet discussed in Table 1.2 comes from entry **6**. This carbene, namely a DAC, has the overall highest TEP value in the table at 2055.8 cm^{-1}. The value is 10.3 cm^{-1} higher than entry **5** even though both examples are saturated six-membered NHCs. To explain the extremely high TEP value for **6**, the ability for the carbene to compete in TM-d orbital π-backbonding must be considered (Figure 1.14, left). The LUMO of a DAC is much lower than that of an analogous NHC due to the nitrogen lone pairs sharing electron density with the amido π-system (*vide supra*). A lower LUMO means that the carbene competes with the carbonyl groups for the TM-d orbital electron density which increases

the CO bond strength of both carbonyl groups and thus increasing the measured TEP values. This scenario highlights a potential major flaw in comparing carbenes using only TEP values. Since carbenes have a formally empty π-orbital, they can partake in varying levels of π-backbonding depending on the relative energy level of the carbene LUMO. Furthermore, since TEP values are extracted from the bond strengths of the carbonyl ligands, one can only reason that the comparison of carbenes' TEP values is truly only a comparison of the overall donor strength of a carbene (σ-donor minus π-acceptor). This shortcoming is better highlighted by comparing the benzimidazole-2-ylidene (left) to the thioylidene (right) depicted below (Figure 1.14, right).[42] Here, they share identical TEP values even though they belong to different classes of carbenes. It was therefore imperative that a method be developed which could be used in conjunction with TEP values to distinguish between the σ-donor and π-acceptor properties of a carbene (see section 1.3.3).

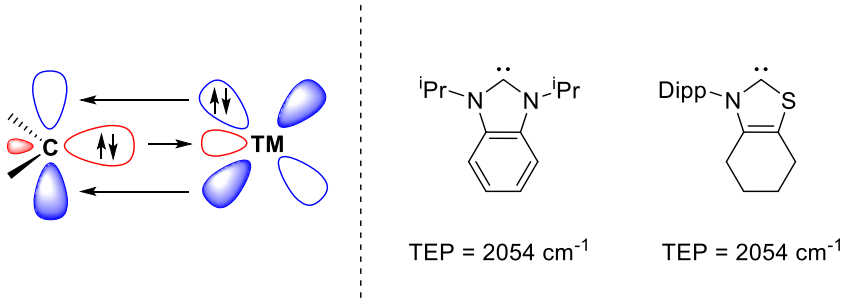

Figure 1.14: Representation of orbitals involved in TM-carbene multiple bonding (left) and its effect on the comparison of TEP values (right).

Although TEP values are by far the most widely used measurement for comparing the overall donor properties of carbenes, several other methods have also been developed.[40, 81] Cavallo and Nolan investigated the $^{1}J_{Pt\text{-}C}$ coupling constants from ^{195}Pt NMR for a series of *cis*-[$PtCl_2$(DMSO)(NHC)] complexes (Figure 1.15).[82] The authors of this report argued that larger coupling constants were due to a greater contribution of electron density in the σ-bond.[83] Indeed, the largest $^{1}J_{Pt\text{-}C}$ coupling constants were recorded for unsaturated NHCs (1479 and 1472 Hz), whereas their saturated counterparts gave the smallest $^{1}J_{Pt\text{-}C}$ coupling constants (1373 and 1358 Hz), with "Ender's carbene"[84] coming right in the

middle (1412 Hz). This method likely needs reinvestigation to better confirm overall trends however, as the original report only included five examples.

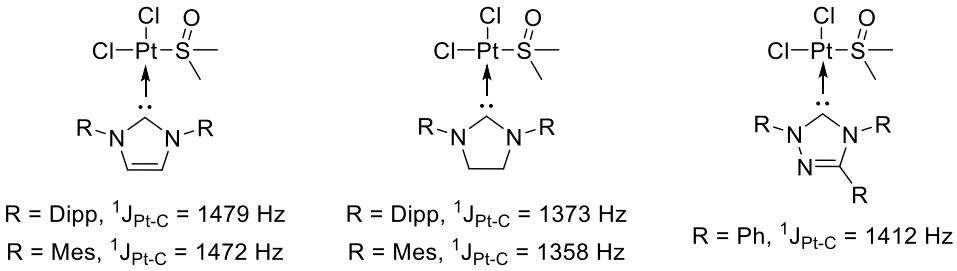

Figure 1.15: Comparing σ-donor character of carbenes through $^1J_{Pt-C}$ coupling constants.

In 2013, Gandon et al. designed a clever set of experiments which were used to compared the overall donor properties of a ligand, including carbenes.[85] In this paper, a series of neutral ligands were reacted with $GaCl_3$ to yield their respective Lewis acid-base adducts $LGaCl_3$. Upon subjecting these complexes to an X-ray diffraction study, the authors noticed that the TEP value of each ligand correlated extremely well with the sum of the internal Cl-Ga-Cl bond angles (R^2 = 0.978). In other words, the stronger σ-donor, the lower the TEP value, and the more pyramidalized the $GaCl_3$ moiety. The obvious drawback of using this comparison method comes from the need for high quality X-ray data for each new ligand one might want to investigate. Thankfully however, Gandon et al. showed that the sum of the calculated Cl-Ga-Cl bond angles at the BP86/def2-SVP level of theory matched well with the experimentally values (R^2 = 0.9689). Therefore, qualitative comparisons of ligand donor strength can be made by simply using the structural data of $LGaCl_3$ complexes acquired from calculated optimized geometries.

1.3.3 Measuring the Accepting Properties of Carbenes

Given the ambiphilic nature of carbenes, methods that compare carbenes' π-accepting properties independent of their σ-donating properties are highly desirable. The first such method was developed in 2013 by Bertand et al. and was expanded to more examples by Hudnall et al. one year later.[86-87] Both groups were able to rank the π-accepting ability for a range of carbenes by comparing the ^{31}P NMR

chemical shift of the corresponding phenylphosphinidene-carbene adducts (Figure 1.16). For highly π-acidic carbenes, adducts more closely resemble the phosphaalkene resonance form **A**. As such, the phosphorus center is greater deshielded and a lower field ^{31}P NMR chemical shift is observed. On the contrary, less π-acidic carbenes favor the carbene phenylphosphinidene resonance form **B** resulting in a much more shielded phosphorus center and a higher field ^{31}P NMR chemical shift. These two resonance forms represent extreme cases in which all known carbenes should fall somewhere in between. Furthermore, since the changes in the ^{31}P NMR chemical shifts are mainly influenced by a π-system, the comparisons are independent of the relative σ-donor strengths of each carbene. Finally, thanks to the sensitivity and wide spectral width of ^{31}P NMR, this technique allows for a more accurate scale in which carbenes can be compared.

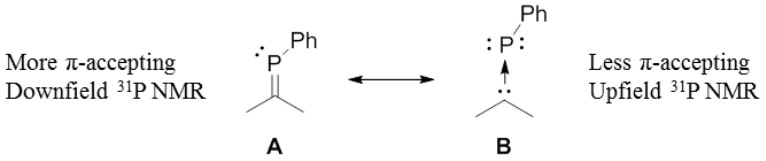

Figure 1.16: Two extreme resonance forms of carbene-phenylphosphinidene adducts giving rise to a ^{31}P NMR scale.

To highlight the power of this method, examples of ^{31}P NMR chemical shifts for certain carbene-phenylphosphinidene adducts are given below with the same carbenes' measured TEP values (Table 1.3). The examples given demonstrate the wide spectral range for the π-accepting scale (-18.2 to 126.3 ppm). Saturated NHC entry **2** is downfield shifted from the analogous unsaturated NHC entry **1** by 8.7 ppm. This arrangement of chemical shifts is expected, as a non-aromatic ring is more π-accepting than its aromatic counterpart. A significant increase in the π-accepting ability of a carbene occurs when the carbene ring size is expanded. For example, entry **3**, a six-membered NHC, has a ^{31}P NMR chemical shift of 24.6 ppm downfield of the five-membered saturated NHC entry **2**. The higher π-acidity can be explained by both less sp mixing of the carbene LUMO, as well as the increased ring size allowing for both more flexibility of the atoms within the ring. This effectively decreases the amount of nitrogen lone-

pair electron density donating into the empty π-orbital of the carbene which makes the carbene more π-acidic. The same logic can be extended to explain the highly deshielded ^{31}P NMR signal of entry **9**. Indeed, the nitrogen lone-pair in the AAAC is no longer restricted to be in plane with the carbene empty orbital by the effect of a closed ring system. The downfield ^{31}P NMR shift of entry **9** also benefits from reduced heteroatom stability of the carbene LUMO. With only one nitrogen lone-pair adjacent to the carbene center, the LUMO is significantly lowered, giving rise to the most π-acidic isolable carbene to date. The same effect can be seen when comparing the ^{31}P NMR chemical shift of the CAACs, entries **6** and **7**. Compared to the saturated NHC entry **2**, the ^{31}P NMR signal of the CAAC-phenylphosphinidene adducts are downfield shifted by 78.2 ppm on average. The large variation between the chemical shifts of the two CAACs (12.7 ppm) does point to imperfectness of this scale. Like TEP values, the π-scale can be heavily influenced by steric bulk, and thus some caution must be taken when comparing species with large substituents. Nonetheless, this measurement is highly useful and even gives evidence to show how DACs like entry **8** are indeed superior π-accepting carbenes.

The true power of this method however, is best seen when comparing both the ^{31}P NMR chemical shift and TEP values of entries **4** and **5**. The TEP values for these two species are identical (2054.0 cm^{-1}), therefore implying that the overall donating ability of these two carbenes is the same. When also considering the ^{31}P NMR data however, it becomes clear that the thioylidene (entry **5**) is a much better π-acceptor than the benzimidazole-2-ylidene (entry **4**). By extension, this means that the thioylidene must also be a better σ-donor to have an identical TEP value (TEP ≈ σ-donor minus π-acceptor). The combination of both TEP values and ^{31}P NMR chemical shifts now allows for a full comparison of the most important electronic properties of carbenes.

Table 1.3: ^{31}P NMR chemical shifts (ppm) and TEP values (cm^{-1}) of carbene-phenylphosphinidene adducts.

Entry	Carbene	^{31}P NMR TEP	Entry	Carbene	^{31}P NMR TEP
1	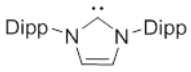	-18.9 2051.5	6	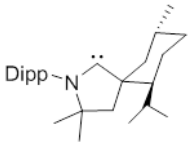	56.2 2042.2
2	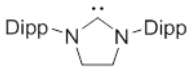	-10.2 2052.2			
3	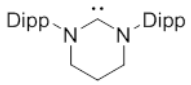	14.8 2044.0	7	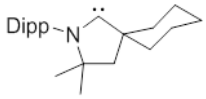	68.9 2048.5
4	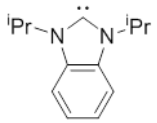	-34.6 2054.0	8	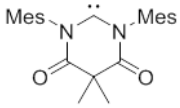	83.0 2055.8
5	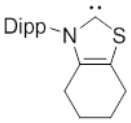	57.0 2054.0	9	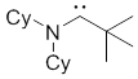	126.3 2043.8

Soon after the first report of the ^{31}P NMR scale, Ganter et al. developed a similar scale based on ^{77}Se NMR.[88] The original report only compared the ^{77}Se NMR chemical shifts for seven largely different examples of carbene-selenium adducts, however subsequent derivative studies by Cavallo et al.,[89] Siemeling et al.,[90] and Ganter et al.[91] have immensely expanded the data set. In principle, the scale works using the same resonance arguments as the phosphorus scale, except now with selenium as the NMR active nucleus of study (Figure 1.17). Highly π-acidic carbenes favor the selenoketone resonance form **C**, whereas poorly π-acidic carbenes more closely match the carbene stabilized selenium atom resonance form **D**. Like in the case of phosphorus, the higher multiple bond character of the carbene-Se bond, the more deshielded the selenium nucleus becomes, and thus a more downfield ^{77}Se NMR signal is observed.

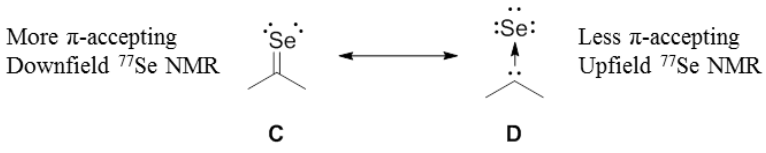

Figure 1.17: Two extreme resonance forms of carbene-selenium adducts giving rise to a ^{77}Se NMR scale.

There are some advantageous for using the selenium scale over the phosphorus scale. First, the selenium scale covers a much wider spectral width (~1200 ppm) allowing for better delineation of the π-accepting properties of closely matching carbenes. Second, elemental selenium, also known as black selenium, can be used as a trapping agent for transient carbenes. This means that carbene generation can be done *in situ* with an excess of black selenium powder, thus allowing for the determination of π-accepting properties of carbenes that would normally decompose at ambient temperatures. For example, both Bertrand et al.[92] and Biewlawski et al.[93] have recently taken advantage of this trapping technique to evaluate the high π-acidity of room temperature unstable cyclic (amino)(aryl)carbenes and a cyclic (alkyl)(amido)carbene, respectively (Scheme 1.7). The latter of the two species has the lowest field ^{77}Se NMR signal recorded for any carbene-selenium adduct to date, therefore making this carbene the most π-accepting singlet carbene reported.

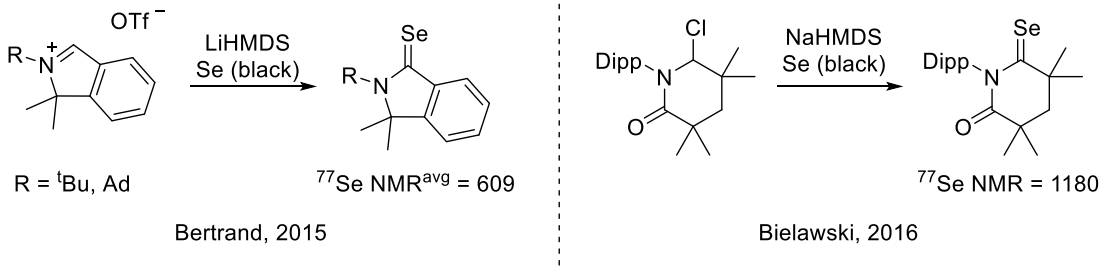

Scheme 1.7: Trapping experiments with Se (black) to give carbene-selenium adducts of cyclic (amino)(aryl)carbenes (left) and cyclic (alkyl)(amido)carbenes (right) and their highly downfield ^{77}Se NMR chemical shifts (ppm).

Although useful, this technique is particularly NMR solvent sensitive. By convention, all measurements have been made in D_6-acetone. Changing to an aromatic solvent like C_6D_6 can give shifts in the ^{77}Se NMR signal by up to 100 ppm which could potentially lead to an incorrectly assigned ranking system. Luckily however, Siemeling et al. surveyed all known examples of carbene-selenium adducts where the ^{77}Se NMR signal was reported in both D_6-acetone and $CDCl_3$.[90] From these data, his group

found an excellent relationship ($R^2 = 0.9976$) for converting between the two solvents, thus also allowing for comparisons in which $CDCl_3$ was used as a solvent (Equation 1.5).

$$\delta(D_6\text{-acetone}) = 1.051\delta(CDCl_3) \quad (1.5)$$

As a final note, it is worth mentioning that the author of this thesis discovered an additional potential flaw with using the selenium scale. Due to the relatively large size of a selenium atom, proximity forced non-classical hydrogen bonding has been observed in carbene-selenium adduct systems. This interaction deshields the selenium nucleus more than would be expected for normal systems, thus giving highly misleading ^{77}Se NMR chemical shifts. A more detailed description of this phenomenon is given in section 4.3.3.

1.4 Supporting Info

Calculations for the HOMO-LUMO gap and ΔE_{ST} of the simplified 5-memebered NHC and CAAC were carried out with the Gaussian 09 package.[94] Geometry optimizations and frequency calculations were performed with B3LYP employing Weigend's def2-TZVPP basis set.[95-96]

NHC singlet

N	1.07256800	0.20730300	-0.03549100
C	0.00000200	1.01233500	-0.00006100
C	-0.76599300	-1.23284700	-0.03345500
H	-1.22900800	-1.77362700	0.79482300
H	-1.14600100	-1.66294600	-0.96530600
N	-1.07256800	0.20730100	0.03538300
C	-2.43855100	0.66335500	0.00281700
H	-2.43758100	1.74874000	0.04768500
H	-2.94430600	0.34594200	-0.91594400
H	-3.00681000	0.27077800	0.85199100
C	2.43855500	0.66335800	-0.00272800
H	2.43756400	1.74873600	-0.04775500
H	2.94412200	0.34609300	0.91618400
H	3.00696900	0.27066300	-0.85173700
C	0.76599400	-1.23287400	0.03346700
H	1.14600600	-1.66286100	0.96536100

H	1.22900100	-1.77370800	-0.79477400

NHC triplet

N	1.08692900	-0.29445100	0.44910700
C	0.00000800	-1.02998100	-0.00009700
C	2.36850600	-0.48271000	-0.23090300
H	2.61278100	-1.54269800	-0.23199000
H	2.35231100	-0.13353000	-1.27329700
H	3.15194400	0.04668500	0.31206300
C	0.57604800	1.09462100	0.51711500
H	1.36988800	1.80402400	0.28830500
H	0.20175300	1.30510800	1.52114700
C	-0.57607600	1.09464900	-0.51708200
H	-1.36991900	1.80403700	-0.28823500
H	-0.20178000	1.30518300	-1.52110200
N	-1.08695200	-0.29443000	-0.44914900
C	-2.36847300	-0.48274100	0.23095800
H	-3.15195200	0.04671900	-0.31188600
H	-2.61276100	-1.54272600	0.23196000
H	-2.35218100	-0.13366600	1.27338500

CAAC singlet

N	-0.64861500	0.90511900	0.04811300
C	0.59902800	1.28088100	0.08315400
C	0.44778200	-1.12521400	-0.38583200
H	0.52303200	-1.37880400	-1.44420100
H	0.64752200	-2.03763100	0.17653000
C	1.44244900	0.02170800	-0.04238700
C	-1.74666000	1.85888100	0.17533200
H	-2.36422600	1.86487300	-0.72347900
H	-2.38031800	1.61239400	1.02837100
H	-1.31006400	2.84104700	0.32062700
C	2.49819700	0.21124100	-1.13935900
H	3.15843500	1.04291300	-0.89416800
H	3.10338000	-0.69203900	-1.25098100
H	2.03329700	0.42810100	-2.10267600
C	2.15189300	-0.20344100	1.30589300
H	2.78942900	-1.08908700	1.25344400
H	2.77337600	0.65594800	1.55666500
H	1.44144800	-0.34703100	2.12126200
C	-0.95787200	-0.57256700	-0.08449700
C	-1.94155200	-0.82732400	-1.22953300
H	-2.04243700	-1.90117200	-1.39359700
H	-2.93630400	-0.43624200	-1.01192500
H	-1.58711000	-0.37676000	-2.15736500
C	-1.53590500	-1.10599700	1.23294100
H	-2.48799900	-0.63310800	1.47683900
H	-1.71567500	-2.17887700	1.15110400
H	-0.84964200	-0.93936000	2.06248800

CAAC triplet

N	-1.38847600	-0.17891100	-0.34478600
C	-0.23653300	-0.92432600	-0.15621400
C	0.45191800	1.28453100	-0.27955700
H	0.96336900	2.05130800	0.30210400
H	0.57157100	1.52002400	-1.33736700
C	1.03360900	-0.14433800	-0.00130700
C	-2.66785700	-0.70180600	0.08511500
H	-2.74821900	-0.76236600	1.18120900
H	-3.46844500	-0.06310600	-0.28918100
H	-2.80766300	-1.70147700	-0.32383500
C	1.61083300	-0.23964700	1.42611500
H	1.88120100	-1.26981600	1.66076500
H	2.50850600	0.37758200	1.52229600
H	0.88576700	0.09029100	2.17067500
C	2.11893800	-0.52609300	-1.01761300
H	2.98034500	0.14172900	-0.93668400
H	2.46926600	-1.54434900	-0.84170300
H	1.73468500	-0.47381300	-2.03617700
C	-1.04187600	1.19126000	0.05812900
H	-1.21423000	1.33130200	1.13544900
H	-1.65101600	1.91759100	-0.48206000

1.5 Acknowledgements

Thanks are due Glen P. Junor for chemical computation assistance to which the data presented is adapted from unpublished results. Permission for the use of this data was obtained from Glen P. Junor.

1.6 References

[1] G. N. Lewis, *J. Am. Chem. Soc.*, 1916, **38**, 762-785.

[2] S. Shaik, D. Danovich, W. Wu, P. F. Su, H. S. Rzepa and P. C. Hiberty, *Nat. Chem.*, 2012, **4**, 195-200.

[3] D. W. O. de Sousa and M. A. C. Nascimento, *J. Chem. Theory Comput.*, 2016, **12**, 2234-2241.

[4] S. Shaik, D. Danovich, B. Braida and P. C. Hiberty, *Chem. Eur. J.*, 2016, **22**, 18977-18980.

[5] S. Shaik, D. Danovich, B. Braida and P. C. Hiberty, *Chem. Eur. J.*, 2016, **22**, 4116-4128.

[6] M. Piris, X. Lopez and J. M. Ugalde, *Chem. Eur. J.*, 2016, **22**, 4109-4115.

[7] G. Frenking and M. Hermann, *Chem. Eur. J.*, 2016, **22**, 18975-18976.

[8] M. Hermann and G. Frenking, *Chem. Eur. J.*, 2016, **22**, 4100-4108.

[9] W. L. Zou and D. Cremer, *Chem. Eur. J.*, 2016, **22**, 4087-4099.

[10] M. Gomberg, *J. Am. Chem. Soc.*, 1900, **22**, 757-771.

[11] E. Herbst and E. F. van Dishoeck, *Annu. Rev. Astron. Ast.*, 2009, **47**, 427-480.

[12] A. P. C. Mann and D. A. Williams, *Nature*, 1980, **283**, 721-725.

[13] M. N. Hopkinson, C. Richter, M. Schedler and F. Glorius, *Nature*, 2014, **510**, 485-496.

[14] D. Bourissou, O. Guerret, F. P. Gabbai and G. Bertrand, *Chem. Rev.*, 2000, **100**, 39-91.

[15] F. Glorius, *N-Heterocyclic Carbenes in Transisiton Metal Catalysis*, Springer, New York, 2007.

[16] S. P. Nolan, *N-Heterocyclic Carbenes in Synthesis*, John Wiley & Sons, Hoboken, NJ, 2006.

[17] F. Z. Dorwald, *Metal Carbenes in Organic Synthesis*, John Wiley & Sons, Hoboken, NJ, 2008.

[18] J. Hine, *Divalent Carbon*, Ronald Press, New York, 1964.

[19] S. Diez-Gonzalez, *N-Heterocyclic Carbenes: From Labratory Curiosities to Effecient Synthetic Tools*, The Royal Society of Chemistry, Cambridge, UK, 2016.

[20] O. S. Mills and A. D. Redhouse, *Chem. Commun.*, 1966, 444-445.

[21] O. S. Mills and A. D. Redhouse, *J. Chem. Soc.*, 1968, 1282-1292.

[22] P. Jensen and P. R. Bunker, *J. Chem. Phys.*, 1988, **89**, 1327-1332.

[23] J. P. Gu, G. Hirsch, R. J. Buenker, M. Brumm, G. Osmann, P. R. Bunker and P. Jensen, *J. Mol. Struct.*, 2000, **517**, 247-264.

[24] I. Shavitt, *Tetrahedron*, 1985, **41**, 1531-1542.

[25] K. Hirai, T. Itoh and H. Tomioka, *Chem. Rev.*, 2009, **109**, 3275-3332.

[26] J. B. Dumas and E. Peligot, *Ann. Chim. Phys.*, 1835, **58**.

[27] J. U. Nef, *Justus Liebigs Ann. Chem.*, 1897, **298**, 202-374.

[28] H. Staudinger and O. Kupfer, *Ber. Bunsen-Ges. Chem. Ges.*, 1912, **45**, 501-509.

[29] W. von E. Doering and A. K. Hoffmann, *J. Am. Chem. Soc.*, 1954, **76**, 6162-6165.

[30] H. W. Wanzlick, *Angew. Chem. Int. Ed. Engl.*, 1962, **1**, 75-80.

[31] H. W. Wanzlick and E. Schikora, *Angew. Chem.*, 1960, **72**, 494-494.

[32] L. Tschugajeff, M. Grigorjewa and A. Posnjak, *Z. Anorg. Allg. Chem.*, 1925, **148**, 37-42.

[33] A. Burke, A. L. Balch and J. H. Enemark, *J. Am. Chem. Soc.*, 1970, **92**, 2555-2557.

[34] G. Rouschia and B. L. Shaw, *J. Chem. Soc. D, Chem. Commun.*, 1970, 183-183.

[35] D. J. Cardin, B. Cetinkay, M. F. Lappert, L. Manojlov and K. W. Muir, *J. Chem. Soc. D, Chem. Commun.*, 1971, 400-401.

[36] R. R. Schrock, *J. Am. Chem. Soc.*, 1974, **96**, 6796-6797.

[37] A. Igau, H. Grutzmacher, A. Baceiredo and G. Bertrand, *J. Am. Chem. Soc.*, 1988, **110**, 6463-6466.

[38] A. Igau, A. Baceiredo, G. Trinquier and G. Bertrand, *Angew. Chem. Int. Ed. Engl.*, 1989, **28**, 621-622.

[39] A. J. Arduengo III, R. L. Harlow and M. Kline, *J. Am. Chem. Soc.*, 1991, **113**, 361-363.

[40] T. Droge and F. Glorius, *Angew. Chem. Int. Ed. Engl.*, 2010, **49**, 6940-6952.

[41] A. J. Arduengo and G. Bertrand, *Chem. Rev.*, 2009, **109**, 3209-3210.

[42] F. E. Hahn and M. C. Jahnke, *Angew. Chem. Int. Ed.*, 2008, **47**, 3122-3172.

[43] A. V. Zhukhovitskiy, M. J. MacLeod and J. A. Johnson, *Chem. Rev.*, 2015, **115**, 11503-11532.

[44] L. Mercs and M. Albrecht, *Chem. Soc. Rev.*, 2010, **39**, 1903-1912.

[45] S. Diez-Gonzalez, N. Marion and S. P. Nolan, *Chem. Rev.*, 2009, **109**, 3612-3676.

[46] M. Poyatos, J. A. Mata and E. Peris, *Chem. Rev.*, 2009, **109**, 3677-3707.

[47] W. A. Herrmann, M. Elison, J. Fischer, C. Kocher and G. R. J. Artus, *Angew. Chem. Int. Ed. Engl.*, 1995, **34**, 2371-2374.

[48] M. Scholl, T. M. Trnka, J. P. Morgan and R. H. Grubbs, *Tetrahedron Lett.*, 1999, **40**, 2247-2250.

[49] S. Grundemann, A. Kovacevic, M. Albrecht, J. W. Faller and R. H. Crabtree, *J. Am. Chem. Soc.*, 2002, **124**, 10473-10481.

[50] R. W. Alder, P. R. Allen and S. J. Williams, *J. Chem. Soc., Chem. Commun.*, 1995, 1267-1268.

[51] A. M. Magill and B. F. Yates, *Aust. J. Chem.*, 2004, **57**, 1205-1210.

[52] A. Kovacevic, S. Grundemann, J. R. Miecznikowski, E. Clot, O. Eisenstein and R. H. Crabtree, *Chem. Commun.*, 2002, 2580-2581.

[53] O. Schuster, L. Yang, H. G. Raubenheimer and M. Albrecht, *Chem. Rev.*, 2009, **109**, 3445-3478.

[54] P. L. Arnold and S. Pearson, *Coord. Chem. Rev.*, 2007, **251**, 596-609.

[55] S. D. U. Paul and U. Radius, *Eur. J. Inorg. Chem.*, 2017, 3362-3375.

[56] E. Aldeco-Perez, A. J. Rosenthal, B. Donnadieu, P. Parameswaran, G. Frenking and G. Bertrand, *Science*, 2009, **326**, 556-559.

[57] D. Martin, M. Melaimi, M. Soleilhavoup and G. Bertrand, *Organometallics*, 2011, **30**, 5304-5313.

[58] M. Melaimi, M. Soleilhavoup and G. Bertrand, *Angew. Chem. Int. Ed.*, 2010, **49**, 8810-8849.

[59] V. Lavallo, J. Mafhouz, Y. Canac, B. Donnadieu, W. W. Schoeller and G. Bertrand, *J. Am. Chem. Soc.*, 2004, **126**, 8670-8671.

[60] V. Lavallo, Y. Canac, C. Präsang, B. Donnadieu and G. Bertrand, *Angew. Chem. Int. Ed.*, 2005, **44**, 5705-5709.

[61] M. Melaimi, R. Jazzar, M. Soleilhavoup and G. Bertrand, *Angew. Chem. Int. Ed.*, 2017, **56**, 10046-10068.

[62] V. Lavallo, Y. Canac, B. Donnadieu, W. W. Schoeller and G. Bertrand, *Science*, 2006, **312**, 722-724.

[63] R. H. Crabtree, *Coord. Chem. Rev.*, 2013, **257**, 755-766.

[64] Y. Han and H. V. Huynh, *Dalton Trans.*, 2011, **40**, 2141-2147.

[65] A. Schmidt and Z. Guan, *Synthesis*, 2012, **44**, 3251-3268.

[66] J. P. Moerdyk, D. Schilter and C. W. Bielawski, *Acc. Chem. Res.*, 2016, **49**, 1458-1468.

[67] J. P. Moerdyk and C. W. Bielawski, *Chem. Commun.*, 2014, **50**, 4551-4553.

[68] T. W. Hudnall, A. G. Tennyson and C. W. Bielawski, *Organometallics*, 2010, **29**, 4569-4578.

[69] T. W. Hudnall and C. W. Bielawski, *J. Am. Chem. Soc.*, 2009, **131**, 16039-16041.

[70] T. A. Perera, E. W. Reinheimer and T. W. Hudnall, *J. Am. Chem. Soc.*, 2017, **139**, 14807-14814.

[71] D. M. Flanigan, F. Romanov-Michailidis, N. A. White and T. Rovis, *Chem. Rev.*, 2015, **115**, 9307-9387.

[72] A. C. Hillier, W. J. Sommer, B. S. Yong, J. L. Petersen, L. Cavallo and S. P. Nolan, *Organometallics*, 2003, **22**, 4322-4326.

[73] A. Gomez-Suarez, D. J. Nelson and S. P. Nolan, *Chem. Commun.*, 2017, **53**, 2650-2660.

[74] A. Poater, B. Cosenza, A. Correa, S. Giudice, F. Ragone, V. Scarano and L. Cavallo, *Eur. J. Inorg. Chem.*, 2009, 1759-1766.

[75] M. M. D. Roy, P. A. Lummis, M. J. Ferguson, R. McDonald and E. Rivard, *Chem. Eur. J.*, 2017, **23**, 11249-11252.

[76] L. Falivene, R. Credendino, A. Poater, A. Petta, L. Serra, R. Oliva, V. Scarano and L. Cavallo, *Organometallics*, 2016, **35**, 2286-2293.

[77] C. A. Tolman, *Chem. Rev.*, 1977, **77**, 313-348.

[78] R. A. Kelly, H. Clavier, S. Giudice, N. M. Scott, E. D. Stevens, J. Bordner, I. Samardjiev, C. D. Hoff, L. Cavallo and S. P. Nolan, *Organometallics*, 2008, **27**, 202-210.

[79] S. Wolf and H. Plenio, *J. Organomet. Chem.*, 2009, **694**, 1487-1492.

[80] D. G. Gusev, *Organometallics*, 2009, **28**, 6458-6461.

[81] D. J. Nelson and S. P. Nolan, *Chem. Soc. Rev.*, 2013, **42**, 6723-6753.

[82] S. Fantasia, J. L. Petersen, H. Jacobsen, L. Cavallo and S. P. Nolan, *Organometallics*, 2007, **26**, 5880-5889.

[83] T. J. Venanzi, *J. Chem. Educ.*, 1982, **59**, 144-148.

[84] D. Enders, K. Breuer, G. Raabe, J. Runsink, J. H. Teles, J. P. Melder, K. Ebel and S. Brode, *Angew. Chem. Int. Ed. Engl.*, 1995, **34**, 1021-1023.

[85] A. El-Hellani, J. Monot, S. Tang, R. Guillot, C. Bour and V. Gandon, *Inorg. Chem.*, 2013, **52**, 11493-11502.

[86] O. Back, M. Henry-Ellinger, C. D. Martin, D. Martin and G. Bertrand, *Angew. Chem. Int. Ed.*, 2013, **52**, 2939-2943.

[87] R. R. Rodrigues, C. L. Dorsey, C. A. Arceneaux and T. W. Hudnall, *Chem. Commun.*, 2014, **50**, 162-164.

[88] A. Liske, K. Verlinden, H. Buhl, K. Schaper and C. Ganter, *Organometallics*, 2013, **32**, 5269-5272.

[89] S. V. C. Vummaleti, D. J. Nelson, A. Poater, A. Gomez-Suarez, D. B. Cordes, A. M. Z. Slawin, S. P. Nolan and L. Cavallo, *Chem. Sci.*, 2015, **6**, 1895-1904.

[90] T. Schulz, D. Weismann, L. Wallbaum, R. Guthardt, C. Thie, M. Leibold, C. Bruhn and U. Siemeling, *Chem. Eur. J.*, 2015, **21**, 14107-14121.

[91] K. Verlinden, H. Buhl, W. Frank and C. Ganter, *Eur. J. Inorg. Chem.*, 2015, 2416-2425.

[92] B. Rao, H. R. Tang, X. M. Zeng, L. Liu, M. Melaimi and G. Bertrand, *Angew. Chem. Int. Ed.*, 2015, **54**, 14915-14919.

[93] Z. R. McCarty, D. N. Lastovickova and C. W. Bielawski, *Chem. Commun.*, 2016.

[94] M. J. Frisch, G. W. Trucks, H. B. Schlegel, G. E. Scuseria, M. A. Robb, J. R. Cheeseman, G. Scalmani, V. Barone, B. Mennucci, G. A. Petersson, H. Nakatsuji, M. Caricato, X. Li, H. P. Hratchian, A. F. Izmaylov, J. Bloino, G. Zheng, J. L. Sonnenberg, M. Hada, M. Ehara, K. Toyota, R. Fukuda, J. Hasegawa, M. Ishida, T. Nakajima, Y. Honda, O. Kitao, H. Nakai, T. Vreven, J. A. Montgomery, J. E. Peralta, F. Ogliaro, M. Bearpark, J. J. Heyd, E. Brothers, K. N. Kudin, V. N. Staroverov, R. Kobayashi, J. Normand, K. Raghavachari, A. Rendell, J. C. Burant, S. S. Iyengar, J. Tomasi, M. Cossi, N. Rega, J. M. Millam, M. Klene, J. E. Knox, J. B. Cross, V. Bakken, C. Adamo, J. Jaramillo, R. Gomperts, R. E. Stratmann, O. Yazyev, A. J. Austin, R. Cammi, C. Pomelli, J. W. Ochterski, R. L. Martin, K. Morokuma, V. G. Zakrzewski, G. A. Voth, P. Salvador, J. J. Dannenberg, S. Dapprich, A. D. Daniels, Farkas, J. B. Foresman, J. V. Ortiz, J. Cioslowski and D. J. Fox, Wallingford CT, 2009.

[95] F. Weigend, *Phys. Chem. Chem. Phys.*, 2006, **8**, 1057-1065.

[96] F. Weigend and R. Ahlrichs, *Phys. Chem. Chem. Phys.*, 2005, **7**, 3297-3305.

Chapter 2 : Exploring the Reactivity of White Phosphorus with Electrophilic Carbenes

2.1 Introduction

2.1.1 Elemental Phosphorus: Production and Uses

Phosphorus is predominantly found in its elemental form as one of its three allotropes: black, red, and white phosphorus. The most thermodynamically favorable form is black phosphorus, which exists as a polymeric network of cyclo-P_6 units.[1] Red phosphorus is also a network solid, however its lower thermodynamic stability can be attributed to its amorphous nature. Due to the large ring strain of the tetrahedral molecule, white phosphorus (P_4) is the least thermodynamically stable, and therefore presents the most interesting reactivity of the three allotropes.

P_4 is produced on an industrial scale from the reaction of phosphate rock (worldwide production 223 million tons in 2015)[2] with metallurgical-grade coke and silica at temperatures between 1200 and 1500 ºC, giving CO and $CaSiO_3$ as byproducts (Equation 2.1).[3]

$$2Ca_3(PO_4)_2 + 6SiO_2 + 10C \rightarrow 6CaSiO_3 + 10CO + P_4 \quad (2.1)$$

The high reactive potential of P_4 has not been ignored by the chemical industry as a large portion of organophosphorus compounds can find their "P-atom" source from P_4. Indeed, chlorination, or oxychlorination, of P_4 with Cl_2 gas gives PCl_3 and PCl_5, or $POCl_3$, respectively. Subsequent alkylation with Grignard or alkyl lithium reagents can yield the desired organophosphorus compounds, but this also produces a stoichiometric equivalent of salt waste.[4] Although useful, this process is highly toxic and environmentally combative. It has therefore been a recent goal among synthetic chemists to develop new

ways to activate P_4, which has led to a wealth of reactivity studies ranging from early to late TMs,[5-6] main-group species,[7-8] and nucleophilic carbanions and carboradicals.[9] It is the goal of this chapter, however, to focus on the reactivity of P_4 with carbenes, including results obtained by the author of this thesis.

2.1.2 P_4 Reactivity with Carbenes

Damrauer et al. have investigated the reaction of P_4 with both singlet and triplet CH_2.[10] Calculations at B3LYP/6-311++G(3df,3p)//B3LYP/6- 311++G(3df,3p) level of theory revealed that only the excited state singlet methylene exhibited a likely reaction pathway (Figure 2.1). The first step in the reaction involves the nucleophilic attack of singlet methylene onto a σ* orbital of the P_4 tetrahedron forming **2.A^{Int1}** (ΔG = -46 kcal mol^{-1}). The cyclotriphosphirene (CTP) **2.A^{Int2}** then forms, assisted by the elimination of a zwitterion and formation of a phosphaalkene ($\Delta G^{\ddagger}$ = 9 kcal mol^{-1}, ΔG = -20 kcal mol^{-1}). Finally, rotation about the P-P single bond, followed by an intramolecular [2+2] cycloaddition generates the formal carbene insertion product **2.A** ($\Delta G^{\ddagger}$ = 25 kcal mol^{-1}, ΔG = -24 kcal mol^{-1}). It should be mentioned the Damrauer et al. did look for a viable reaction pathway with methylene in its triplet ground state, however they could only find one likely intermediate **2.B** which exists 19 kcal mol^{-1} higher in energy. **2.B** is a diradical species, with an unpaired electron localized on both the carbon atom and the terminal phosphorus of the P_4 butterfly. These calculations help explain why the field of P_4 activation with carbenes has been monopolized by the singlet state with currently no reports of triplet carbenes reacting with P_4.

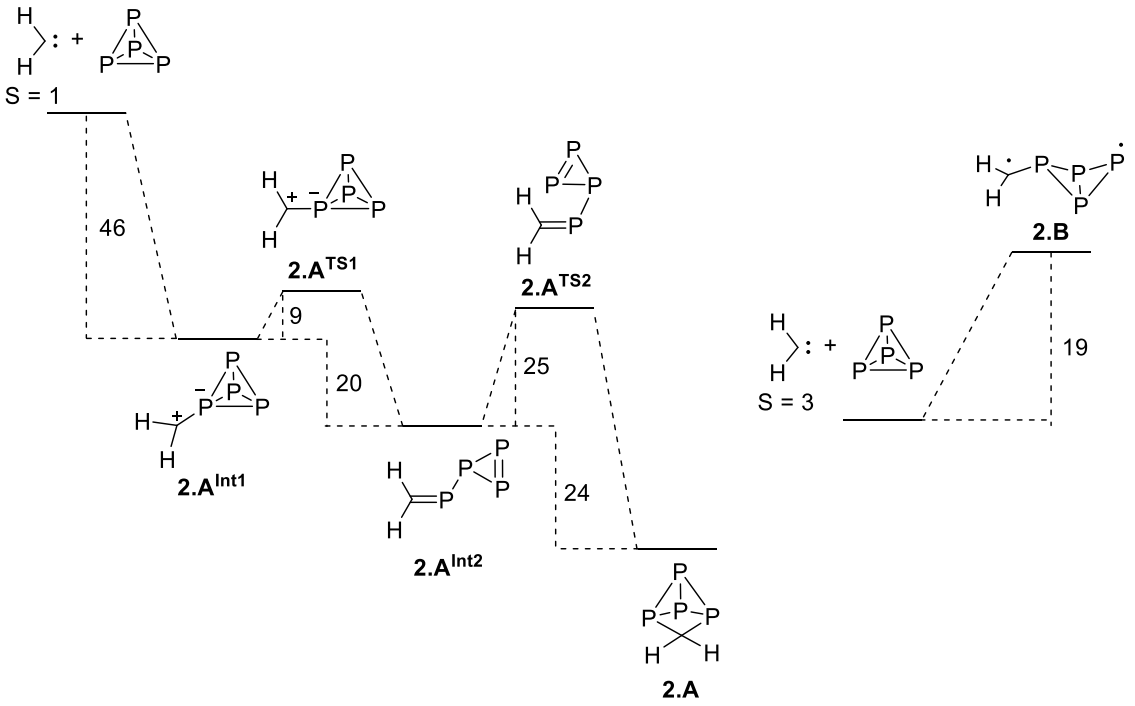

Figure 2.1: Calculated reaction pathway of P_4 with singlet (left) and triplet (right) methylene. Energies given in kcal mol^{-1}.

The first experimental example of a singlet carbene reacting with P_4 was reported in 2008 by Bertrand et al.[11] In this publication, hexanes was added to a mixture of P_4 and a CAAC featuring a bulky menthyl substituent yielding a dark blue solution (Scheme 2.1). ^{31}P NMR and X-ray diffraction studies revealed the product to be the P_4 chain **2.C** as a mixture of (*E*) and (*Z*)-diphosphene isomers in a 9:1 ratio, respectively. The central phosphorus double bond was shown to be reactive towards 2,3-dimethylbutadiene (DMB) yielding the [4+2] cycloaddition product **2.D**. Calculations predicted the first intermediate in this reaction to be a CTP, mimicking **2.A^{Int1}**. Indeed, trapping experiments with DMB yielded **2.E**, confirming the existence of the CTP intermediate.

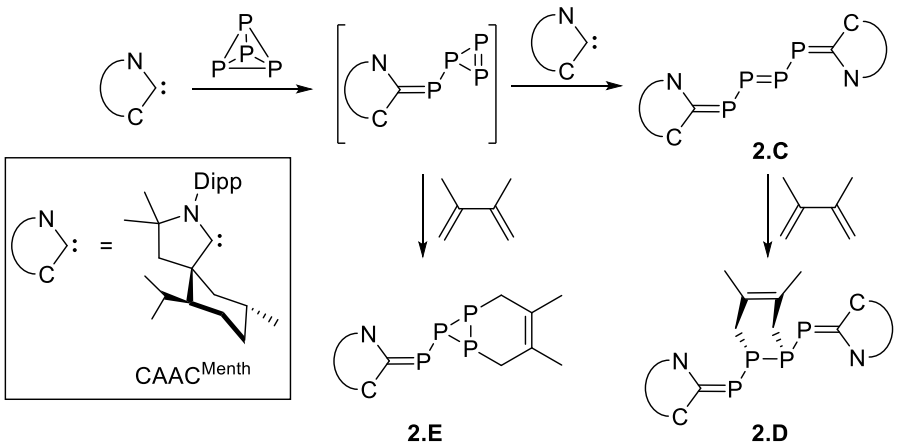

Scheme 2.1: Carbene activation of white phosphorus giving a linear P_4 chain **2.C** and subsequent derivatization.

The stability of the P_4 chain has been shown to be highly sensitive to kinetic protection. For example, when a CAAC with a cyclohexyl substituent was used instead of the menthyl version, vastly different functionalization of P_4 was observed (Scheme 2.2).[12] An ether solution of $CAAC^{Cy}$ and P_4 yielded both **2.F** and **2.G**, which are formed from the additional attack of CAAC onto both the γ-phosphorus of the CTP intermediate or onto the β-phosphorus of the analogous P_4 chain, respectively. The latter represented the first example of P_4 fragmentation with a neutral organic species. The same publication presented more evidence for the existence of an intermediate like $\mathbf{2.A^{Int2}}$ as the reaction of an AAAC with P_4 yielded compound **2.H** in which one equivalent of AAAC underwent a cyclopropanation with the two γ-phosphorus atoms of the CTP. Finally, direct fragmentation of the CTP intermediate could be achieved when the sterically unhindered BAC was reacted with P_4. In this case, the bis(carbene) P_1 cation **2.I** was isolated, likely resulting from the attack of another carbene onto the α-phosphorus of the CTP intermediate. The fate of the resulting P_3^- anion was never resolved, however an anion exchange with Cl^- allowed for X-ray confirmation of the P_1 moiety in **2.I.**

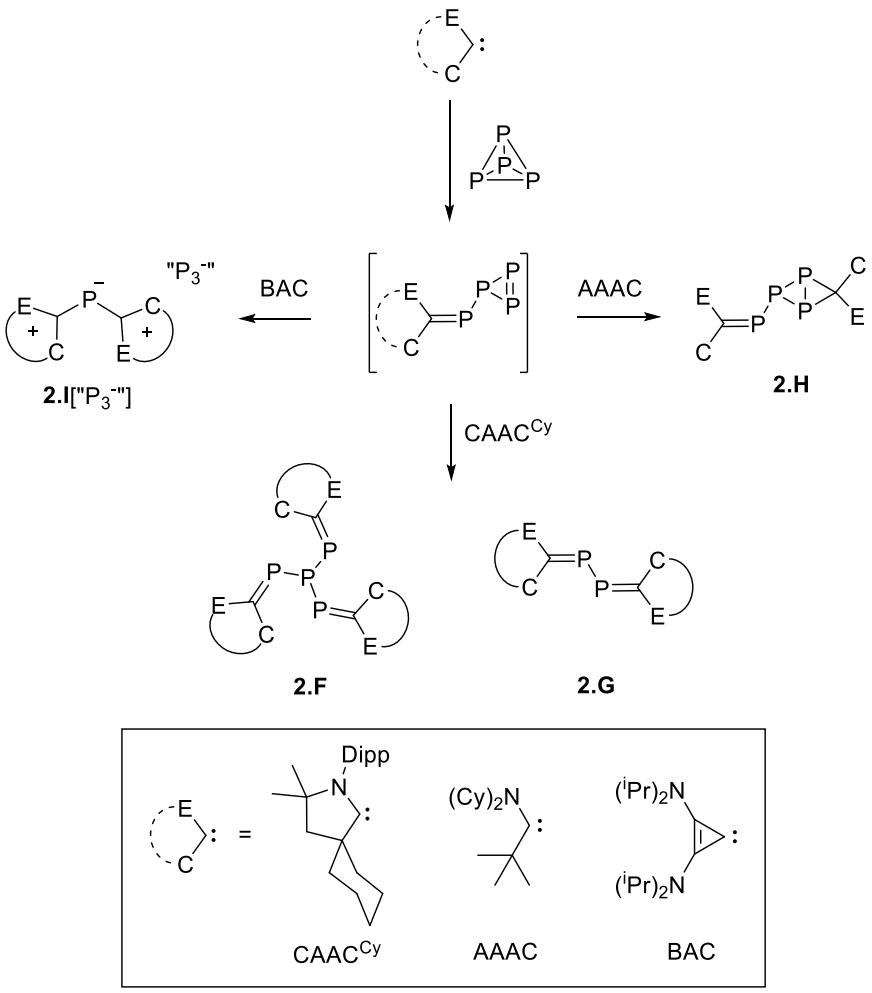

Scheme 2.2: Carbene activation of P_4 yielding trapped intermediate **2.H**, tris(carbene) P_4 adduct **2.F**, and bis(carbene) P_1 and P_2 species, **2.I** and **2.G**, respectively.

When P_4 functionalization was attempted with an NHC, none of the previous phosphorus containing isomers were isolated, and instead the P_{12} species **2.J** was formed (Scheme 2.3).[13] It was proposed that the first step of this reaction involves the formation of the analogous NHC stabilized P_4 chain, and by extension the CTP intermediate. Due to the decreased steric hindrance about the central P-P double bond, a [3+2] cycloaddition can occur. Since NHCs are less nucleophilic and electrophilic than CAACs (see Chapter 1), they are also better leaving groups. Thus a step was proposed which required the loss of two equivalents of NHC. This step fits with the experimental observation that higher temperatures are needed to drive the reaction to completion. From here, only one more equivalent of the NHC

stabilized CTP is required to arrive at the final P_{12} isomer. It should be noted that only the P_4 chain and CTP intermediates were observed through trapping experiments with DMB.

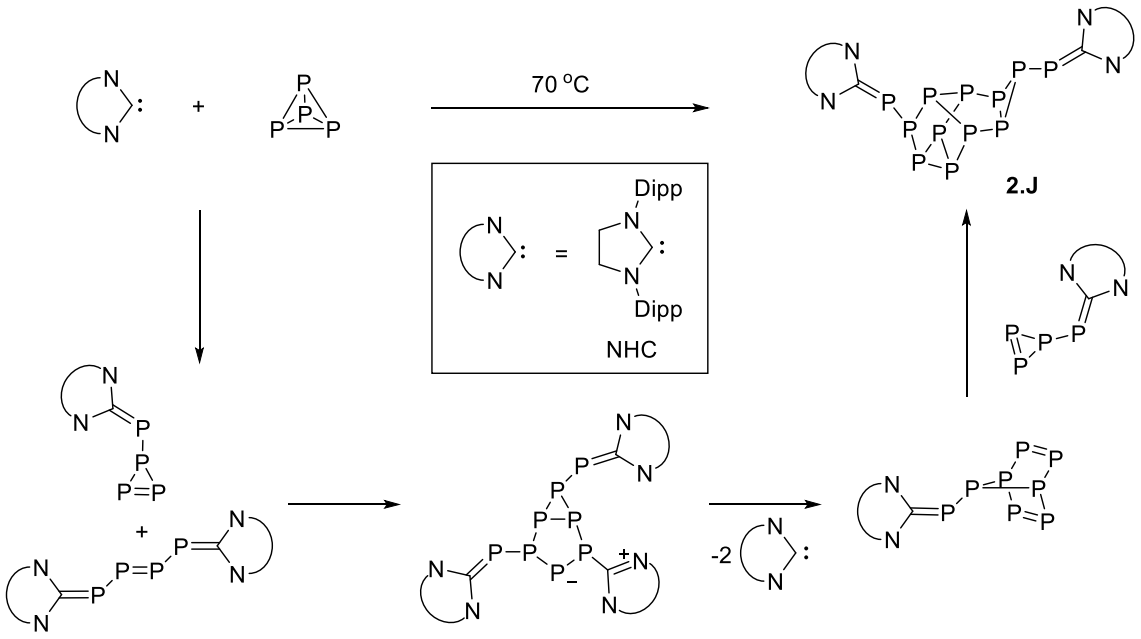

Scheme 2.3: NHC activation of white phosphorus giving P_{12} isomer **2.J** and proposed intermediates.

Grützmacher and Gudat et al. demonstrated that unsaturated NHCs with small steric protection could also yield bis(carbene) P_1 cations through the fragmentation of P_4.[14] Through either *in situ* deprotonation of imidazolium salts **2.Ka**,**b** with KO^{t}Bu in the presence of P_4, or by adding a solution of P_4 to a mixture of the free NHC and ^{t}BuOH, bis(carbene) P_1 cations **2.La**,**b** could be isolated, in addition to the presence of phosphaalkenes **2.Ma**,**b** and other polyphosphorus compounds (Scheme 2.4). The mixture of phosphorus containing products highlights the unselective nature of this reaction. When repeating reaction conditions with imidazolium salts **2.Kc**,**d**, featuring bulkier Mes and Dipp groups, respectively, only phosphaalkenes **2.Mc**,**d** and polyphosphorus compounds could be identified in the reaction mixtures. This was likely due to the increased steric hindrance of the aromatic substituents preventing attack on the α-phosphorus of the CTP intermediate. The authors claimed that the hydrogen atom of phosphaalkenes **2.Ma-d** originated from ^{t}BuOH. They corroborated this hypothesis with deutero exchange experiments,

however they did not report a reaction of pure NHCs with P_4 in the absence of ^{t}BuOH, and thus it homolytic cleavage of a P-P bond followed by H-atom abstraction cannot be excluded.

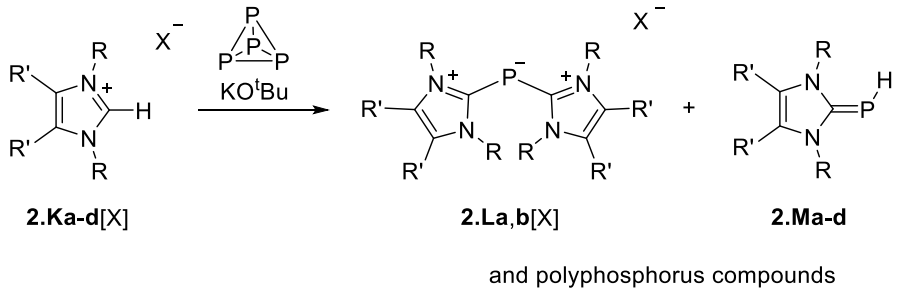

Scheme 2.4: *In situ* reaction of P_4 with imidazolium salts **2.Ka-d**. (**2.Ka**[X]-**2.Ma**: X = I, R = Me, R' = H; **2.Kb**[X]-**2.Mb**: X = I, R = Me, R' = Me; **2.Kc**[X]-**2.Mc**: X = Cl, R = Mes, R' = H; **2.Kd**[X]-**2.Md**: X = Cl, R = Dipp, R' = H).

Finally, Tamm et al. demonstrated that the strong Lewis acid tris(pentafluorophenyl)borane (BCF) could mitigate the unwanted formation of polyphosphorus and secondary fragmentation species.[15] Indeed, the reaction of unsaturated NHC **2.N** with P_4 remarkably yielded the abnormal NHC P_4 butterfly species **2.O** (Scheme 2.5). From calculations, the authors showed that the abnormal coordination mode of **2.O** is 14.3 kcal mol^{-1} more thermodynamically stable than the normal coordination mode **2.O^{Int1}**. Thus, they argue that **2.O** is simply formed from the favorable rearrangement of **2.O^{Int1}**. The most striking feature about **2.O** is not the rearrangement of the carbene however, but is instead the P_4 butterfly. This suggests that when P_4 is activated by carbenes with low π-accepting abilities,[16-20] the phosphaalkene moiety in the CTP intermediate is not formed, and thus the reaction instead proceeds through a butterfly intermediate. This likely explains why activation of P_4 with unsaturated NHCs without the presence of a Lewis acid yield complex mixtures of polyphosphorus compounds, as the terminal phosphorus atom of the P_4 butterfly can act as a nucleophile.

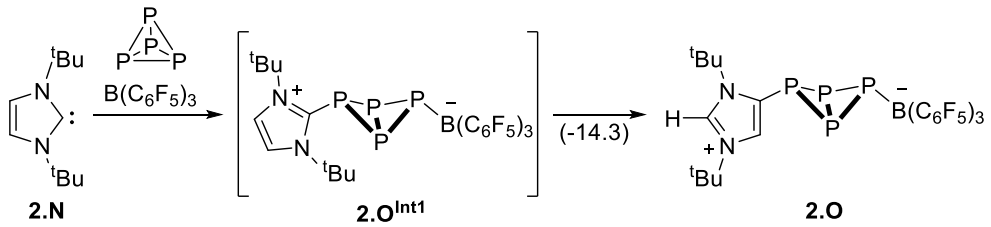

Scheme 2.5: Lewis acid trapped P_4 butterfly **2.O^{Int1}** and subsequent rearrangement product **2.O**. ΔG is given in parenthesis in kcal mol^{-1}.

Upon an analysis of these literature experiments, it is clear that when mildly π-accepting carbenes activate P_4, the CTP intermediate is present. Additionally, P_4 chains similar to **2.C** are also commonly found in reaction mixtures. Such compounds feature a phosphorus-phosphorus double bond that is prone to dimerization in the absence of steric protection.[21] Thus, it was surprising that there were no examples of P_8 clusters derived from the dimerization of either the CTP intermediate or the P_4 chain. In this chapter, the author reports the first examples of white phosphorus activation with carbenes yielding P_8 clusters. Additionally, the isolation of a carbene P_4 adduct, resulting from the insertion into a P-P bond of white phosphorus, is also reported.

2.2 Synthesis of a P_4 Cage, P_8 Clusters and Other Carbene-P_4 Reactivity Studies

We first attempted to facilitate the dimerization of species like **2.A^{Int1}**. It was reasoned that we could prevent the attack of an additional carbene simply by using a large excess of P_4. Unfortunately, all efforts failed, which suggests that the attack of the second carbene to the CTP intermediate is not only faster than the dimerization process, but also faster than the reaction of carbenes with P_4. We therefore hoped that kinetic protection of the CTP intermediate might slow the second attack of a carbene, and allow for the dimerization product to form. As such, P_4 was reacted with one equivalent of NHC **2.1**, which featured exceedingly bulky aromatic substituents and has been shown to successfully kinetically

stabilize other highly reactive phosphorus species (Scheme 2.6).[22-24] Upon addition of THF to the mixture of solids, a green color was immediately formed which quickly dissipated into a yellow solution with a white ppt. The ^{31}P NMR spectrum of the crude mixture exhibited a doublet at -134 ppm ($^{1}J_{P\text{-}H}$ = 150 Hz), which was resolved as a singlet in $^{31}P\{^{1}H\}$ NMR spectrum, clearly implying that phosphaalkene **2.2** was the major product, similar to product **2.Ma-d**

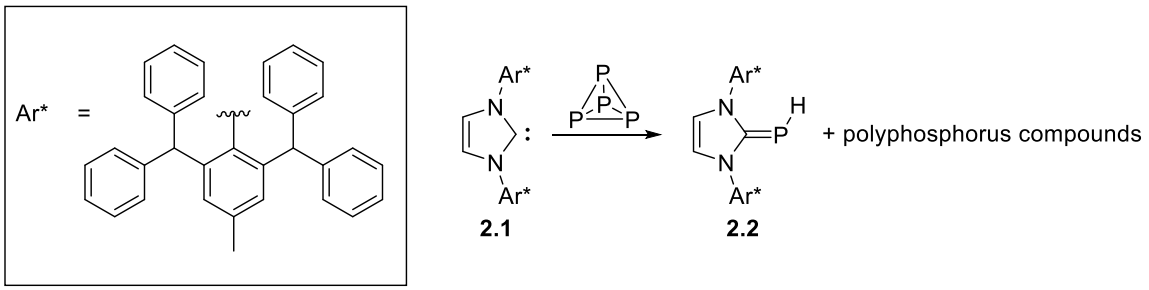

Scheme 2.6: Reaction of a highly sterically encumbering NHC with P_4.

Unable to achieve the desired P_8 cluster through this route, we turned our attention to the dimerization of a species analogous to (*Z*)-**2.C**. Our hypothesis was that the unusual reluctance of **2.C** to dimerize was likely not only due to steric hindrance, but also due to the strong polarization of the PC bond, which makes the central P_4 chain highly electron rich. To favor a P_4 chain with a "regular" phosphorus-phosphorus double bond, a highly π-acidic carbene was necessary. Therefore, the six-membered DAC **2.3** seemed to be a good candidate (Scheme 2.7).[25-26]

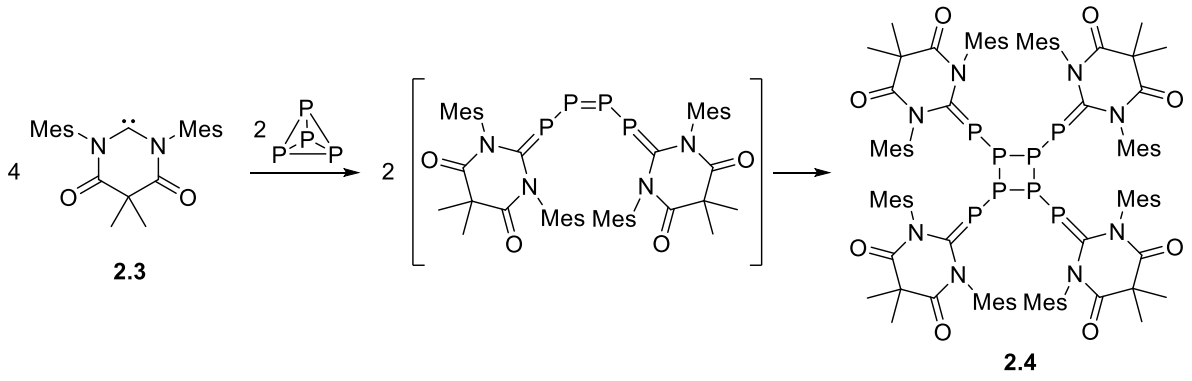

Scheme 2.7: Dimerization of the P_4 chain diphosphene giving the tetra(carbene)P_8 cluster **2.4**.

The addition of a benzene solution of P_4 to a solution of **2.3** in the same solvent produced a deep red color. After removing the solvent *in vacuo*, the solid residue was dissolved in $CDCl_3$, and the $^{31}P\{^1H\}$ NMR spectrum revealed a singlet at -520 ppm (white phosphorus), a doublet and a quartet (δ = 109.7 ppm and -16.1 ppm, respectively; $^1J_{P\text{-}P}$ = 284 Hz) which could be assigned to a compound of type **2.F**,[12] as well as two additional broad signals at δ = 107.9 and -37.9 ppm (Figure 2.2). Washing the solid residue with benzene and hexane, then drying *in vacuo*, afforded the compound corresponding to the broad set of ^{31}P NMR signals.

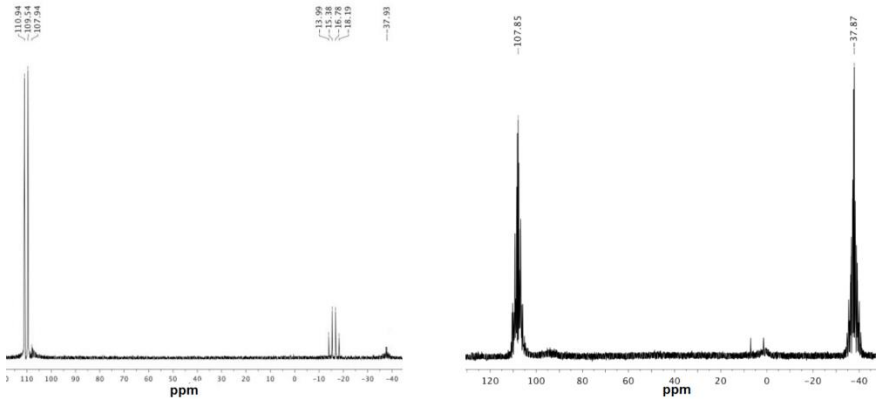

Figure 2.2: $^{31}P\{^1H\}$ NMR spectrum of the crude reaction of **2.3** with P_4 (left) and isolated **2.4** (right).

It should be mentioned that independent of this research, Hudnall et al. concurrently reported that the exact same reaction in Et_2O exclusively yielded a product like **2.F**, confirming what we observed in solution but were not able to isolate.[27]

Single crystals of the compound which exhibited the broad set of $^{31}P\{^1H\}$ NMR signals were obtained by recrystallization from a saturated benzene solution at room temperature, and an X-ray diffraction study revealed the structure of the tetra(carbene)P_8 cluster **2.4** (Figure 2.3). As expected from the dimerization of a compound analogous to (*Z*)-**2.C**, **2.4** features a four-membered phosphorus ring with each of the phosphorus atoms bound to another phosphorus anchored with a carbene.

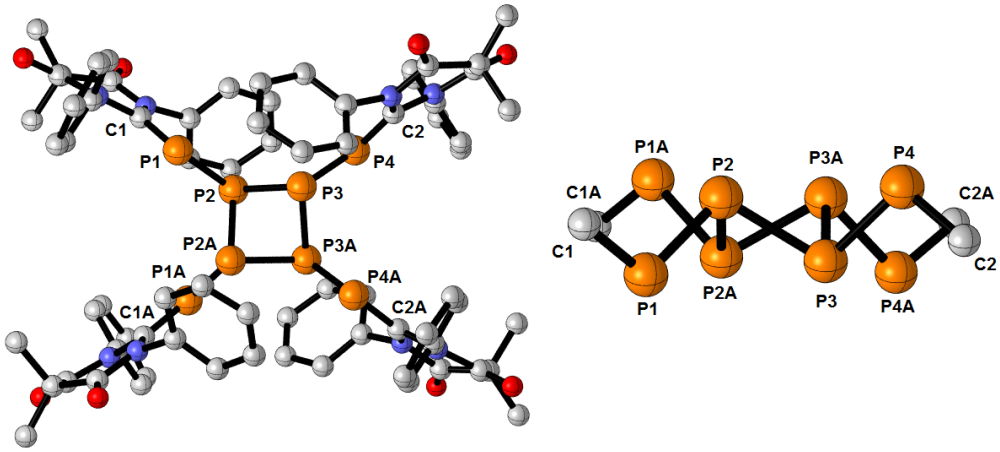

Figure 2.3: Solid state structure of **2.4** viewed from a top-down perspective (left) and along the P_4 ring (right). All hydrogen atoms, solvates, and methyl groups on the phenyl substituents (left) are omitted for clarity.

The central P_4 ring is puckered with each phosphorus assuming a strained trigonal pyramidal geometry. The P-P bond lengths within the central ring are on average 0.0498(2) Å longer than the respective P-P bonds of the central ring to each outer phosphorus atom [P-P 2.259(2) and 2.2092(15) Å, averaged respectively]. The longer internal P-P bonds are likely due to the fact that each of the internal phosphorus bonds result from the linear combination of two sp^3 hybridized orbitals, whereas each of the external phosphorus bonds result from a mix of sp^3 and sp^2 hybridized orbitals. Finally, each of the outer phosphorus atoms features a bent geometry [P-P-C 107.79(14) ° averaged] and short P-C bonds [P-C 1.738(4) Å averaged] as would be expected for a phosphaalkene.

Reconsidering the influence of the stoichiometry on the fate of the reaction of P_4 with carbenes, we reinvestigated the reaction in the case of $CAAC^{Cy}$.[28-29] Indeed, the formation of the corresponding bis(carbene)P_2 adduct **2.G** was observed when the reaction was conducted in Et_2O,[12] a solvent in which P_4 has limited solubility, meaning $CAAC^{Cy}$ was present in a large excess. To determine if the P_8 cluster could also be formed with $CAAC^{Cy}$, the same reaction conditions used for **2.4** were followed (Scheme 2.8). The $^{31}P\{^1H\}$ NMR spectrum of the orange powder obtained after work up showed two second order resonances at δ = +62.1 and -44.5 ppm (Figure 2.4)

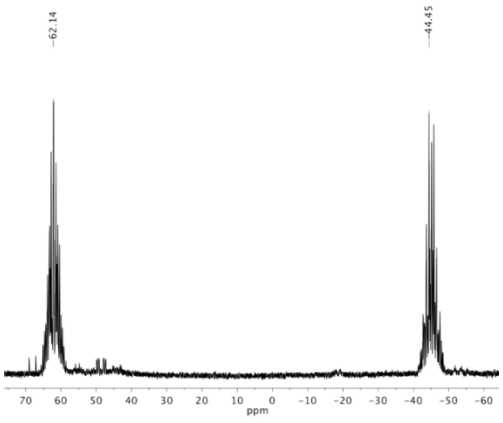

Figure 2.4: $^{31}P\{^{1}H\}$ NMR spectrum of **2.5**.

The signal at low field, assigned to the phosphaalkene moiety, is downfield shifted by 45.5 ppm compared to that of **2.4**, but this is easily rationalized by the higher π-accepting properties of **2.3** versus $CAAC^{Cy}$.[16-18] A solid-state structure from crystals grown by vapor diffusion of hexanes into a saturated benzene solution of the powder confirmed the formation of the P_8 cluster **2.5** (Figure 2.5).

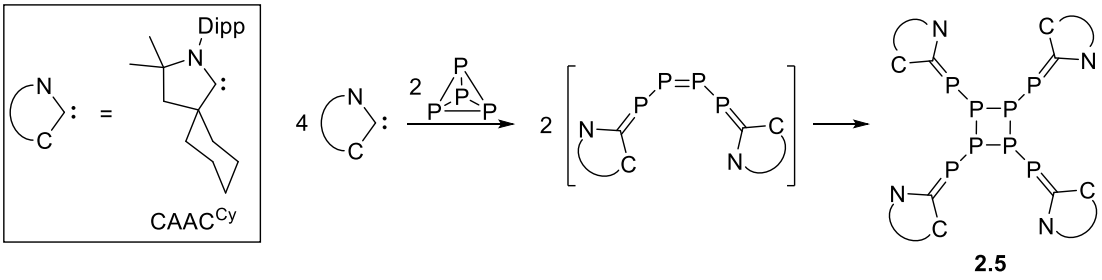

Scheme 2.8: Formation of tetra(carbene) P_8 cluster **2.5**.

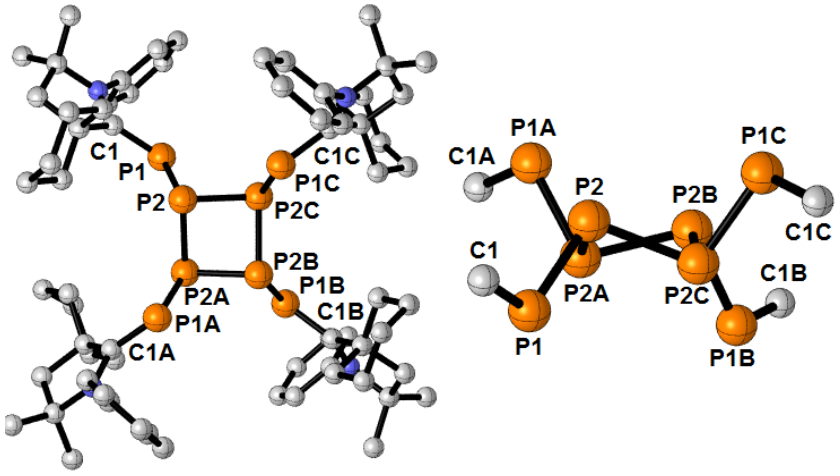

Figure 2.5: Solid state structure of **2.5** viewed from a top-down perspective (left) and along the P_4 ring (right). All hydrogen atoms, solvates, and isopropyl groups on the phenyl substituents (left) are omitted for clarity.

The P_8 cluster **2.5** is isostructural to **2.4** with only minor geometric changes in the P_8 core. The phosphaalkene [P1-C1 1.737(2) Å] and exocyclic phosphorus-phosphorus [P1-P2 2.1982(8)] bonds are essentially identical in length to the analogous bonds in **2.4**. This was a minor surprise as carbene **2.3** is more π-accepting than $CAAC^{Cy}$, and therefore should make stronger phosphaalkene bonds, however it is possible that steric crowding of the cyclic carbon substituents might be inhibiting geometries most favorable for efficient π-overlap. Although still minor, the biggest structural differences between **2.4** and **2.5** come from within the central four-membered phosphorus ring. Indeed, the phosphorus-phosphorus bonds are slightly shorter [P-P 2.2454(1) Å, averaged] and internal angles slightly larger [P2A-P2-P2C 84.855(15) º] than in **2.4**, respectively.

To further generalize the synthesis of P_8 clusters, we investigated the reaction of white phosphorus with the seven-membered DAC **2.6** (Scheme 2.9).[30] Due to the combination of a seven-membered ring, and benzamido functionality, **2.6** was the most electrophilic stable carbene reported at the time these experiments were conducted. The reaction of **2.6** with P_4 in benzene produced a yellow precipitate. To our surprise, the $^{31}P\{^1H\}$ NMR spectrum of the redissolved precipitate did not reveal any peaks indicative of a compound like **2.4**/**2.5**. Instead, an ABX_2 spin system was observed (δ_A = -10.5

ppm, δ_B = -14.5 ppm, δ_X = -325.6 ppm; J_{AX} = 85 Hz, J_{AB} = 19 Hz, J_{BX} = 89 Hz) resembling the reported spectrum for the insertion of a silylene into a single P-P bond of white phosphorus (Figure 2.6).[31]

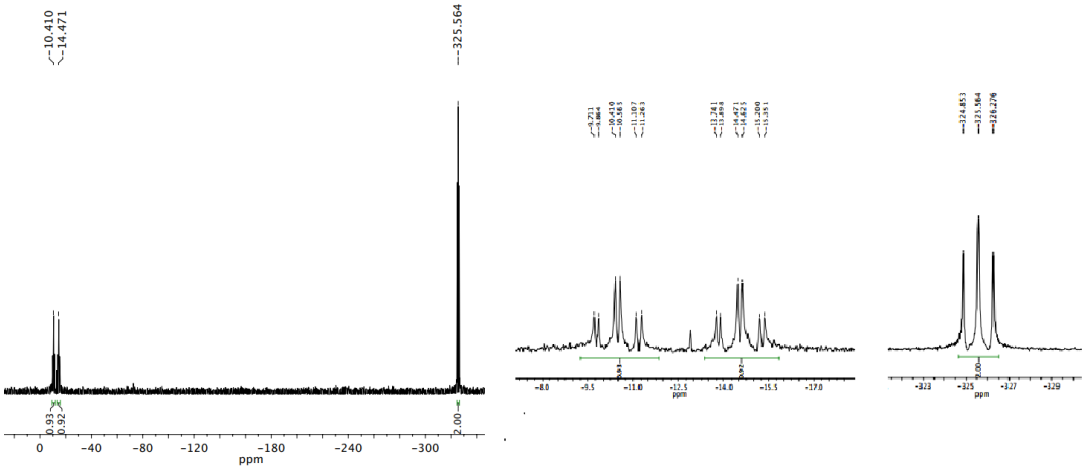

Figure 2.6: $^{31}P\{^1H\}$ NMR spectrum of **2.7** (left) and magnified sections AB (middle) and X_2 (right).

An X-ray diffraction study confirmed the identity of this species as the carbene-P_4 adduct **2.7** (Figure 2.7). Although this type of product is common for reactions of P_4 with TMs and main-group carbenoids,[32-39] the insertion of a carbene into a single P-P bond of white phosphorus had never been observed. The electronic properties of carbene **2.6** are likely similar to the heavier p-block congeners,[40] *i.e.* less nucleophilic and more electrophilic than all carbenes mentioned prior in this chapter, rationalizing the isolation of **2.7**. In fact, the P_4 adduct **2.7** mimics **2.A**, the lowest energy isomer in the reaction of singlet methylene with P_4.[10] Indeed, with weaker electrophilic carbenes, adducts of type **2.7** cannot form and instead follow subsequent reactivity on intermediates like **2.A^{Int1}**, leading to the large variety of organophosphorus compounds mentioned above.

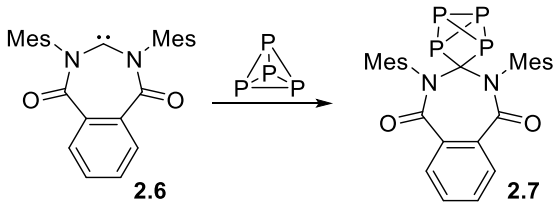

Scheme 2.9: Reaction of P_4 with seven-member DAC **2.6** yielding insertion product **2.7**.

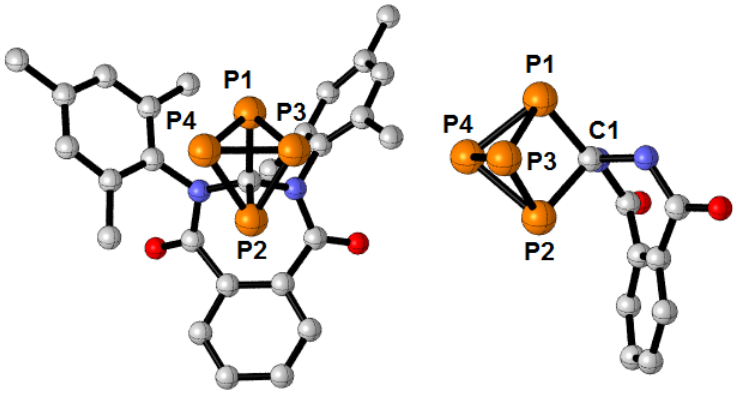

Figure 2.7: Solid state structure of **2.7** viewed from top-down (left) and side-on (right) perspectives. All hydrogen atoms (both) and the Mes groups (right) are omitted for clarity. Selected bond lengths (Å): P1-C1 1.916(3), P2-C1 1.917(3), P1-P4 2.214(1), P1-P3 2.225(1), P2-P3 2.215(1), P2-P4 2.237(1), P3-P4 2.178(1).

As the reactivity of electrophilic carbenes with P_4 was now well understood, we were curious what would happen to white phosphorus in the presence of a strong neutral carbon based donor with relatively no π-accepting ability. Therefore, we chose cyclic bent allene (CBA) **2.8**, which features a central carbone resonance form, as the candidate.[41] When C_6D_6 was added to a mixture of P_4 and **2.8**, the solution immediately turned red and gave a product that was highly insoluble in hexanes and pentane, as would be expected for an ionic species (Scheme 2.10). The ^{31}P NMR spectrum of the precipitate exhibited only one singlet at 144 ppm, not including residual white phosphorus (-526 ppm), which implied that the product contains only one chemically and magnetically independent phosphorus atom. This was surprising because the ^{31}P chemical shift is nearly 237, 263, and 257 ppm downfield shifted from the bis(carbene) P_1 fragments **2.I** and **2.La**, and **2.Lb**, respectively. This shift does not fit for the analogous bis(CBA) P_1 fragment as the central carbon of the CBA has no concernable π-accepting ability, and thus cannot form a phosphaalkene. Nonetheless, the groups of Ong and Chen et al. recently reported that the γ-carbon of bent allenes does have rather unusual π-accepting ability.[42] Therefore, it is possible that the product of this reaction is indeed bis(CBA) P_1 **2.9**[X^-], in which the phosphorus atom is involved in a three-membered phosphorane with one of the CBA units. Unfortunately, all attempts to crystalize this

species failed, and only the decomposition product **2.10** could ever be retrieved as X-ray quality crystals from this reaction, suggesting that other complicated pathways might be involved (Figure 2.8)**.**

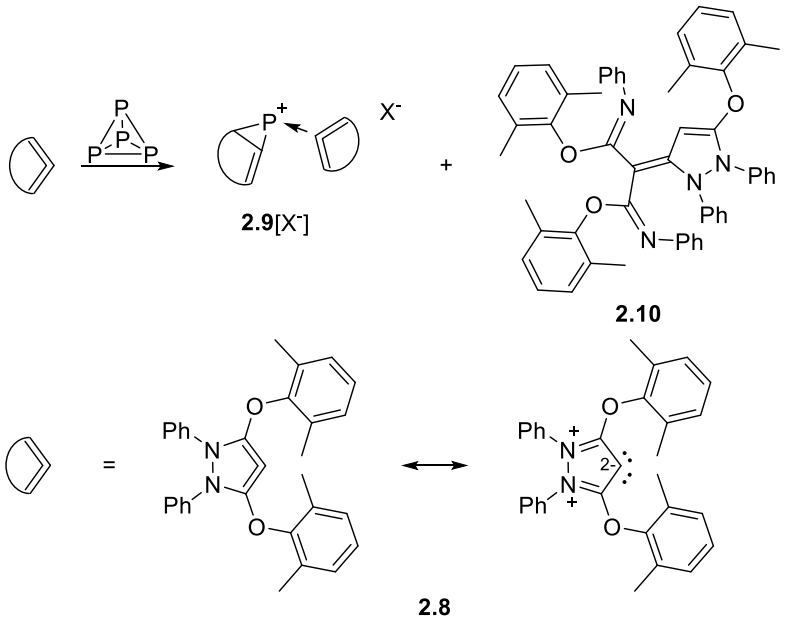

Scheme 2.10: Reaction of CBA **2.8** with P_4 yielding proposed **2.9**[X^-] and **2.10**.

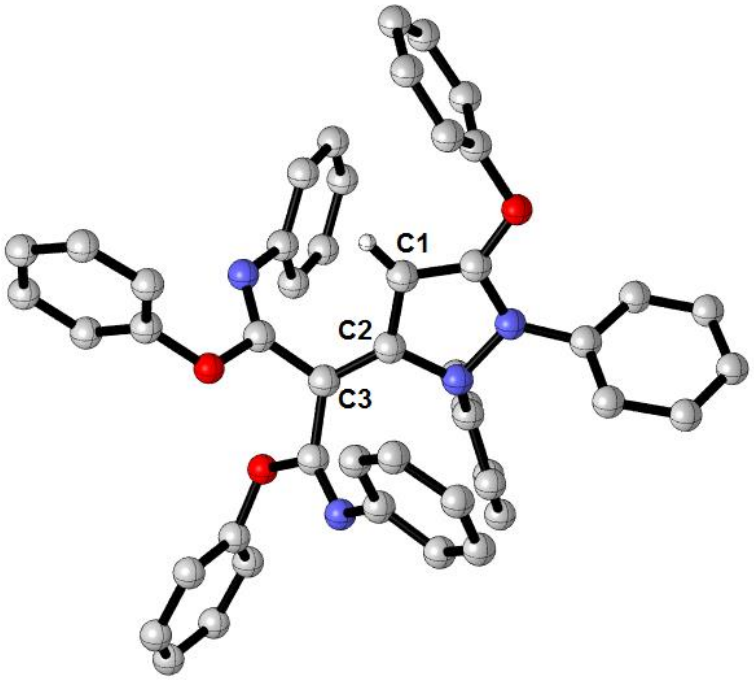

Figure 2.8: X-ray structure of decomposition product **2.10**. Methyl groups and all hydrogen atoms, except on C1, removed for clarity. Selected bond lengths (Å): C1-C2 1.415(3), C2-C3 1.397(3).

2.3 Conclusion

In summary, we have demonstrated that by utilizing an electrophilic six-membered DAC, a donor stabilized P_8 allotrope can be prepared from white phosphorus. This P_8 cluster could also be prepared with the less electrophilic cyclic (alkyl)(amino)carbene if P_4 is in excess, suggesting that the outcome of the reactions with white phosphorus could be influenced by stoichiometry. In addition, the reaction of white phosphorus with the extremely electrophilic seven-membered benzamido carbene led to the isolation of a carbene-P_4 adduct. The latter compound represents the missing link of the reaction of singlet methylene with P_4. In general, these observations expand the understanding of the fundamental processes in the activation of white phosphorus. Furthermore, given these unique findings, the highly electrophilic nature of both six- and seven-membered DACs should be further investigated.

2.4 Experimental

2.4.1 General Considerations

All manipulations were performed using standard glovebox and Schlenk techniques. Glassware was dried in an oven overnight at 150 ºC. Toluene, benzene and hexanes were freshly distilled over Na metal. $CDCl_3$ used for ^1H NMR spectroscopy was purchased from Cambridge Isotope Laboratories and dried over CaH_2. The carbenes **2.1**, **2.3**, **2.6**, and $CAAC^{Cy}$ were prepared via literature procedures.[26, 28-30, 43-44] White phosphorus was sublimed and stored in Argon in the dark prior to use. CAUTION: P_4 is extremely pyrophoric and the proper safety procedure should be followed when handling.

Multinuclear NMR data were recorded on a Varian INOVA 500MHz or JEOL 500 MHz spectrometers. NMR signals are listed in ppm, relative to residual solvent signals, and were taken at room temperature. Coupling constants are in Hertz (Hz). NMR multiplicities are abbreviated as follows: s = singlet, d = doublet, t = triplet, sept = septet, m = multiplet, br = broad.

Melting points were measured with an electrothermal MEL-TEMP apparatus. When reported, pure crystals of each compound were added to a capillary tube which was then sealed from air with vacuum grease.

High resolution mass spectrometry (HRMS) data was collected on an Agilent 6230 TOF-MS.

Single crystal X-Ray diffraction data were collected on a Bruker Apex II-CCD detector using either Mo-K_α radiation (λ = 0.71073 Å). Crystals were selected under oil, mounted on nylon loops then immediately placed in a cold stream of N_2. Structures were solved and refined using SHELXTL and Olex2 software.[45] All hydrogen atoms were included in the refinement in calculated positions depending on the connecting carbon atoms. Visualized structures were generated with CYLview.

2.4.2 Synthetic Procedures

2.2: THF (5 mL) was added to a vial containing carbene **2.1** (100 mg, 1 eq) and P_4 (14 mg, 1 eq) in the glovebox. The mixture was stirred for 12 hrs giving a yellow color. The crude solution was checked

by NMR without any further purification. **^{31}P NMR** (121 MHz, THF) -134 (d, $^{1}J_{P\text{-}H}$ = 150 Hz), -526 (s, P_4). **^{31}P{^{1}H} NMR** -134 (s), -526 (s, P_4). No other experimental data was recorded.

2.4: A solution of **2.3** (0.500 g, 1 eq) in benzene (40 mL) was cannula transferred dropwise to a solution of P_4 in toluene (0.330 g, 2 eq; 20 mL). The colorless solution immediately began acquiring an orange color, which then became red. After stirring for 2 hrs, the solvent was removed *in vacuo*. The solids were washed with benzene (10 mL), then hexanes (2 x 15 mL) and dried *in vacuo* to give a red powder (0.582 g, 66 % yield). Single crystals were grown by slow evaporation of a benzene solution. **MP**: 160-162 ºC. **^{31}P{^{1}H} NMR** (121 MHz, $CDCl_3$) δ = 107.9 (m, 4P), -37.9 (m, 4P). **HRMS**: *m/z* calculated for $C_{96}H_{112}O_8N_8P_8Na$ $(M+Na)^+$ = 1775.6373, found 1775.6396.

2.5: A solution of $CAAC^{Cy}$ (0.500 g, 1 eq) in benzene (40 mL) was cannula transferred to a solution of P_4 in toluene (0.382, 2 eq; 25 mL) in the dark. The colorless solution immediately began acquiring a green color, which then became red. After stirring for 2 hrs, the toluene was removed *in vacuo* to produce an orange powder. The product was extracted with THF and the solvent removed *in vacuo*. The solids were washed with cold pentane (2 x 15 mL) and dried *in vacuo* to give an orange powder (0.351 g, 40 % yield). Single crystals of **2.5** for X-ray diffraction studies were grown by vapor diffusion of hexanes into a saturated benzene solution. **MP:** 204-206 ºC. **^{1}H NMR** (500 MHz, $CDCl_3$) δ = 7.28 (t, *J* = 7.5 Hz, 4H), 7.14 (d, *J* = 7.5 Hz, 8H), 3.03-2.90 (m, 8H), 2.80 (sept, *J* = 7.0 Hz, 16H), 2.01 (s, 8H), 1.55-1.35 (m, 32H), 1.29 (d, *J* = 7.0 Hz, 24H), 1.27-1.13 (m, 8H), 1.18 (d, *J* = 7.0 Hz, 24H). **^{13}C{^{1}H} NMR** (126 MHz, $CDCl_3$) δ = 212.3 (br d, *J* = 84 Hz), 148.1 (d, *J* = 3 Hz), 134.6 (d, *J* = 3 Hz), 128.3, 124.9, 68.2 (d, *J* = 1 Hz), 56.1 (d, *J* = 11 Hz), 50.5, 29.7, 29.0, 27.7, 27.6, 25.1, 24.5, 23.5. **^{31}P{^{1}H} NMR** (121 MHz, $CDCl_3$) δ = 66.4 (m, 4P), -44.5 (m, 4P). **HRMS**: *m/z* calculated for $C_{92}H_{141}N_4P_8$ $(M+H)^+$ 1549.9052, found 1549.9033.

2.7: Carbene **2.6** (0.090 g, 1 eq) was added to an NMR tube with P_4 (0.027 g, 1 eq). C_6D_6 was the added to the mixture of solids. The solution immediately turned a red-orange color. Over time a yellow precipitate formed which was primarily **2.7**. Although we could not obtain a pure bulk sample, the reaction proceeded in >50 % yield. Single crystals of **2.7** for X-ray diffraction studies were grown by

vapor diffusion of hexanes into a saturated $CDCl_3$ solution. **$^{31}P\{^1H\}$ NMR** (121 MHz, $CDCl_3$) δ = -10.5 (td, $^1J_{P\text{-}P}$ = 85 Hz and $^2J_{P\text{-}P}$ = 19 Hz, 1P), -14.5 (td, $^1J_{P\text{-}P}$ = 85 Hz and $^2J_{P\text{-}P}$ = 19 Hz, 1P), -326 (dd, $^1J_{P\text{-}P}$ = 89 Hz and $^2J_{P\text{-}P}$ = 85 Hz, 2P).

2.9: Crude experiment - carbene **2.8** (36 mg, 1 eq) and P_4 (10 mg, 1 eq) were added to an NMR tube with C_6D_6. The solution immediately turned red and was shaken for 10 min. The benzene was removed *in vacuo* and washed with pentane (2 x 5 mL) giving a red, oily solid. The solid was dissolved again in C_6D_6 and an NMR of the crude was taken. **$^{31}P\{^1H\}$ NMR** (121 MHz, C_6D_6) δ = 144 (s), 520 (s, P_4). No other experimental data is reported.

2.10: Orange, X-ray quality crystals were grown from the crude precipitate is **2.9** by a slow evaporation of C_6D_6. No other experimental data was recorded on said crystals.

2.4.3 Crystallographic Data

Compound	**2.4**
Empirical formula	$C_{120}H_{136}N_8O_8P_8$
Formula weight	2066.12
Temperature/K	100(2)
Crystal system	monoclinic
Space group	P2/c
a/Å	12.600(4)
b/Å	16.320(5)
c/Å	26.808(9)
α/°	90
β/°	92.213(11)
γ/°	90
Volume/Å^3	5508(3)
Z	2
ρ_{calc}g/cm^3	1.246
μ/mm^{-1}	0.187
F(000)	2192.0
Crystal size/mm^3	0.210 × 0.110 × 0.100
Radiation	MoKα (λ = 0.71073)
2Θ range for data collection/°	5.846 to 53.562
Index ranges	$-15 \leq h \leq 15$, $0 \leq k \leq 20$, $0 \leq l \leq 33$
Reflections collected	15639
Independent reflections	15639 [R_{int} = 0.0820, R_{sigma} = 0.0988]
Data/restraints/parameters	15639/0/651
Goodness-of-fit on F^2	1.009

Final R indexes [I>=2σ (I)]	R_1 = 0.0625, wR_2 = 0.1524
Final R indexes [all data]	R_1 = 0.1043, wR_2 = 0.1766
Largest diff. peak/hole / e Å^{-3}	0.44/-0.41

Compound	**2.5**
Empirical formula	$C_{98}H_{146}N_4P_8$
Formula weight	1628.0482
Temperature/K	100(2)
Crystal system	orthorhombic
Space group	Fddd
a/Å	12.0923(12)
b/Å	29.578(3)
c/Å	53.934(5)
α/°	90.00
β/°	90.00
γ/°	90.00
Volume/Å^3	19290(3)
Z	8
ρ_{calc}g/cm^3	1.121
μ/mm^{-1}	0.190
F(000)	7056.0
Crystal size/mm^3	0.15 × 0.13 × 0.12
Radiation	MoKα (λ = 0.71073)
2Θ range for data collection/°	6.28 to 52.88
Index ranges	-15 ≤ h ≤ 15, -36 ≤ k ≤ 36, -67 ≤ l ≤ 67
Reflections collected	48349
Independent reflections	4945 [R_{int} = 0.1266, R_{sigma} = N/A]
Data/restraints/parameters	4945/0/249
Goodness-of-fit on F^2	1.008
Final R indexes [I>=2σ (I)]	R_1 = 0.0432, wR_2 = 0.0934
Final R indexes [all data]	R_1 = 0.0756, wR_2 = 0.1067
Largest diff. peak/hole / e Å^{-3}	0.29/-0.28

Compound	**2.7**
Empirical formula	$C_{27}H_{26}N_2O_2P_4$
Formula weight	534.38
Temperature/K	100(2)
Crystal system	hexagonal
Space group	R-3
a/Å	34.4341(10)
b/Å	34.4341(10)
c/Å	11.4555(4)
α/°	90.00
β/°	90.00

γ/°	120.00
Volume/Å^3	11763.1(6)
Z	18
ρ_{calc}g/cm^3	1.459
μ/mm^{-1}	0.421
F(000)	5004.0
Crystal size/mm^3	0.18 × 0.15 × 0.13
Radiation	MoKα (λ = 0.71073)
2Θ range for data collection/°	4.74 to 52.74
Index ranges	-42 ≤ h ≤ 43, -42 ≤ k ≤ 42, -14 ≤ l ≤ 14
Reflections collected	38581
Independent reflections	5356 [R_{int} = 0.1185, R_{sigma} = N/A]
Data/restraints/parameters	5356/0/322
Goodness-of-fit on F^2	1.077
Final R indexes [I>=2σ (I)]	R_1 = 0.0645, wR_2 = 0.1355
Final R indexes [all data]	R_1 = 0.1090, wR_2 = 0.1495
Largest diff. peak/hole / e Å^{-3}	0.57/-0.37

Compound	**2.10**
Empirical formula	$C_{54}H_{49}N_4O_3$
Formula weight	801.97
Temperature/K	296.15
Crystal system	monoclinic
Space group	$P2_1/n$
a/Å	11.899(3)
b/Å	18.769(4)
c/Å	20.324(4)
α/°	90
β/°	100.772(11)
γ/°	90
Volume/Å^3	4459.1(16)
Z	4
ρ_{calc}g/cm^3	1.195
μ/mm^{-1}	0.074
F(000)	1700.0
Crystal size/mm^3	0.3 × 0.2 × 0.2
Radiation	MoKα (λ = 0.71073)
2Θ range for data collection/°	2.978 to 48.862
Index ranges	-13 ≤ h ≤ 13, -21 ≤ k ≤ 20, -23 ≤ l ≤ 23
Reflections collected	24699
Independent reflections	7286 [R_{int} = 0.0674, R_{sigma} = 0.0729]
Data/restraints/parameters	7286/0/556
Goodness-of-fit on F^2	1.018
Final R indexes [I>=2σ (I)]	R_1 = 0.0566, wR_2 = 0.1445

Final R indexes [all data] $R_1 = 0.0835$, $wR_2 = 0.1644$
Largest diff. peak/hole / e $Å^{-3}$ 0.62/-0.49

2.5 Acknowledgments

Chapter 2 is adapted, in part, from Caleb D. Martin, Cory M. Weinstein, Curtis E. Moore, Arnold L. Rheingold, and Guy Bertrand "Exploring the reactivity of white phosphorus with electrophilic carbenes: synthesis of a P_4 cage and P_8 clusters," *Chemical Communications*, 2013, **49**, 4486-4488. Copyright 2013 the Royal Society of Chemistry. Permission to use copyrighted images and data was obtained from Caleb D. Martin, Curtis E. Moore, Arnold L. Rheingold, Guy Bertrand and the Royal Society of Chemistry. The dissertation author was the second author of the manuscript.

2.6 References

[1] A. Brown and S. Rundqvist, *Acta Cryst.*, 1965, **19**, 684-685.

[2] S. M. Jasinski, *U. S. Geological Survey, Mineral Commodity Summaries*, 2016.

[3] W. Gleason, *JOM*, 2007, **59**, 17-19.

[4] D. E. C. Corbridge, *Phosphorus 2000: Chemistry, Biochemistry & Technology*, Elsevier, Amsterdam; New York, 2000.

[5] B. M. Cossairt, N. A. Piro and C. C. Cummins, *Chem. Rev.*, 2010, **110**, 4164-4177.

[6] M. Caporali, L. Gonsalvi, A. Rossin and M. Peruzzini, *Chem. Rev.*, 2010, **110**, 4178-4235.

[7] N. A. Giffin and J. D. Masuda, *Coord. Chem. Rev.*, 2011, **255**, 1342-1359.

[8] M. Scheer, G. Balazs and A. Seitz, *Chem. Rev.*, 2010, **110**, 4236-4256.

[9] J. E. Borger, A. W. Ehlers, J. C. Slootweg and K. Lammertsma, *Chem. Eur. J.*, 2017, **23**, 11738-11746.

[10] R. Damrauer, S. E. Pusede and G. A. Staton, *Organometallics*, 2008, **27**, 3399-3402.

[11] J. D. Masuda, W. W. Schoeller, B. Donnadieu and G. Bertrand, *Angew. Chem. Int. Ed.*, 2007, **46**, 7052-7055.

[12] O. Back, G. Kuchenbeiser, B. Donnadieu and G. Bertrand, *Angew. Chem. Int. Ed.*, 2009, **48**, 5530-5533.

[13] J. D. Masuda, W. W. Schoeller, B. Donnadieu and G. Bertrand, *J. Am. Chem. Soc.*, 2007, **129**, 14180-14181.

[14] M. Cicac-Hudi, J. Bender, S. H. Schlindwein, M. Bispinghoff, M. Nieger, H. Grutzmacher and D. Gudat, *Eur. J. Inorg. Chem.*, 2016, 649-658.

[15] D. Holschumacher, T. Bannenberg, K. Ibrom, C. G. Daniliuc, P. G. Jones and M. Tamm, *Dalton Trans.*, 2010, **39**, 10590-10592.

[16] O. Back, M. Henry-Ellinger, C. D. Martin, D. Martin and G. Bertrand, *Angew. Chem. Int. Ed.*, 2013, **52**, 2939-2943.

[17] A. Liske, K. Verlinden, H. Buhl, K. Schaper and C. Ganter, *Organometallics*, 2013, **32**, 5269-5272.

[18] R. R. Rodrigues, C. L. Dorsey, C. A. Arceneaux and T. W. Hudnall, *Chem. Commun.*, 2014, **50**, 162-164.

[19] S. V. C. Vummaleti, D. J. Nelson, A. Poater, A. Gomez-Suarez, D. B. Cordes, A. M. Z. Slawin, S. P. Nolan and L. Cavallo, *Chem. Sci.*, 2015, **6**, 1895-1904.

[20] K. Verlinden, H. Buhl, W. Frank and C. Ganter, *Eur. J. Inorg. Chem.*, 2015, 2416-2425.

[21] T. Sasamori and N. Tokitoh, *Dalton Trans.*, 2008, 1395-1408.

[22] M. M. Hansmann and G. Bertrand, *J. Am. Chem. Soc.*, 2016, **138**, 15885-15888.

[23] M. M. Hansmann, R. Jazzar and G. Bertrand, *J. Am. Chem. Soc.*, 2016, **138**, 8356-8359.

[24] L. Liu, D. A. Ruiz, D. Munz and G. Bertrand, *Chem*, 2016, **1**, 147-153.

[25] T. W. Hudnall, J. P. Moerdyk and C. W. Bielawski, *Chem. Commun.*, 2010, **46**, 4288-4290.

[26] T. W. Hudnall and C. W. Bielawski, *J. Am. Chem. Soc.*, 2009, **131**, 16039-16041.

[27] C. L. Dorsey, B. M. Squires and T. W. Hudnall, *Angew. Chem. Int. Ed.*, 2013, **52**, 4462-4465.

[28] R. Jazzar, R. D. Dewhurst, J. B. Bourg, B. Donnadieu, Y. Canac and G. Bertrand, *Angew. Chem. Int. Ed.*, 2007, **46**, 2899-2902.

[29] V. Lavallo, Y. Canac, C. Präsang, B. Donnadieu and G. Bertrand, *Angew. Chem. Int. Ed.*, 2005, **44**, 5705-5709.

[30] T. W. Hudnall, A. G. Tennyson and C. W. Bielawski, *Organometallics*, 2010, **29**, 4569-4578.

[31] Y. Xiong, S. Yao, M. Brym and M. Driess, *Angew. Chem. Int. Ed.*, 2007, **46**, 4511-4513.

[32] M. Donath, E. Conrad, P. Jerabek, G. Frenking, R. Frohlich, N. Burford and J. J. Weigand, *Angew. Chem. Int. Ed.*, 2012, **51**, 2964-2967.

[33] M. H. Holthausen, K. O. Feldmann, S. Schulz, A. Hepp and J. J. Weigand, *Inorg. Chem.*, 2012, **51**, 3374-3387.

[34] M. H. Holthausen and J. J. Weigand, *Z. Anorg. Allg. Chem.*, 2012, **638**, 1103-1108.

[35] M. H. Holthausen, C. Richter, A. Hepp and J. J. Weigand, *Chem. Commun.*, 2010, **46**, 6921-6923.

[36] M. H. Holthausen and J. J. Weigand, *J. Am. Chem. Soc.*, 2009, **131**, 14210-14211.

[37] J. J. Weigand, M. Holthausen and R. Frohlich, *Angew. Chem. Int. Ed.*, 2009, **48**, 295-298.

[38] Y. Peng, H. J. Fan, H. P. Zhu, H. W. Roesky, J. Magull and C. E. Hughes, *Angew. Chem. Int. Ed.*, 2004, **43**, 3443-3445.

[39] A. R. Fox, R. J. Wright, E. Rivard and P. P. Power, *Angew. Chem. Int. Ed.*, 2005, **44**, 7729-7733.

[40] H. M. Tuononen, R. Roesler, J. L. Dutton and P. J. Ragogna, *Inorg. Chem.*, 2007, **46**, 10693-10706.

[41] V. Lavallo, C. A. Dyker, B. Donnadieu and G. Bertrand, *Angew. Chem. Int. Ed.*, 2008, **47**, 5411-5414.

[42] W. C. Chen, W. C. Shih, T. Jurca, L. L. Zhao, D. M. Andrada, C. J. Peng, C. C. Chang, S. K. Liu, Y. P. Wang, Y. S. Wen, G. P. A. Yap, C. P. Hsu, G. Frenking and T. G. Ong, *J. Am. Chem. Soc.*, 2017, **139**, 12830-12836.

[43] R. Jazzar, J. B. Bourg, R. D. Dewhurst, B. Donnadieu and G. Bertrand, *J. Org. Chem.*, 2007, **72**, 3492-3499.

[44] S. G. Weber, C. Loos, F. Rominger and B. F. Straub, *Arkivoc*, 2012, 226-242.

[45] O. V. Dolomanov, L. J. Bourhis, R. J. Gildea, J. A. K. Howard and H. Puschmann, *J. Appl. Crystallogr.*, 2009, **42**, 339-341.

Chapter 3 : Cross-coupling Reactions between Stable Carbenes

3.1 Introduction

In a seminal study, Wanzlick et al. [1-3] demonstrated that thermolysis of the imidazolidine **3.A** gave tetraazafulvalene **3.B$_2$**, presumably resulting from the dimerization of a short-lived intermediate, namely imidazolidin-2-ylidene **3.B** (Scheme 3.1). Wanzlick proposed that a potential equilibrium might exist between **3.B** and **3.B$_2$**, which colloquially became known as the "Wanzlick equilibrium". Since this discovery, the existence of a potential equilibrium between singlet carbenes and their homodimer has been a subject of controversy.[4-10]

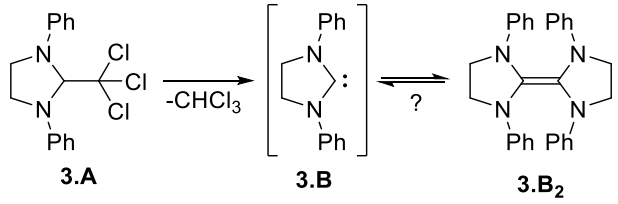

Scheme 3.1: Hypothetical "Wanzlick equilibrium".

Many groups have attempted to find conclusive evidence to support Wanzlick's original hypothesis (Scheme 3.2). Two of the most convincing pieces of evidence for the spontaneous dissociation of the dimer into two identical carbene units were independently reported by Hahn et al.[11] and Lemal et al.[12] Both groups were able to observe by NMR spectroscopy the formation of the benzimidazolin-2-ylidenes **3.C** from solutions of the dibenzotetraazafulvalenes **3.C$_2$**, however Lemal et al. were cautious, suggesting that adventitious electrophilic catalysis of equilibration might be occurring. Arduengo et al.[13] isolated both the thiazol-2-ylidene **3.D** and its dimer **3.D$_2$**, and Alder et al.[14-15] reported the spectroscopic characterization of the acyclic bis(amino)carbene **3.E** while also isolating the corresponding

tetra(amino)alkene **3.E₂**.[16-17] In both cases however, it has been demonstrated that the dimerization only occurs in the presence of an acid catalyst.

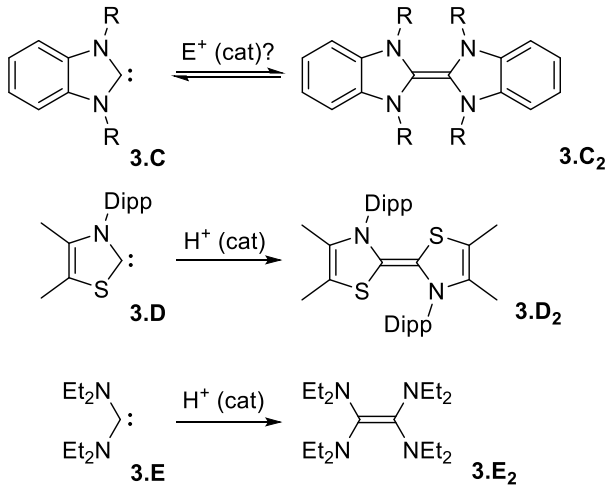

Scheme 3.2: Carbene dimerization proceeding by electrophilic catalysis. Dipp = 2,6-$^{i}Pr_2C_6H_3$

The formation of **3.C₂-E₂** by adventitious electrophilic catalysis can be rationalized by the fact that **3.C-E** are formed via deprotonation of their respective conjugate acids. Indeed, with small kinetic protection the carbene can add to its conjugate acid giving the protonated form of the homodimer. This species can next be deprotonated by another equivalent of carbene, completing the catalytic cycle. Alder et al.[4] gave evidence towards the intermediate of this process by isolating **3.G** from the reaction of 0.5 eq. LiHMDS with the iminium salt **3.F** (Scheme 3.3, top). A more recent striking example was the isolation by Bielawski et al.[18] of diamidocarbene **3.I** prepared by reduction of the corresponding dichloro derivative **3.H**, while Ganter et al.[19] reported that **3.I** spontaneously dimerizes to **3.I₂** when generated by deprotonation of **3.H'** (Scheme 3.3, bottom).

Lemal et al. and Denk et al., attempting to test the propensity of dissociation of the carbene heterodimer, performed crossover experiments with several different carbenes.[4-5, 7] Although carbene exchange was observed in some cases, the reaction proceeded only in the presence of an electrophilic catalyst, adding to the current hypothesis that the "Wanzlick equilibrium" required an electrophile.

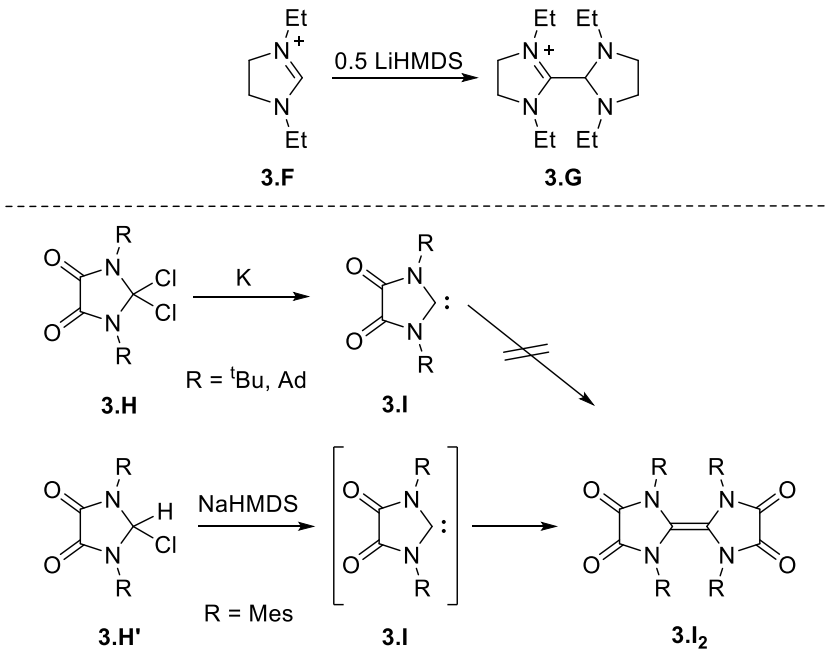

Scheme 3.3: Intermediate in acid-induced carbene dimerization (top) and prevention of dimerization by reduction (bottom). Mes = 2,4,6-$Me_3C_6H_2$

Although up to this point not confirmed experimentally, many groups have calculated reaction pathways and energies for the non-catalyzed dimerization of singlet carbenes.[20-22] Steric protection of the carbene center does play a large role in the kinetics of this reaction, thus even in the presence of an electrophilic catalyst, carbenes with large substituents adjacent to the carbene center do not dimerize. Nolan et al. introduced a model which included a steric parameter to help calculate the energy of dimerization for two carbenes,[23] however when only small substituents are considered, the Carter-Goddard model can be applied to determine if dimerization is thermodynamically possible.[20] Their model estimates that the energy of the resulting alkene (E_{CC}) is approximately equal to the C=C bond energy of ethylene (172 kcal mol^{-1})[24] minus the sum of the singlet-triplet gap energies (ΔE_{ST}) of the free carbenes (Equation 3.1). It is important to note here that positive E_{CC} values imply that dimerization is favorable.

$$E_{CC} = 172 \text{ kcal mol}^{-1} - \Sigma\Delta E_{ST} \quad (3.1)$$

Singlet carbene dimerization follows a non-least motion pathway which involves the attack of the occupied in-plane σ orbital (HOMO) of one carbene on the out-of-plane vacant p_π orbital (LUMO) of a second carbene, giving a transition state with C_2 symmetry (Figure 3.1). As described above, this reaction is thermodynamically favorable (formation of a C=C double bond), however resistance to dimerization has been attributed to a large energy of the transition state, which results from the stabilization of the vacant orbital by the denotation of the lone pairs from the substituents.[25] It is therefore readily understandable that protonation of the carbene, which considerably decreases the energy of the LUMO, facilitates the dimerization reaction.

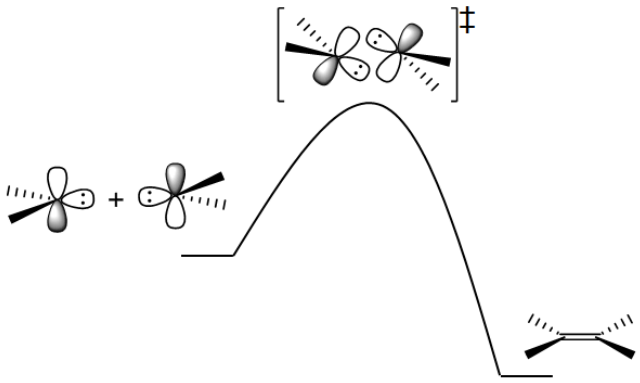

Figure 3.1: Reaction pathway for the dimerization of singlet carbenes.

This short analysis indicates that the coupling reaction involving stable carbenes featuring a rather low-energy LUMO should be possible,[26-36] especially if the other carbene partner has a high-energy HOMO. Following this hypothesis, we sought to demonstrate the first unambiguous example of a non-catalyzed cross-coupling reaction between stable singlet carbenes.

3.2 Synthesis of Carbene Heterodimers and Subsequent Rearrangement Reactions

As the activation energy barrier is sensitive to steric hindrance about the carbene center, we focused on using small carbenes **3.1**-**3.3** as the potential nucleophilic partner in this reaction (Figure 3.2). Indeed, NHCs **3.1** and **3.2**, feature methyl and isopropyl groups, respectively. Furthermore, the two amino groups of BAC **3.3** are directed towards the back of the ring, thus leaving the carbene center of **3.3** readily accessible.[37]

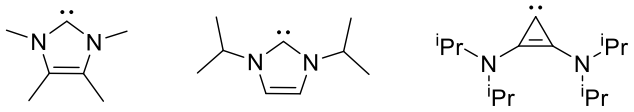

Figure 3.2: Nucleophilic carbenes with minimal steric hindrance.

With the nucleophilic partners decided on, the electrophilic partners needed careful consideration. Since a large portion of the activation energy barrier of carbene dimerization comes from an energetically inaccessible π-orbital, carbenes **3.4**-**3.6** were chosen due to their relatively low-lying LUMOs and strong π-accepting properties (Figure 3.3).[32-34] The reduced heteroatom stabilization of the CAAC[38] **3.4** greatly lowers the LUMO of this species relative to classical NHCs. Additionally, DACs **3.5** and **3.6**, popularized by Bielawski et al.,[31, 39-40] feature amido resonance forms that further reduce their LUMO energy level (see section 1.2). Finally, 7-DAC **3.6** also features a seven-membered ring, and thus widest carbene bond angle of the series, further lowering its LUMO (see section 1.3.3).

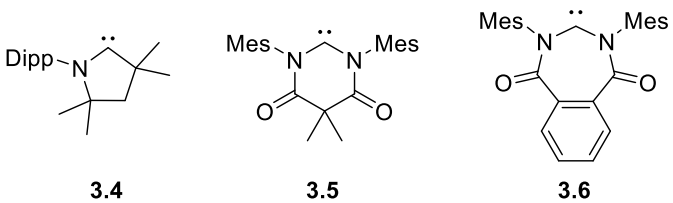

Figure 3.3: Highly electrophilic CAAC **3.4**, 6-DAC **3.5** and 7-DAC **3.6**.

Cross-coupling reactions were first performed by adding benzene or toluene to a 1:1 mixture of NHC **3.1** and each of the electrophilic partners **3.4**-**3.6**, respectively (Scheme 3.4). Although the ^{1}H and ^{13}C NMR clearly indicated complete consumption of starting materials, unfortunately for reactions involving **3.4** and **3.6**, a mixture of unidentifiable products was obtained, and no X-ray quality crystals could be grown. However, some insight into the unexpected behavior of these reactions could be determined in the case of **3.5**. Indeed, upon recrystallization by slow diffusion of hexane into benzene, pure orange crystals of **3.7** were obtained and subjected to an X-ray diffraction study (Figure 3.4).

Although an exact mechanism was not determined, it is evident from the structure of **3.7** that the first step of this reaction is likely the desired cross-coupling of the two carbenes. This is evident as there is clearly formation of a new C-C bond [C1-C2 1.462(3) Å] coming from the two former carbene carbon atoms. Strangely however, intramolecular deprotonation at C3, followed by nucleophilic attack at C4, and subsequent leaving of N2, lead to formation of an enolate [C3-C4 1.373(3), C4-O1 1.278 Å] and subsequent ring opening of the DAC species. This result made clear that although the methyl groups are not sterically hindering dimerization, the proximity of acidic C-H bonds to the resulting heterodimer caused undesired rearrangements.

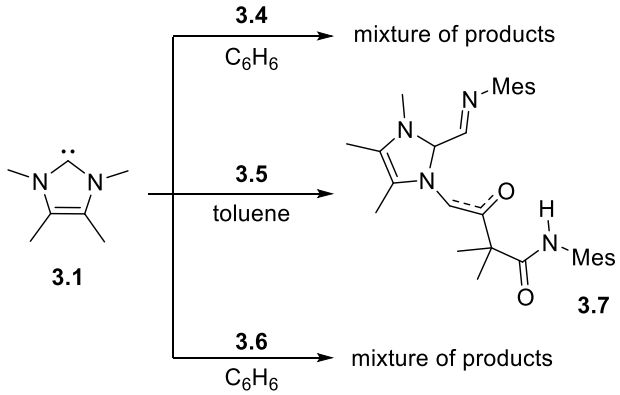

Scheme 3.4: Carbene cross-coupling with NHC **3.1** as the nucleophilic partner.

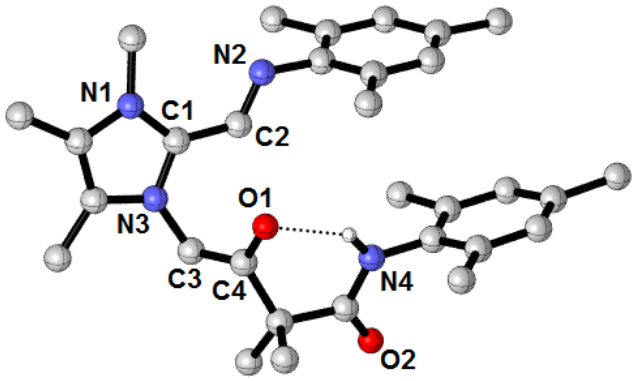

Figure 3.4: X-ray structure of rearrangement product **3.7**. One molecule in the asymmetric unit is depicted and hydrogen atoms, except on N4, have been removed for clarity.

The analogous reactions of NHC **3.2** with 6-DAC **3.5** and 7-DAC **3.6** were both slow, likely due to the increased steric hindrance of the isopropyl groups, and yielded a mixture of unidentifiable products. We believe that the instability of the resulting heterodimers is due to proximity of an acidic C-H from the isopropyl group, similar to the case of the formation of **3.7**. With this in mind, the reaction between **3.2** and CAAC **3.4** was not attempted, and instead we proceeded to focus exclusively on reactions pertaining to BAC **3.3**.

A stirred solution of a stoichiometric mixture of **3.3** and **3.4** in hexanes over 12 h led to formation of compound **3.8**, which was isolated as single crystals in 33 % yield (Scheme 3.5). Although mass spectrometry was consistent with the formation of a cross-coupled product, a singlet at δ = 3.85 ppm in the ^{1}H NMR spectrum, integrating for one proton, suggested the **3.8** was not the expected alkene heterodimer. Indeed, a single-crystal X-ray diffraction study showed that **3.8** was a rearrangement product, in which the cyclopropenylidene moiety underwent a ring-expansion to form a rare example of a stable bent allene (Figure 3.5, middle).[41-45]

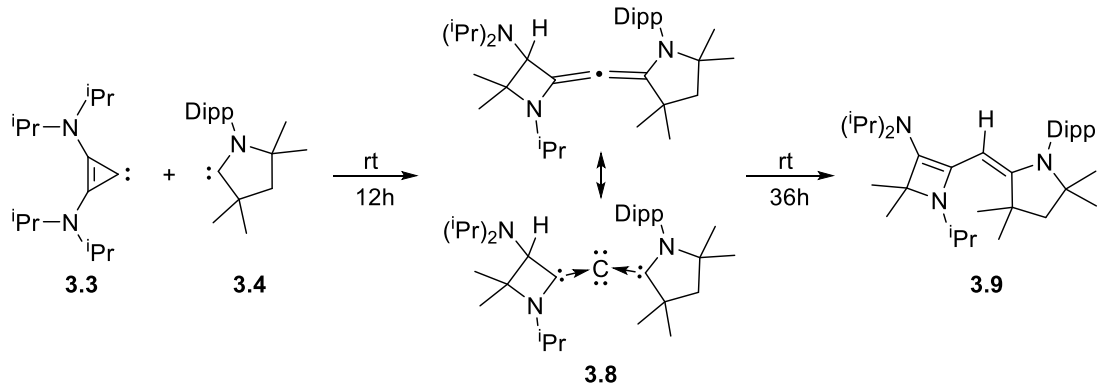

Scheme 3.5: Cross-coupling reaction between **3.3** and **3.4** leading to bent allene **3.8** and intramolecular deprotonation product **3.9**.

Although allenes are traditionally linear, **3.8** is bent with a C1-C2-C3 bond angle of 164.4(1) º. The slight bending can be explained if **3.8** is pictured as a carbodicarbene[46-54] (shown in Scheme 3.2 as the bottom resonance form). Here, the central carbon has two lone pairs and is sandwiched between CAAC **3.4** and the newly formed 4-membered CAAC, giving a bent molecular geometry. This resonance form description also gives explanation to the formation of **3.9** when the reaction is allowed to continue for 36 h. The highly basic central carbone deprotonates the 4-membered ring, resulting in clean formation of diene **3.9**. This compound was unambiguously determined through an X-ray diffraction study from crystals grown in a concentrated pentane solution at -20 ºC (Figure 3.5, right). The movement of a double bond from allene to a diene is clearly seen as C2-C3 is lengthened [1.311(2), 1.468(1) Å] and C3-C4 is shortened [1.541(1), 1.353(1) Å] in the transformation of **3.8** into **3.9**, respectively. Furthermore, C2 is now trigonal planar with C1-C2-C3 bond angle of 127.77(1) º.

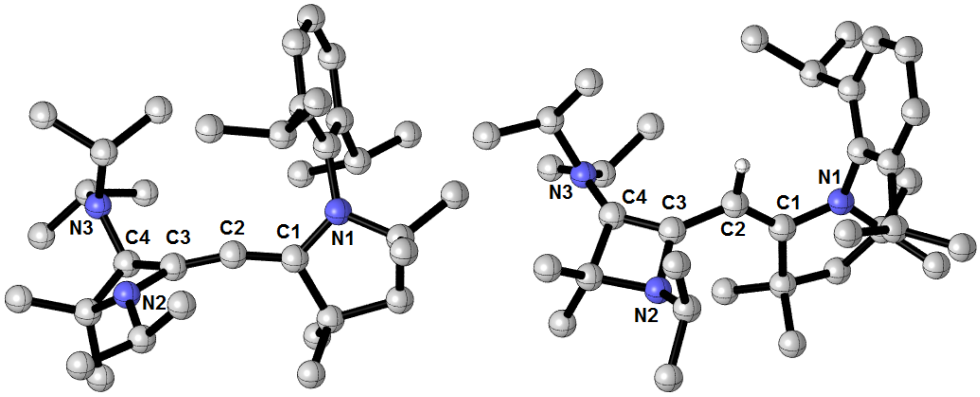

Figure 3.5: X-ray structures of bent allene **3.8** (left) and diene **3.9** (right). Hydrogen atoms, except on C2 in **3.9**, removed for clarity.

Next, we considered the cross-coupling reaction of **3.3** with the electrophilic 6-DAC **3.5** (Scheme 3.6). By stirring a toluene solution of **3.3** and **3.5** overnight, compound **3.10** was isolated after workup. Once again however, the ^{1}H NMR spectrum showed a singlet representing one hydrogen atom at $\delta = 2.86$ ppm, thus suggesting that **3.10** was similar to bent allene **3.8**. This hypothesis was confirmed by a single-crystal X-ray diffraction study from crystals grown in concentrated hexanes at -20 ºC (Figure 3.6). The central allene in **3.10** features a highly bent angle [C1-C2-C3 152.1(2) º] which can also be viewed as a carbodicarbene. Surprisingly however, this allene is stable in solution for days and does not rearrange into the diene **3.11**, analogous to **3.9**. This is likely due to the increased π-accepting nature of 6-DAC **3.5** vs. CAAC **3.4**, therefore reducing the basicity of the resulting carbone, and preventing the subsequent intramolecular deprotonation reaction.

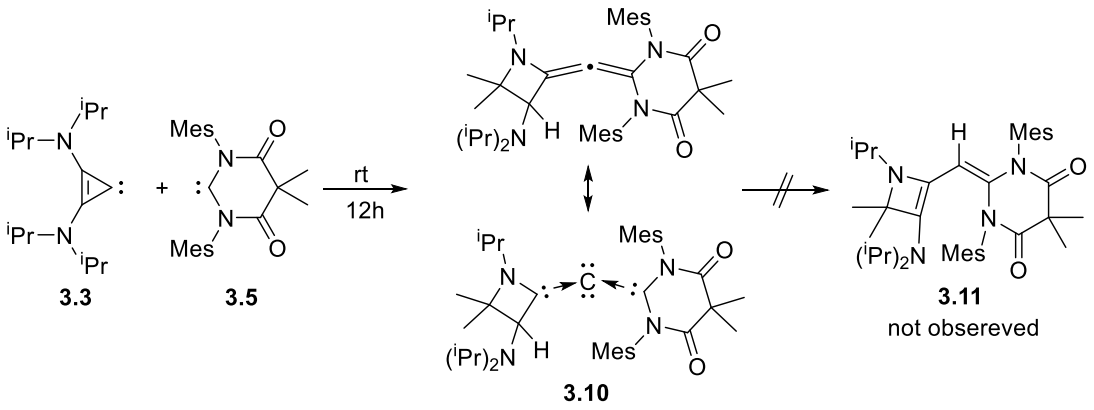

Scheme 3.6: Cross-coupling reaction between **3.3** and **3.5** leading to bent allene **3.10**.

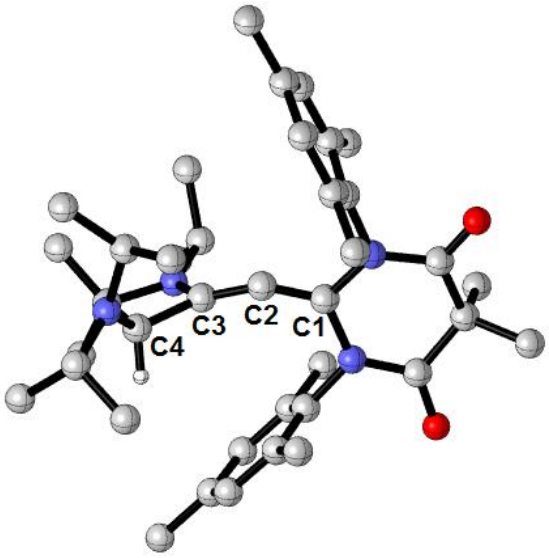

Figure 3.6: X-ray structure of **3.10** with hydrogen atoms, except on C4, removed for clarity.

The final cross-coupling reaction considered was between **3.3** and 7-DAC **3.6**, the most electrophilic singlet carbene known at the time of this research. Following the same experimental procedure used for **3.5**, but now using carbene **3.6**, the heterodimer **3.12** was isolated in 57 % yield (Scheme 3.7). To our delight, two ^{13}C NMR signals corresponding to the formation of a polarized alkene were observed at δ = 118.3 and 91.4 ppm. A single-crystal X-ray diffraction study confirmed that **3.12** was the desired carbene-carbene heterodimer (Figure 3.7). As expected for a polarized alkene,[55-56] it is slightly twisted [N1-C1-C2-C3 = 17.71(3) º], but the C1-C2 bond length is in the typical range for regular

alkenes [1.351(3) Å]. Quite remarkably however, was that the benzannulated backbone of **3.12** is nearly perpendicular to the central alkene. This causes the nitrogen lone pairs to no longer be in plane with the π-system of the alkene, reducing the electronic occupancy of the π* orbital, and thus stabilizing the alkene. This likely explains why **3.12** does not undergo a rearrangement reaction to form a bent allene analogous to **3.8** and **3.10**, but computational calculations were needed to confirm this hypothesis.

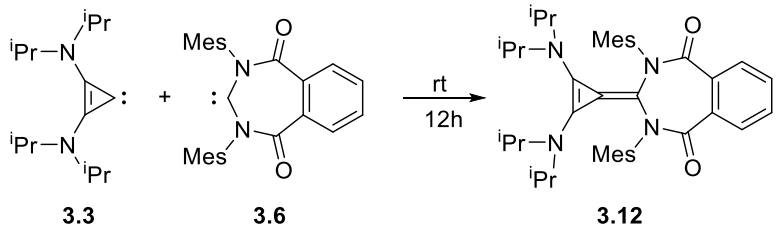

Scheme 3.7: Cross-coupling reaction between **3.3** and **3.6** leading to carbene heterodimer **3.12**.

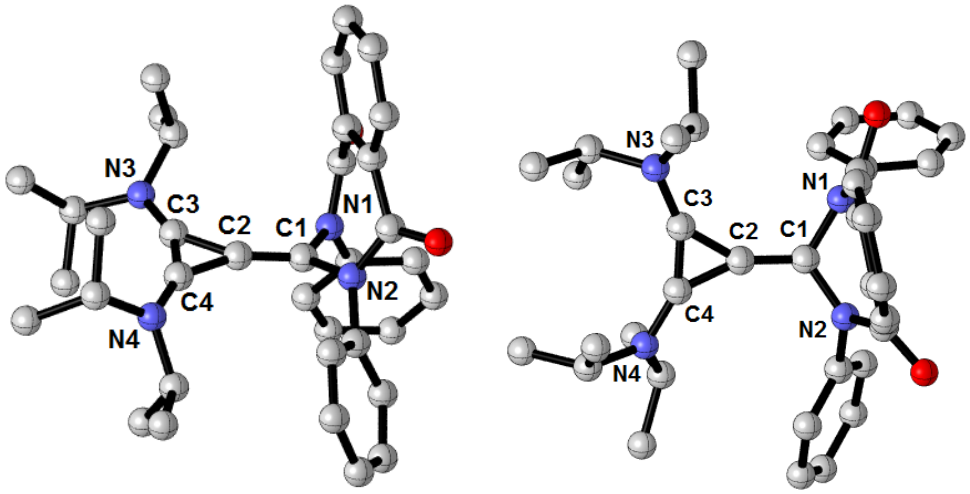

Figure 3.7: X-ray structure of **3.12** in two separate orientations. CH_3 groups of Mes and all hydrogen atoms have been removed for clarity.

3.3 Computational Calculations

To better understand the process leading to **3.8**-**3.10**, and by extension the stability of **3.11**, ab-initio calculations were performed at the B3LYP/6-311++G-(2d,p)//B3LYP/6-31G(d) level of theory. To

reduce computational cost, the Dipp group in **3.4** as well as the Mes groups in **3.5** and **3.6** were replaced with phenyl groups.

Calculations confirmed that the first step in the formation of **3.8** is indeed the generation of the carbene-carbene heterodimer **3.8^{Int1}**, as this was found to be exothermic by 22.3 kcal mol^{-1} (Scheme 3.8). We then tested two separate transition states. First, it was hypothesized that the conjugated aminocyclopropene backbone of the heterodimer might deprotonate a tertiary C-H group of one of the isopropyl substituents, resulting in the **3.8$^{TS1'}$** transition state. This was found to cost 53.8 kcal mol^{-1}, and thus an unlikely candidate. Instead, we believe the process proceeds through the transition state **3.8^{TS1}**, which is only endergonic by 19.8 kcal mol^{-1}. **3.8^{TS1}** can be formally described as an opening of the three-membered ring to form the acyclic aminocarbene **3.8^{Int2}**. This intermediate is 4.7 kcal mol^{-1} lower in energy than **3.8^{Int1}**. Finally, the transient carbene undergoes a C-H insertion with one of the neighboring isopropyl groups, costing 18.2 kcal mol^{-1} (**3.8^{TS2}**), which results in the formation of the bent allene **3.8**. The final step of this reaction is overall 13.8 and 18.5 kcal mol^{-1} downhill from **3.8^{Int2}** and **3.8^{Int1}**, respectively.

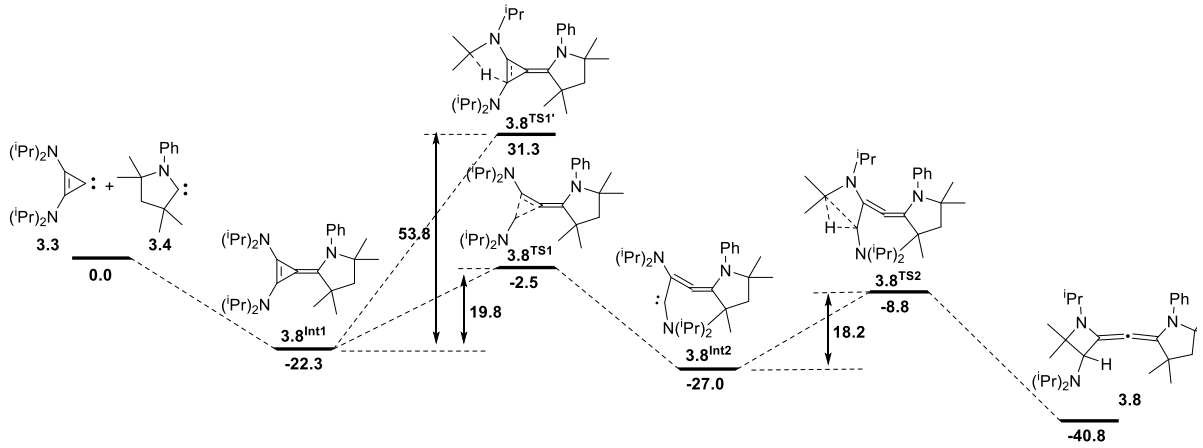

Scheme 3.8: Calculated reaction mechanism for the formation of bent allene **3.8**. Energies are given in kcal mol^{-1}.

The formation of bent allene **3.10** followed an analogous reaction pathway to that of **3.8**, however the energies of the transition states and intermediates varied slightly with several key differences (Scheme 3.9). The intermediate of this reaction, namely **3.10^{Int1}**, is lower in energy than the reagents by 37.0 kcal

mol^{-1}, which is relatively 14.7 kcal mol^{-1} more downhill than **3.8^{Int1}**. Furthermore, the ring opening transition state **3.10^{TS1}** is 3.8 kcal mol^{-1} higher in energy than the analogous **3.8^{TS1}** transition state. These results implied that by moving to a more π-accepting carbene, the formation of the resulting heterodimer is not only more thermodynamically favored, but also that the subsequent undesired rearrangement reactions are inhibited by higher activation energy, therefore further stabilizing the heterodimer. For **3.10^{Int1}** however, these two stabilizing factors are not enough to overcome the additional 14.7 kcal mol^{-1} gained from the formation of **3.10**.

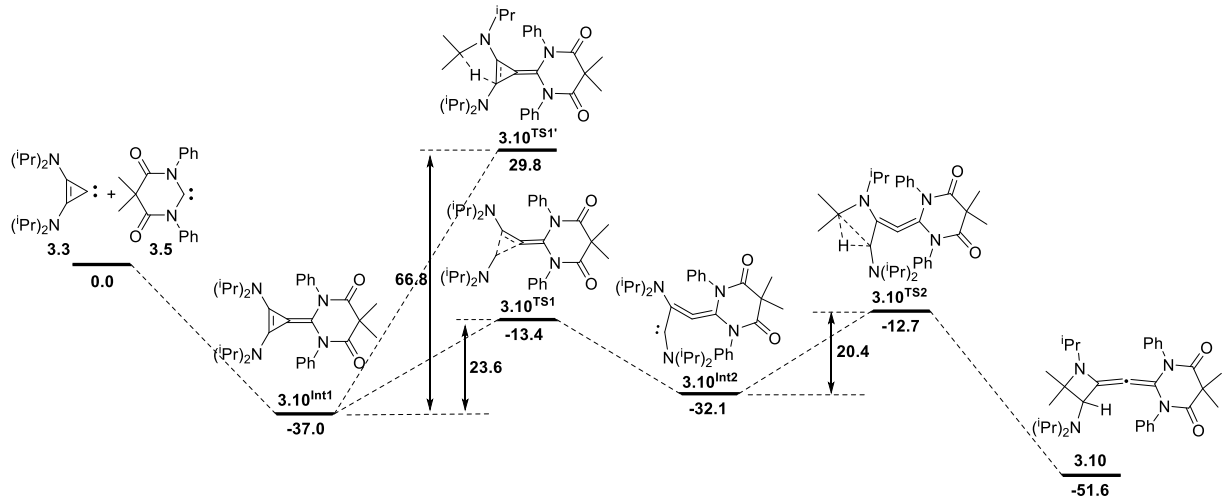

Scheme 3.9: Calculated reaction mechanism for the formation of bent allene **3.10**. Energies are given in kcal mol^{-1}.

To rationalize why **3.10** is stable as a bent allene, whereas **3.8** undergoes an intramolecular deprotonation reaction to form the diene **3.9**, we compared the overall energies of these three compounds, as well as the non-observed diene **3.11** (Scheme 3.10). Indeed, the higher basicity of the carbone in **3.8** leads to the 4.1 kcal mol^{-1} energy gain in the formation of **3.9**. In contrast however, the reduced basicity of the carbone in **3.10**, resulting from the higher π-acidity of 6-DAC **3.5** vs CAAC **3.4**, causes the intramolecular deprotonation product **3.11** to be endergonic by 3.3 kcal mol^{-1}. These results as a whole explain why **3.9** was experimentally observed, whereas **3.11** was not observed even when **3.10** was stirred in toluene for several days.

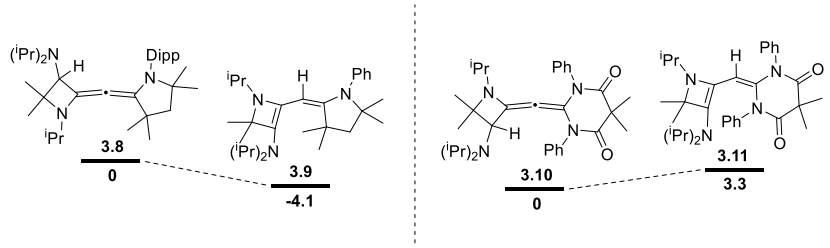

Scheme 3.10: Intramolecular deprotonation reactions to form dienes **3.9** (left) and **3.11** (right). Relative energies are given in kcal mol^{-1} and are arbitrarily set to 0 for both **3.8** and **3.10**.

Lastly, the identical reaction pathway was calculated for the cross-coupling between **3.3** and DAC-7 **3.6** (Scheme 3.11). It was experimentally shown that the carbene-carbene heterodimer **3.12** was stable both in the solid state and solution for multiple days. The room temperature stability of **3.12** can be attributed to the relatively large activation energy barrier (30.6 kcal mol^{-1}) of **3.13^{TS1}**. Furthermore, the total difference in energy between **3.12** and the non-observed bent allene **3.13** is only 4.8 kcal mol^{-1}, which is significantly smaller than the same energy comparison in the reactions involving **3.4** (18.5 kcal mol^{-1}) and **3.5** (14.6 kcal mol^{-1}). Although never experimentally observed, the overall lower energy of **3.13** likely explains why compound **3.12** does not cleanly melt, and instead decomposes in the solid state at 125 ºC.

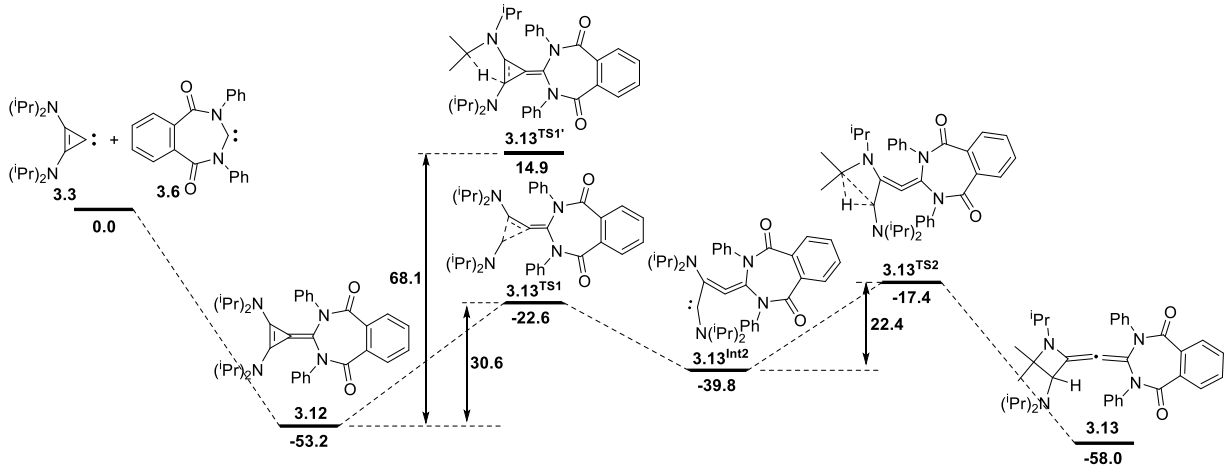

Scheme 3.11: Calculated Gibbs free energy for carbene-carbene heterodimer **3.12**, and reaction pathway for the non-observed allene **3.13**. Energies are given in kcal mol^{-1}.

To further study the electronics of **3.12**, we ran a molecular orbital analysis at the B3LYP/6-311g(d,p) level of theory. As apparent from the HOMO, the majority of the electron density from the π orbital of the newly formed alkene is localized on the 7-DAC carbene carbon atom (Figure 3.8). Moreover, the computed nucleus independent chemical shift[57] NICS(0) (at the center of the three-membered ring) and NICS(1) (at 1 Å above the ring plane) values are -29.1 and -8.5 ppm, respectively. This data is a clear indication that the three-membered ring of **3.12** is a 2π-electron aromatic, thus further demonstrating the polarization of the double bond.

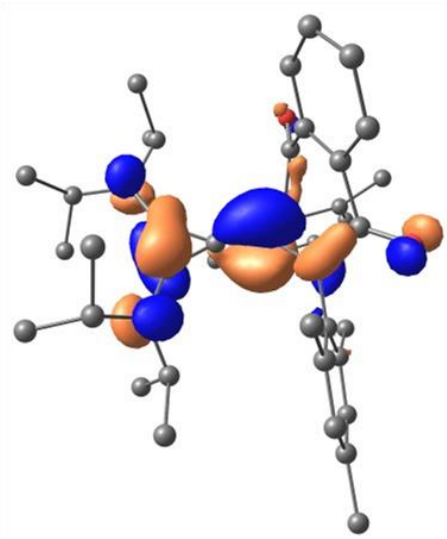

Figure 3.8: HOMO of **3.12** (isovalue = 0.04). Hydrogen atoms removed for clarity.

3.4 Conclusion

These results represent the first demonstration that non-catalyzed cross-coupling reactions between stable carbenes are possible. By utilizing stable carbenes with low-lying LUMOs, coupling with nucleophilic and sterically unhindered carbenes was achieved. Furthermore, by using a bis(amino)cyclopropenylidene as the nucleophilic partner, this reaction resulted in the formation of two new and rare examples of a bent allene, as well as the isolation of the first carbene-carbene heterodimer. It is quite likely that this process has a broad scope of applications. Specifically, this reaction gives access to

polarized alkenes, which could be used for the fine tuning of organic reducing agents,[58-62] as well as bent allenes, which have been shown to be extremely strong donor ligands capable of stabilizing highly electron deficient species.[43, 63]

3.5 Experimental

3.5.1 General Considerations

All manipulations were performed using standard glovebox and Schlenk techniques. Glassware was dried in an oven overnight at 150 ºC. Toluene was freshly distilled over Na metal. Benzene and hexanes were freshly distilled over CaH_2. Additionally, benzene (C_6D_6) used for NMR spectroscopy was purchased from Cambridge Isotope Laboratories and dried over CaH_2. The carbenes **3.1**-**3.6** were prepared following previously described procedures.[37, 39-40, 64-67]

Multinuclear NMR data were recorded on a Varian INOVA 500MHz spectrometer. NMR signals are listed in ppm, relative to residual solvent signals, and were taken at room temperature. Coupling constants are in Hertz (Hz). NMR multiplicities are abbreviated as follows: s = singlet, d = doublet, sept = septet, m = multiplet, br = broad.

Melting points were measured with an electrothermal MEL-TEMP apparatus. When reported, pure crystals of each compound were added to a capillary tube which was then sealed from air with vacuum grease.

High resolution mass spectrometry (HRMS) data was collected on an Agilent 6230 TOF-MS.

Single crystal X-Ray diffraction data were collected on a Bruker Apex II-CCD detector using either Mo-K_α radiation (λ = 0.71073 Å) or Cu-K_α (λ = 1.54178). Crystals were selected under oil, mounted on nylon loops then immediately placed in a cold stream of N_2. Structures were solved and refined using SHELXTL and Olex2 software.[68] All hydrogen atoms were included in the refinement in calculated positions depending on the connecting carbon atoms. Visualized structures were generated with CYLview.

3.5.2 Synthetic Procedures

3.7: NHC **3.1** (113 mg, 1 eq.) and 6-DAC **3.5** (344 mg, 1 eq.) were added to a Schlenk. 20 mL of toluene was added to the mixture of solids and the resulting solution was stirred for 12h. The toluene was removed *in vacuo* and the resulting dark red-brown oil was washed with pentane (2 x 10 mL). The residual pentane was removed *in vacuo*, and the mixture was dissolved in toluene (5 mL), concentrated to near precipitation, and stored in the freezer at -20 ºC over 12h which yielded **3.7** as pure orange microcrystals (104 mg, 23 % yield). X-ray quality crystals of **3.7** were grown by vapor diffusion of hexanes into a benzene solution. No additional characterization data is given.

3.8: Cyclopropenylidene **3.3** (0.705 g, 1 eq) was added to a Schlenk flask containing CAAC **3.4** (0.937 g, 1 eq). The mixture of solids was dissolved in hexanes (12 mL) upon which a yellow colored solution was formed. The reaction was stirred for 16h, at which point the hexanes solution was concentrated to half volume and stored in a -20 ºC freezer overnight, yielding yellow X-ray quality crystals (0.536 g, 32.6 % yield). **MP**: 119-121 ^{0}C. **^{1}H NMR** (500 MHz, C_6D_6) δ 1.17 (s, 3H), 1.30 (d, *J* = 6.8 Hz, 3H) 1.43 (s, 3H), 1.46-1.49 (m, 12H) 1.53-1.55 (m, 6H) 1.61-1.63 (m, 6H) 1.69 (s, 3H), 2.02 (d, *J* = 12 Hz, 1H), 2.17 (d, *J* = 12 Hz, 1H), 3.43 (sept, 1H), 3.51 (sept, *J* = 6.8, 1H), 3.67 (sept, *J* = 6.8 Hz, 2H), 3.82 (sept, *J* = 6.8 Hz, 1H), 3.85 (s, 1H), 7.27-7.37 (m, 3H). **^{13}C{^{1}H} NMR** (126 MHz, C_6D_6) δ 21.64, 22.12, 22.59, 23.05, 23.21, 24.45, 25.82, 25.86, 26.33, 26.88, 27.74, 28.86, 29.03, 30.72, 31.32, 33.99, 41.18, 47.64, 53.58, 62.59, 67.23, 68.49, 124.19, 124.47, 127.68, 127.95, 128.15, 128.34, 131.93, 135.45, 137.83, 149.97, 151.71, 161.64. **HRMS**: *m/z* calculated for $C_{35}H_{60}N_3$ $(M+H)^+$ 522.4782, found 522.4781.

3.9: Allene **3.8** from the previous synthetic procedure was stirred at in hexanes (15 mL) at room temperature for an additional 16h. This solution was then concentrated to half volume and stored in a -20 ºC giving crystals of both **3.8** (yellow) and **3.9** (colorless). No additional characterization data is given.

3.10: Cyclopropenylidene **3.3** (0.150 g, 1eq) and 6-DAC **3.5** (0.240 g, 1 eq) were added to a Schlenk flask. The mixture was dissolved in toluene (6 mL), resulting in a yellow colored solution, which was stirred for 1.5h. The toluene was then removed under reduced pressure, and the product was

dissolved in hexanes and triturated for 30 min. The hexanes was then filtered off and any excess was removed *in vacuo* yielding **3.10** as dark yellow-orange solid. Yellow block crystals suitable for X-ray diffraction were obtained from a concentrated solution in hexanes stored at -20 ºC (0.280 g, 71.9 % yield). **MP**: 136-138 ºC. **^{1}H NMR** (500 MHz, C_6D_6) δ 0.74 (m, 15H), 0.83 (d, *J* = 6.8, 3H), 0.90 (d, *J* = 6.8 Hz, 3H), 0.93 (s, 3H), 1.86 (s, 3H), 1.91 (s, 3H), 2.10 (s, 6H), 2.19 (s, 3H), 2.25 (s, 3H), 2.28 (s, 6H), 2.81 (sept, *J* = 6.6 Hz, 2H,), 2.86 (s, 1H), 3.20 (sept, *J* = 6.8 Hz, 1H), 6.73 (m, 4H). **^{13}C{^{1}H} NMR** (126 MHz, C_6D_6) δ 18.16, 18.49, 18.19, 18.99, 20.73, 20.91, 21.04, 21.88, 23.93, 24.05, 25.32, 26.91, 46.63, 47.32, 68.07, 70.47, 115.56 (C*C*C), 127.94, 128.14, 128.33, 128.99, 129.38, 129.44, 129.60, 129.61, 135.87, 135.97, 136.04, 136.13, 136.26 (*C*O), 136.28 (*C*O). **HRMS**: *m/z* calculated for $C_{39}H_{57}N_4O_2$ $(M+H)^+$ 613.4476, found 613.4475.

3.12: Cyclopropenylidene **3.3** (0.120 g, 1 eq) and 7-DAC **3.6** (0.208 g, 1 eq) were added to a Schlenk flask. The mixture was then dissolved in toluene (20 mL) resulting in an orange colored solution. After stirring for 3h, the toluene was removed *in vacuo*. The resulting solid was then washed with hexanes (2 x 25 mL), and remaining volatiles were removed *in vacuo* yielding **3.12** as a yellow-orange solid. Crystals suitable for X-ray diffraction were obtained from a concentrated toluene solution stored in a -20 ºC freezer for 3 days (0.186 g, 56.7 %). **MP**: 125 ºC (dec.). **^{1}H NMR** (500 MHz, C_6D_6) δ 0.78 (d, *J* = 6.5 Hz, 12H), 0.84 (d, *J* = 6.5 Hz, 12H), 2.09 (s, 12H), 2.39 (s, 6H), 3.25 (sept, *J* = 6.5 Hz, 4H), 6.66 (s, 2H), 6.80 (s, 2H), 7.22 (m, 2H), 8.40 (m, 2H). **^{13}C{^{1}H} NMR** (126 MHz, C_6D_6) δ 20.06, 20.75, 21.26, 22.43, 50.81, 91.46 (N*C*=CC), 118.31 (NC=*C*C), 126.08, 127.97, 128.35, 130.03, 130.37, 130.45, 130.90, 135.13, 135.65, 135.95, 136.74, 139.32, 171.63 (*C*O). **HRMS**: *m/z* calculated for $C_{42}H_{55}N_4O_2$ $(M+H)^+$ 647.4320, found 647.4322.

3.5.3 Crystallographic Data

Compound	**3.7**
Empirical formula	$C_{34}H_{43}N_4O_2$
Formula weight	539.72
Temperature/K	100.0
Crystal system	triclinic

Space group	P-1
a/Å	11.3853(2)
b/Å	16.8361(4)
c/Å	17.8286(4)
α/°	93.5350(10)
β/°	106.1800(10)
γ/°	109.3940(10)
Volume/Å^3	3050.69(11)
Z	4
ρ_{calc}g/cm^3	1.175
μ/mm^{-1}	0.575
F(000)	1164.0
Crystal size/mm^3	0.2 × 0.1 × 0.1
Radiation	CuKα (λ = 1.54178)
2Θ range for data collection/°	78.72 to 140.2
Index ranges	$-13 \leq h \leq 12$, $-19 \leq k \leq 20$, $-21 \leq l \leq 12$
Reflections collected	6407
Independent reflections	6407 [R_{int} = 0.0000, R_{sigma} = 0.0647]
Data/restraints/parameters	6407/0/743
Goodness-of-fit on F^2	1.036
Final R indexes [I>=2σ (I)]	R_1 = 0.0526, wR_2 = 0.1293
Final R indexes [all data]	R_1 = 0.0665, wR_2 = 0.1352
Largest diff. peak/hole / e Å^{-3}	0.17/-0.16

Compound	**3.8**
Empirical formula	$C_{35}H_{59}N_3$
Formula weight	521.85
Temperature/K	100
Crystal system	triclinic
Space group	P-1
a/Å	9.8338(16)
b/Å	11.7838(18)
c/Å	15.706(3)
α/°	72.001(5)
β/°	80.072(6)
γ/°	70.424(5)
Volume/Å^3	1626.0(5)
Z	2
ρ_{calc}g/cm^3	1.066
μ/mm^{-1}	0.061
F(000)	580.0
Crystal size/mm^3	0.2 × 0.2 × 0.1
Radiation	MoKα (λ = 0.71073)
2Θ range for data collection/°	2.74 to 51.62

Index ranges	$-11 \leq h \leq 12$, $-14 \leq k \leq 14$, $-19 \leq l \leq 19$
Reflections collected	22558
Independent reflections	6171 [R_{int} = 0.0468, R_{sigma} = 0.0424]
Data/restraints/parameters	6171/0/359
Goodness-of-fit on F^2	1.069
Final R indexes [I>=2σ (I)]	R_1 = 0.0429, wR_2 = 0.1064
Final R indexes [all data]	R_1 = 0.0522, wR_2 = 0.1132
Largest diff. peak/hole / e Å^{-3}	0.25/-0.23

Compound	**3.9**
Empirical formula	$C_{35}H_{59}N_3$
Formula weight	521.85
Temperature/K	100
Crystal system	monoclinic
Space group	$P2_1/n$
a/Å	11.9840(7)
b/Å	14.4541(8)
c/Å	19.7806(12)
α/°	90.00
β/°	105.892(3)
γ/°	90.00
Volume/Å^3	3295.4(3)
Z	4
ρ_{calc}g/cm^3	1.052
μ/mm^{-1}	0.450
F(000)	1160.0
Crystal size/mm^3	0.2 × 0.2 × 0.1
Radiation	CuKα (λ = 1.54178)
2Θ range for data collection/°	7.68 to 139.04
Index ranges	$-14 \leq h \leq 14$, $-13 \leq k \leq 16$, $-23 \leq l \leq 22$
Reflections collected	21373
Independent reflections	5936 [R_{int} = 0.0501, R_{sigma} = 0.0389]
Data/restraints/parameters	5936/0/419
Goodness-of-fit on F^2	1.038
Final R indexes [I>=2σ (I)]	R_1 = 0.0465, wR_2 = 0.1190
Final R indexes [all data]	R_1 = 0.0544, wR_2 = 0.1253
Largest diff. peak/hole / e Å^{-3}	0.25/-0.18

Compound	**3.10**
Empirical formula	$C_{39}H_{56}N_4O_2$
Formula weight	612.88
Temperature/K	100
Crystal system	triclinic
Space group	P-1

a/Å	9.5145(9)
b/Å	11.5250(11)
c/Å	18.4317(17)
α/°	105.780(4)
β/°	91.807(5)
γ/°	107.521(4)
Volume/Å^3	1840.5(3)
Z	2
ρ_{calc}g/cm^3	1.106
μ/mm^{-1}	0.068
F(000)	668.0
Crystal size/mm^3	0.2 × 0.1 × 0.05
Radiation	MoKα (λ = 0.71073)
2Θ range for data collection/°	3.88 to 50.88
Index ranges	-10 ≤ h ≤ 11, -13 ≤ k ≤ 13, -22 ≤ l ≤ 22
Reflections collected	17882
Independent reflections	5979 [R_{int} = 0.0772, R_{sigma} = 0.1303]
Data/restraints/parameters	5979/0/422
Goodness-of-fit on F^2	0.853
Final R indexes [I>=2σ (I)]	R_1 = 0.0454, wR_2 = 0.0805
Final R indexes [all data]	R_1 = 0.1106, wR_2 = 0.0929
Largest diff. peak/hole / e Å^{-3}	0.20/-0.26

Compound	**3.12**
Empirical formula	$C_{42}H_{54}N_4O_2$
Formula weight	646.89
Temperature/K	100
Crystal system	monoclinic
Space group	$P2_1/c$
a/Å	16.3875(15)
b/Å	15.1926(16)
c/Å	14.6652(17)
α/°	90.00
β/°	96.640(5)
γ/°	90.00
Volume/Å^3	3626.7(7)
Z	4
ρ_{calc}g/cm^3	1.185
μ/mm^{-1}	0.073
F(000)	1400.0
Crystal size/mm^3	0.2 × 0.16 × 0.1
Radiation	MoKα (λ = 0.71073)
2Θ range for data collection/°	2.5 to 52.86
Index ranges	-20 ≤ h ≤ 17, -19 ≤ k ≤ 18, -18 ≤ l ≤ 18

Reflections collected	44771
Independent reflections	7401 [R_{int} = 0.0576, R_{sigma} = 0.0503]
Data/restraints/parameters	7401/0/447
Goodness-of-fit on F^2	1.045
Final R indexes [I>=2σ (I)]	R_1 = 0.0587, wR_2 = 0.1477
Final R indexes [all data]	R_1 = 0.0953, wR_2 = 0.1644
Largest diff. peak/hole / e $Å^{-3}$	0.78/-0.38

3.5.4 Computational Details

All calculations were carried out with the Gaussian 09 package.[69] Geometry optimizations and frequency calculations were performed with B3LYP. The 6-31G(d)[70-73] basis set was used for C, H, N and O. Transition states were examined by vibrational analysis and then submitted to intrinsic reaction coordinate [74] calculations to determine two corresponding minima. For compounds that had multiple conformations, efforts were made to find the lowest-energy conformation by comparing the structures optimized from different starting geometries. To calculate the single-point electronic energies in solution, the same method with a basis set employing 6-311++G(2d,p)[75-77] was used for C, H, N and O. The default self-consistent reaction field polarizable continuum model was used with *n*-hexane (dielectric constant ε = 1.8819) for the reaction of cyclopropenylidene **3.3** with CAAC **3.4**, or toluene (ε = 2.3741) for the reaction of cyclopropenylidene **3.3** with 6-DAC **3.5** and 7-DAC **2.6**, while Bondi radii[78] were chosen as the atomic radii to define the molecular cavity. The gas-phase geometry was used for all the solution phase calculations. The dispersion correction calculations using the corresponding B3LYP-D functional were performed with the DFT-D3 program of Grimme.[79-81] The Gibbs energy corrections from frequency calculations and dispersion corrections were added to the single-point energies to obtain the Gibbs free energies in solution. All the solution-phase free energies reported in this chapter correspond to the reference state of 1 mol L^{-1}, 298 K. To reduce the computational cost, the 2,6-diisopropylphenyl and 2,4,6-trimethylphenyl groups were replaced by phenyl groups. Nucleus independent chemical shift was computed at the B3LYP/6-311++G(2d,p)//B3LYP/6-311G(d,p) level of

theory in the gas-phase. Cartesian coordinates for the optimized structures and the first frequency from calculations are given following Table 3.1.

Table 3.1: Energies of Intermediates and Transition States

Compound	Solvation Energies (Hartree)	Thermal Corrections of Gibbs Free Energies (Hartree)	Dispersion Corrections (kcal mol^{-1})
3.3	-698.0638945 (hexane)	0.358473	-52.8188
3.4	-599.7981252	0.256704	-43.6558
3.8^{Int1}	-1297.899621	0.645424	-114.1502
3.8^{TS1}	-1297.864108	0.642314	-114.6491
3.8$^{TS1'}$	-1297.804418	0.639559	-116.4403
3.8^{Int2}	-1297.90268	0.641884	-114.6382
3.8^{TS2}	-1297.86881	0.637238	-114.7848
3.8	-1297.940466	0.642999	-113.4177
3.3	-698.0657944 (toluene)	0.358473	-52.8188
3.5	-955.7507267	0.25435	-54.4891
3.10^{Int1}	-1653.87071	0.641955	-128.5367
3.10^{TS1}	-1653.831542	0.641822	-129.4488
3.10$^{TS1'}$	-1653.757138	0.639054	-131.172
3.10^{Int2}	-1653.860896	0.640451	-128.8964
3.10^{TS2}	-1653.822381	0.634233	-128.7842
3.10	-1653.893879	0.639765	-127.3143
3.6	-1068.869467	0.247882	-59.7669
3.12	-1767.015879	0.637352	-134.6055
3.13^{TS1}	-1766.965955	0.636617	-134.8991
3.13$^{TS1'}$	-1766.898894	0.6333	-137.3987
3.13^{Int2}	-1766.991521	0.636459	-135.9172
3.13^{TS2}	-1766.951545	0.6324	-136.0816
3.13	-1767.023552	0.637243	-134.5234

3.3 (23.59)

7	1.965967	-0.145974	-0.000692
7	-1.859833	-0.116400	-0.000190
6	-0.637343	-0.681941	-0.000300
6	0.049682	-1.915344	-0.000726
6	0.726183	-0.677131	-0.000537
6	-2.049122	1.343688	0.000328
6	-3.040073	-1.018476	-0.000040
1	-3.914281	-0.358390	-0.000227
6	3.095213	-1.105966	0.000144
1	2.609952	-2.086023	0.000057
6	2.226854	1.304361	-0.000387
1	3.317185	1.402125	-0.001018
1	-1.039327	1.761245	0.001033
6	3.945506	-0.995335	-1.273247
1	4.460772	-0.029273	-1.342984
1	4.714588	-1.776383	-1.281517
1	3.324339	-1.119581	-2.166221
6	3.944238	-0.994836	1.274344
1	3.322212	-1.118645	2.166786
1	4.713269	-1.775921	1.283717
1	4.459494	-0.028772	1.344147
6	1.712322	1.979786	1.279722
1	1.946923	3.050572	1.272323

1	0.627648	1.872441	1.379865
1	2.174324	1.531330	2.165092
6	1.711058	1.980352	-1.279673
1	1.946059	3.051049	-1.272127
1	2.171979	1.532016	-2.165669
1	0.626248	1.873481	-1.378701
6	-2.753062	1.837352	-1.273667
1	-3.778649	1.457216	-1.343826
1	-2.806790	2.932205	-1.278714
1	-2.209275	1.514180	-2.167481
6	-2.754232	1.836701	1.273942
1	-2.211511	1.512739	2.168111
1	-2.807269	2.931586	1.279501
1	-3.780121	1.457177	1.342799
6	-3.088173	-1.878438	-1.271306
1	-3.101658	-1.251075	-2.169440
1	-2.214779	-2.535115	-1.318317
1	-3.991592	-2.499629	-1.273229
6	-3.088167	-1.878019	1.271486
1	-3.101800	-1.250459	2.169473
1	-3.991473	-2.499387	1.273560
1	-2.214704	-2.534609	1.318681

3.4 (29.53)

7	0.189056	-0.080919	-0.163300
6	-1.844808	-1.062474	0.787677
6	0.948392	-1.100602	-0.509742
6	-2.043156	0.456755	-1.083683
6	0.853451	1.180707	0.398152
6	-3.429940	0.295798	-1.061320
1	-4.041419	0.816327	-1.793442
6	-3.229891	-1.219756	0.806993
1	-3.685573	-1.881100	1.538968
6	-1.247839	-0.218502	-0.153634
6	2.389525	-0.647514	-0.288417
6	-4.027159	-0.536795	-0.114181
1	-5.106457	-0.661111	-0.100109
6	2.333366	0.867659	0.084123
1	2.979807	1.117133	0.932528
1	2.668855	1.477199	-0.762877
6	0.562613	1.271877	1.905011
1	-0.512707	1.352267	2.097504
1	1.046789	2.159518	2.328254
1	0.940254	0.392699	2.437000
6	0.368235	2.454361	-0.304683
1	0.510015	2.387128	-1.388902
1	0.948320	3.311623	0.056584
1	-0.687787	2.658968	-0.101784
6	3.204578	-0.895831	-1.570472
1	3.184727	-1.956664	-1.839820
1	4.249881	-0.590262	-1.432402
1	2.795863	-0.329231	-2.415620
6	2.967159	-1.509353	0.856005
1	2.424739	-1.354254	1.796084
1	4.020792	-1.256720	1.030019
1	2.900778	-2.572919	0.605943
1	-1.577065	1.082226	-1.837395
1	-1.210364	-1.604387	1.481585

3.8$^{\mathbf{Int1}}$ (24.93)

7	-1.019937	2.160809	-0.697600
7	-2.982336	-0.610753	0.320950
6	-0.275773	-0.431480	-0.264625
6	-1.711569	-0.242994	-0.128458
6	-0.981233	0.835911	-0.457126
6	-2.374981	2.756168	-0.809649
1	-3.051359	1.996766	-0.407650
6	-3.311087	-0.147649	1.689819
1	-2.945739	0.887665	1.731967
6	-3.766497	-1.671100	-0.337211
6	0.155083	2.971686	-1.093688
1	-0.268584	3.862692	-1.569662
1	-4.818524	-1.386323	-0.209741
6	-2.577748	-0.914929	2.806697
1	-2.735212	-0.422059	3.774518
1	-2.932455	-1.947145	2.894642
1	-1.500996	-0.939585	2.612068
6	-4.821766	-0.090702	1.948004
1	-5.274162	-1.086664	2.011106
1	-5.004193	0.409440	2.905508
1	-5.339717	0.475097	1.165812
6	-3.617962	-3.081219	0.268670
1	-4.225678	-3.800826	-0.294194
1	-2.580708	-3.426364	0.250290
1	-3.960086	-3.105502	1.307933
6	-3.500577	-1.670951	-1.847628
1	-4.168053	-2.385789	-2.341381
1	-3.684255	-0.678356	-2.271917
1	-2.470223	-1.953730	-2.082453
6	-2.774679	2.996163	-2.274601
1	-3.812424	3.344985	-2.330760
1	-2.145977	3.756395	-2.752560
1	-2.692713	2.070006	-2.852838
6	-2.527569	4.021123	0.045054
1	-1.888848	4.837621	-0.310175
1	-3.564269	4.374495	0.003669
1	-2.274962	3.819476	1.091060
6	1.016991	2.264789	-2.145864
1	1.464581	1.346614	-1.754290
1	0.416768	2.010513	-3.026910
1	1.826788	2.930892	-2.465522
6	0.953978	3.437258	0.130958

1	1.799996	4.060773	-0.179959
1	0.323769	4.029134	0.803040
1	1.350554	2.588543	0.691821
7	2.178008	-0.561095	-0.439108
6	2.272950	0.244221	1.908634
6	0.867388	-1.147793	-0.221279
6	3.774140	1.157974	0.260855
6	3.007249	-1.631816	-1.099191
6	4.344228	1.976117	1.233564
1	5.142045	2.659657	0.952211
6	2.833277	1.080857	2.873300
1	2.450754	1.046191	3.890987
6	2.742277	0.251692	0.580795
6	0.970002	-2.680105	-0.095964
6	3.879844	1.947137	2.550210
1	4.314808	2.596141	3.305182
6	2.467298	-2.921701	-0.423763
1	3.031137	-3.085440	0.503334
1	2.618709	-3.807187	-1.052649
6	4.521788	-1.544439	-0.878883
1	4.978972	-0.699472	-1.401722
1	4.975348	-2.459723	-1.277602
1	4.782141	-1.474636	0.180749
6	2.720320	-1.592101	-2.611358
1	1.645891	-1.563779	-2.810217
1	3.145543	-2.467974	-3.116527
1	3.163381	-0.692981	-3.054676
6	0.074559	-3.415160	-1.114400
1	-0.976825	-3.157856	-0.971059
1	0.170390	-4.503293	-1.002219
1	0.338363	-3.159903	-2.145206
6	0.631359	-3.197294	1.318853
1	1.259003	-2.716219	2.076955
1	0.790207	-4.282058	1.392784
1	-0.415926	-2.995946	1.571764
1	4.110618	1.230816	-0.767797
1	1.454238	-0.415797	2.172256

3.8^{TS1} (-249.06)

7	-1.236559	2.032431	-0.095262
7	-3.120618	-0.598139	-0.228947
6	-0.048282	-0.262273	0.021401
6	-1.859715	-0.375218	-0.642392
6	-1.012918	0.669865	-0.279672
6	-2.300566	2.609547	-0.954715
1	-2.995011	1.785659	-1.134893
6	-3.717051	0.137368	0.930522
1	-3.253410	1.124748	0.905526
6	-3.913777	-1.691869	-0.863269
6	-0.199736	2.930359	0.455665
1	-0.680728	3.910842	0.526314
1	-4.902106	-1.262447	-1.069737
6	-3.306657	-0.481624	2.278418
1	-3.614507	0.178370	3.099152
1	-3.762395	-1.461359	2.448956
1	-2.219466	-0.594830	2.326990
6	-5.232949	0.344825	0.829430
1	-5.797559	-0.587891	0.931786
1	-5.556041	1.010041	1.638521
1	-5.513453	0.814157	-0.120231
6	-4.130998	-2.922875	0.034253
1	-4.719232	-3.671908	-0.509132
1	-3.178521	-3.381470	0.315114
1	-4.677964	-2.681439	0.949810
6	-3.315585	-2.104559	-2.209570
1	-3.997597	-2.810695	-2.699021
1	-3.178685	-1.239298	-2.864057
1	-2.340732	-2.581436	-2.086197
6	-1.798000	3.069134	-2.336239
1	-2.651039	3.308843	-2.982845
1	-1.176137	3.967894	-2.266518
1	-1.214416	2.279395	-2.819580
6	-3.091682	3.726452	-0.257879
1	-2.510062	4.649205	-0.154857
1	-3.977688	3.972484	-0.854150
1	-3.424827	3.421113	0.739476
6	1.036493	3.090175	-0.444721
1	1.483469	2.126649	-0.687410
1	0.779564	3.589303	-1.383221
1	1.799686	3.692769	0.059482
6	0.151076	2.514194	1.890852
1	0.879572	3.210055	2.321420
1	-0.747517	2.518861	2.517828
1	0.581631	1.510593	1.919851
7	2.321494	-0.860585	-0.376391
6	3.243953	0.772534	1.224319
6	1.010104	-1.054739	0.182382
6	3.905223	0.851322	-1.095450
6	2.914595	-2.201103	-0.679869
6	4.758316	1.918274	-0.814887
1	5.341530	2.362678	-1.617695
6	4.081097	1.852703	1.496760
1	4.148866	2.233690	2.513053
6	3.139931	0.252986	-0.078540
6	0.958500	-2.454269	0.851308
6	4.848977	2.429283	0.481237
1	5.507448	3.266046	0.697715
6	2.323089	-3.076633	0.454470
1	3.010783	-3.051655	1.308820
1	2.225744	-4.124732	0.149146
6	4.445798	-2.234967	-0.630789
1	4.904422	-1.652750	-1.435459

1	4.774413	-3.274780	-0.742355
1	4.828606	-1.858340	0.322742
6	2.433661	-2.656838	-2.071390
1	1.344779	-2.592975	-2.153737
1	2.738290	-3.691190	-2.273753
1	2.861891	-2.015315	-2.850033
6	-0.214701	-3.307917	0.348081
1	-1.161512	-2.797763	0.530783
1	-0.229610	-4.276727	0.863628
1	-0.147234	-3.496851	-0.728060
6	0.847668	-2.311317	2.383258
1	1.660962	-1.697474	2.787422
1	0.897531	-3.294045	2.871095
1	-0.101827	-1.841958	2.664103
1	3.807165	0.479215	-2.110919
1	2.667507	0.313854	2.021496

3.8$^{TS1'}$ (-1555.52)

7	-1.045783	2.226230	-0.487056
7	-2.708946	-0.801725	0.491015
6	-0.224112	-0.250760	-0.307434
6	-1.745692	-0.049213	-0.230284
6	-0.832925	1.002727	0.011969
6	-2.418501	2.392884	-0.899771
1	-2.408790	0.790490	-1.090870
6	-2.221946	-1.370563	1.767953
1	-1.137541	-1.496035	1.644578
6	-3.922965	-1.352504	-0.147962
6	0.061717	3.100320	-0.961812
1	-0.426065	3.981219	-1.382423
1	-3.916756	-2.439161	0.008051
6	-2.772511	-2.758947	2.125104
1	-2.286140	-3.099316	3.046135
1	-3.851980	-2.755158	2.310722
1	-2.558687	-3.499836	1.347412
6	-2.429537	-0.382688	2.930310
1	-3.494942	-0.233658	3.140366
1	-1.949432	-0.750994	3.846179
1	-1.989116	0.590460	2.689276
6	-3.983880	-1.157413	-1.668023
1	-4.835740	-1.727608	-2.056198
1	-4.126699	-0.109912	-1.948012
1	-3.077506	-1.520075	-2.161319
6	-5.210663	-0.813050	0.503513
1	-6.092489	-1.315885	0.085842
1	-5.214597	-0.977393	1.585773
1	-5.312716	0.262872	0.327871
6	-2.664557	3.386230	-2.014844
1	-3.681597	3.222865	-2.389879
1	-2.619300	4.442810	-1.696396
1	-1.984976	3.256873	-2.863479
6	-3.420446	2.541778	0.234592
1	-3.365882	3.548523	0.684221
1	-4.440493	2.415262	-0.146182
1	-3.268166	1.804590	1.024269
6	0.902257	2.437557	-2.058833
1	1.434553	1.561554	-1.679923
1	0.273883	2.123598	-2.899496
1	1.642426	3.153671	-2.434518
6	0.900905	3.565161	0.234446
1	1.662914	4.276856	-0.103182
1	0.270140	4.064386	0.977579
1	1.408357	2.726921	0.718002
7	2.222075	-0.556597	-0.408746
6	2.040498	0.204592	1.921184
6	0.866622	-1.016820	-0.477359
6	3.841735	1.026967	0.545213
6	3.117100	-1.405920	-1.265156
6	4.319424	1.770304	1.624001
1	5.206907	2.384190	1.489243
6	2.517316	0.961874	2.987484
1	1.988812	0.925880	3.937291
6	2.696576	0.212657	0.671514
6	0.881467	-2.487245	-0.876278
6	3.663393	1.750095	2.854926
1	4.031392	2.339342	3.689872
6	2.147441	-2.518440	-1.766889
1	2.635898	-3.499254	-1.763210
1	1.857264	-2.306303	-2.802446
6	4.291817	-2.011877	-0.475390
1	4.961094	-1.244296	-0.078796
1	4.878203	-2.658486	-1.138021
1	3.940192	-2.617255	0.365137
6	3.655182	-0.626428	-2.482869
1	2.836810	-0.119252	-3.004124
1	4.131971	-1.317928	-3.189140
1	4.403026	0.122666	-2.205135
6	-0.359175	-2.926684	-1.663728
1	-1.260353	-2.872915	-1.044831
1	-0.249574	-3.962621	-2.008366
1	-0.514529	-2.288712	-2.540662
6	1.048091	-3.398732	0.362683
1	1.879689	-3.077432	0.997656
1	1.234601	-4.437824	0.060243
1	0.140298	-3.385997	0.975960
1	4.352715	1.093468	-0.407837
1	1.153699	-0.405729	2.046706

3.8^{Int2} (9.97)

7	-1.524607	1.387166	1.200388
7	-2.398542	-1.090021	-0.896706
6	0.122570	-0.380696	0.780411

6	-1.657304	-0.013816	-0.800147
6	-0.988015	0.317984	0.479429
6	-2.678314	2.119993	0.645856
1	-3.048093	1.504439	-0.178315
6	-2.781197	-2.021417	0.219606
1	-2.153841	-1.708592	1.055889
6	-2.980813	-1.402733	-2.248097
6	-0.837274	1.988800	2.359740
1	-1.437972	2.868432	2.611751
1	-3.651016	-2.255214	-2.106340
6	-2.454255	-3.485979	-0.095630
1	-2.597098	-4.089069	0.808742
1	-3.105085	-3.906333	-0.870471
1	-1.415353	-3.599443	-0.415043
6	-4.255410	-1.835686	0.600547
1	-4.930405	-2.119403	-0.215616
1	-4.498013	-2.468286	1.462382
1	-4.464830	-0.796611	0.873213
6	-1.874327	-1.808813	-3.224809
1	-2.304552	-2.079902	-4.195750
1	-1.183417	-0.972726	-3.368013
1	-1.305335	-2.666399	-2.850579
6	-3.806780	-0.227246	-2.776173
1	-4.243303	-0.481294	-3.748884
1	-4.624323	0.021260	-2.090117
1	-3.169878	0.653936	-2.888819
6	-2.274240	3.470727	0.030451
1	-3.141719	3.954750	-0.434969
1	-1.877933	4.160149	0.785288
1	-1.507715	3.319938	-0.735924
6	-3.827976	2.268919	1.655873
1	-3.564944	2.923300	2.495011
1	-4.703299	2.709581	1.164021
1	-4.117380	1.295546	2.066582
6	0.581132	2.505429	2.067488
1	1.287496	1.688255	1.914288
1	0.594425	3.135658	1.173123
1	0.930617	3.105852	2.917046
6	-0.873514	1.063543	3.587384
1	-0.415349	1.560232	4.451279
1	-1.906052	0.805819	3.847673
1	-0.326366	0.138772	3.393568
7	2.471619	-0.179167	0.041225
6	3.111243	2.086934	-0.611887
6	1.373990	-0.807348	0.704078
6	1.361101	0.976254	-1.845383
6	3.569249	-1.151409	-0.224146
6	1.226251	2.101914	-2.658787
1	0.475733	2.102989	-3.445178
6	2.990758	3.203045	-1.439915
1	3.625915	4.068917	-1.270380
6	2.306058	0.954446	-0.811535
6	1.936146	-2.050987	1.432556
6	2.044754	3.216306	-2.466888
1	1.940962	4.090124	-3.104965
6	3.418353	-2.106875	0.980269
1	4.067290	-1.759527	1.792295
1	3.737428	-3.123590	0.725382
6	4.953748	-0.489679	-0.222195
1	5.082112	0.194694	-1.066622
1	5.727609	-1.263016	-0.297271
1	5.119156	0.067996	0.705642
6	3.357464	-1.876105	-1.570787
1	2.386112	-2.380187	-1.603921
1	4.138331	-2.628854	-1.733547
1	3.394412	-1.164483	-2.402802
6	1.167343	-3.323617	1.038255
1	0.116523	-3.233066	1.328261
1	1.588525	-4.201212	1.545584
1	1.205297	-3.508112	-0.040920
6	1.844014	-1.876142	2.959861
1	2.337741	-0.951966	3.280097
1	2.326923	-2.716908	3.475382
1	0.798920	-1.834276	3.283627
1	0.703984	0.127500	-1.988372
1	3.819949	2.090036	0.209803

3.8^{TS2} (-1018.76)

7	-1.808907	1.563005	1.079573
7	-2.154818	-1.256453	-1.007006
6	0.109294	0.778112	-0.287890
6	-2.252805	-0.008889	-0.546138
6	-1.179271	0.773939	0.074999
6	-2.999770	0.898598	1.502740
1	-3.215999	0.344039	0.117298
6	-1.082628	-2.215137	-0.620762
1	-0.414754	-1.641926	0.022519
6	-3.234725	-1.753932	-1.903907
6	-1.541090	2.991025	1.295609
1	-2.293460	3.317784	2.020861
1	-2.964149	-2.781856	-2.163207
6	-0.270876	-2.685270	-1.834283
1	0.557545	-3.318798	-1.498764
1	-0.872057	-3.275440	-2.536253
1	0.149290	-1.828402	-2.368129
6	-1.635541	-3.392918	0.195300
1	-2.294405	-4.039473	-0.396991
1	-0.803672	-4.009027	0.556059
1	-2.193901	-3.036845	1.066834
6	-3.289311	-0.930222	-3.195781
1	-4.071485	-1.311976	-3.862145
1	-3.506221	0.117099	-2.963111

1	-2.332376	-0.970026	-3.726445
6	-4.596771	-1.795766	-1.197040
1	-5.346622	-2.248704	-1.855833
1	-4.549537	-2.386566	-0.276192
1	-4.938929	-0.787549	-0.942902
6	-4.246812	1.733885	1.701035
1	-5.120147	1.079125	1.807749
1	-4.207024	2.347015	2.617260
1	-4.429707	2.408030	0.856551
6	-2.809143	-0.191309	2.542588
1	-1.875020	-0.736189	2.376494
1	-2.767261	0.228695	3.563102
1	-3.640800	-0.908410	2.526196
6	-1.730306	3.823784	0.017127
1	-1.051450	3.482108	-0.769198
1	-2.753751	3.731981	-0.361428
1	-1.528426	4.884181	0.209573
6	-0.168094	3.237395	1.942578
1	-0.052916	4.298346	2.197055
1	-0.068457	2.649793	2.861536
1	0.640884	2.956458	1.263118
7	2.354903	-0.197788	-0.253383
6	2.440199	-2.270245	1.047329
6	1.340806	0.681166	-0.745657
6	1.788645	-0.224910	2.150018
6	3.708887	0.168572	-0.750880
6	1.642924	-0.921994	3.348852
1	1.329016	-0.388906	4.242833
6	2.308232	-2.962987	2.252837
1	2.509511	-4.030977	2.282611
6	2.195882	-0.889413	0.981412
6	1.935659	1.458501	-1.944850
6	1.906738	-2.292664	3.408656
1	1.795699	-2.832237	4.345405
6	3.358010	0.862279	-2.087947
1	3.362989	0.110610	-2.885953
1	4.104911	1.618836	-2.352850
6	4.593874	-1.061569	-1.003045
1	4.868254	-1.565476	-0.070862
1	5.521583	-0.750029	-1.498157
1	4.085774	-1.781850	-1.653080
6	4.435352	1.109285	0.234276
1	3.850295	2.011009	0.437609
1	5.407269	1.417259	-0.169602
1	4.612125	0.603024	1.189534
6	1.981664	2.973684	-1.665210
1	0.972086	3.373266	-1.533115
1	2.448033	3.501433	-2.507116
1	2.553691	3.211931	-0.762904
6	1.095889	1.218063	-3.211609
1	1.057771	0.151828	-3.462533
1	1.521554	1.753353	-4.070393
1	0.068212	1.565939	-3.063064
1	1.585476	0.838772	2.110468
1	2.722840	-2.798970	0.143141

3.8 (14.62)

7	-1.815289	1.383888	1.270530
7	-2.525595	-1.206740	-0.704681
6	0.183019	0.778624	-0.125787
6	-2.391717	0.177735	-0.358322
6	-1.086775	0.795317	0.228251
6	-3.130937	0.823333	0.899458
1	-2.670561	0.773838	-1.233409
6	-1.688507	-2.230071	-0.060693
1	-1.193428	-1.723868	0.773230
6	-3.183203	-1.543341	-1.974813
6	-1.514137	2.468881	2.190955
1	-2.367809	2.505206	2.881593
1	-3.136544	-2.635182	-2.048482
6	-0.575049	-2.783672	-0.970124
1	0.055131	-3.483687	-0.410369
1	-0.987768	-3.326456	-1.829761
1	0.062124	-1.975265	-1.338796
6	-2.527155	-3.383735	0.520431
1	-3.039700	-3.948193	-0.268663
1	-1.884091	-4.090295	1.059156
1	-3.287096	-3.009859	1.212603
6	-2.483794	-0.979152	-3.229923
1	-2.967094	-1.357165	-4.139319
1	-2.535237	0.115498	-3.266923
1	-1.428733	-1.265887	-3.255813
6	-4.675004	-1.165768	-1.966879
1	-5.169475	-1.508702	-2.884025
1	-5.182090	-1.618891	-1.108668
1	-4.811865	-0.079440	-1.907217
6	-4.193430	1.863851	0.528599
1	-5.095127	1.369859	0.146802
1	-4.494229	2.462162	1.398366
1	-3.827922	2.550095	-0.243799
6	-3.676539	-0.155709	1.939134
1	-2.911668	-0.874616	2.243600
1	-4.012976	0.380974	2.835782
1	-4.533988	-0.709562	1.540465
6	-1.403694	3.840527	1.497681
1	-0.586860	3.834469	0.768783
1	-2.328842	4.096280	0.972107
1	-1.198271	4.630153	2.230772
6	-0.256603	2.170594	3.020464
1	-0.119989	2.933579	3.795783
1	-0.330756	1.189863	3.500607
1	0.630313	2.172781	2.379808

7	2.443707	-0.119212	-0.456843
6	2.674102	-2.367993	0.487375
6	1.379217	0.787450	-0.688074
6	2.276964	-0.510470	1.974257
6	3.728197	0.343312	-1.056533
6	2.321720	-1.376088	3.066055
1	2.184251	-0.981048	4.069520
6	2.734739	-3.231457	1.583268
1	2.910745	-4.291881	1.421258
6	2.454772	-0.995151	0.669372
6	1.827179	1.796449	-1.768154
6	2.555764	-2.740205	2.876640
1	2.595480	-3.412996	3.729120
6	3.221389	1.268266	-2.187217
1	3.127568	0.681638	-3.108380
1	3.932046	2.076950	-2.389395
6	4.545411	-0.820488	-1.637885
1	4.921362	-1.485861	-0.854245
1	5.410838	-0.424768	-2.182825
1	3.941931	-1.410207	-2.336056
6	4.595643	1.096034	-0.025508
1	4.064152	1.952022	0.400906
1	5.514657	1.466268	-0.495189
1	4.881163	0.433516	0.798385
6	1.896122	3.225679	-1.194104
1	0.901269	3.556473	-0.879799
1	2.262985	3.926703	-1.954783
1	2.559361	3.294025	-0.325963
6	0.848461	1.788855	-2.955171
1	0.763537	0.786428	-3.388920
1	1.186202	2.475609	-3.742040
1	-0.150003	2.100596	-2.631361
1	2.107003	0.548872	2.125838
1	2.783306	-2.755224	-0.519838

3.5 (30.28)

8	2.339838	2.118122	-0.187425
8	-2.297669	2.014569	-0.663520
7	-1.155557	0.104795	-0.036975
7	1.164577	0.135682	-0.023149
6	-4.678743	-2.256349	-0.075933
6	-4.625737	-1.092463	0.693024
1	-5.481646	-0.793134	1.291463
6	-3.474218	-0.306346	0.703206
6	-2.372044	-0.688274	-0.063875
6	0.012148	-0.599357	0.033890
6	4.711219	-2.187389	0.121137
6	4.546040	-1.235849	-0.886124
1	5.319097	-1.094968	-1.636382
6	3.388085	-0.459493	-0.943333
6	2.393721	-0.640096	0.019131
6	1.273263	1.551935	-0.081137
6	-0.034872	2.319226	0.090800
6	0.003907	3.622017	-0.723104
1	0.876371	4.210924	-0.434311
1	-0.907379	4.196147	-0.545347
1	0.069085	3.413425	-1.795531
6	-1.271228	1.506333	-0.268734
6	-3.570780	-2.632662	-0.836695
1	-3.601578	-3.537683	-1.437053
6	-2.416896	-1.849646	-0.835191
6	-0.149427	2.642106	1.613869
1	-0.188302	1.732854	2.222588
1	-1.058153	3.224518	1.793758
1	0.719392	3.231570	1.920781
6	2.549492	-1.591287	1.027971
6	3.708260	-2.364758	1.075961
1	3.824973	-3.106182	1.861503
1	1.751833	-1.731542	1.749473
1	5.614991	-2.789166	0.160296
1	3.262659	0.278759	-1.726110
1	-3.436058	0.597894	1.300698
1	-5.577860	-2.866248	-0.081183
1	-1.541057	-2.137910	-1.405388

3.10$^{\mathbf{Int1}}$ (17.72)

8	-3.512019	1.252882	2.139649
8	-2.038636	-3.045473	1.897058
7	-1.312393	-1.540558	0.298891
7	1.969181	2.357515	0.001374
7	-1.955306	0.771350	0.504274
7	2.750092	-1.205842	0.064515
6	-1.248184	-4.045768	-3.144897
6	-1.928200	-4.448731	-1.995391
1	-2.454645	-5.399816	-1.980739
6	-1.952832	-3.654301	-0.849713
6	-1.289560	-2.413286	-0.836958
6	-0.905653	-0.160123	0.194233
6	0.419033	0.163565	0.196376
6	1.793039	-0.234503	0.149920
6	1.507133	1.094375	0.108450
6	3.415901	2.587339	0.216924
1	3.843162	1.592265	0.358810
6	-3.737153	3.133632	-2.545429
6	-3.148378	1.904538	-2.847429
1	-3.143959	1.536246	-3.870167
6	-2.571346	1.129477	-1.842530
6	-2.568954	1.578414	-0.514276
6	-2.606223	0.550832	1.717658
6	-2.129303	-0.703178	2.494751
6	-3.266290	-1.141357	3.437392
1	-3.514002	-0.325743	4.119511

1	-2.956210	-2.021270	4.004249
1	-4.169166	-1.397847	2.876255
6	-1.816689	-1.895049	1.544304
6	-0.586285	-2.818883	-3.133324
1	-0.050176	-2.477058	-4.015438
6	-0.601353	-2.012094	-1.995654
6	3.895093	-0.978383	-0.845733
1	3.699361	-0.007667	-1.312782
6	2.758174	-2.402809	0.938623
6	1.072690	3.522615	-0.187409
1	1.741539	4.388813	-0.198715
6	-0.889173	-0.352847	3.359118
1	-0.047923	0.009353	2.764291
1	-0.570285	-1.241459	3.914530
1	-1.161063	0.423865	4.081885
6	-3.166462	2.810468	-0.207585
6	-3.744991	3.574726	-1.221897
1	-4.204767	4.526539	-0.967843
1	-3.190732	3.154178	0.816643
1	-4.188463	3.735476	-3.329519
1	-2.127455	0.170470	-2.084084
1	3.707843	-2.896780	0.710925
1	-2.474010	-3.994245	0.032137
1	-1.234111	-4.675147	-4.030318
1	-0.080312	-1.063665	-2.006609
6	3.925675	-2.027002	-1.970147
1	4.716788	-1.791238	-2.691799
1	4.124794	-3.030809	-1.577808
1	2.967554	-2.054054	-2.498256
6	5.250298	-0.887778	-0.123992
1	5.542637	-1.845473	0.320422
1	6.034933	-0.607643	-0.836169
1	5.230399	-0.139143	0.675172
6	1.644866	-3.411974	0.637841
1	1.837643	-4.343151	1.183666
1	0.666057	-3.046361	0.953267
1	1.595908	-3.642005	-0.429912
6	2.785290	-2.012233	2.423328
1	2.871315	-2.906024	3.051517
1	3.631393	-1.352743	2.645048
1	1.863676	-1.493926	2.708970
6	3.692144	3.388045	1.499207
1	4.772337	3.456045	1.672233
1	3.305639	4.411238	1.435343
1	3.236038	2.902229	2.367667
6	4.089267	3.215365	-1.012011
1	3.718889	4.227620	-1.208196
1	5.170911	3.287762	-0.851671
1	3.913869	2.610102	-1.907594
6	0.111496	3.702362	0.994504
1	-0.547545	2.838704	1.108005
1	0.667536	3.837644	1.928363
1	-0.517717	4.585016	0.838087
6	0.370664	3.468372	-1.548883
1	-0.263511	4.350466	-1.687080
1	1.107666	3.441694	-2.359088
1	-0.270023	2.588059	-1.636473

3.10^{TS1} (-239.25)

8	4.188895	-0.952921	-1.772474
8	1.428720	-4.029819	-0.077330
7	0.927543	-1.833916	0.405635
7	-1.312934	2.488767	-0.032464
7	2.436331	-0.193251	-0.499040
7	-2.927661	-0.233580	-0.887114
6	-1.268601	-2.630154	3.955435
6	-1.296660	-3.535470	2.894235
1	-1.877091	-4.450935	2.974556
6	-0.588290	-3.287528	1.717993
6	0.176630	-2.116608	1.591176
6	1.088677	-0.467635	-0.056225
6	0.053299	0.343112	-0.207414
6	-1.695859	0.202766	-1.116393
6	-0.983220	1.206793	-0.432272
6	-2.429347	3.141322	-0.759455
1	-2.992298	2.323332	-1.211561
6	4.693728	3.047464	1.024169
6	4.026377	2.183163	1.894165
1	4.095615	2.327506	2.969103
6	3.286383	1.113797	1.390473
6	3.188766	0.914613	0.008672
6	3.062361	-1.114338	-1.331309
6	2.223700	-2.364361	-1.638865
6	3.150423	-3.479783	-2.139967
1	3.670702	-3.148511	-3.041217
1	2.565487	-4.375756	-2.357987
1	3.901689	-3.738011	-1.389297
6	1.494904	-2.844164	-0.366122
6	-0.514213	-1.463079	3.827742
1	-0.472617	-0.745278	4.642911
6	0.203059	-1.209330	2.660234
6	-3.790946	0.190232	0.260278
1	-3.252235	1.018813	0.723563
6	-3.431071	-1.368832	-1.722449
6	-0.370385	3.356355	0.711774
1	-0.923235	4.285282	0.880164
6	1.180457	-2.021851	-2.740716
1	0.462025	-1.258030	-2.429695
1	0.629825	-2.930211	-3.008469
1	1.705435	-1.667432	-3.634553
6	3.865498	1.774248	-0.864649
6	4.615825	2.832700	-0.353283

1	5.140507	3.493484	-1.038074
1	3.808681	1.603839	-1.932603
1	5.278729	3.874610	1.416876
1	2.802455	0.415895	2.065996
1	-4.449663	-1.569433	-1.377399
1	-0.605605	-4.008257	0.913825
1	-1.822164	-2.831910	4.868226
1	0.787811	-0.301819	2.577887
6	-3.912918	-0.922452	1.311289
1	-4.464044	-0.546191	2.181341
1	-4.461454	-1.789494	0.926206
1	-2.929174	-1.257567	1.649560
6	-5.169420	0.695724	-0.189536
1	-5.792953	-0.110485	-0.590844
1	-5.703047	1.120717	0.668347
1	-5.087706	1.473185	-0.955938
6	-2.601949	-2.639537	-1.519902
1	-3.027320	-3.462448	-2.106021
1	-1.572031	-2.476736	-1.845468
1	-2.583234	-2.939312	-0.468081
6	-3.497489	-0.953168	-3.195059
1	-3.883046	-1.775657	-3.808019
1	-4.153417	-0.085990	-3.332155
1	-2.497991	-0.687527	-3.552765
6	-1.955076	4.044018	-1.912005
1	-2.818469	4.384118	-2.495958
1	-1.436083	4.935520	-1.544011
1	-1.281351	3.501811	-2.582822
6	-3.382816	3.898688	0.177550
1	-2.928247	4.807908	0.585873
1	-4.274732	4.208718	-0.378367
1	-3.703184	3.273389	1.016622
6	0.899333	3.710746	-0.076715
1	1.455375	2.819223	-0.365159
1	0.661083	4.271136	-0.984940
1	1.562742	4.327836	0.538962
6	-0.057212	2.772996	2.094988
1	0.523113	3.492623	2.682998
1	-0.980261	2.542801	2.637378
1	0.533808	1.858345	2.013312

3.10$^{TS1'}$ (-1515.67)

8	-3.845175	-0.481913	-1.657964
8	-1.227498	3.093433	-2.541398
7	-0.642406	1.792796	-0.734091
7	0.835474	-2.903972	0.006578
7	-2.097191	-0.053488	-0.202854
7	3.028487	-0.178834	0.334597
6	0.415300	5.094346	1.710176
6	0.844412	5.036167	0.383610
1	1.447914	5.840035	-0.029600
6	0.507750	3.952260	-0.427864
6	-0.269555	2.907695	0.089882
6	-0.741251	0.455290	-0.219306
6	0.329516	-0.336098	-0.006679
6	1.789143	-0.723709	-0.098803
6	0.822095	-1.616108	0.405931
6	2.061403	-3.237875	-0.640772
1	2.148102	-1.661707	-1.034445
6	-3.836076	-1.307338	3.483550
6	-2.549215	-0.773278	3.435935
1	-1.967004	-0.662242	4.347203
6	-1.985210	-0.377116	2.223992
6	-2.703924	-0.495572	1.018830
6	-2.751018	0.015763	-1.431125
6	-2.000316	0.796519	-2.544050
6	-3.041251	1.305983	-3.556271
1	-3.578566	0.461419	-3.991667
1	-2.539415	1.873935	-4.342023
1	-3.771007	1.964007	-3.077066
6	-1.246688	2.016892	-1.966863
6	-0.370366	4.059344	2.219954
1	-0.727281	4.097280	3.245849
6	-0.719020	2.975410	1.415106
6	3.117723	0.269301	1.745075
1	2.365695	-0.327895	2.274089
6	3.851627	0.531119	-0.670803
6	-0.360301	-3.795181	-0.046744
1	0.035073	-4.772259	-0.331430
6	-1.007997	-0.139955	-3.286762
1	-0.223245	-0.530304	-2.634924
1	-0.535612	0.414655	-4.104401
1	-1.558665	-0.982972	-3.717652
6	-4.000427	-1.044594	1.069434
6	-4.547329	-1.436873	2.291491
1	-5.551984	-1.852115	2.300064
1	-4.570556	-1.151981	0.160514
1	-4.273158	-1.618168	4.428202
1	-0.979034	0.019740	2.214782
1	4.537407	1.159376	-0.093004
1	0.825672	3.920979	-1.461258
1	0.682826	5.940343	2.337227
1	-1.349765	2.187267	1.810234
6	2.790239	1.752661	1.978934
1	2.789636	1.973392	3.053209
1	3.535145	2.408348	1.512981
1	1.809119	2.015546	1.580539
6	4.488458	-0.086899	2.343910
1	5.298746	0.474887	1.864463
1	4.509121	0.161820	3.411547
1	4.705910	-1.153808	2.233664
6	3.055606	1.462212	-1.597221

1	3.738134	2.007301	-2.260044
1	2.361040	0.897290	-2.229271
1	2.477343	2.192082	-1.026140
6	4.719501	-0.442438	-1.485146
1	5.381975	0.111336	-2.161682
1	5.338258	-1.057502	-0.824251
1	4.102394	-1.109509	-2.097609
6	2.004678	-4.329725	-1.685844
1	2.903396	-4.242638	-2.306680
1	2.021745	-5.344836	-1.256847
1	1.139068	-4.248812	-2.348503
6	3.298247	-3.343268	0.234461
1	3.319432	-4.332187	0.721629
1	4.205563	-3.256882	-0.370824
1	3.335360	-2.572082	1.001305
6	-1.395847	-3.371110	-1.091681
1	-1.892380	-2.441488	-0.814092
1	-0.941737	-3.241440	-2.079237
1	-2.164311	-4.147838	-1.172176
6	-0.959253	-3.934733	1.357673
1	-1.774301	-4.666157	1.334202
1	-0.204164	-4.283020	2.070046
1	-1.364946	-2.985423	1.716297

3.10^{Int2} (21.55)

8	-2.783288	3.069691	1.429957
8	-4.397015	-1.081749	0.466683
7	-2.282005	-0.545865	-0.212550
7	2.363863	0.037983	-1.280870
7	-1.403241	1.612776	0.337196
7	1.944688	-1.176840	1.865818
6	-2.353843	-3.666234	-3.071469
6	-2.316853	-3.969543	-1.709097
1	-2.320240	-5.005667	-1.381189
6	-2.282981	-2.946436	-0.761636
6	-2.284133	-1.613294	-1.176812
6	-1.095930	0.261219	-0.067578
6	0.104929	-0.205895	-0.356791
6	1.978111	-0.104223	1.120708
6	1.454975	-0.117760	-0.255615
6	3.804629	0.128145	-0.964700
1	3.858784	0.111051	0.127810
6	0.884516	4.898822	-1.043379
6	-0.354448	4.607343	-1.618937
1	-0.747199	5.231084	-2.417356
6	-1.095626	3.517083	-1.165565
6	-0.600205	2.715495	-0.133202
6	-2.498385	1.920189	1.131013
6	-3.296570	0.717482	1.649512
6	-4.701961	1.168390	2.066776
1	-4.629380	1.944511	2.831456
1	-5.264953	0.315417	2.451441
1	-5.251064	1.581193	1.215878
6	-3.403607	-0.379532	0.582859
6	-2.363825	-2.332277	-3.483759
1	-2.404163	-2.087563	-4.541734
6	-2.334622	-1.306830	-2.538692
6	1.520424	-2.555247	1.435313
1	1.190596	-2.430628	0.403087
6	2.412848	-1.039469	3.290886
6	1.976470	0.044921	-2.708503
1	2.918935	0.192722	-3.244533
6	-2.544152	0.132121	2.876040
1	-1.524234	-0.174073	2.622709
1	-3.087794	-0.737006	3.261416
1	-2.488634	0.888006	3.666370
6	0.631347	3.008740	0.452701
6	1.373902	4.097594	-0.010405
1	2.332779	4.324551	0.448582
1	1.018139	2.376358	1.244408
1	1.461325	5.750729	-1.393823
1	-2.065491	3.289060	-1.596878
1	2.374356	-2.042893	3.723187
1	-2.272902	-3.174176	0.298996
1	-2.382219	-4.464944	-3.807655
1	-2.354855	-0.266387	-2.848892
6	0.324895	-3.067153	2.246115
1	-0.001200	-4.030320	1.837581
1	0.569869	-3.226449	3.302291
1	-0.516073	-2.371116	2.184325
6	2.702479	-3.532131	1.466281
1	3.062810	-3.721214	2.483723
1	2.388919	-4.494403	1.046094
1	3.541347	-3.160072	0.869317
6	1.469645	-0.130921	4.082168
1	1.804498	-0.055870	5.122772
1	1.460135	0.871211	3.643647
1	0.445849	-0.518357	4.080633
6	3.861027	-0.546625	3.340527
1	4.203669	-0.493559	4.379843
1	4.530095	-1.221108	2.794851
1	3.931808	0.448950	2.894041
6	4.405661	1.470743	-1.409852
1	5.443366	1.549266	-1.065012
1	4.414983	1.580263	-2.500507
1	3.834724	2.302710	-0.986797
6	4.610025	-1.067301	-1.497798
1	4.629379	-1.095391	-2.593378
1	5.649154	-1.002919	-1.154299
1	4.189977	-2.014871	-1.143928
6	1.064489	1.215733	-3.097678
1	0.065809	1.106372	-2.671315

1	1.476935	2.169006	-2.754748
1	0.966567	1.253309	-4.189492
6	1.413499	-1.312758	-3.159343
1	1.195270	-1.287653	-4.233370
1	2.139421	-2.113017	-2.978843
1	0.489818	-1.558378	-2.631515

3.10^{TS2} (-1026.22)

8	-4.288248	1.672310	0.650971
8	-3.513447	-2.887237	-0.030388
7	-1.810083	-1.394935	-0.288687
7	2.127082	0.442830	-1.644661
7	-2.207975	0.952888	0.059361
7	2.305049	-0.061796	1.849083
6	0.558500	-4.484031	-1.960303
6	0.252335	-4.495436	-0.598055
1	0.609423	-5.303463	0.034816
6	-0.523356	-3.476083	-0.045193
6	-0.991531	-2.439018	-0.854756
6	-1.230286	-0.079179	-0.170941
6	0.053687	0.146577	-0.317751
6	2.324591	0.521419	0.651638
6	1.378085	0.323254	-0.443516
6	3.473250	0.078067	-1.356619
1	3.378653	0.626482	0.009710
6	-1.107394	5.016293	-0.378245
6	-1.915852	4.400543	-1.335508
1	-2.283617	4.967341	-2.186440
6	-2.260525	3.055501	-1.200817
6	-1.800360	2.327038	-0.102646
6	-3.508165	0.743926	0.495803
6	-3.904706	-0.688267	0.849732
6	-5.396403	-0.895500	0.534775
1	-5.991403	-0.158918	1.077643
1	-5.695565	-1.906219	0.818308
1	-5.592597	-0.770539	-0.535103
6	-3.083989	-1.752932	0.125737
6	0.074355	-3.454562	-2.769969
1	0.294507	-3.447822	-3.834102
6	-0.705262	-2.436814	-2.220292
6	1.598302	-1.336333	2.153352
1	1.068602	-1.585690	1.233393
6	3.111435	0.560257	2.938954
6	1.743629	1.324217	-2.764431
1	2.605832	1.311340	-3.438474
6	-3.663317	-0.871092	2.374408
1	-2.609321	-0.732226	2.639224
1	-3.966065	-1.879401	2.673387
1	-4.258807	-0.139068	2.928417
6	-0.999063	2.940811	0.861243
6	-0.647490	4.283351	0.717758
1	-0.020709	4.758069	1.467776
1	-0.654826	2.366366	1.714838
1	-0.839631	6.064153	-0.483732
1	-2.899718	2.570059	-1.931370
1	2.993333	-0.089033	3.811385
1	-0.786000	-3.490039	1.007946
1	1.161307	-5.279189	-2.390462
1	-1.096848	-1.641262	-2.844543
6	0.556109	-1.161000	3.265060
1	-0.016716	-2.087573	3.385069
1	1.013573	-0.934333	4.235075
1	-0.142336	-0.356529	3.015717
6	2.583368	-2.473901	2.460884
1	3.142051	-2.300611	3.388114
1	2.034890	-3.415436	2.580390
1	3.300413	-2.602174	1.644093
6	2.562817	1.947689	3.292058
1	3.155891	2.402691	4.093495
1	2.600245	2.600164	2.413876
1	1.522441	1.885353	3.628774
6	4.605670	0.608281	2.594136
1	5.173808	0.985229	3.451984
1	4.988425	-0.386417	2.342027
1	4.792683	1.276431	1.747741
6	4.590760	0.903008	-1.960838
1	5.539956	0.648436	-1.475232
1	4.725590	0.697598	-3.034868
1	4.425926	1.978755	-1.841949
6	3.755796	-1.414277	-1.329373
1	2.902648	-1.976542	-0.939926
1	3.962351	-1.792945	-2.344143
1	4.637480	-1.639905	-0.715501
6	1.503041	2.773088	-2.317208
1	0.656874	2.834130	-1.629270
1	2.382971	3.180532	-1.808406
1	1.283833	3.407441	-3.184059
6	0.552948	0.770492	-3.559929
1	0.394180	1.374862	-4.461092
1	0.740137	-0.263987	-3.863804
1	-0.364675	0.798084	-2.965955

3.10 (11.57)

8	3.699352	2.548501	-1.030019
8	4.111970	-2.008736	-0.701369
7	2.174084	-1.034883	0.017832
7	-2.157004	0.287258	1.547269
7	1.980051	1.350127	-0.128830
7	-2.716678	-0.574958	-1.610496
6	1.257591	-4.471217	2.314433
6	1.274655	-4.546537	0.920920
1	1.066359	-5.489662	0.423068

6	1.564567	-3.414941	0.158121
6	1.837696	-2.201832	0.791857
6	1.297865	0.100072	0.065980
6	0.010182	0.010934	0.322111
6	-2.471637	0.332340	-0.531205
6	-1.294231	0.161261	0.476616
6	-3.405735	0.392265	0.760962
1	-2.407200	1.344652	-0.941354
6	0.212084	4.932176	1.265066
6	1.175091	4.278562	2.036167
1	1.483459	4.693911	2.991657
6	1.751764	3.092782	1.578711
6	1.364997	2.562991	0.347692
6	3.139809	1.473953	-0.880756
6	3.625458	0.192732	-1.566326
6	5.127043	0.301005	-1.862545
1	5.317030	1.178396	-2.483971
1	5.469649	-0.600998	-2.373536
1	5.703402	0.406944	-0.938926
6	3.357227	-1.049493	-0.710525
6	1.540564	-3.257925	2.945651
1	1.543742	-3.193915	4.030411
6	1.835026	-2.125275	2.186764
6	-2.298850	-1.983253	-1.517056
1	-2.054247	-2.150095	-0.463459
6	-2.978014	-0.009412	-2.943297
6	-1.972311	0.291522	2.993520
1	-2.922303	0.666078	3.397847
6	2.833366	0.041385	-2.895857
1	1.753797	-0.034144	-2.727577
1	3.166039	-0.860214	-3.420337
1	3.024449	0.909298	-3.535148
6	0.413564	3.221238	-0.433578
6	-0.166344	4.402877	0.028900
1	-0.904466	4.916431	-0.581395
1	0.141976	2.809176	-1.400485
1	-0.234524	5.856778	1.620728
1	2.509427	2.580639	2.163892
1	-3.076742	-0.870403	-3.612626
1	1.594424	-3.470158	-0.924246
1	1.033504	-5.354447	2.906265
1	2.071487	-1.181790	2.669552
6	-1.028475	-2.310737	-2.324996
1	-0.733687	-3.353618	-2.159654
1	-1.188722	-2.183183	-3.402196
1	-0.199579	-1.668397	-2.015414
6	-3.437319	-2.950340	-1.889105
1	-3.720251	-2.854681	-2.944400
1	-3.123149	-3.988914	-1.731071
1	-4.328900	-2.762972	-1.283704
6	-1.838625	0.866458	-3.505013
1	-2.057704	1.162356	-4.537997
1	-1.712728	1.789044	-2.925608
1	-0.885411	0.329858	-3.497587
6	-4.318795	0.743420	-2.989716
1	-4.541072	1.081316	-4.009073
1	-5.135688	0.097119	-2.652534
1	-4.301899	1.632101	-2.346811
6	-4.122991	1.732821	0.946522
1	-4.948354	1.830131	0.230931
1	-4.551823	1.822716	1.952701
1	-3.432336	2.570377	0.797067
6	-4.372806	-0.774593	0.952628
1	-3.862307	-1.738643	0.887514
1	-4.862212	-0.714588	1.932801
1	-5.155082	-0.748482	0.186351
6	-0.863122	1.256940	3.429619
1	0.109835	0.931363	3.049910
1	-1.047701	2.267534	3.053789
1	-0.806723	1.295078	4.523593
6	-1.746157	-1.127222	3.544907
1	-1.647086	-1.102606	4.636849
1	-2.585209	-1.784325	3.293651
1	-0.834058	-1.565757	3.128152

3.6 (8.07)

8	2.499910	1.163183	-1.294582
8	-2.499762	1.162451	1.295222
7	1.185360	-0.240851	-0.060265
6	3.499893	-3.146995	-0.579945
1	3.544726	-4.062975	-1.162649
6	2.398851	-2.301980	-0.713271
6	2.342455	-1.126381	0.032577
6	1.224237	3.458237	-0.645442
1	2.188208	3.433458	-1.139651
6	4.538855	-2.820070	0.293965
6	-3.372446	-0.793208	-0.911521
6	1.493496	1.050487	-0.619307
6	0.628207	2.224886	-0.319055
6	-1.493555	1.050110	0.619607
6	-2.342187	-1.126845	-0.032605
6	-2.398289	-2.302632	0.712965
6	4.471683	-1.641700	1.039207
1	5.272218	-1.382660	1.726577
6	-0.628683	2.224731	0.319118
6	3.372542	-0.792790	0.911707
6	-1.225130	3.457930	0.645330
1	-2.189078	3.432901	1.139576
6	0.614617	4.664529	-0.331467
1	1.098780	5.600300	-0.595801
6	-4.538344	-2.820828	-0.294116
6	-0.615933	4.664378	0.331141

1	-1.100414	5.600029	0.595318
6	-3.499212	-3.147794	0.579575
1	-3.543816	-4.063923	1.162065
6	-4.471464	-1.642266	-1.039081
1	-5.272130	-1.383194	-1.726288
7	-1.185237	-0.241135	0.060288
6	0.000121	-0.895968	-0.000073
1	-3.312446	0.122500	-1.492507
1	-1.572579	-2.550805	1.370206
1	-5.393874	-3.482653	-0.396612
1	3.312327	0.122776	1.492897
1	1.573273	-2.550126	-1.370688
1	5.394479	-3.481780	0.396418

3.12 (17.59)

8	-1.846425	2.190418	2.641827
8	-2.220173	-3.066429	1.409720
7	-1.443752	-1.337517	0.110802
7	2.268621	2.141674	-0.398393
7	-1.585873	1.007594	0.675494
7	2.613416	-1.486152	-0.774386
6	-3.180135	-2.760939	-3.497251
6	-3.896493	-2.831699	-2.301312
1	-4.905584	-3.235379	-2.294416
6	-3.338878	-2.379632	-1.106137
6	-2.041663	-1.849754	-1.095244
6	-0.799954	-0.056343	0.116701
6	0.529604	0.100212	-0.145932
6	1.815347	-0.425826	-0.469415
6	1.680316	0.924523	-0.348307
6	3.745267	2.203959	-0.312159
1	4.065690	1.170227	-0.164168
6	-4.312479	3.111640	-1.836881
6	-3.389027	2.209278	-2.362569
1	-3.361538	2.010609	-3.430914
6	-2.494583	1.540763	-1.528890
6	-2.500799	1.757168	-0.141283
6	-1.491074	1.173207	2.052604
6	-1.645403	-1.986060	1.322261
6	-1.889541	-2.231438	-3.487293
1	-1.316129	-2.169482	-4.408842
6	-1.321156	-1.783443	-2.295019
6	3.800012	-1.249756	-1.626583
1	3.714563	-0.209070	-1.952450
6	2.469587	-2.804569	-0.107372
6	1.513737	3.407786	-0.569781
1	2.290037	4.169556	-0.691623
6	-3.432038	2.670887	0.387540
6	-4.322630	3.330074	-0.459476
1	-5.033175	4.028672	-0.024502
1	-3.450885	2.869659	1.447751
1	-5.010359	3.632886	-2.486322
1	-1.800225	0.827046	-1.952762
1	3.355250	-3.366438	-0.419555
1	-3.902499	-2.442217	-0.185009
1	-3.622868	-3.113441	-4.424824
1	-0.316093	-1.376065	-2.292401
6	3.760872	-2.124780	-2.889422
1	4.604969	-1.881803	-3.545245
1	3.829204	-3.190764	-2.645247
1	2.832442	-1.960722	-3.445237
6	5.134460	-1.402892	-0.876598
1	5.317772	-2.440264	-0.575846
1	5.965003	-1.100709	-1.524795
1	5.160889	-0.782551	0.025465
6	1.245556	-3.595100	-0.581402
1	1.265368	-4.602605	-0.149973
1	0.311762	-3.121733	-0.273412
1	1.236590	-3.690289	-1.671639
6	2.522841	-2.669813	1.419680
1	2.475871	-3.658254	1.890250
1	3.449943	-2.181685	1.739598
1	1.679777	-2.083389	1.796248
6	4.213787	3.000439	0.915676
1	5.305459	2.950318	1.000257
1	3.937800	4.058397	0.846665
1	3.778107	2.591569	1.832654
6	4.390441	2.718221	-1.608650
1	4.135909	3.766092	-1.802440
1	5.482233	2.654556	-1.537450
1	4.067025	2.127483	-2.472372
6	0.692343	3.791974	0.666426
1	-0.141084	3.109617	0.836634
1	1.317685	3.802499	1.565084
1	0.271893	4.795338	0.533142
6	0.681508	3.397612	-1.857095
1	0.205933	4.373405	-2.005385
1	1.312165	3.185475	-2.727570
1	-0.115097	2.650705	-1.813608
6	-0.635938	-2.288965	3.524010
6	-0.052740	-1.894092	4.723778
6	0.099159	-0.534675	5.000474
6	-0.351223	0.406567	4.081349
6	-0.913203	0.026152	2.852370
6	-1.044423	-1.353061	2.559879
1	-0.792954	-3.338932	3.302999
1	0.270417	-2.643068	5.441782
1	0.545643	-0.208675	5.936124
1	-0.299750	1.466575	4.304294

3.13^{TS1} (-83.87)

8	-3.487533	0.709374	-2.480620

8	-1.687119	3.208309	1.830901
7	-1.074491	1.089651	1.188377
7	1.573315	-2.329790	-0.930406
7	-2.303343	0.050975	-0.626013
7	3.115453	0.497305	-0.278521
6	0.386707	-0.182420	4.976544
6	0.489951	1.156218	4.595166
1	0.952728	1.878869	5.262385
6	0.006829	1.592500	3.362401
6	-0.602989	0.683956	2.479437
6	-1.031198	0.176228	0.062690
6	0.068695	-0.424280	-0.335891
6	1.991488	0.193981	-0.893686
6	1.232628	-0.996263	-0.758746
6	2.875563	-2.626415	-1.572080
1	3.464058	-1.714270	-1.471339
6	-5.036118	-2.987337	0.510644
6	-4.544972	-2.085800	1.455743
1	-4.866922	-2.148311	2.491816
6	-3.656594	-1.079839	1.074224
6	-3.228749	-0.985801	-0.256752
6	-2.611521	0.928074	-1.653304
6	-1.450536	2.409734	0.932055
6	-0.213187	-1.086069	4.100572
1	-0.310319	-2.133497	4.374354
6	-0.703203	-0.660681	2.866461
6	3.799026	-0.337894	0.763497
1	3.265690	-1.290118	0.750990
6	3.661840	1.878509	-0.496370
6	0.530189	-3.383378	-1.006450
1	1.079885	-4.298427	-1.246342
6	-3.730798	-1.882393	-1.208309
6	-4.632788	-2.873641	-0.820935
1	-5.021262	-3.560396	-1.568452
1	-3.432521	-1.784303	-2.243606
1	-5.736111	-3.763989	0.806599
1	-3.311187	-0.354568	1.802268
1	4.555597	1.957452	0.129273
1	0.079307	2.637691	3.098506
1	0.762378	-0.512976	5.940852
1	-1.170911	-1.377955	2.205385
6	3.622666	0.272117	2.161030
1	4.035281	-0.409947	2.913435
1	4.150741	1.227240	2.258930
1	2.566292	0.433433	2.391750
6	5.276789	-0.598731	0.439411
1	5.879775	0.312869	0.509991
1	5.687630	-1.316066	1.159003
1	5.408489	-1.014655	-0.564827
6	2.659286	2.945935	-0.053159
1	3.085059	3.945330	-0.198875
1	1.741307	2.863992	-0.640073
1	2.401623	2.833951	1.005336
6	4.075266	2.050112	-1.960430
1	4.485529	3.052229	-2.127974
1	4.836409	1.315430	-2.246764
1	3.202767	1.913943	-2.606994
6	2.762635	-2.909067	-3.080840
1	3.764974	-3.003585	-3.514680
1	2.227895	-3.842721	-3.285532
1	2.245222	-2.092580	-3.594327
6	3.633908	-3.749362	-0.848138
1	3.137833	-4.719919	-0.958729
1	4.640302	-3.851280	-1.269858
1	3.728859	-3.539268	0.221893
6	-0.492622	-3.152260	-2.132100
1	-1.022726	-2.208030	-1.999792
1	-0.010222	-3.138298	-3.113321
1	-1.235289	-3.957667	-2.127336
6	-0.149361	-3.619675	0.348012
1	-0.762979	-4.526674	0.303724
1	0.594534	-3.740924	1.142325
1	-0.808523	-2.789477	0.610786
6	-0.924017	4.205728	-0.633940
6	-0.798062	4.811225	-1.879738
6	-1.207188	4.130185	-3.028504
6	-1.751676	2.857337	-2.910276
6	-1.850376	2.221805	-1.664345
6	-1.419763	2.896686	-0.502300
1	-0.643350	4.737875	0.267988
1	-0.393781	5.817325	-1.951578
1	-1.123234	4.598036	-4.005574
1	-2.136631	2.331624	-3.777488

3.13$^{\mathbf{TS1'}}$ (-1499.45)

8	2.673351	-2.909756	0.956843
8	1.340072	1.588150	3.386691
7	1.111643	1.090048	1.147104
7	-1.952925	-1.900579	-1.417472
7	1.809523	-0.973256	0.068981
7	-2.674186	1.444036	-0.660976
6	2.458269	4.866901	-0.282013
6	1.763690	4.780171	0.924656
1	1.555796	5.678877	1.499739
6	1.324207	3.550583	1.414739
6	1.578767	2.372678	0.691402
6	0.790906	0.039034	0.213600
6	-0.427341	-0.057571	-0.356603
6	-1.886469	0.276728	-0.459411
6	-1.309979	-0.722247	-1.271663
6	-3.290247	-1.840620	-0.928715
1	-2.762178	-0.646920	0.042330

6	4.385882	-0.950036	-3.310741
6	3.045672	-0.586583	-3.436277
1	2.647998	-0.283888	-4.401537
6	2.200103	-0.606676	-2.325745
6	2.688728	-0.986650	-1.066899
6	1.921868	-1.945527	1.056712
6	1.073809	0.783419	2.501142
6	2.712905	3.698132	-0.998675
1	3.257917	3.737862	-1.938241
6	2.280686	2.462571	-0.518557
6	-2.323019	2.298463	-1.821548
1	-1.876644	1.608936	-2.547907
6	-3.237295	2.101727	0.539992
6	-1.307143	-3.182819	-1.821850
1	-2.121893	-3.908230	-1.850672
6	4.040593	-1.341101	-0.940143
6	4.873680	-1.324307	-2.057149
1	5.918366	-1.599769	-1.939662
1	4.432470	-1.635913	0.023494
1	5.043123	-0.937781	-4.175713
1	1.163351	-0.308695	-2.430702
1	-3.458453	3.129510	0.233595
1	0.805710	3.501585	2.360439
1	2.798579	5.828900	-0.655310
1	2.492690	1.568759	-1.089584
6	-1.292973	3.400627	-1.527570
1	-1.041655	3.937356	-2.450354
1	-1.684575	4.138313	-0.817301
1	-0.369115	2.989272	-1.116774
6	-3.586800	2.888531	-2.468691
1	-4.088732	3.602618	-1.805482
1	-3.321832	3.428881	-3.385000
1	-4.305928	2.104655	-2.726894
6	-2.273674	2.180453	1.732936
1	-2.736575	2.741638	2.553288
1	-2.028157	1.181994	2.111293
1	-1.341455	2.680905	1.460589
6	-4.571938	1.460361	0.954932
1	-5.017436	2.008589	1.793996
1	-5.282472	1.468056	0.122270
1	-4.429815	0.421907	1.275103
6	-3.864938	-3.127179	-0.379184
1	-4.704750	-2.862790	0.273299
1	-4.274158	-3.790982	-1.157660
1	-3.147847	-3.693283	0.221545
6	-4.301236	-1.048991	-1.738075
1	-4.657386	-1.665274	-2.580110
1	-5.171980	-0.798470	-1.124417
1	-3.890781	-0.119971	-2.128435
6	-0.243158	-3.681657	-0.845097
1	0.662683	-3.076880	-0.892046
1	-0.610141	-3.683282	0.185630
1	0.033678	-4.708157	-1.109838
6	-0.761115	-3.046419	-3.249786
1	-0.396702	-4.019890	-3.595613
1	-1.538454	-2.703002	-3.939958
1	0.075181	-2.341624	-3.284252
6	0.639285	-0.611704	2.889183
6	-0.112981	-0.673627	4.072949
6	-0.521135	-1.890318	4.609004
6	-0.131646	-3.081494	3.993051
6	0.653780	-3.036941	2.846428
6	1.025825	-1.815159	2.262679
1	-0.355963	0.259305	4.569696
1	-1.121625	-1.909252	5.514432
1	-0.422490	-4.039987	4.414451
1	1.012477	-3.949293	2.382462

3.13^{Int2} (21.52)

8	2.010461	-0.523396	3.337510
8	3.019666	-2.787975	-1.440181
7	1.089751	-1.888282	-0.623702
7	-2.653096	1.037243	-0.457467
7	0.648760	-0.916300	1.556601
7	0.230896	2.901614	-0.699156
6	-1.279130	-4.549236	-2.920076
6	-0.386633	-3.681250	-3.553342
1	-0.300870	-3.682667	-4.636748
6	0.399137	-2.807239	-2.803430
6	0.299293	-2.800513	-1.408316
6	0.400795	-0.857171	0.125607
6	-0.460757	-0.045820	-0.458481
6	-0.630522	2.283822	0.059424
6	-1.280623	1.038290	-0.338087
6	-3.385907	2.313442	-0.320298
1	-2.635050	3.035522	0.015549
6	-2.574461	-1.527940	4.235541
6	-1.819530	-2.613077	3.787533
1	-2.049994	-3.618235	4.130118
6	-0.754736	-2.408551	2.908321
6	-0.452656	-1.118431	2.466110
6	1.867091	-0.596910	2.121539
6	2.464793	-1.945262	-0.741997
6	-1.377070	-4.541603	-1.528278
1	-2.063100	-5.217289	-1.024436
6	-0.585529	-3.675295	-0.772789
6	0.589593	2.545318	-2.117284
1	0.016248	1.640301	-2.324204
6	0.909865	4.117023	-0.123886
6	-3.428550	-0.159828	-0.858321
1	-4.459017	0.200196	-0.933358
6	-1.197418	-0.027516	2.922909

6	-2.257649	-0.237007	3.805648
1	-2.832011	0.612671	4.166141
1	-0.944228	0.971309	2.581245
1	-3.399105	-1.686027	4.925512
1	-0.139203	-3.240787	2.580046
1	1.575505	4.489842	-0.906677
1	1.098133	-2.137068	-3.290951
1	-1.890140	-5.229070	-3.507685
1	-0.653468	-3.673879	0.310045
6	2.074659	2.199083	-2.261079
1	2.264092	1.846708	-3.281559
1	2.726017	3.063182	-2.087913
1	2.361254	1.403892	-1.568845
6	0.146215	3.645293	-3.089694
1	0.704378	4.577860	-2.949771
1	0.321523	3.310732	-4.118302
1	-0.921501	3.864088	-2.982655
6	1.752771	3.733564	1.093265
1	2.267140	4.618262	1.485176
1	1.111064	3.323468	1.878603
1	2.505643	2.982117	0.837257
6	-0.115922	5.205258	0.202522
1	0.393982	6.100207	0.575793
1	-0.696110	5.488194	-0.682687
1	-0.806571	4.849918	0.972824
6	-4.452505	2.247839	0.783065
1	-4.896995	3.238861	0.930530
1	-5.267429	1.557973	0.536141
1	-4.005367	1.925385	1.728363
6	-3.963497	2.812107	-1.654202
1	-4.741701	2.143621	-2.040138
1	-4.416624	3.801617	-1.522234
1	-3.180067	2.892792	-2.415526
6	-3.426618	-1.272975	0.196745
1	-2.441822	-1.732839	0.294364
1	-3.723727	-0.889739	1.177033
1	-4.134349	-2.056397	-0.099566
6	-3.038452	-0.674303	-2.254422
1	-3.694717	-1.505489	-2.535595
1	-3.148791	0.117182	-3.004010
1	-2.008199	-1.034754	-2.281242
6	4.490266	-0.579539	-0.705961
6	5.391891	0.336475	-0.178441
6	5.130713	0.926728	1.061003
6	3.971512	0.591020	1.750224
6	3.027999	-0.298568	1.207886
6	3.291749	-0.895468	-0.041453
1	4.697041	-1.088331	-1.640850
1	6.302966	0.574289	-0.720900
1	5.836385	1.629185	1.496336
1	3.772527	0.993680	2.737178

3.13^{TS2} (-1013.87)

8	0.685747	1.767814	3.327343
8	2.334881	3.294747	-1.510264
7	1.666021	1.215008	-0.843462
7	-1.047143	-2.764625	-0.373252
7	1.105146	0.557628	1.422182
7	-3.139404	0.009607	-0.404509
6	4.372595	-0.558072	-3.585127
6	3.002425	-0.793604	-3.702496
1	2.624619	-1.429239	-4.499192
6	2.105429	-0.204972	-2.809162
6	2.581115	0.611000	-1.779232
6	0.817826	0.387496	-0.001682
6	-0.052453	-0.474243	-0.488792
6	-2.422745	-1.005168	0.070828
6	-1.057019	-1.379476	-0.256133
6	-2.378984	-3.243087	-0.586718
1	-2.941010	-2.091702	0.228584
6	3.442551	-2.374668	3.410825
6	3.800429	-1.918315	2.141521
1	4.690322	-2.303827	1.650944
6	3.030526	-0.952054	1.495099
6	1.879460	-0.437533	2.108193
6	0.640432	1.666541	2.104800
6	1.609557	2.597462	-0.808225
6	4.844781	0.270950	-2.565410
1	5.909287	0.467092	-2.469346
6	3.955341	0.854689	-1.664163
6	-2.852119	0.720445	-1.685652
1	-1.886139	0.325796	-2.009574
6	-4.381501	0.385422	0.333032
6	0.103939	-3.678205	-0.210257
1	-0.272095	-4.646755	-0.557147
6	1.513000	-0.902885	3.379668
6	2.298462	-1.860389	4.022318
1	2.005191	-2.208284	5.009426
1	0.631643	-0.505956	3.862802
1	4.048824	-3.120241	3.918037
1	3.329310	-0.592727	0.516857
1	-4.828907	1.204261	-0.236564
1	1.038949	-0.379730	-2.891320
1	5.067750	-1.012506	-4.285986
1	4.316805	1.510579	-0.879924
6	-2.697824	2.230861	-1.483504
1	-2.345077	2.686741	-2.415076
1	-3.646504	2.714785	-1.223620
1	-1.969259	2.450475	-0.702326
6	-3.906750	0.404024	-2.757328
1	-4.895108	0.792305	-2.484448
1	-3.619943	0.879565	-3.702485

1	-3.996866	-0.671707	-2.931507
6	-4.039854	0.901956	1.734934
1	-4.951506	1.213985	2.256987
1	-3.555319	0.115258	2.322221
1	-3.359120	1.757157	1.683191
6	-5.399528	-0.762169	0.376188
1	-6.331765	-0.411760	0.832730
1	-5.630333	-1.130704	-0.628908
1	-5.030661	-1.599666	0.977115
6	-2.809283	-4.458819	0.206292
1	-3.891500	-4.603357	0.107695
1	-2.337207	-5.387291	-0.154771
1	-2.573538	-4.356733	1.270672
6	-2.874123	-3.225559	-2.020155
1	-2.477121	-2.368751	-2.571284
1	-2.561156	-4.137133	-2.557096
1	-3.970537	-3.192439	-2.065134
6	0.528222	-3.831760	1.255171
1	0.855849	-2.879253	1.674825
1	-0.298273	-4.208438	1.866520
1	1.360606	-4.540018	1.335870
6	1.277258	-3.309061	-1.125738
1	2.029528	-4.104796	-1.084575
1	0.947622	-3.201355	-2.163892
1	1.758067	-2.377862	-0.822210
6	0.067733	4.461765	-0.472807
6	0.552973	3.249404	0.048516
6	0.075076	2.807146	1.299218
6	-0.885701	3.579633	1.974528
6	-1.395441	4.747615	1.420587
6	-0.907647	5.196564	0.189962
1	0.487297	4.810292	-1.409852
1	-1.194332	3.250985	2.960930
1	-2.148498	5.319162	1.956399
1	-1.276216	6.122361	-0.243506

3.13 (18.77)

8	-2.076994	2.039243	-3.038634
8	-1.649343	3.155873	2.137261
7	-1.424962	1.139400	1.087983
7	1.262346	-2.656246	0.001068
7	-1.672523	0.638909	-1.273455
7	3.433084	-0.210479	0.337248
6	-3.516672	-0.864844	4.180120
6	-2.190008	-1.196580	3.903500
1	-1.688874	-1.969263	4.480435
6	-1.492474	-0.530093	2.894414
6	-2.129403	0.462735	2.145737
6	-0.930923	0.398714	-0.050992
6	0.062324	-0.457045	0.000217
6	2.591433	-1.068395	-0.436005
6	1.082935	-1.289459	-0.107579
6	2.705876	-2.658262	-0.352624
1	2.677513	-0.774555	-1.485145
6	-4.041249	-2.531575	-2.794330
6	-4.142994	-2.148781	-1.456190
1	-4.831587	-2.661904	-0.790224
6	-3.373135	-1.094967	-0.963903
6	-2.481118	-0.421756	-1.807830
6	-1.542245	1.838257	-1.954082
6	-1.267747	2.513458	1.166768
6	-4.146514	0.138408	3.440249
1	-5.177768	0.407424	3.651874
6	-3.459195	0.800829	2.424002
6	3.176623	-0.019917	1.775672
1	2.495109	-0.828347	2.060950
6	4.219134	0.810921	-0.378100
6	0.307213	-3.763075	-0.053748
1	0.923372	-4.665373	0.055367
6	-2.374578	-0.806255	-3.150299
6	-3.157132	-1.853797	-3.635760
1	-3.069656	-2.141958	-4.680012
1	-1.696775	-0.278149	-3.808296
1	-4.647254	-3.347233	-3.179112
1	-3.469019	-0.790531	0.073261
1	4.725660	1.387266	0.403111
1	-0.456930	-0.772995	2.683616
1	-4.055601	-1.380724	4.970098
1	-3.940924	1.586937	1.852967
6	2.470865	1.304706	2.121314
1	2.235995	1.341529	3.191664
1	3.104313	2.170654	1.895975
1	1.536576	1.407082	1.564164
6	4.458337	-0.182864	2.611932
1	5.185082	0.608659	2.393494
1	4.226360	-0.122108	3.681845
1	4.939960	-1.145215	2.415428
6	3.381589	1.806875	-1.203334
1	4.030506	2.573173	-1.644246
1	2.857468	1.313473	-2.030431
1	2.633156	2.309423	-0.585685
6	5.321084	0.168439	-1.238230
1	5.959945	0.937014	-1.689308
1	5.948406	-0.492958	-0.631616
1	4.896757	-0.424421	-2.058195
6	3.027263	-3.300004	-1.707116
1	4.082777	-3.138645	-1.957149
1	2.856201	-4.383311	-1.690735
1	2.417660	-2.870886	-2.509725
6	3.599223	-3.242340	0.738940
1	3.334895	-2.859547	1.727024
1	3.508193	-4.335513	0.764469

1	4.649091	-2.999062	0.543241
6	-0.442654	-3.844672	-1.393842
1	-1.020407	-2.934380	-1.577208
1	0.250675	-3.985281	-2.228676
1	-1.140735	-4.689443	-1.386780
6	-0.662050	-3.711504	1.134507
1	-1.301529	-4.601197	1.137712
1	-0.114898	-3.673785	2.082178
1	-1.312245	-2.833126	1.077902
6	0.217572	4.311814	0.427471
6	-0.548784	3.201963	0.034966
6	-0.668893	2.903343	-1.338684
6	-0.017492	3.726253	-2.272222
6	0.773419	4.794781	-1.866697
6	0.892122	5.089886	-0.506135
1	0.253981	4.553479	1.484046
1	-0.163956	3.511692	-3.325039
1	1.280633	5.405529	-2.608536
1	1.492437	5.933380	-0.176261

3.6 Acknowledgements

Chapter 3 is adapted, in part, from Cory M. Weinstein, Caleb D. Martin, Liu Liu, and Guy Bertrand "Cross-Coupling Reactions between Stable Carbenes," *Angewandte Chemie International Edition*, 2014, **53**, 6550-6553. Copyright 2014 John Wiley & Sons, Inc. Permission to use copyrighted images and data was also obtained from Caleb D. Martin, Liu Liu, and Guy Bertrand. The dissertation author was the first author of the manuscript.

3.7 References

[1] H. W. Wanzlick and E. Schikora, *Angew. Chem.*, 1960, **72**, 494-494.

[2] H. W. Wanzlick, *Angew. Chem. Int. Ed. Engl.*, 1962, **1**, 75-80.

[3] H. J. Schoenherr and H. W. Wanzlick, *Chem. Ber. Recl.*, 1970, **103**, 1037-1046.

[4] R. W. Alder, M. E. Blake, L. Chaker, J. N. Harvey, F. Paolini and J. Schütz, *Angew. Chem. Int. Ed.*, 2004, **43**, 5896-5911.

[5] D. M. Lemal, R. A. Lovald and K. I. Kawano, *J. Am. Chem. Soc.*, 1964, **86**, 2518-2519.

[6] H. E. Winberg, J. E. Carnahan, D. D. Coffman and M. Brown, *J. Am. Chem. Soc.*, 1965, **87**, 2055-2056.

[7] M. K. Denk, K. Hatano and M. Ma, *Tetrahedron Lett.*, 1999, **40**, 2057-2060.

[8] Y. Liu and D. M. Lemal, *Tetrahedron Lett.*, 2000, **41**, 599-602.

[9] T. A. Taton and P. Chen, *Angew. Chem. Int. Ed. Engl.*, 1996, **35**, 1011-1013.

[10] M.-J. Cheng, C.-L. Lai and C.-H. Hu, *Mol. Phys.*, 2004, **102**, 2617-2621.

[11] F. E. Hahn, L. Wittenbecher, D. Le Van and R. Fröhlich, *Angew. Chem. Int. Ed.*, 2000, **39**, 541-544.

[12] Y. Liu, P. E. Lindner and D. M. Lemal, *J. Am. Chem. Soc.*, 1999, **121**, 10626-10627.

[13] A. J. Arduengo III, J. R. Goerlich and W. J. Marshall, *Liebigs Ann. Recl.*, 1997, 365-374.

[14] R. W. Alder, L. Chaker and F. P. V. Paolini, *Chem. Commun.*, 2004, 2172-2173.

[15] R. W. Alder and M. E. Blake, *Chem. Commun.*, 1997, 1513-1514.

[16] P. I. Jolly, S. Zhou, D. W. Thomson, J. Garnier, J. A. Parkinson, T. Tuttle and J. A. Murphy, *Chem. Sci.*, 2012, **3**, 1675-1679.

[17] M. Otto, S. Conejero, Y. Canac, V. D. Romanenko, V. Rudzevitch and G. Bertrand, *J. Am. Chem. Soc.*, 2004, **126**, 1016-1017.

[18] J. P. Moerdyk and C. W. Bielawski, *Chem. Commun.*, 2014, **50**, 4551-4553.

[19] M. Braun, W. Frank and C. Ganter, *Organometallics*, 2012, **31**, 1927-1934.

[20] E. A. Carter and W. A. Goddard III, *J. Phys. Chem.*, 1986, **90**, 998-1001.

[21] J. P. Malrieu and G. Trinquier, *J. Am. Chem. Soc.*, 1989, **111**, 5916-5921.

[22] H. Jacobsen and T. Ziegler, *J. Am. Chem. Soc.*, 1994, **116**, 3667-3679.

[23] A. Poater, F. Ragone, S. Giudice, C. Costabile, R. Dorta, S. P. Nolan and L. Cavallo, *Organometallics*, 2008, **27**, 2679-2681.

[24] S. I. Miller, *J. Chem. Educ.*, 1978, **55**, 778-780.

[25] D. Bourissou, O. Guerret, F. P. Gabbai and G. Bertrand, *Chem. Rev.*, 2000, **100**, 39-91.

[26] T. Droge and F. Glorius, *Angew. Chem. Int. Ed. Engl.*, 2010, **49**, 6940-6952.

[27] M. Melaimi, M. Soleilhavoup and G. Bertrand, *Angew. Chem. Int. Ed.*, 2010, **49**, 8810-8849.

[28] D. Martin, M. Melaimi, M. Soleilhavoup and G. Bertrand, *Organometallics*, 2011, **30**, 5304-5313.

[29] F. E. Hahn and M. C. Jahnke, *Angew. Chem. Int. Ed.*, 2008, **47**, 3122-3172.

[30] D. J. Nelson and S. P. Nolan, *Chem. Soc. Rev.*, 2013, **42**, 6723-6753.

[31] J. P. Moerdyk, D. Schilter and C. W. Bielawski, *Acc. Chem. Res.*, 2016, **49**, 1458-1468.

[32] O. Back, M. Henry-Ellinger, C. D. Martin, D. Martin and G. Bertrand, *Angew. Chem. Int. Ed.*, 2013, **52**, 2939-2943.

[33] R. R. Rodrigues, C. L. Dorsey, C. A. Arceneaux and T. W. Hudnall, *Chem. Commun.*, 2014, **50**, 162-164.

[34] A. Liske, K. Verlinden, H. Buhl, K. Schaper and C. Ganter, *Organometallics*, 2013, **32**, 5269-5272.

[35] S. V. C. Vummaleti, D. J. Nelson, A. Poater, A. Gomez-Suarez, D. B. Cordes, A. M. Z. Slawin, S. P. Nolan and L. Cavallo, *Chem. Sci.*, 2015, **6**, 1895-1904.

[36] K. Verlinden, H. Buhl, W. Frank and C. Ganter, *Eur. J. Inorg. Chem.*, 2015, **2015**, 2416-2425.

[37] V. Lavallo, Y. Canac, B. Donnadieu, W. W. Schoeller and G. Bertrand, *Science*, 2006, **312**, 722-724.

[38] V. Lavallo, Y. Canac, C. Präsang, B. Donnadieu and G. Bertrand, *Angew. Chem. Int. Ed.*, 2005, **44**, 5705-5709.

[39] T. W. Hudnall and C. W. Bielawski, *J. Am. Chem. Soc.*, 2009, **131**, 16039-16041.

[40] T. W. Hudnall, A. G. Tennyson and C. W. Bielawski, *Organometallics*, 2010, **29**, 4569-4578.

[41] C. A. Dyker, V. Lavallo, B. Donnadieu and G. Bertrand, *Angew. Chem. Int. Ed.*, 2008, **47**, 3206-3209.

[42] V. Lavallo, C. A. Dyker, B. Donnadieu and G. Bertrand, *Angew. Chem. Int. Ed.*, 2008, **47**, 5411-5414.

[43] W. C. Chen, Y. C. Hsu, C. Y. Lee, G. P. A. Yap and T. G. Ong, *Organometallics*, 2013, **32**, 2435-2442.

[44] M. Melaimi, P. Parameswaran, B. Donnadieu, G. Frenking and G. Bertrand, *Angew. Chem. Int. Ed.*, 2009, **48**, 4792-4795.

[45] C. Pranckevicius, L. Liu, G. Bertrand and D. W. Stephan, *Angew. Chem. Int. Ed.*, 2016, **55**, 5536-5540.

[46] G. Frenking and R. Tonner, *Pure Appl. Chem.*, 2009, **81**, 597-614.

[47] M. M. Deshmukh, S. R. Gadre, R. Tonner and G. Frenking, *PCCP*, 2008, **10**, 2298-2301.

[48] R. Tonner and G. Frenking, *Chem. Eur. J.*, 2008, **14**, 3260-3272.

[49] R. Tonner and G. Frenking, *Chem. Eur. J.*, 2008, **14**, 3273-3289.

[50] G. Frenking, B. Neumuller, W. Petz, R. Tonner and F. Oxler, *Angew. Chem. Int. Ed.*, 2007, **46**, 2986-2987.

[51] R. Tonner and G. Frenking, *Angew. Chem. Int. Ed.*, 2007, **46**, 8695-8698.

[52] R. Tonner, G. Heydenrych and G. Frenking, *Chem. Asian J.*, 2007, **2**, 1555-1567.

[53] M. Alcarazo, C. W. Lehmann, A. Anoop, W. Thiel and A. Furstner, *Nature Chemistry*, 2009, **1**, 295-301.

[54] D. A. Ruiz, M. Melaimi and G. Bertrand, *Chem. Asian J.*, 2013, **8**, 2940-2942.

[55] R. W. Saalfrank and H. Maid, *Chem. Commun.*, 2005, 5953-5967.

[56] A. Forni and R. Destro, *Chem. Eur. J.*, 2003, **9**, 5528-5537.

[57] P. V. Schleyer, C. Maerker, A. Dransfeld, H. J. Jiao and N. J. R. V. Hommes, *J. Am. Chem. Soc.*, 1996, **118**, 6317-6318.

[58] N. Wiberg, *Angew. Chem. Int. Ed.*, 1968, **7**, 766-779.

[59] J. Broggi, T. Terme and P. Vanelle, *Angew. Chem. Int. Ed.*, 2014, **53**, 384-413.

[60] J. A. Murphy, *J. Org. Chem.*, 2014, **79**, 3731-3746.

[61] J. Garnier, D. W. Thomson, S. Z. Zhou, P. I. Jolly, L. E. A. Berlouis and J. A. Murphy, *Beilstein J. Org. Chem.*, 2012, **8**.

[62] D. Munz, J. X. Chu, M. Melaimi and G. Bertrand, *Angew. Chem. Int. Ed.*, 2016, **55**, 12886-12890.

[63] W. C. Chen, C. Y. Lee, B. C. Lin, Y. C. Hsu, J. S. Shen, C. P. Hsu, G. P. A. Yap and T. G. Ong, *J. Am. Chem. Soc.*, 2014, **136**, 914-917.

[64] F. Hanasaka, K. Fujita and R. Yamaguchi, *Organometallics*, 2005, **24**, 3422-3433.

[65] S. J. Ryan, S. D. Schimler, D. C. Bland and M. S. Sanford, *Org. Lett.*, 2015, **17**, 1866-1869.

[66] R. Jazzar, J. B. Bourg, R. D. Dewhurst, B. Donnadieu and G. Bertrand, *J. Org. Chem.*, 2007, **72**, 3492-3499.

[67] R. Jazzar, R. D. Dewhurst, J. B. Bourg, B. Donnadieu, Y. Canac and G. Bertrand, *Angew. Chem. Int. Ed.*, 2007, **46**, 2899-2902.

[68] O. V. Dolomanov, L. J. Bourhis, R. J. Gildea, J. A. K. Howard and H. Puschmann, *J. Appl. Crystallogr.*, 2009, **42**, 339-341.

[69] M. J. Frisch, G. W. Trucks, H. B. Schlegel, G. E. Scuseria, M. A. Robb, J. R. Cheeseman, G. Scalmani, V. Barone, B. Mennucci, G. A. Petersson, H. Nakatsuji, M. Caricato, X. Li, H. P. Hratchian, A. F. Izmaylov, J. Bloino, G. Zheng, J. L. Sonnenberg, M. Hada, M. Ehara, K. Toyota, R. Fukuda, J. Hasegawa, M. Ishida, T. Nakajima, Y. Honda, O. Kitao, H. Nakai, T. Vreven, J. A. Montgomery, J. E. Peralta, F. Ogliaro, M. Bearpark, J. J. Heyd, E. Brothers, K. N. Kudin, V. N. Staroverov, R. Kobayashi, J. Normand, K. Raghavachari, A. Rendell, J. C. Burant, S. S. Iyengar, J. Tomasi, M. Cossi, N. Rega, J. M. Millam, M. Klene, J. E. Knox, J. B. Cross, V. Bakken, C. Adamo, J. Jaramillo, R. Gomperts, R. E. Stratmann, O. Yazyev, A. J. Austin, R. Cammi, C. Pomelli, J. W. Ochterski, R. L. Martin, K. Morokuma, V. G. Zakrzewski, G. A. Voth, P. Salvador, J. J. Dannenberg, S. Dapprich, A. D. Daniels, Farkas, J. B. Foresman, J. V. Ortiz, J. Cioslowski and D. J. Fox, Wallingford CT, 2009.

[70] R. Ditchfield, W. J. Hehre and J. A. Pople, *J. Chem. Phys.*, 1971, **54**, 724-728.

[71] W. J. Hehre, R. Ditchfield and J. A. Pople, *J. Chem. Phys.*, 1972, **56**, 2257-2261.

[72] J. D. Dill and J. A. Pople, *J. Chem. Phys.*, 1975, **62**, 2921-2923.

[73] M. M. Francl, W. J. Pietro, W. J. Hehre, J. S. Binkley, M. S. Gordon, D. J. Defrees and J. A. Pople, *J. Chem. Phys.*, 1982, **77**, 3654-3665.

[74] K. Fukui, *Acc. Chem. Res.*, 1981, **14**, 363-368.

[75] R. Krishnan, J. S. Binkley, R. Seeger and J. A. Pople, *J. Chem. Phys.*, 1980, **72**, 650-654.

[76] T. Clark, J. Chandrasekhar, G. W. Spitznagel and P. V. Schleyer, *J. Comput. Chem.*, 1983, **4**, 294-301.

[77] A. D. Mclean and G. S. Chandler, *J. Chem. Phys.*, 1980, **72**, 5639-5648.

[78] A. Bondi, *J. Phys. Chem.*, 1964, **68**, 441-451.

[79] S. Grimme, *J. Comput. Chem.*, 2004, **25**, 1463-1473.

[80] S. Grimme, *J. Comput. Chem.*, 2006, **27**, 1787-1799.

[81] S. Grimme, J. Antony, S. Ehrlich and H. Krieg, *J. Chem. Phys.*, 2010, **132**, 154104-154104.

Chapter 4 : Development and Reactivity Studies of Cyclic (Alkyl)(amino)carbenes with Expanded Ring Sizes

4.1 Introduction

First introduced by Bertrand et al. in 2005,[1] CAACs are categorically defined as "cyclic" species with an sp^3 "alkyl" and "amino" substituent adjacent to the "carbene" center. This atomic arrangement leads to CAACs being both better σ-donors (higher HOMO) and π-acceptors (lower LUMO) when compared to "classical" NHCs (Figure 4.1). Furthermore, the reduced heteroatom stabilization of the carbene center in CAACs versus NHCs also gives rise to a smaller ΔE_{ST} (48.3 vs 72.7 kcal mol^{-1}). Due to the more ambiphilic electronic properties, CAACs have started to replace NHCs as extremely powerful ligands for a wide range of chemical disciplines.[2-5]

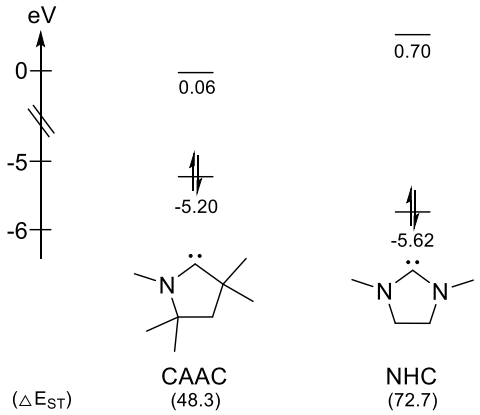

Figure 4.1: Calculated HOMO-LUMO gaps (eV) and ΔE_{ST} (kcal mol^{-1}) of a CAAC and NHC.

The synthesis of CAACs as free species has so far only been achieved through deprotonation of the corresponding cyclic iminium salt precursors (Scheme 4.1) These salts were initially prepared via

alkylation of aza-allyl anions with 1,2-epoxy-2-methylpropane, followed by hydrolysis and cyclization with trifluoromethansulfonic acid anhydride (TfOTf).[1] As the unique properties of CAACs started to be more realized, Bertand et al. developed a cheaper "hydro-iminiumation" method which allows for large scale synthesis of iminium salt precursors.[6-7] In this route, alkylation of the aza-allyl anion is instead achieved with 3-chloro-2-methylpropene. Protonation of the alkenyl ketimine with HCl and subsequent heating gives the corresponding cyclized five-membered iminium salt. The final cyclization step proceeds via an intramolecular proton transfer from the ketiminium moiety to the vinyl carbon. This gives a short lived tertiary carbocation intermediate which is quickly attacked by the ketimine lone pair. Although incredibly reliable, the hydro-iminiumation is limited in its scope due to the cyclization step. Indeed, if the nitrogen atom features an alkyl group, the resulting ketimine has a much higher basicity, and therefore cannot be deprotonated by the alkenyl group even at temperatures up to 200 ºC. As a result of this limitation, only CAACs featuring an aryl group on the nitrogen atom have been synthesized to date Furthermore, although CAACs with many different aryl substituents have been synthesized and coordinated to TMs *in situ*,[8] the bulky Dipp has been the only aryl substituent that has allowed for the isolation of CAACs at room temperature.

Another structural similarity shared by all CAACs is a quaternary carbon adjacent to the nitrogen. The purpose of this functionality is to remove any potentially acidic protons on the ring from possible deprotonation. Given the high basicity of CAACs, if the carbon group was instead secondary or tertiary, deprotonation of the aldiminium proton would occur, leading to an azomethine-ylide.[9] Therefore, all CAACs as free species feature a *gem*-dimethyl group on their backbone. The specificity of this group can be simply explained by its synthetic simplicity, but CAACs could hypothetically be synthesized with any alkyl group that gives a quaternary carbon at this position.

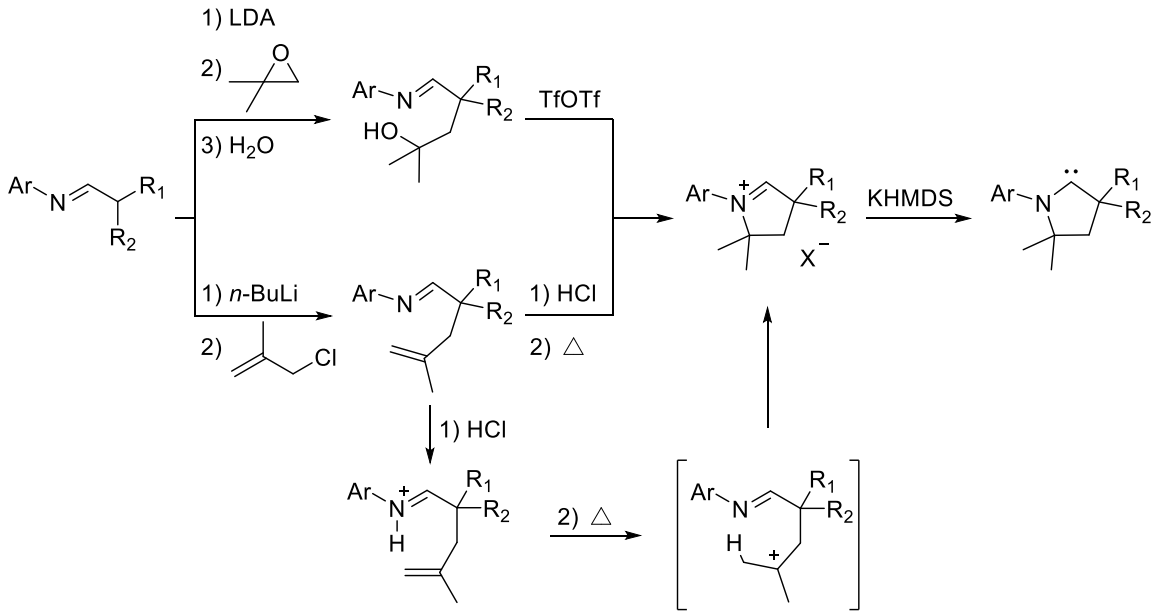

Scheme 4.1: Synthetic routes for CAACs (LDA = lithium diisopropylamide, KHMDS = potassium hexamethyldisilylamide, TfOTf = trifluoromethansulfonic acid anhydride).

Given the synthetic requirements described above, CAACs are indefinitely stable at room temperature in solution and the solid state in the absence of air and moisture. Caution should be taken when deciding on solvent choice for reactions involving CAACs are they are very strong bases. Indeed, Turner et al. reported that CAACs react with weakly acidic solvents like $CHCl_3$ to give the C-H insertion product **4.A** (Scheme 4.2).[10] In the same paper it was shown that at elevated temperatures, CAACs can also inter- and intramolecularly insert into the benzylic CH bonds of toluene or the Dipp group giving **4.B** or **4.C**, respectively.

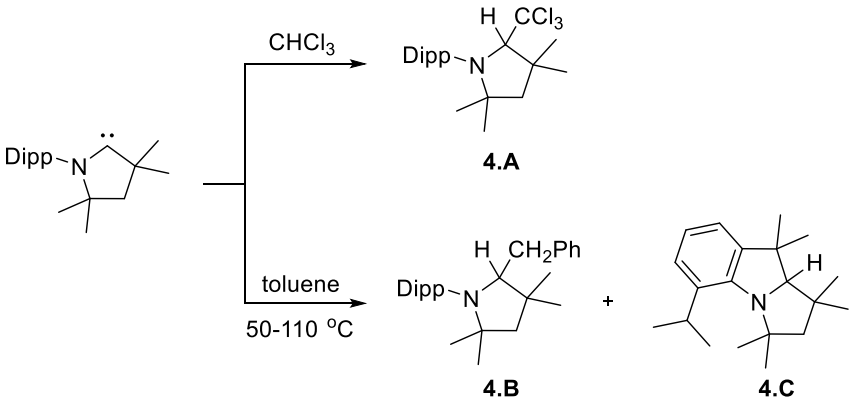

Scheme 4.2: Examples of inter- and intramolecular CH-insertion reactions with CAACs.

Examples of insertion reactions involving CAACs go well beyond the C-H insertion products reported above. Indeed, the small HOMO-LUMO gap of CAACs has allowed for many examples of E-H insertion products (Scheme 4.3). In one report by Bertrand et al., CAACs with varying substituents at the quaternary carbon were shown to inert into R_3Si-H, R_2P-H, and R_2B-H bonds.[11] Subsequent studies by Roesky et al.[12] and Radius et al.[13] have generalized this reaction for other silanes and boranes, respectively. Perhaps unsurprisingly however, was the observation that B-H insertion reactions were only observed when the boron was bonded to π-donor substituents. When BH_3 was reacted with a CAAC, the classical Lewis acid-base adduct was obtained instead of the B-H insertion product.[11] This might be rationalized by the fact that the LUMO p-orbital of BH_3 is much lower in energy than the same orbital of boranes with π-donors.

Although BH_3 did not show insertion chemistry with CAACs, Bertrand et al. demonstrated that its close chemical neighbor NH_3 could be activated by a CAAC.[14] Perhaps even more remarkably, the Bertrand group also demonstrated that CAACs could even split H_2 at slightly elevated temperatures. This seminal report marked the first time that a single carbon center could mimic small molecule "oxidative addition" reactivity traditionally reserved for TM centers.

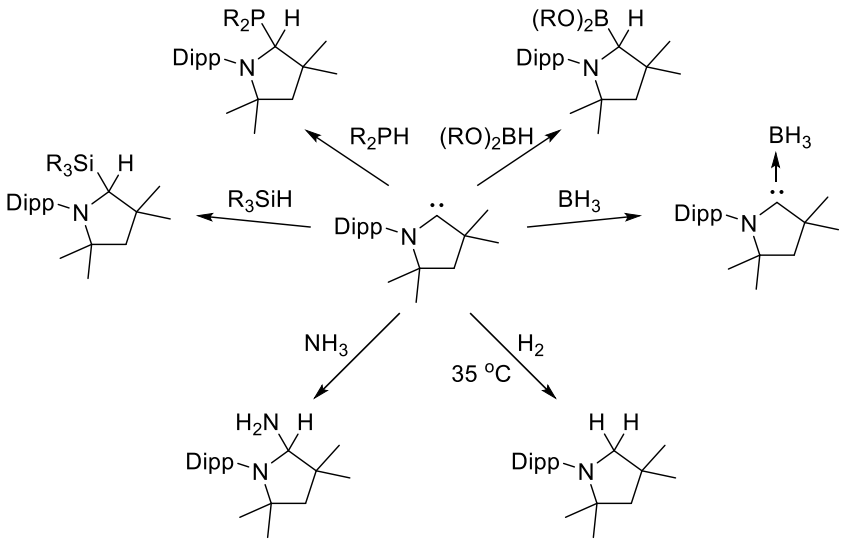

Scheme 4.3: Insertion of CAACs into a variety of E-H bonds, with the exception of BH_3.

The mechanism for all of the above E-H insertion reactions proceeds through a concerted pathway. The CAAC HOMO lone pair first attacks the σ*-orbital of the substrate which initiates the breaking of the E-H bond (Scheme 4.4).[14] Due to the low LUMO of the CAAC, a three-membered transition state can then be envisioned which involves a new bond forming between the carbene empty π-orbital and the former CH σ-bond of the substrate. Ring opening of this short-lived species yields the observed R-H insertion products.

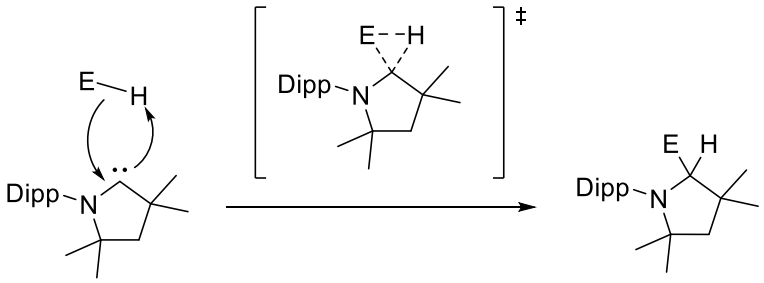

Scheme 4.4: CAAC E-H insertion reactions proceed through a three-membered transition state.

Inspired by the E-H insertion chemistry available by CAACs, Johnson et al. recently reported that the same reactivity could be translated to functionalizing solid-state materials.[15] In this report, it was shown that CAACs could inset into terminal Si-H bonds of both Si(111) wafers and silicon nanoparticles

(SiNps). In the case of the wafers, up to ~21 ± 3% of the surface could be covered with low concentrations of CAAC in as quickly as three days. The main limitation of surface coverage was attributed to the relatively large size of the CAAC Dipp substituent. Nonetheless, this method leaves unreacted Si-H bonds at the surface which could give rise to further functionalization by other means.

In addition to their ability to undergo insertion reactions, CAACs have been instrumental ligands for the field of main-group chemistry due to their small HOMO-LUMO gap. One primary example of such was shown by Bertrand et al. in 2011 when the ($CAAC^{Cy}$)BBr_3 adduct **4.D** was reduced with KC_8 in the presence of additional $CAAC^{Cy}$ yielding product **4.E** (Scheme 4.5).[16] It should be noted that the new B-H bond likely formed via H-atom abstraction from solvent in these harsh reducing conditions.[17] That being said, **4.E** can be viewed as a bis($CAAC^{Cy}$) stabilized borylene in which the boron is now isolobal to an amine. Fantastically, **4.E** did indeed react like an amine, as the boron center now acted as a Brønsted base when subjected to HOTf giving adduct **4.F**. This marked the first example of neutral nucleophilic boron, and was only possible due to the ambiphilic ability of the CAAC ligands.

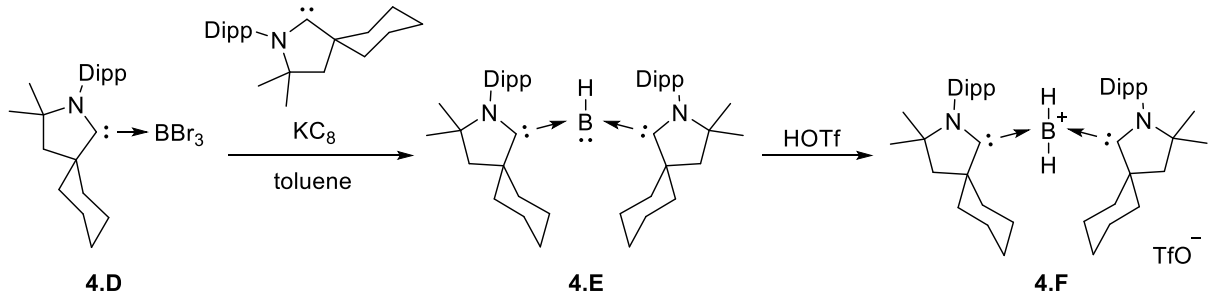

Scheme 4.5: Strong donor properties of CAACs translate to a nucleophilic boron center (HOTf = trifluoromethanesulfonic acid).

In a very similar experiment, Braunschweig et al. reduced ($CAAC^{Me}$)B(CN)Br_2 **4.G** in the presence of PEt_3 giving ($CAAC^{Me}$)(PEt_3)BCN **4.H** (Scheme 4.6).[18] The absence of a B-H bond in this product suggests that the H-atom abstraction step forming **4.E** occurs only upon a third reduction of the boron center. What was most surprising however, was that when the reduction was performed in the absence of an external Lewis base, tetramer **4.I** was instead isolated as the major product. This reaction

simply highlights the fact that small changes to molecules involving CAACs as ligands have the potential to lead to a wide variety of products.

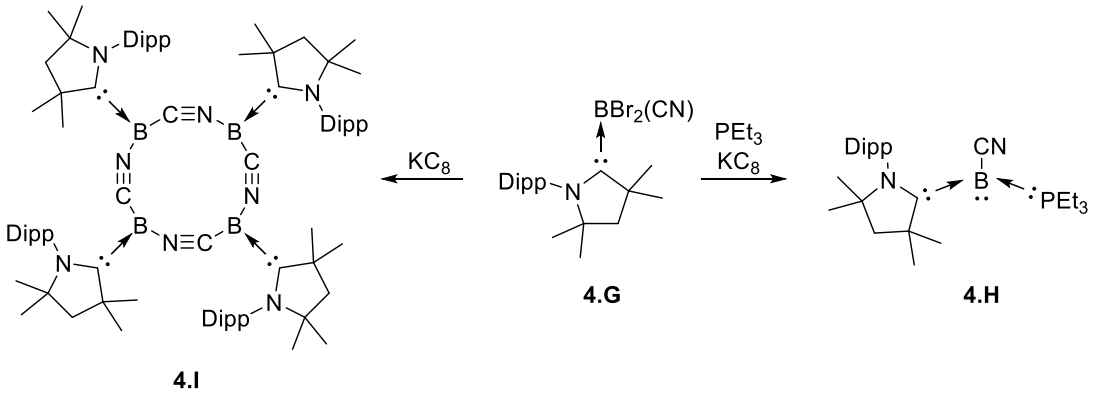

Scheme 4.6: Reduction of (CAAC^{Me})B(CN)Br$_2$ with and without the presence of Lewis external base.

Beyond their strong σ-donor properties, the high π-acidity of CAACs has also led to the stabilization of many rare main-group species. One recent example includes the isolation of a bis(CAAC^{Me}) stabilized Be^0 atom **4.J** by Braunschweig et al. (Figure 4.2).[19] The reduced Be^0 center (normally found as Be^{2+}) was formally described as a ground state singlet with an electronic configuration of $1s^2 2s^0 2p^2$. This electronic description allows for significant stabilization of the two additional electrons on the Be center due to the formation of a three-center two-electron π-bond between the Be filled p-orbital and the two CAACs' empty π-orbitals. In fact, the combined π-backbonding stabilization was found to be significantly more energetically important (-148.6 kcal mol^{-1}) than the electronic stabilization from the σ-donating lone pairs of the CAACs (-71.6 kcal mol^{-1}).

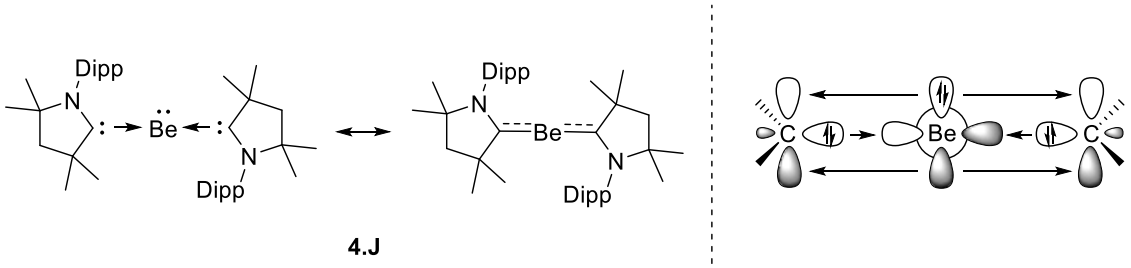

Figure 4.2: Bis(CAAC^{Me}) stabilized Be^0 atom **4.J** (left) and its major electronic description (right).

The π-backbonding ability of CAACs has also been instrumental for stabilizing a variety of main-group radicals and radical ions.[20] To name just a few examples, neutral boron,[21] aluminum,[22] and phosphorus[23] radicals **4.K**, **4.L**, and **4.Ma-c** featuring CAAC ligand(s) have been isolated and crystallographically characterized (Figure 4.3). All of these radical species are significantly stabilized by the π-backbonding available from CAAC ligands. In fact, **4.Ma-c** might even be better described as a neutral phosphorus center with the radical completely localized on the CAAC. Indeed, singly occupied molecular orbital (SOMO) calculations gave spin densities as high as 70.5% and 20.9% for the CAAC carbon and nitrogen, respectively. CAAC-stabilized radical cations of both boron and phosphorus, **4.N** and **4.O**, have also been reported.[16, 24] Here, these oxidized species are stabilized not only from π-backbonding, but also the high σ-donating ability of the CAAC.

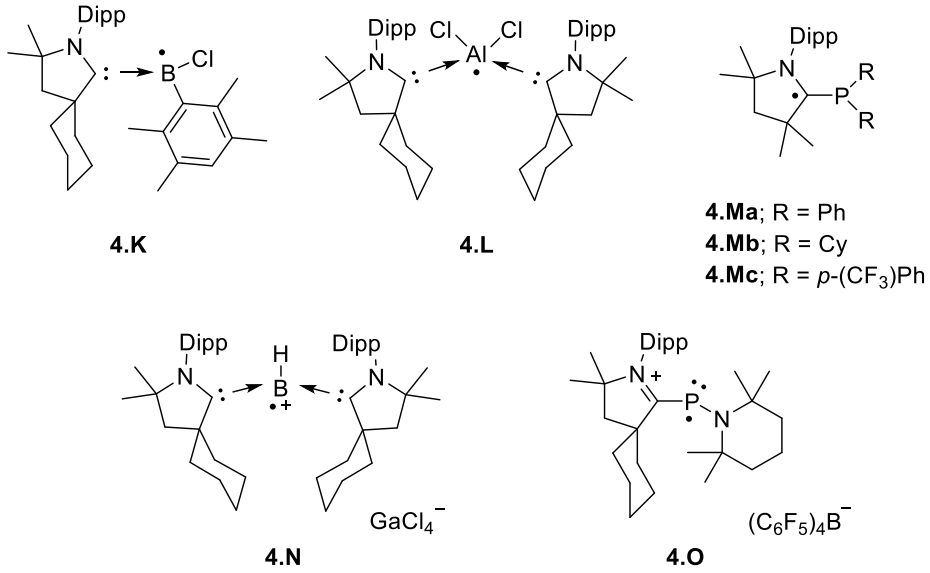

Figure 4.3: CAAC-supported main-group radicals and radical cations.

Perhaps one of the best examples of how CAACs can support different oxidation states of a main-group species came from Bertrand et al. in 2014.[25] In this report, $CAAC^{Cy}$ was first reacted with $SbCl_3$ to give the corresponding adduct **4.P** (Scheme 4.7). A single electron reduction of this species yielded the neutral antimony radical **4.Q**. Unlike the "phosphorus" radicals **4.Ma-c**, the SOMO of **4.Q** was calculated to have a spin density of 90.7% localized on the antimony center, with only minor spin densities found on

the two chlorine atoms (4.6% and 3.9%). Although single crystals of **4.Q** could not be grown, EPR studies gave evidence toward its likely bonding arrangements. When **4.P** was instead reacted with two equivalents of KC_8, the Lewis base stabilized chloro-stibinidene **4.R** was isolated. Finally, upon a three electron reduction of **4.P** with three equivalents of KC_8, the bis($CAAC^{Cy}$) stabilized diatomic antimony species **4.S** was formed. In all, **4.P**-**S** represent four different oxidation states of antimony species stabilized by a CAAC ligand.

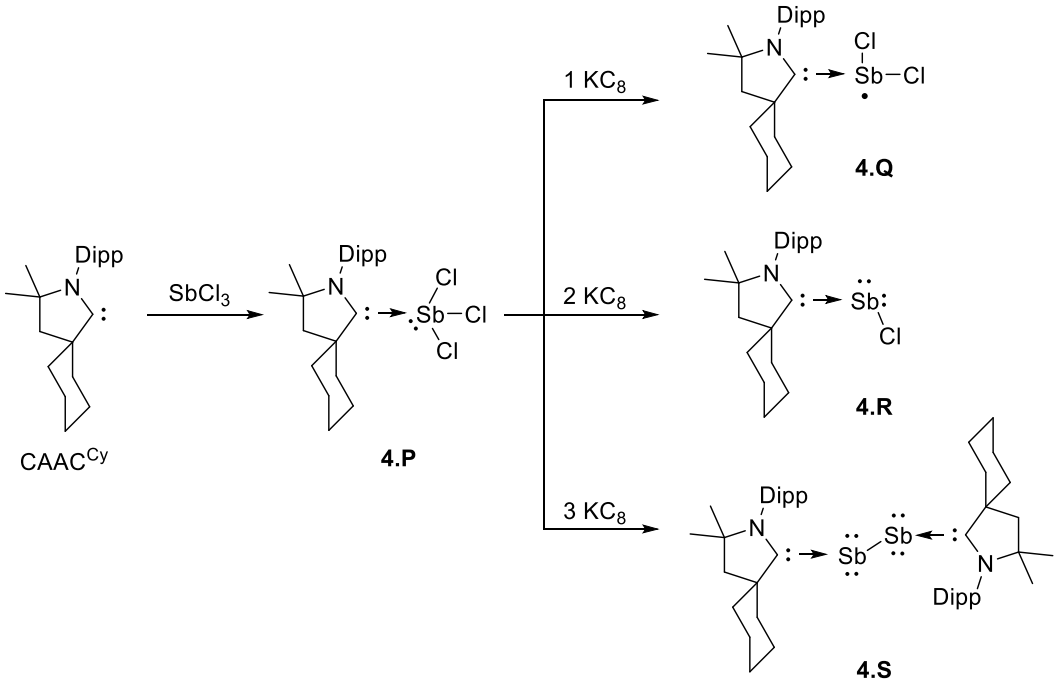

Scheme 4.7: Four different oxidation states of antimony stabilized by CAACs.

In addition to main-group radicals, CAACs have also been widely used to stabilize organic radicals. Mono, bis, and tris(amino)(carboxy) radicals have been reported featuring one (**4.T**), two (**4.U**), or three (**4.V**) CAACs, respectively (Figure 4.4).[26] Although highly sensitive to air and moisture, radicals **4.T**-**V** do not dimerize and could be crystallographically characterized. Subsequent research showed that if a perfluorinated phenyl group (C_6F_5) was used instead of the phenyl group (C_6H_5), the corresponding (amino)(carboxy) monoradical **4.W** was remarkably stable in air for several days.[27]

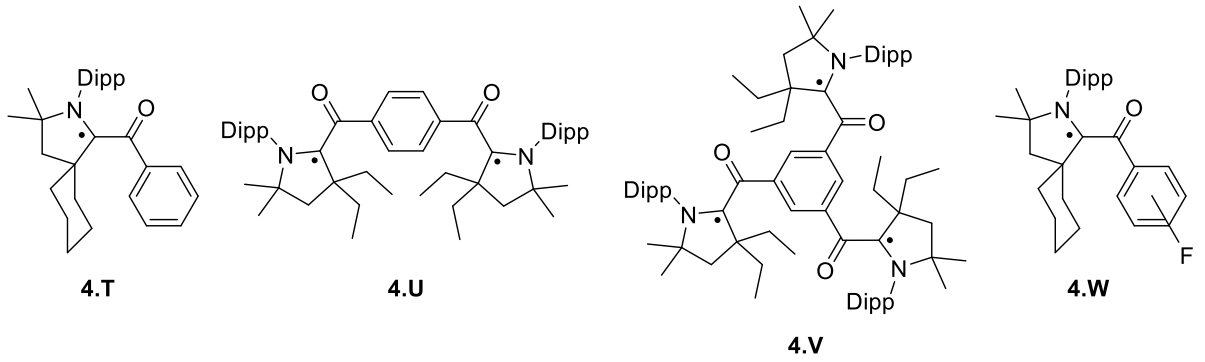

Figure 4.4: Mono, bis, and tris(amino)(carboxy) radicals derived from CAACs.

The stabilization of organic radicals by CAACs extends well beyond (amino)(carboxy) systems. For example, organic mixed valence systems based on bis(CAAC) stabilized C_2 were developed simultaneously by both Bertrand et al. and Roesky et al.[28-29] Here, the central C_2 unit can exist in three separate oxidation states upon either reduction (**4.X**) or oxidation (**4.Z**) of the radical cation **4.Y** (Scheme 4.8). Surprisingly, the radical cation **4.Y** was even determined to be air stable. Similar organic capacitor systems derived from CAACs were also probed by cyclic voltammetry (CV) with either pyridyl (**4.AA**-**4.AC**) or benzimidazole (**4.AD**-**4.AF**) linkers.[30-31] In every case except for **4.AC**, each oxidation state of the series was isolable and crystallographically characterized. What is most remarkable about all of these systems is the reversibility of each series, not just by CV but also via synthetic chemical routes. Given the range of redox states now available in these systems, one might imagine that any one of the molecules would be useful for finely tuned electrochemistry. Furthermore, given proper chemical engineering, large scale capacitor systems derived from CAACs might be possible.

One of the most recent examples of an organic radical stabilized by a CAAC came from the isolation of a monomeric allenyl radical.[32] After an impressive amount of synthetic modification, the Bertrand group was able to crystallize the allenyl radical **2.AG** which is terminated by a triphenylmethyl group (Figure 4.5). Importantly, this novel radical was readily accessible after only three synthetic steps from the free CAAC. Mulliken spin densities were calculated at the UB3LYP/def2-TZVP level of theory,

and showed that the carbene carbon atom had the highest localized spin density at 45%. The next highest spin density was found at the terminal allenyl carbon (38%), followed by the CAAC nitrogen (17%).

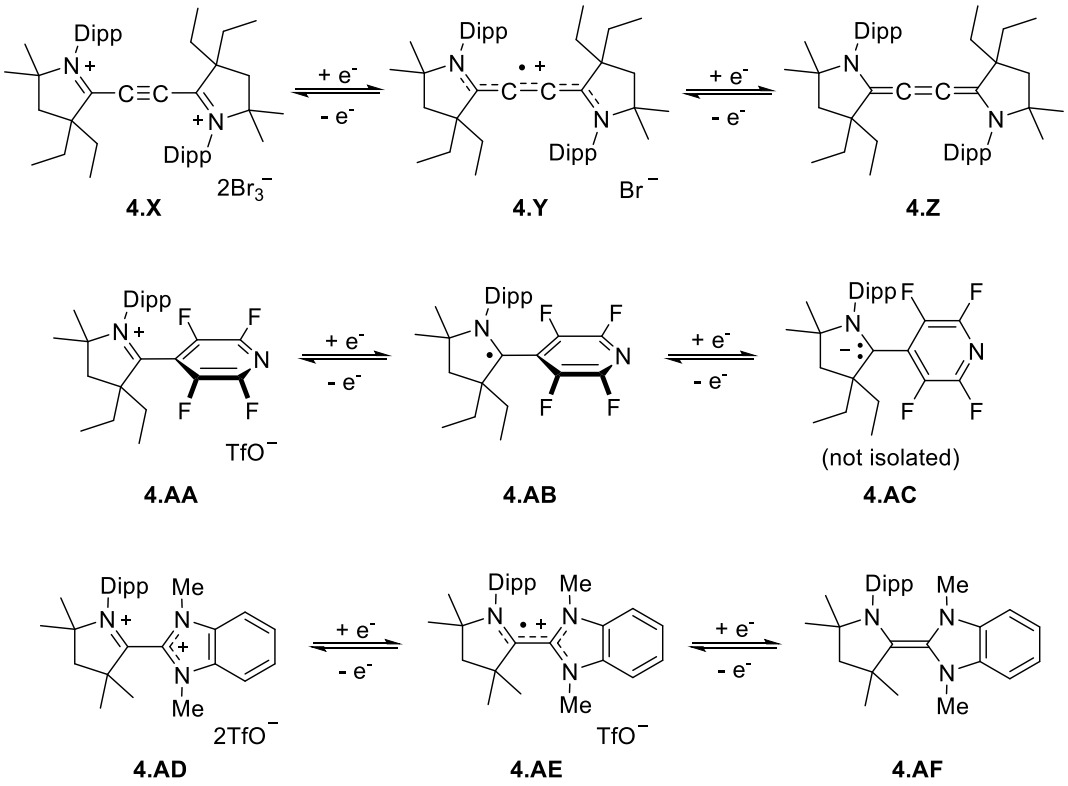

Scheme 4.8: Organic capacitors derived from CAACs.

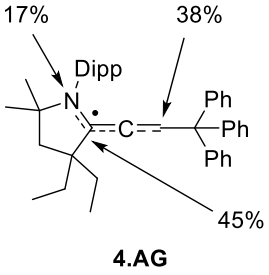

Figure 4.5: A stable, monomeric allenyl radical derived from a CAAC, and the calculated Muliken spin densities of the SOMO at the UB3LYP/def2-TZVP level of theory.

Moving to the d-block, the peculiar electronic properties of CAACs have allowed for the stabilization of many novel low-valent TMs in unique coordination environments. In fact, one of the very

first CAAC publications included examples of coordinatively unsaturated rhodium (**4.AH**) and palladium (**4.AI)** complexes (Figure 4.6).[33] Each complex was stabilized both via the strong σ-donation of the CAAC, and even through agostic interactions with the bulky menthyl substituent. Since this report, many other "naked" transition-metal complexes featuring CAACs as ligands have been synthesized. For example, the $[(CAAC)Au(toluene)]^+$ complex **4.AJ** was isolated and crystallographically characterized following a halide abstraction with the weakly coordinating anion $(C_6F_5)_4B^-$.[34] Staying in group XI, the first copper borohydride complex **4.AK** featuring a monodentate ligand, namely a CAAC, has also been isolated.[35]

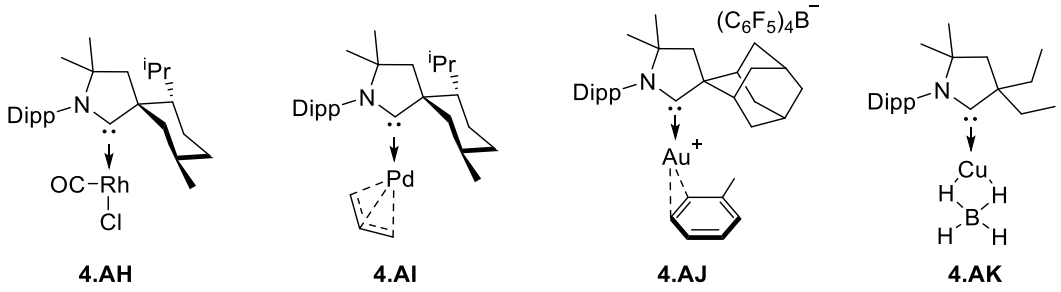

Figure 4.6: CAAC-supported TM complexes in unique coordination environments.

The strong π-accepting properties of CAACs has allowed for the isolation of many highly reduced TM complexes. Indeed, bis(CAAC)-stabilized zero valent complexes of Ni,[36] Pd,[37] Pt,[37] Zn,[38] Mn,[39] Co,[40] Fe,[40] Cu,[41] and Au[42] (**4.ALa-i**) have been spectroscopically and crystallographically studied (Figure 4.7).[3] The three group X complexes **4.ALa-c** are all diamagnetic with classical M^0 d^{10} electronic configurations. The lone group XII complex **4.ALd** might also be best described with a d^{10} electronic configuration. Here however, the Zn atom is formally 2+ while the remaining two electrons are antiferromagnetically coupled and each localized on one CAAC unit, respectively. The remaining complexes **4.Ale-i** are all paramagnetic. For the coinage metal complexes **4.ALh**,**i** however, calculations showed that the remaining unpaired electron is formally in a metal p-orbital and delocalized across the $(L)_2M^0$ π-system.[43] If a CAAC featuring a bulkier menthyl substituent was instead used as the supporting ligand, the diatomic Au^0 complex **4.AM** could be isolated after a lithium sand reduction of the

corresponding (CAAC)AuCl precursor.[42] Finally, although its fully reduced neutral form was not synthesized, the $[(CAAC)_2Cr]^+$ complex **4.AN** has also been reported.[44]

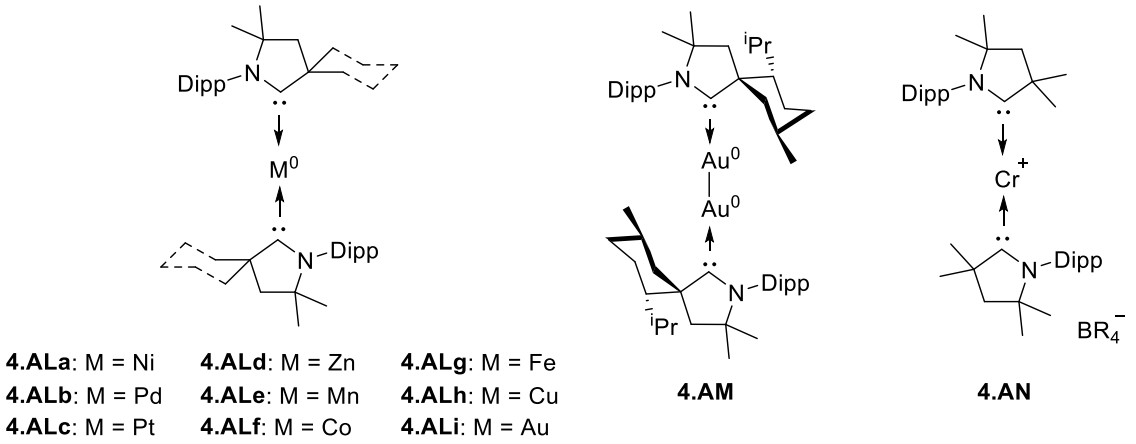

Figure 4.7: Low valent L_2 TM complexes featuring CAAC ligands (R = $(C_6H_3(CF_3)_2)$).

Beyond the mono and diatomic Au^0 complexes **4.Ali** and **4.AM**, a trinuclear gold complex supported by CAAC ligands has also been reported.[45] The (CAAC)AuCl complex **4.AO** was first reacted with Ag_2O in the presence of $NaBF_4$ to give the $[((CAAC)Au)_3O]^+[BF_4]^-$ complex **4.AP** in which oxygen is bridging all three gold atoms (Scheme 4.9). This species can be easily reduced at room temperature by CO, generating both CO_2 and the new trinuclear gold species **4.AQ**. Here, each gold center has a formal charge of +1/3. Unfortunately, all attempts to further reduce **4.AQ** failed, and thus no higher nuclearity gold complexes could be synthesized. One potential problem preventing higher nucleation might be the steric hindrance exhibited by the three Dipp groups. Therefore, if new CAACs could be synthesized with smaller substituents on the nitrogen atom, perhaps larger gold clusters could be constructed.

CAAC coinage metal complexes have also shown to have promising luminescent properties. Recently, Bochmann et al. demonstrated that the lack of strong intermolecular interactions in (CAAC)MCl (M = Cu, Au) complexes **4.ARa**,**b** led to high solid-state photoluminescence quantum efficiencies for these species (Figure 4.8).[46] In a following study, the same group probed the use of (CAAC)MCz (M = Cu, Au; Cz = carbazole) **4.ASa**,**b** in organic light-emitting diodes (OLEDs).[47] The gold complex **4.ASb** was found to have a remarkably fast emission lifetime of 350 ns, considerably faster

than iridium-based phosphorescent emitters. The fast emission would be highly beneficial for use in OLED operation. Finally, Thompson et al. studied the emissive properties of two, three, and four coordinate (CAAC)CuTp (Tp = trispyrazolborate) complexes and found that the four coordinate complex **4.AT** was the most photoefficient.[48]

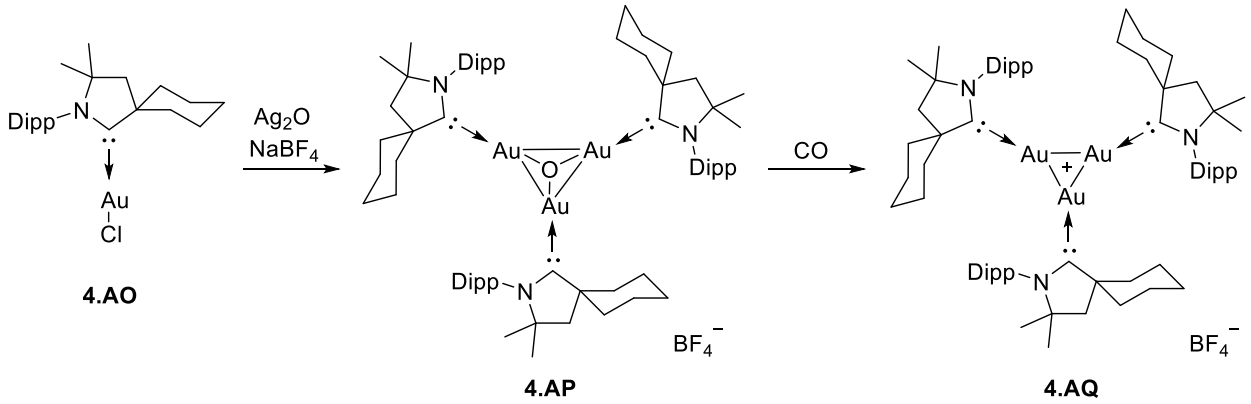

Scheme 4.9: Synthesis of a trinuclear gold cluster in the +1 oxidation state stabilized by three CAACs.

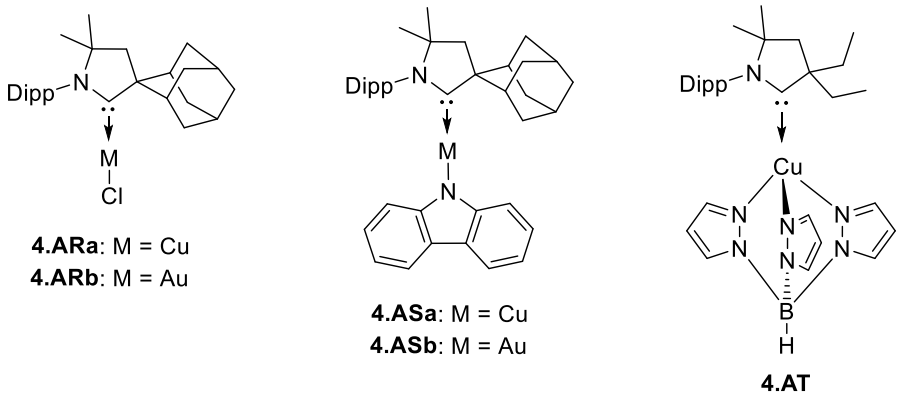

Figure 4.8: Photoluminescent coinage metal complexes featuring a CAAC ligand.

In addition to their high quantum efficiencies, CAAC coinage metal complexes have been shown to be excellent precatalysts for a diverse set of organic transformations. For example, the gold complex **4.ARb** was found to be highly efficient at coupling enamines and terminal alkynes to yield allenes in the presence of a halide abstracting agent (Scheme 4.10).[34] These reactions were performed at relatively mild temperature (90 ºC) with yields of up to 99% over 16 hours. The same $[(CAAC)Au]^+$ catalyst has

also been reported to facilitate the hydroamination of unactivated alkenes and alkynes using either ammonia or hydrazine as the amine source.[49-50] This reaction requires high temperatures, sometimes up to 175 ºC, in order to dissociate the thermodynamically favored Werner complexes made between Au^+ and the amines. Although this might be viewed negatively, it actually highlights the superior electronic properties of CAACs. First, the σ-donor strength of the carbene exhibits a strong trans effect, and thus assists in the dissociation of the amine in the rate limiting step. Second, hydrazine is a strong reducing agent and is often guilty of killing catalysts by generating inactive metal(0) particles.[51] Fortunately however, the high π-accepting property of CAACs strengthens the carbene-Au bond, therefore making the catalyst more robust and thus remaining active at higher temperatures.

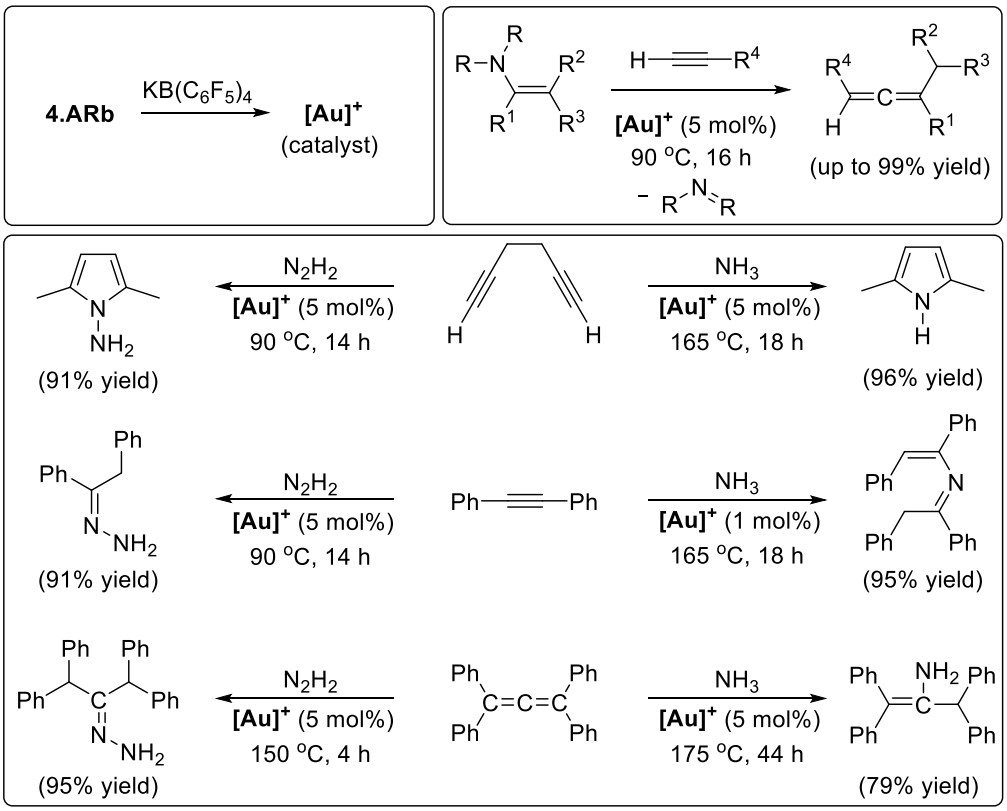

Scheme 4.10: Preparation of the active $[(CAAC)Au]^+$ gold catalyst (top left) in the coupling reactions of enamines and alkynes (top right), as well as the hydroamination of alkynes or allenes using ammonia or hydrazine as the nitrogen source (bottom).

CAACs are also excellent ligands for rhodium catalyzed hydrogenation of arenes. Zeng et al. showed that (CAAC)Rh(cod)Cl complexes **4.AU** showed impressive catalytic activity for the selective hydrogenation of aryl groups on phenyl ketones and alcohols (Scheme 4.11).[52] In as little as two days at room temperature, up to 99% conversion of the starting material could be converted to the respective cyclohexyl product with only 3 mol% catalyst loading. This reaction was even functional group tolerant to unsaturated amides, amino acids, carboxylic acids, esters, and ketones. Building off of these results, Glorius et al. recently reported that the same catalyst was also highly active for the *cis*-hydrogenation of 32 diverse (multi)fluorinated arenes.[53] Remarkably, the catalyst was selective for hydrogenation over hydrodefluorination, and therefore gave easy access to many previously synthetically challenging all-*cis*-(multi)fluorinated cyclohexane derivatives. All of these transformations were possible thanks to the overall strong donor abilities of CAACs making the Rh center electron rich.

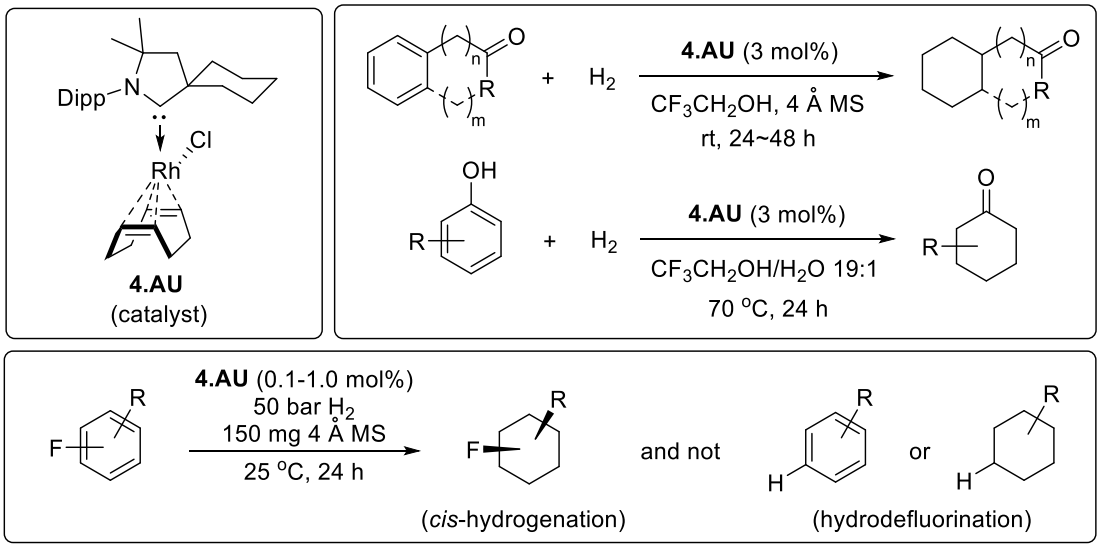

Scheme 4.11: (CAAC)Rh(cod)Cl catalyst (top left) active in the hydrogenation of aryl groups in phenyl ketones and alcohols (top right), as well as the *cis*-hydrogenation of (multi)fluorinated arenes (MS = molecular sieves).

Although many other catalytic transformations facilitated by CAAC TM complexes exist and are worth reader attention,[2] the last example given in this chapter focuses on potentially one of the most industrially viable transformations, namely ruthenium catalyzed olefin metathesis. Hoveyda-Grubbs

ruthenium catalysts featuring CAAC supporting ligands **4.AV** were easily synthesized via the room temperature *in situ* deprotonation and ligand substitution/complexation of the respective iminium and $RuP(Cy)_3$ precursors, respectively (Scheme 4.12).[8, 54] Many variations of the catalyst were synthesized, in which small steric changes were introduced by substituting different groups on both the aryl ring and quaternary carbon. Initially, these catalysts were found to have good activity for both cross- and ring closing-metathesis.[54] However, it wasn't until seven years later that these catalysts were discovered to be highly useful for the ethenolysis of seed-oil derivative methyl oleate.[8] Indeed, depending on the purity of ethylene used, catalyst loadings as low as 1 ppm gave turnover numbers (TONs) as high as 340,000. The high TONs and cheap cross-metathesis linker (ethylene) make this system incredibly valuable for the production of linear α-olefins on the industrial scale.

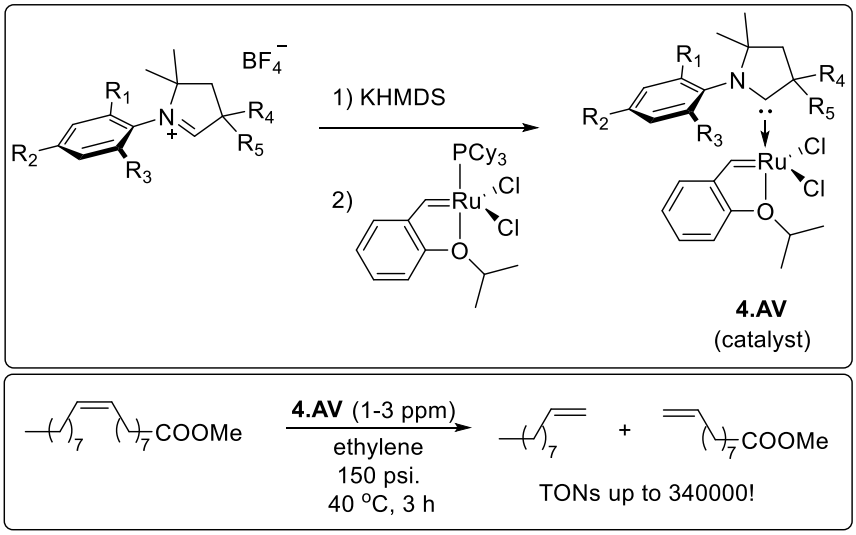

Scheme 4.12: Synthesis of Hoveyda-Grubbs type ruthenium catalysts supported by CAAC ligands (top) which are highly active for the ethenolysis of methyl oleate (bottom).

The topics presented thus far in no way come close to describing all of the published material featuring CAACs as a centerpiece of the scientific work. Hopefully however, this mini review of CAACs has painted a clear picture of how these carbon based species have made significant impacts on many different fields of chemistry. Similar to how NHCs essentially replaced phosphines as the universal ligand

in organometallic and inorganic chemistry, CAACs have now begun replace NHCs because of their superior electronic properties. It is therefore clear that the development of new CAACs, or CAAC-like species, with higher HOMOs, lower LUMOs, and smaller ΔE_{ST} could be highly desirable for chemists in the future. In this vein, Bertrand et al. recently synthesized a series of cyclic (amino)(aryl)carbenes (CAArCs) (Figure 4.9).[55] Clearly from the new name, these species only differ from CAACs by the replacement of the quaternary carbon "alkyl" group with an annulated "aryl" substituent. The added inductive effect of the aryl linker gives these variants lower HOMOs and LUMOs than CAACs, however they were not stable as free species. Iwamoto et al. and Kinjo et al. have reported heavier group XIV congeners of CAACs, namely a silylene (CAASi) and germylene (CAAGe), respectively.[56-57] Although they have lower LUMOs than CAACs and are even stable as free species, they unfortunately also have lower HOMOs, as is normally expected with the heavier congeners of carbenes.[58]

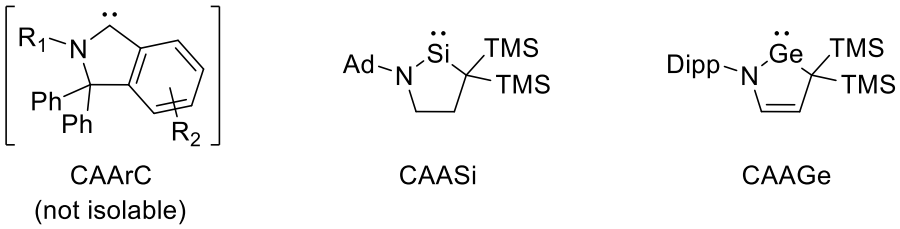

CAArC (not isolable) CAASi CAAGe

Figure 4.9: Closely related species to CAACs (Ad = adamantyl; TMS = trimethylsilyl).

As it is evident that changing the α-quaternary or carbene carbon atom to a different hybridization or element, respectively, does not yield isolable CAAC variants with all-around improved electronic properties, a different approach must be taken. Reflecting on what is known for NHCs, it is well established that increasing the carbene bond angle induces greater p-character of both the HOMO and LUMO of the carbene, effectively shrinking the ΔE_{ST}.[59-63] Indeed, DFT calculations at the B3LYP/def2-TZVPP level of theory found that expanding the ring size of NHCs from five to six decreases the HOMO-LUMO gap and ΔE_{ST} by 0.64 eV and 13.3 kcal mol^{-1}, respectively (Figure 4.10). Therefore, CAACs designed with larger internal bond angles should also benefit in the same manner. To test this theory, we recently synthesized and published several stable bicyclic (alkyl)(amino)carbenes (BICAACs) in which

the carbene is formally part of two six-membered rings.[64] ^{31}P NMR, ^{77}Se NMR, and TEP values corroborated with results from DFT calculations that BICAACs were indeed better π-acceptors and σ-donors than their five-membered analogues. BICAACs suffer from one limiting factor however, in that the strained bicyclic system causes the internal carbene bond angle to be more acute than in a simple monocyclic system. Indeed, the calculated HOMO-LUMO gap and ΔE_{ST} of CAAC-6 were found to be smaller than those of BICAAC by 0.08 eV and 8.3 kcal mol^{-1}, respectively. By extension, these values are also considerably smaller than those of CAAC-5 (0.39 eV and 11.8 kcal mol^{-1}) and NHC-6 (0.81 eV and 22.9 kcal mol^{-1}). It was therefore with great interest that monocyclic six-membered ring CAACs were synthesized and isolated, and their electronic and chemical properties studied.

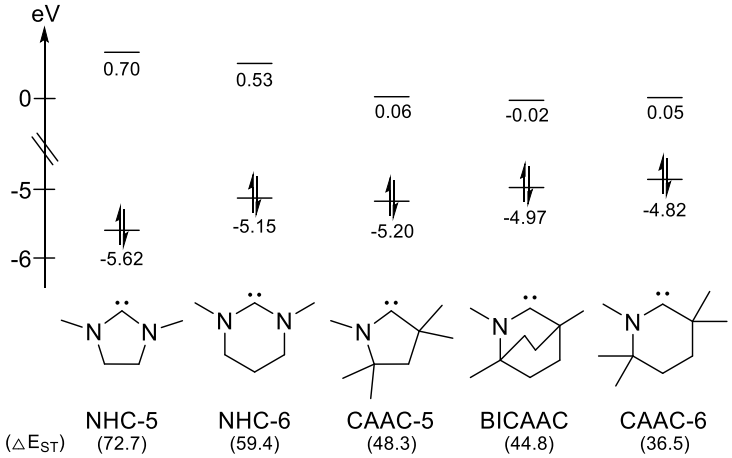

Figure 4.10: Calculated HOMO-LUMO gap (eV) and ΔE_{ST} (kcal mol^{-1}) of representative carbenes at the B3LYP/def2-TZVPP level of theory.

4.2 Highly Ambiphilic Room Temperature Stable Six-Membered Cyclic (Alkyl)(amino)carbenes

4.2.1 Synthesis

Referring to the published routes for CAAC-5 synthesis (Scheme 4.1),[6-7] the atoms that make up the 5-membered iminium precursors originate from two individual pieces, namely an imine and an

alkenyl halide. As imine **4.2a** was synthesized through a condensation reaction between 2,6-diisopropylaniline ($DippNH_2$) and aldehyde **4.1a**, respectively, it therefore seemed an obvious choice that expanding to a six-membered ring CAAC iminium precursor would be best achieved with an alkylation agent featuring one extra carbon link (Scheme 4.13). In order to disfavor the formation of undesired elimination side products greatly decreasing the overall yield, internal alkene 4-chloro-2-methyl-2-butene was first investigated as a likely alkylation reagent. Indeed, as a proof of principle for this method, deprotonation of imine **4.2a** with *n*-BuLi followed by addition of 4-chloro-2-methyl-2-butene at low temperatures easily yielded the respective alkenyl imine **4.3a**.

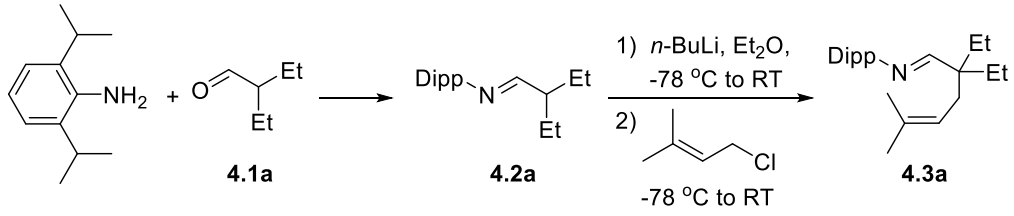

Scheme 4.13: Synthesis of an internal alkenyl imine precursor for a CAAC-6 species.

With the end goal of a six-membered iminium salt in mind, three potential cyclization routes were considered. First, simply following the published procedure for CAAC-5 synthesis might be a viable option. Unfortunately, cyclization through the addition of HCl and subsequent heating gave a mixture of both the 6-*endo* and 5-*exo* iminium salts **4.4a** and **4.5a**, respectively (Scheme 4.14). The mixture of products by this method was not surprising as the reaction can procede through either a tertiary or secondary carbocation intermediate. The same method is selective in the CAAC-5 synthesis as the carbocation position is heavily favored on the tertiary position instead of a primary one.

As the hydroiminiumation method was no longer a desirable option, we next considered cyclization by oxidation of the alkene. Unfortunately, addition of PhSeBr to **4.3a** gave a ~50:50 mixture of six- and five-membered iminium salts **4.6a** and **4.7a**. On the other hand, oxidation with Br_2 gave the desired six-membered ring iminium salts **4.8a** exclusively. It is well established with NHCs that a hydride can be easily removed from the C2 position in a completely saturated heterocycle to give an iminium

salt.[65] Therefore, we predicted that the addition of a strong hydride source should give a piperidine ring, which would then give us direct access to the CAAC-6 iminium salt precursor. Quite surprisingly however, upon addition of excess $LiAlH_4$ to **4.8a**, the ^1H NMR of the product displayed a quartet at 3.98 ppm. Furthermore, the ^{13}C NMR of the same product contained a doublet and triplet at 67.8 and 65.7 ppm, respectively, with no other signals in the same region. Therefore, reduction of **4.8a** did not yield the desired piperidine, and instead gave the five-membered species **4.9a**. A proposed mechanism for this reaction is given in Scheme 4.14. First, the iminium center is reduced by one equivalent of $LiAlH_4$. The now available nitrogen lone pair attacks the backside of the ring forming a bicyclic aziridinium intermediate, which is quickly quenched by another equivalent of hydride giving the pyrrolidine product.[66]

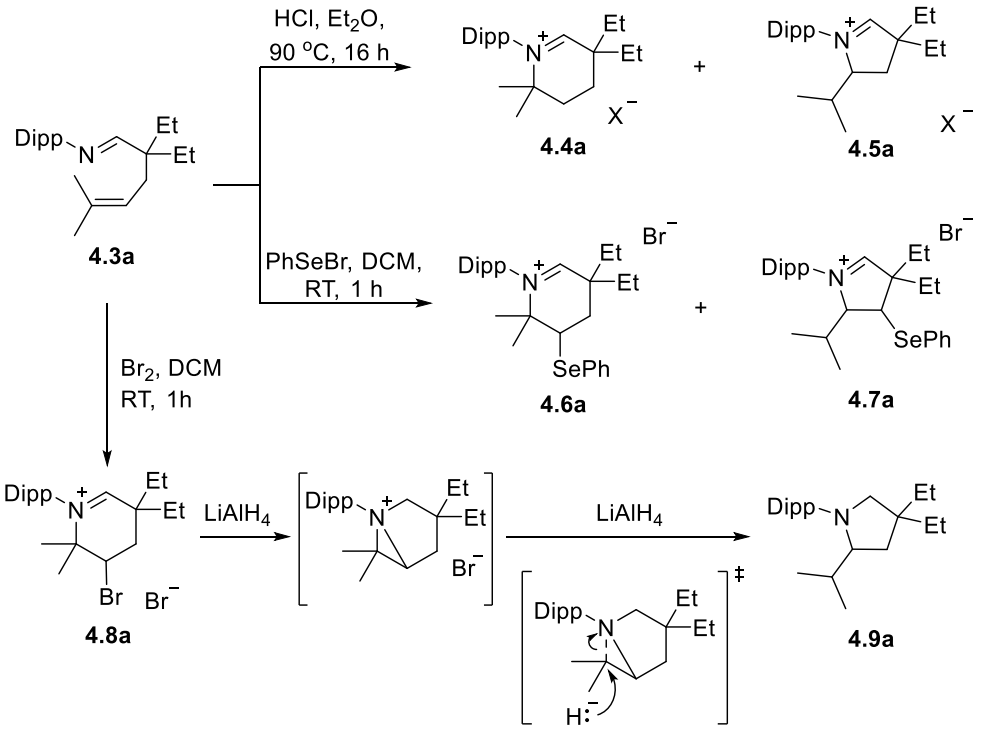

Scheme 4.14: Failed cyclization methods for making a CAAC-6 precursor.

Cleary, generation of a CAAC-6 precursor through an internal alkenyl imine like **4.3a** was not a viable route. As such, we revisited the possibility of using a terminal alkenyl imine instead. Imine **4.2a**

was once again deprotonated with *n*-BuLi, however this time three different 2-methyl-1-butene variants were tried as alkylating agents featuring either Br, I, or *p*-toluenesulfonate (Ts) as the potential leaving group (Scheme 4.15). When the Ts form was used, only imine starting material **4.2a** and an insoluble polymer, likely polyisoprene, could be recovered from the reaction mixture. Given the size of Ts, it's likely that the elimination reaction was more favored in this case. Moving to the smallest leaving group bromine, alkylation of the imine was much more favored as only ~10% of the imine starting material could be observed in the crude product mixture. The best case scenario occurred for the iodobutene however, as all of the imine was converted to the alkenyl imine **4.10a**.

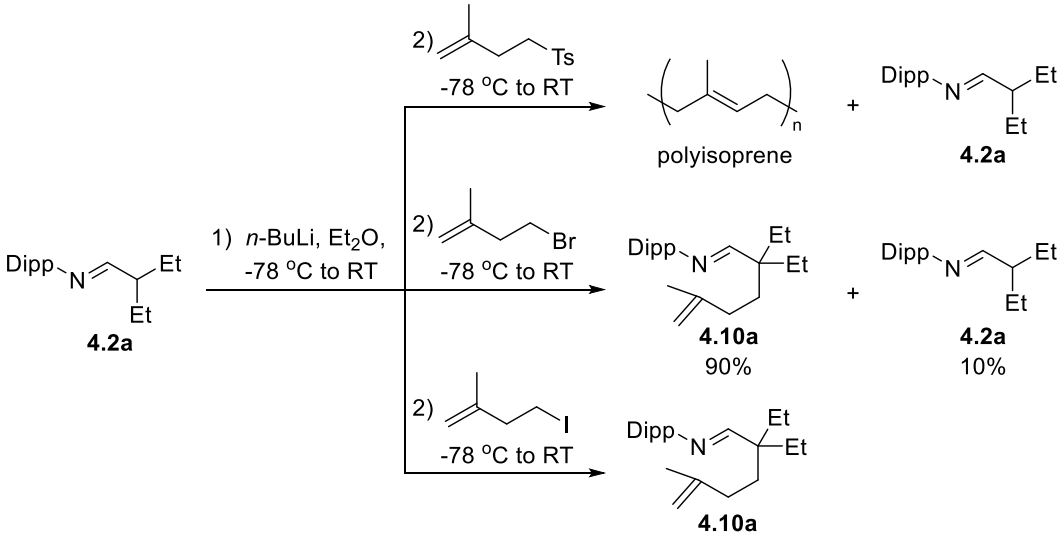

Scheme 4.15: Synthesis of a terminal alkenyl imine. Percentages given were determined from crude NMR spectra.

With a reliable method for generation of terminal alkenyl imine in place, attention was once again turned to the cyclization reaction. Proceeding via the hydroiminiumation route, heating a solution of **4.10a** and HCl in Et_2O overnight and subsequent washings with Et_2O gave a white precipitate. ^{1}H and ^{13}C NMR of the precipitate indicated that the product of this reaction was an ~10:1 mixture of the six- and five-membered iminium salts **4.4a** and **4.5a**, respectively (Scheme 4.16). The formation of **4.5a** was quite confusing as no reasonable reaction pathway giving this product could be hypothesized. Even more perplexing, upon an attempted anion exchange of this mixture with $NaBF_4$, the ratio of **4.4a**:**4.5a**

decreased to 3:1 after 12 h of stirring in a 1:1 DCM:H_2O mixture, as if **4.4a** was isomerizing into **4.5a**. This reaction was repeated several times with only small differences in the ratios of the two compounds being observed. Finally, after several months of frustration, the problem was identified and a solution was implemented.

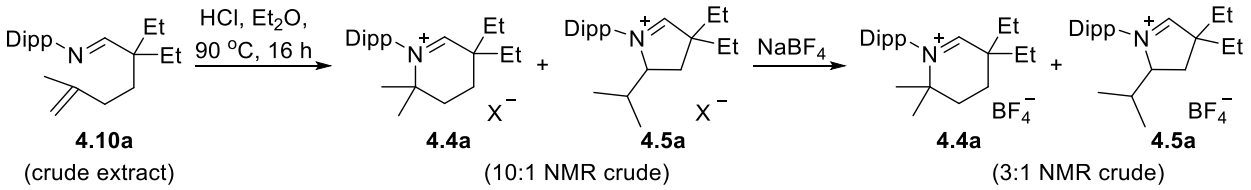

Scheme 4.16: Perplexing mixture of two iminium salts.

Upon alkylation of **4.2a** with 4-iodo-2-methyl-1-butene, the crude solution was always quite red in color. Originally, workup of **4.10a** included the removal of residual solvent *in vacuo* followed by an extraction with pentane. Theoretically, this should have removed all undesired salts from the solution. It did not however, remove the small amount of I_2 also generated from the alkylation reaction. Indeed, if the crude mixture was washed with a $NaHSO_3/H_2O$ mixture instead of a pentane extraction, the subsequent cyclization reaction yielded the six-membered iminium salt **4.4a** exclusively. To further test the hypothesis that it was I_2 causing the undesired mixture, alkenyl imine **4.10a** was first isolated and dissolved in Et_2O (Scheme 4.17). This solution was then divided into four separate high pressure Schlenks. To each was added two equivalents of 2.0 M HCl in Et_2O and then a substoichiometric quantity of one of the following four species: LiCl, LiI, NaI, I_2. For each of the solutions containing an ionic compound additive, the only iminium salt observed from this reaction was **4.4a**. This showed that adventitious Li^+, I^-, or even the combination of both, were not responsible for the isomerization reactions. For the solution containing I_2 however, a mixture of the two iminium salts and other crude products was observed. It is still unclear why I_2 gives a mixture; nonetheless, washing the alkenyl imine crude solution with a $NaHSO_3/H_2O$ mixture prevents this problem from persisting.

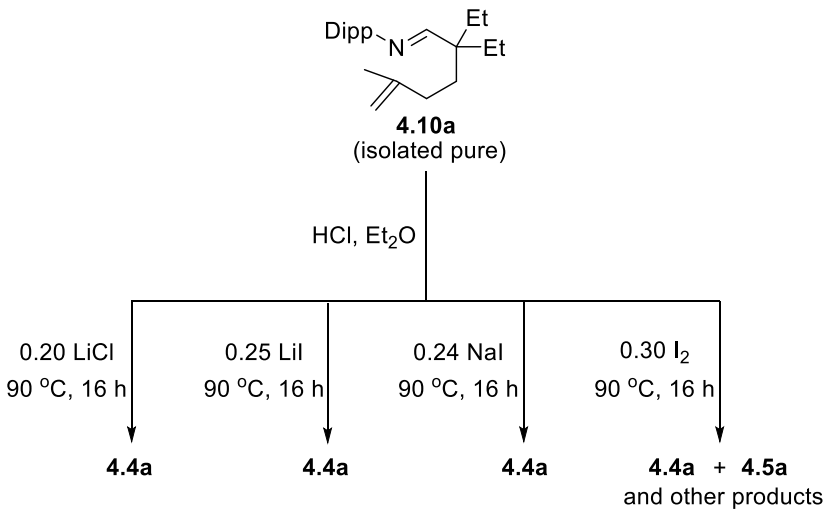

Scheme 4.17: Parallel substoichiometric reactions providing evidence that adventitious I_2 was the root cause of the mixture of iminium salts.

In all, the desired CAAC-6 precursors, namely iminium salts **4.4a-e**, could now be prepared by slight modification of the published CAAC-5 synthesis (Scheme 4.18). Condensation of aldehydes **1a-e** with $DippNH_2$ yielded imines **4.2a-e** in near quantitative yields. Deprotonation with *n*-BuLi followed by alkylation with 4-iodo-2-methyl-1-butene yielded alkenyl imines **4.10a-e**, which after an aqueous workup ($NaHSO_3/H_2O$), were used without further purification. Protonation of the imine with HCl in Et_2O, followed by thermally induced intramolecular hydroiminiumation resulted in the precipitation of the six-membered cationic heterocycles with Cl^- or HCl_2^- anions. Of particular note was the ring formation of compound **4.4d**. Although competing 6-*endo* (BICAAC) and 6-*exo* (CAAC-6) cyclization reactions should result in a mixture of products, nearly exclusive formation of the 6-*exo* product was observed likely due to the Thorpe-Ingold effect.[67] Finally, after an anion exchange with $NaBF_4$ and subsequent workup, compounds **4.4a-e** were isolated as microcrystalline colorless solids. Although the overall yields of these reactions were low, the reactions can be scaled with no apparent loss of yield.

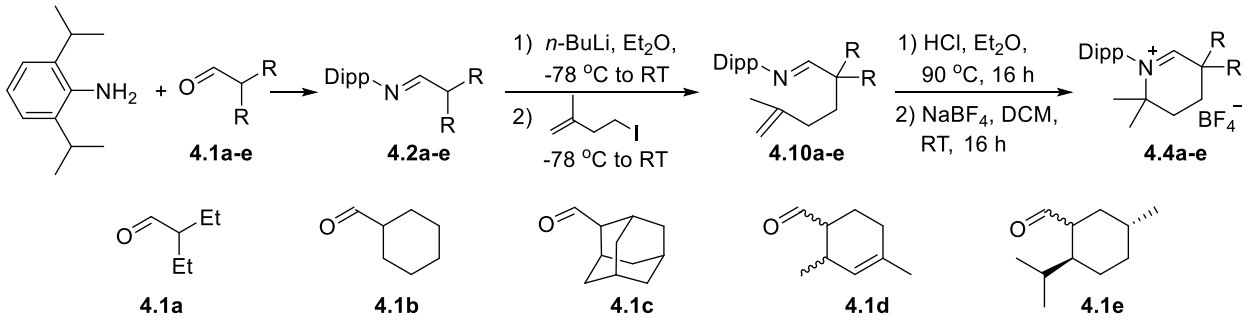

Scheme 4.18: General synthesis of CAAC-6 iminium salts **4.4a-e**. Isolated yields were calculated with respect to the imines **4.2**: **4.4a** (11%), **4.4b** (14%), **4.4c** (19%), **4.4d** (not isolated), **4.4e** (15%).

X-ray quality crystals were obtained for **4.4e** by slow diffusion of pentane into DCM (Figure 4.11). It should be noted that this batch of crystals came from a reaction with which the alkenyl imine **4.10e** was not washed with a $NaHSO_3/H_2O$ solution. As such, the final iminium salt was actually a deep red ionic compound with an I_3^- anion. Therefore, a comparison of bond lengths here might not be appropriate as the I_3^- anion might be weakly coordinating to the iminium proton [H1···I 2.949 Å]. Nonetheless, the structure not only provides unambiguous evidence that a six-membered iminium ring was formed from this reaction, but also that iodine does transfer into the reaction products unless the $NaHSO_3/H_2O$ wash was performed

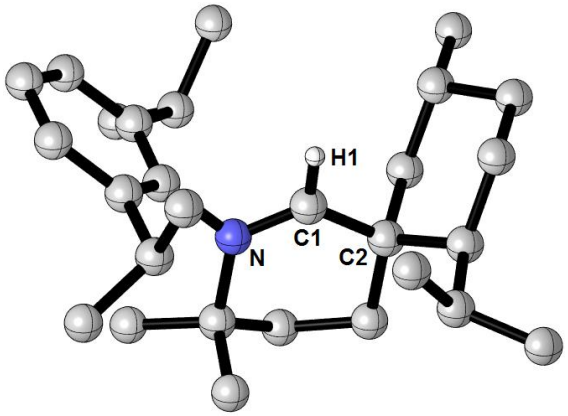

Figure 4.11: Solid state structure of the cationic part of **4.4e**. H-atoms, except for H1, and the I_3^- anion have been removed for clarity. Selected bond lengths (Å) and angles (°): N-C1 1.289(1), C1-C2 1.496(1), N-C1-C2 127.0(1).

With iminiums **4.4** in hand, we investigated whether the free carbene would be stable. C_6D_6 was added to an NMR tube containing KHMDS and either **4.4a** or **4.4b** (Scheme 4.19). To our delight, we observed clean conversion of the starting material into one product giving a sharp ^{13}C NMR signal at 330 ppm for both reactions, indicative of the formation of carbenes **4.11a**,**b**, respectively (Figures 4.12, 4.13). This signal is slightly downfield shifted compared to that of the analogous CAAC-5 species (317 ppm),[68] and close in value to that of BICAACs (335 ppm).[64] Carbenes **4.11a**,**b** are stable in solution for days without any evidence of decomposition; however, attempts to obtain single crystals failed. It should be noted that a six-membered cyclic (alkyl)(amido)carbene was recently postulated as an intermediate, but the free carbene was not observed.[69]

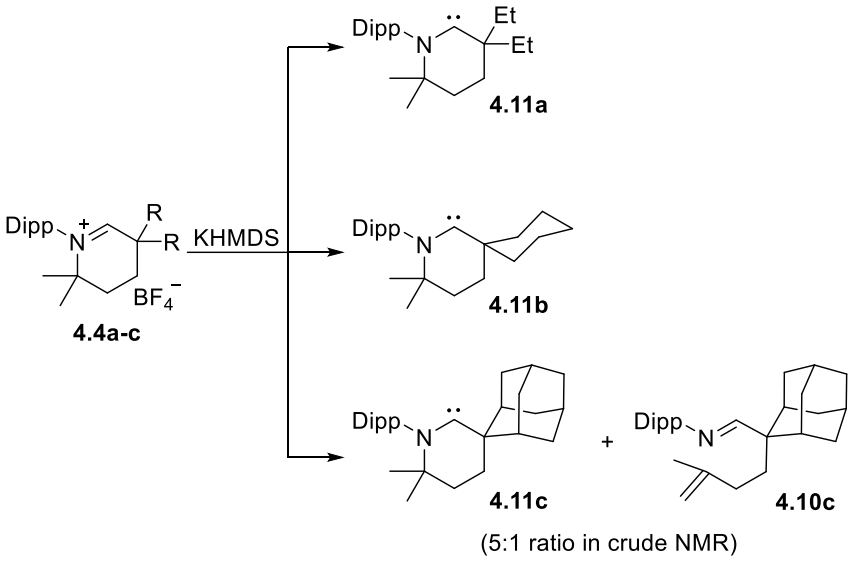

Scheme 4.19: Deprotonation of **4.4a-c** giving CAAC-6 **4.11a**,**b** or mixture of CAAC-6 **4.11c** and alkenyl imine **4.10c**, respectively.

In the hope of obtaining a crystalline CAAC-6 derivative, we moved to **4.4c** featuring the rigid diamondoid adamantyl group. Addition of benzene to a solid mixture of **4.4c** and KHMDS gave a bright yellow solution containing free carbene **4.11c** ($^{13}C_{carbene}$ = 345 ppm) and alkenyl imine **4.10c** in a 5:1 mixture (Figures 4.14, 4.15). Unlike carbene precursors **4.4a**,**b**, the iminium canter in **4.4c** is sandwiched between an adamantyl and a Dipp group, two very sterically hindering substituents. As a result of the

increased bulk, there are now two competing deprotonation pathways: one of which is the kinetic product and involves the deprotonation of one of the *gem*-dimethyl groups to give **4.10c**. Indeed, when this reaction was instead performed at -78 ºC in THF, the major product was now **4.10c**. Therefore, it is highly recommended that all deprotonation reactions involving CAAC-6 precursors be performed at or near room temperature. Synthetic problems aside, **4.11c** can be isolated from the mixture as bright yellow single crystals by recrystallization from a concentrated pentane solution at -20 ºC.

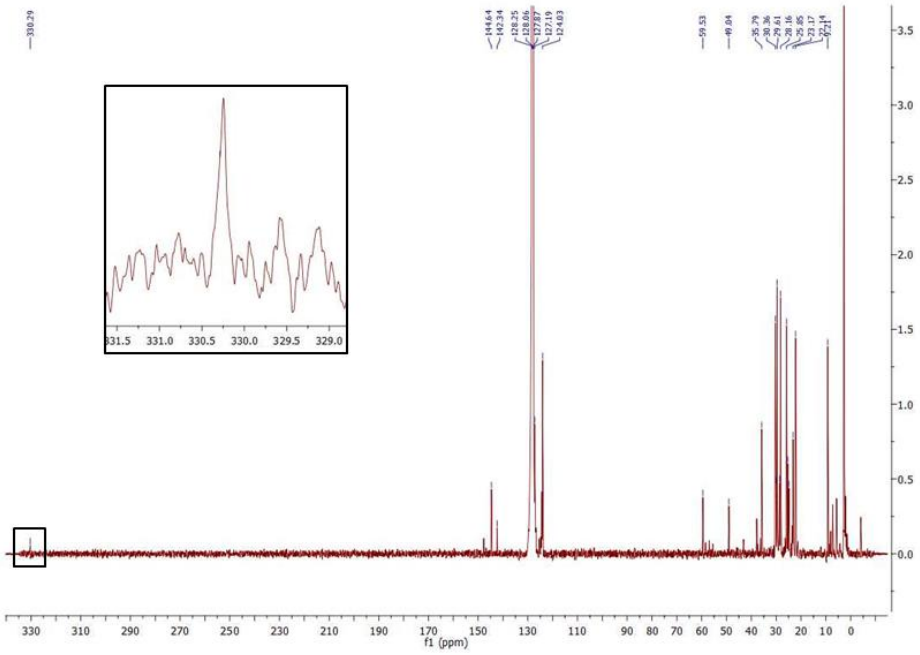

Figure 4.12: Crude $^{13}C\{^{1}H\}$ NMR spectra of deprotonation reaction forming **4.11a** (C_6D_6, 126 MHz).

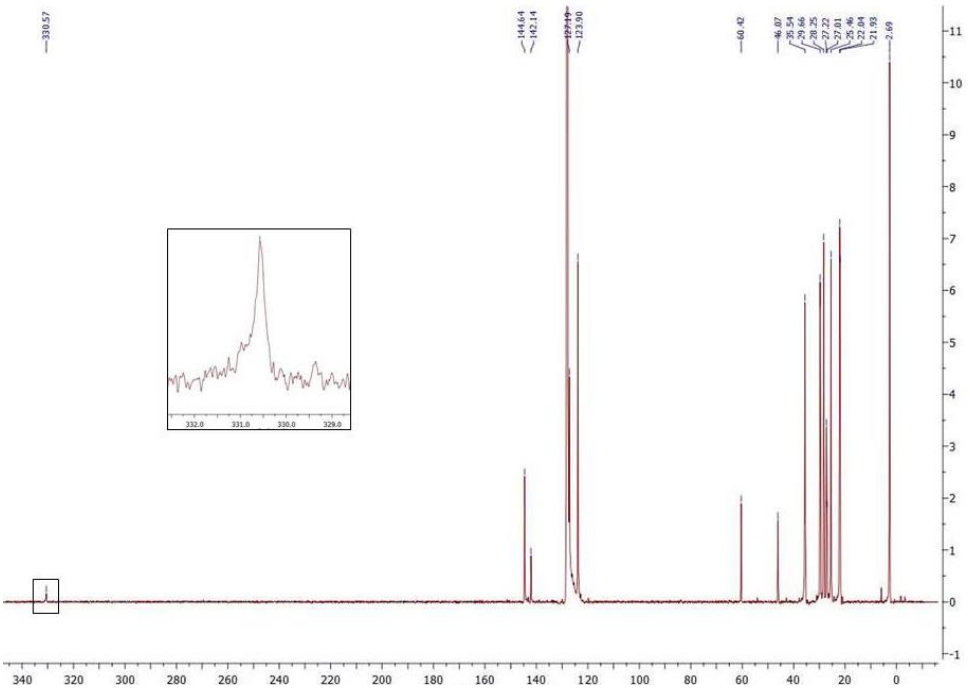

Figure 4.13: Crude $^{13}C\{^{1}H\}$ NMR spectra of deprotonation reaction forming **4.11b** (C_6D_6, 126 MHz).

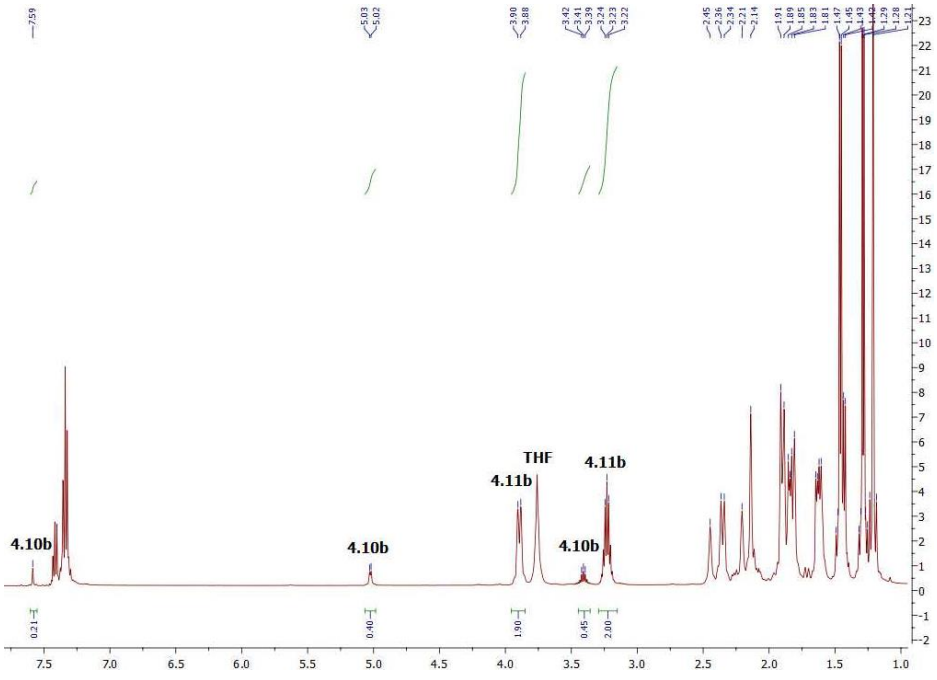

Figure 4.14: ^{1}H NMR of deprotonation reaction forming **4.11c** and **4.10c** showing ~5:1 mixture (C_6D_6, 500 MHz).

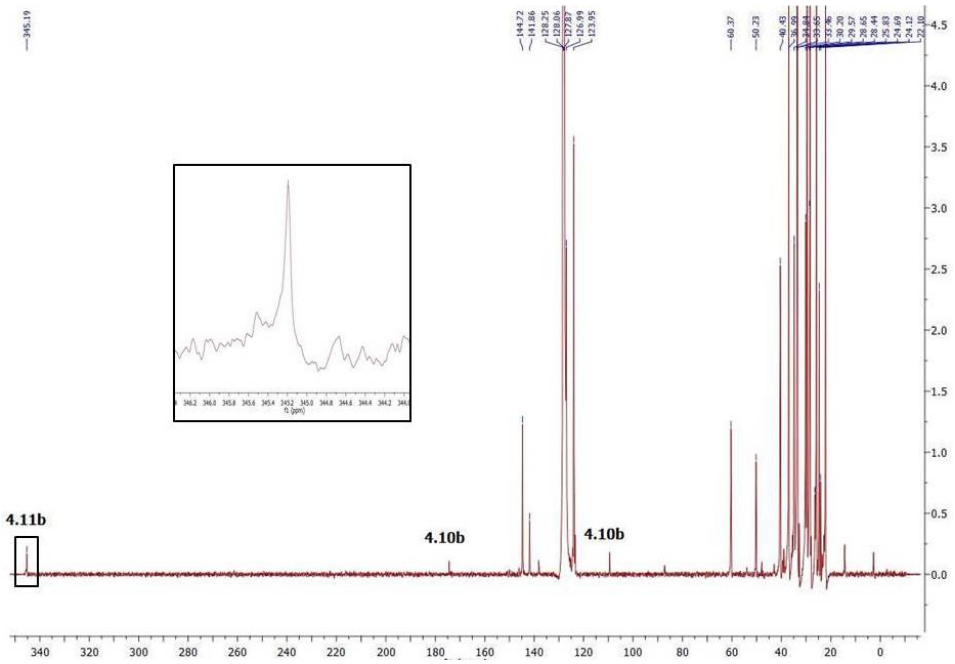

Figure 4.15: $^{13}C\{^{1}H\}$ NMR of deprotonation reaction showing mixture of **4.11c** and **4.10c** (C_6D_6, 126 MHz).

The most striking structural parameter of carbene **4.11c** is the N-C1-C2 bond angle (Figure 4.16, left). At 117.9 degrees, the carbene bond angle is 11.5 degrees larger than the analogous CAAC-5 derivative (Figure 4.16, right).[34] Other than the significantly larger bond angle however, all other important structural parameters are essentially equivalent within the standard deviation error. Nevertheless, the internal bond angle of **4.11c** is also 9.6 degrees larger than the recently published BICAAC. Furthermore, acyclic (alkyl)(amino)carbenes (AAACs),[70] some of the most π-accepting singlet carbenes to date, are only 2.6 degrees more obtuse than **4.11c** (see section 1.3.3 for a more detailed description of π-accepting properties of carbenes).

Although highly air and moisture sensitive, **4.11c** is stable both in solution and in the solid state for weeks at room temperature, and decomposition is only observed above 50 ºC in solution and 120 ºC in the solid state. Indeed, a C_6D_6 solution of **4.11c** heated in a J-Young NMR tube at 50 ºC for 12 h gave a complicated ^{1}H and $^{13}C\{^{1}H\}$ NMR spectra which contained signals for unreacted carbene, alkenyl imine **4.10c**, and likely the C-H insertion product **4.12** in a 6:2:3 ratio, respectively (Scheme 4.20). Benzylic C-H insertion reactions with CAAC-5 have been observed before, however these reactions required

temperatures as high as 110 ºC to favor the intramolecular C-H insertion.[10] The lower temperature required for formation of **4.12** gave the first indication that CAAC-6s like **4.11c** might exhibit different reactivity based on their smaller HOMO-LUMO gaps.

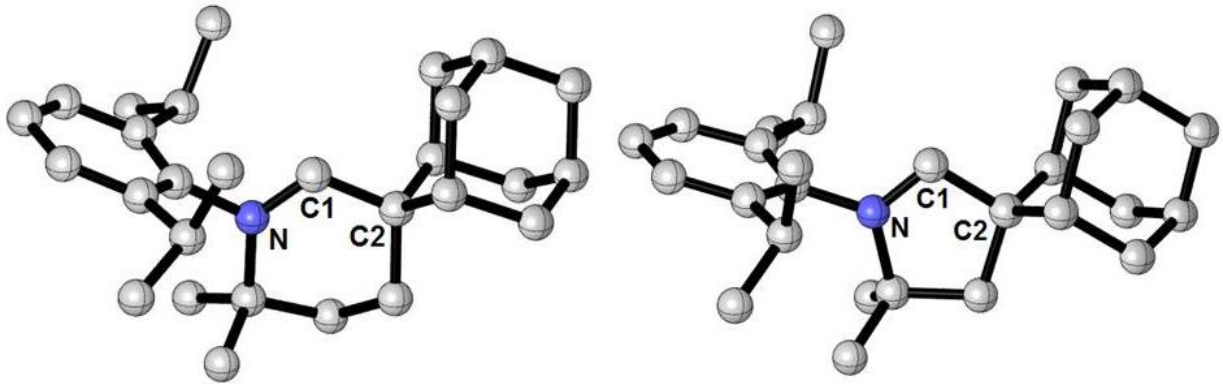

Figure 4.16: Solid state structures of **4.11c** (left) and analogous CAAC-5 derivative (right). H-atoms are omitted for clarity. Selected bond lengths (Å) and angles (º): **4.11c** N-C1 1.3101(14), C1-C2 1.5252(13), N-C1-C2 117.88(9); CAAC-5 N-C1 1.312(1), C1-C2 1.531(1), N-C1-C2 106.36(1).

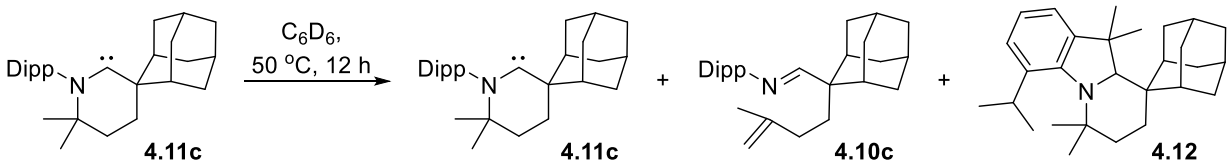

Scheme 4.20: Proposed decomposition products upon mild heating of carbene **4.11c**.

4.2.2 Quantum Mechanical, Spectroscopic, and Reactivity Studies of CAAC-6 Derivatives

With an X-ray structure of CAAC-6 **4.11c** in hand, we used the crystallographic data to investigate the full molecule computationally. The ΔE_{ST} of this carbene was calculated to be 32.2 kcal mol^{-1} at the B3LYP/def2-TZVPP level of theory. It should be noted that this value is 4.3 kcal mol^{-1} smaller than the ΔE_{ST} calculated for the simplified CAAC-6 derivative featuring methyl substituents at both the nitrogen and quaternary carbon atoms. The remarkably small ΔE_{ST} value for **4.11c** is best explained upon a comparison of the singlet and triplet state geometries (Figure 4.17). The most important

geometric change is indeed the puckering of the N-C1-C2 carbene bond (front of image) when transitioning from the singlet to triplet state. The loss of planarity about this bond makes sense as the carbene is no longer sp^2 hybridized in the triplet state. Importantly however, the puckering also results in the six-membered ring conforming to a thermodynamically favored cyclohexyl chair geometry. The more rigid systems of BICAACs and CAAC-5s cannot benefit from this added geometric stabilization energy, therefore giving CAAC-6 species the lowest ΔE_{ST} value.

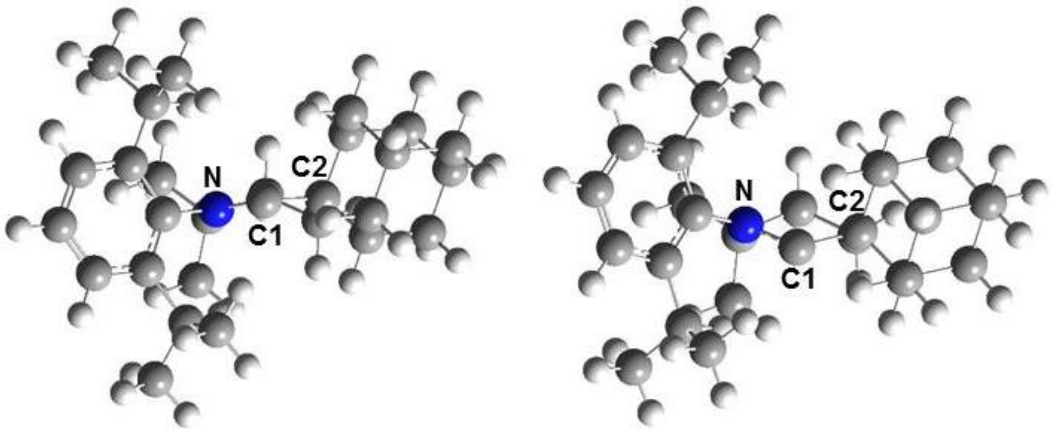

Figure 4.17: Front view of the calculated singlet (left) and triplet (right) geometries of **4.11c** at the B3LYP/def2-TZVPP level of theory (N-C1-C2 is front-facing).

As mentioned before, carbene **4.11c** was isolated as bright yellow single crystals. As such, this carbene is the first CAAC with an n → π* transition trailing into the visible region (Figure 4.18). In an attempt to better understand the electronic transitions, we simulated the UV-Vis spectra at the M062X/def2-TZVPP level of theory employing DFT and TD-DFT with a Tamm-Dancoff approximation (see section **4.5.4** for a more detailed explanation). In order of increasing energy, the three major electronic transitions observed are n → π*, n → π* and π → π* with λ_{max} = 396, 300 and 250 nm, respectively. The low energy first n → π* transition (3.1 eV), also the HOMO-LUMO transition, is best explained upon inspection of the carbene's LUMO (Figure 4.19). Surprisingly, the Dipp group π* orbital is in close enough proximity to the C-N π* orbital. This causes the two orbitals to mix, lowering the overall energy of the orbital and giving rise to the observed yellow color. The close proximity of the two

π* orbitals is likely a result of the wider carbene bond angle positioning the Dipp group closer to the carbene center. In all, the relatively low energy vibronic absorption of **4.11c** highlights the very small HOMO-LUMO gap of CAAC-6 species.

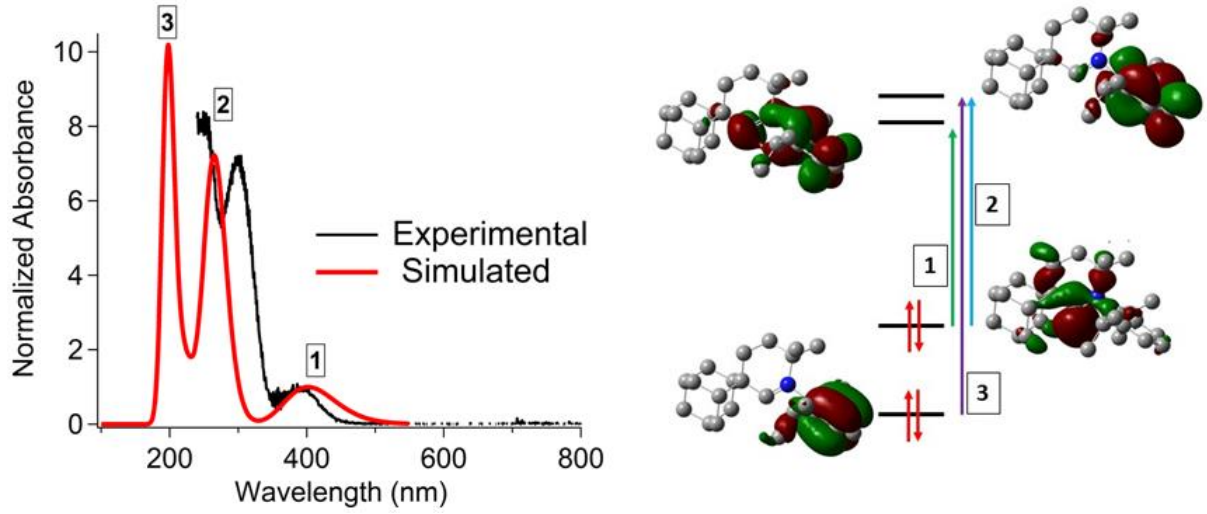

Figure 4.18: Experimental versus simulated UV-Vis spectra (left), and MOs and corresponding electronic transitions for **4.11c** (right). Degenerate states and hydrogen atoms removed for clarity.

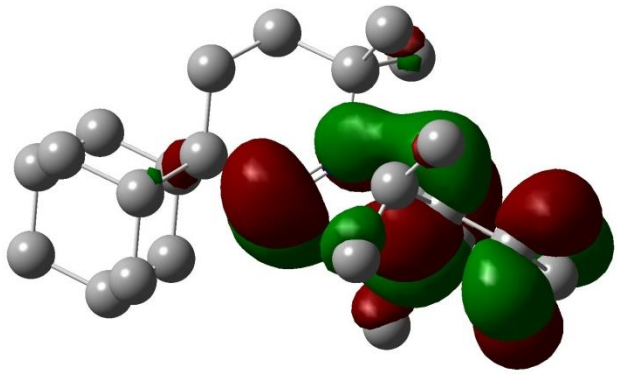

Figure 4.19: LUMO of carbene **4.11c** (isovalue = 0.03). H-atoms removed for clarity.

To better probe the effect of the ring size on the steric environment around the carbene center, carbene **4.11c** was reacted with (tht)AuCl (Scheme 4.21). After workup, colorless crystals of complex **4.13c** were grown by slow diffusion of pentane into DCM at room temperature (Figure 4.20). The 14 e^- complex is nearly linear [C1-Au-Cl 178.1(1) º] with the longest carbene-Au bond [C1-Au 1.990(5) Å]

recorded thus far for a (CAAC)AuCl complex.[34, 50, 71] This was a little surprising as the expected higher π-acidity of CAAC-6 species should have resulted in a shorter carbene-Au bond. However, given the large size of gold, the lengthening of the bond is likely due to steric clashing with the protruding substituents. Indeed, we found carbene **4.11c** to have a relatively high percent buried volume (%V_{bur}) of 51.1%, an increase of 3.2% from the CAAC-5 complex with identical substituents (see section 1.3.1).[72]

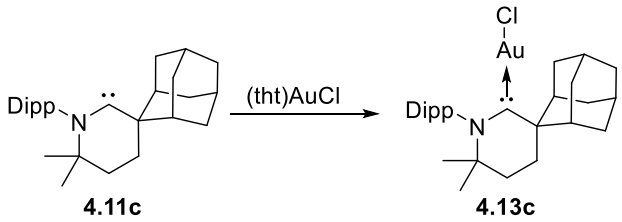

Scheme 4.21: Probing the sterics of a CAAC-6.

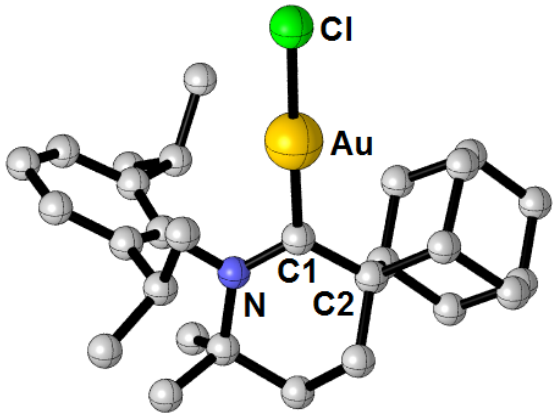

Figure 4.20: Solid-state structure of **4.13c**. H-atoms are omitted for clarity. Selected bond lengths (Å) and angles (°): C1-Au 1.990(5), N-C1 1.323(6), C1-C2 1.533(6), N-C1-C2 117.5(4), C1-Au-Cl 178.7(1).

The increased steric demand of CAAC-6 species can even play a fairly significant role in the stabilization of amino ketenes. It is worth noting that amino ketenes are rare species with only four structurally confirmed examples:[73-75] one of these has been argued to be irreproducible,[76] and another required 100 psi of CO to prevent regeneration of the carbene.[74] In addition to their low ΔE_{ST} and high formation energy barrier, amino ketenes derived from carbenes experience low stability due to the

susceptibility of the central ketene carbon atom to nucleophilic attack.[77] Without proper steric protection, attack of a second carbene is faster than the complexation of CO to that carbene, therefore giving betaine intermediates which frequently undergo subsequent rearrangement reactions to give colorless products.[78-79] For example, of the remaining two known amino ketenes, one was derived from an AAAC, and the other a CAAC-5 featuring the bulky menthyl group.[73] Both of these species have substituents which sterically protect the LUMO from nucleophilic attack. However, if smaller CAAC-5s featuring cyclohexyl or dimethyl groups at the quaternary carbon are instead employed, the betaine formation is favored over the amino ketene (Scheme 4.22).[27, 80] When carbene **4.11a**, which features diethyl groups, was subjected to an atmosphere of CO at room temperature, the solution turned a deep red color. Additionally, we observed clean conversion of the carbene to a single new species with a signal at 235 ppm in the ^{13}C NMR, indicative of the formation of an amino ketene. Single crystals of **4.14a** were grown from a -40 ºC pentane solution confirming the hypothesized structure (Figure 4.21). It is clear from the stability of **4.14a** that the larger carbene bond angle of CAAC-6 species increases the steric protection about the LUMO of the ketene enough to prevent further *in situ* reactivity.

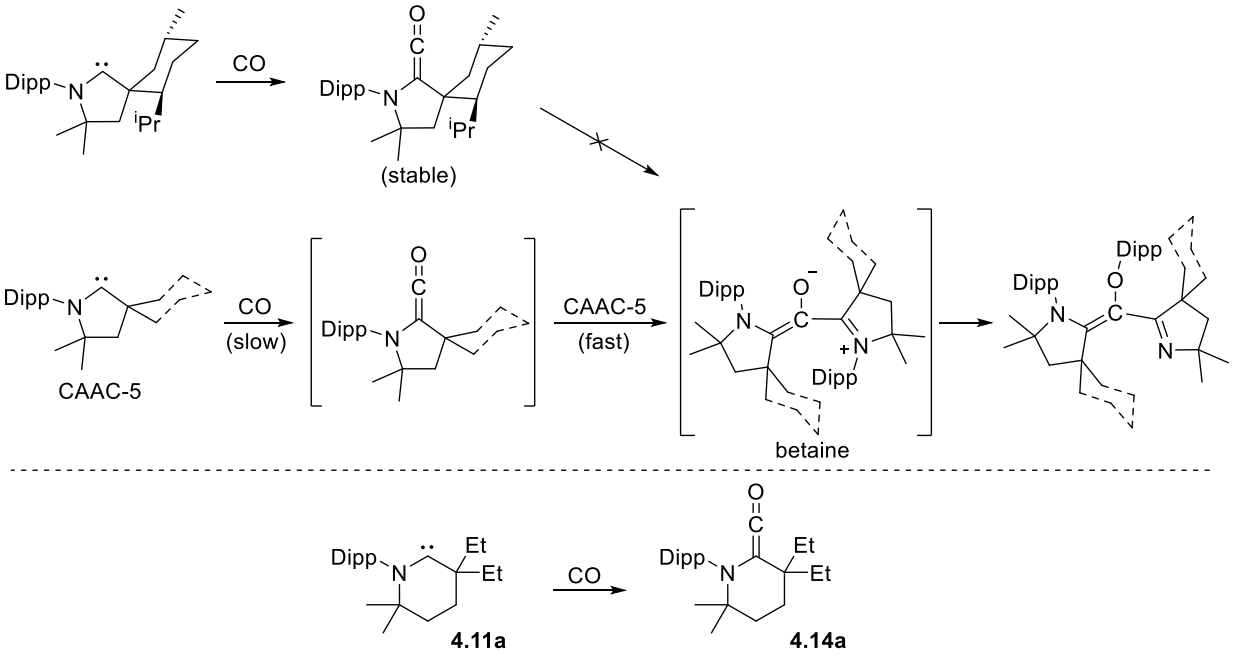

Scheme 4.22: Sterics influencing the stability of amino ketenes derived from CAAC-5 (top) and CAAC-6 (bottom).

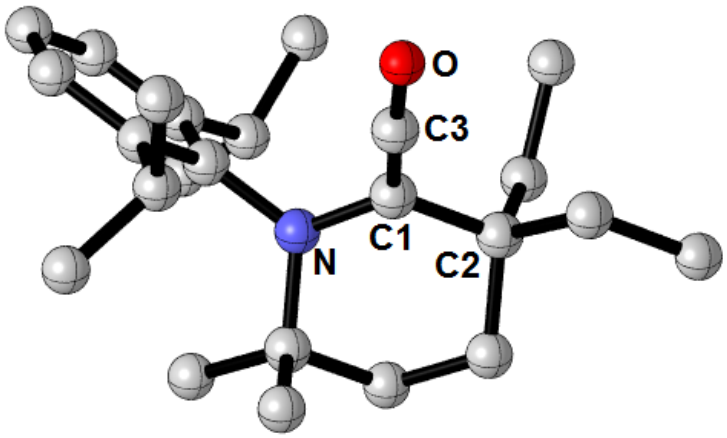

Figure 4.21: Solid state structure of **4.14a**. H-atoms are omitted for clarity. Selected bond lengths (Å) and angles (°): N-C1 1.427(2), C1-C3 1.319(2), C1-C2 1.540(2), C3-O 1.179(2), C1-C3-O 173.3(1).

We then explored the overall donor capabilities of CAAC-6. A stirred THF solution of carbene **4.11c** and $[Rh(cod)Cl]_2$ led to the formation of the corresponding (**4.11c**)Rh(cod)Cl complex (Scheme 4.23). Subjecting a THF solution of this complex to a CO atmosphere, after workup, afforded orange single crystals of **4.15c** (Figure 4.22). The IR spectrum of **4.15c** (KBr, DCM solution) showed two CO stretching frequencies at 2067 and 1990 cm^{-1} (ν^{av}_{CO} = 2029 cm^{-1}). The average value is red-shifted from both CAAC-5 (ν^{av}_{CO} = 2036 cm^{-1}) and BICAAC (ν^{av}_{CO} = 2032 cm^{-1}) proving that **4.11c** is by far the most overall electron-donating CAAC to date (see section 1.3.2).

Comparing the ^{31}P NMR signals of carbene-phenylphosphinidene adducts has been shown to be a useful method for assessing the π-accepting properties of a carbene (see section 1.3.3). Although **4.11c** proved to be too sterically demanding, **4.16a** could be generated *in situ* by heating a mixture of **4.11a** and $(PhP)_5$ at 60 ºC for 3h. The ^{31}P NMR signal of **4.16a** appears at 103 ppm, downfield shifted compared to those of CAAC-5 and BICAAC, by 34 and 13 ppm, respectively, suggesting that CAAC-6 is extremely electrophilic. To further confirm the π-accepting properties of CAAC-6, the Se adduct **4.17a** was synthesized, and gave a ^{77}Se NMR signal at 715 ppm, downfield of both CAAC-5 (492 ppm) and

BICAAC (645 ppm). Surprisingly however, when the analogous Se adduct **4.17c** was synthesized, the ^{77}Se NMR signal appeared at 863 ppm. The 148 ppm difference between these two values was remarkable considering that they should have nearly identical π-accepting properties. We later came to understand that the more deshielded value was actually due to C-H···Se nonclassical hydrogen bonding (NCHB) interactions (see section 4.3.3). Nonetheless, from these results as a whole it can be concluded that CAAC-6 species are highly ambiphilic.

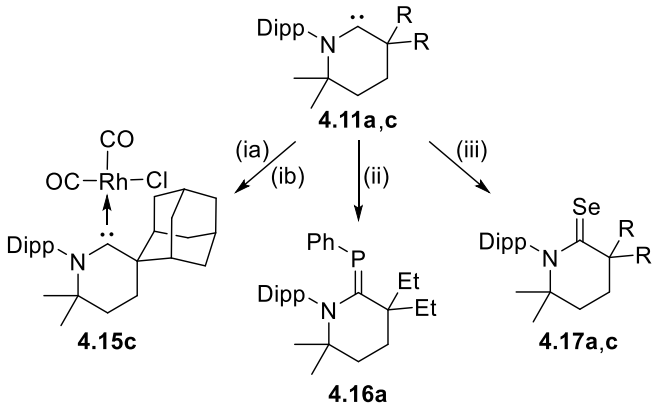

Scheme 4.23: Probing the electronics of CAAC-6: (ia) 0.4 eq. $[Rh(cod)Cl]_2$, THF, RT, (ib) CO, THF, RT; (ii) $(PhP)_5$, C_6D_6, 60 ºC; (iii) Se, THF, RT.

In the hope of preparing an enantiomerically pure CAAC-6, we turned our attention to the deprotonation of **4.4e** (Scheme 4.24). Upon addition of KHMDS, complete consumption of the starting material resulted in a 10:1 mixture of two products (Figures 4.23, 4.24). The minor product was easily identified as alkenyl imine **4.10e** mirroring the deprotonation reaction of **4.4c**. Surprisingly however, the major product was not carbene **4.11e** as no ^{13}C NMR signal could be found downfield of those of the aromatic carbons. Furthermore, DEPT-90 and DEPT-135 experiments revealed the presence of two additional CH groups and one fewer CH_2 group than would have been expected for carbene **4.11e** (Figures 4.25, 4.26). These data suggested that a carbene C-H insertion occurred. Indeed, an X-ray diffraction study of single crystals, grown from a concentrated pentane solution at room temperature, unambiguously identified the product as the tricyclic compound **4.18** (Figure 4.27). The latter clearly

results from the insertion of the carbene into the α-CH_2 group of the menthyl substituent. This is the first example of a CAAC inserting into an unactivated C-H bond, and a further indication of the highly ambiphilic nature of CAAC-6. Note that since such a C-H insertion was not observed in the case of **4.11a**,**b**, it is likely due to the rigidity of the menthyl substituent, which brings the methylene group in close proximity to the carbene center. Although **4.18** is a highly strained tricyclic compound, the C-H insertion reaction was found to be nonreversible. Indeed, heating a THF solution of **4.18** at 80 ºC in the presence of S_8 did not yield the corresponding sulfur adduct or any of the other previous CAAC-6 decomposition products previously observed.

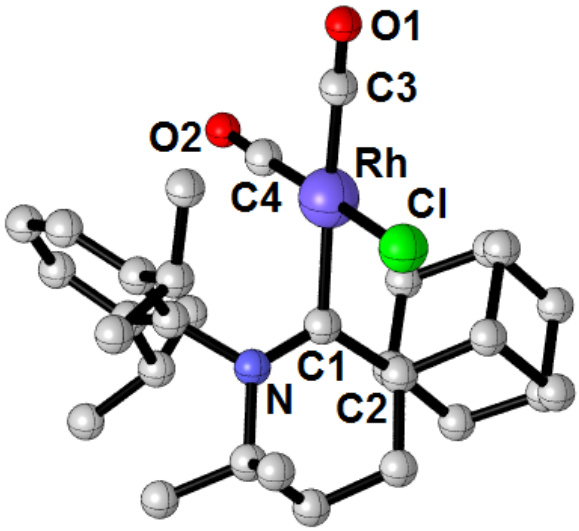

Figure 4.22: Solid-state structure of **4.15c**. H-atoms are omitted for clarity. Selected bond lengths (Å) and angles (°): C1-Rh 2.087(3), N-C1 1.327(5), C1-C2 1.555(6), C3-O1 1.098(5), C4-O2 1.139(5), Rh-Cl 2.408(1), N-C1-C2 119.7(3), C1-Rh-C3 169.9(2), C1-Rh-C4 97.3(2).

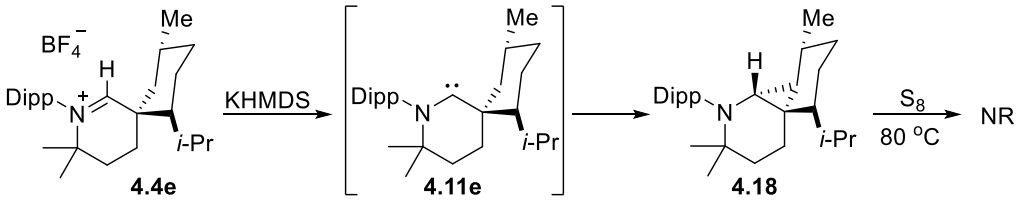

Scheme 4.24: Formation of the carbene C-H insertion product **4.18** is nonreversible. Alkenyl imine **4.10e** was also a minor product of the deprotonation reaction.

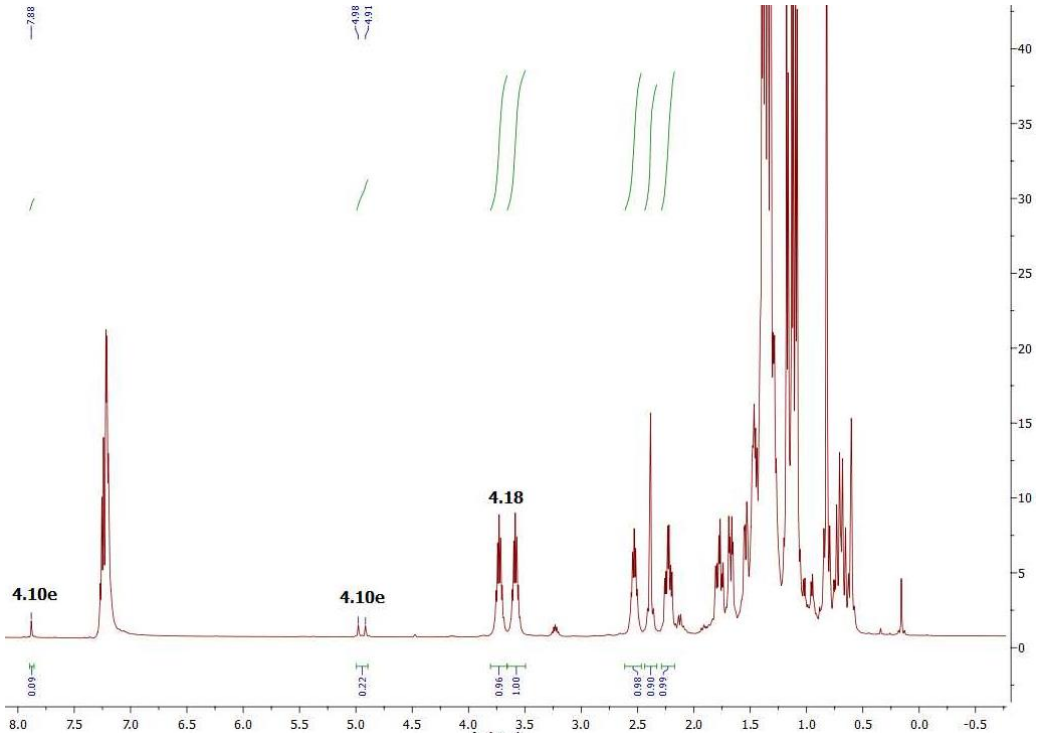

Figure 4.23: ^{1}H NMR of crude mixture **4.18** and **4.10e** showing ~10:1 mixture (C_6D_6, 500 MHz).

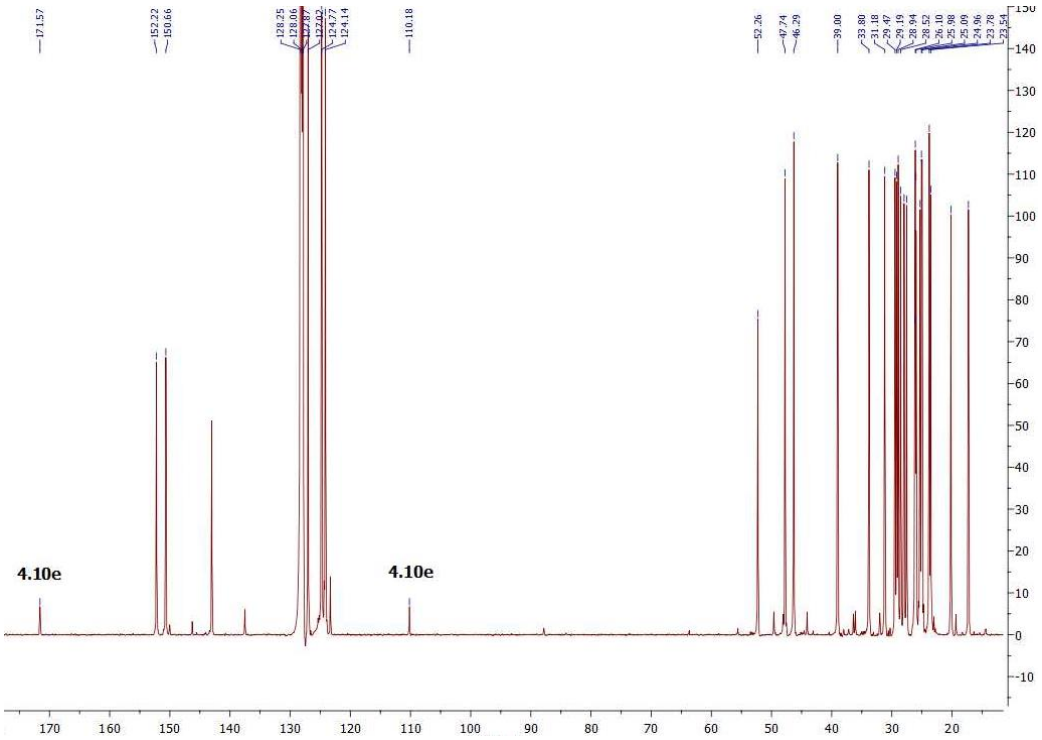

Figure 4.24: $^{13}C\{^{1}H\}$ NMR of crude mixture **4.18** and **4.10e** showing ~10:1 mixture (C_6D_6, 126 MHz).

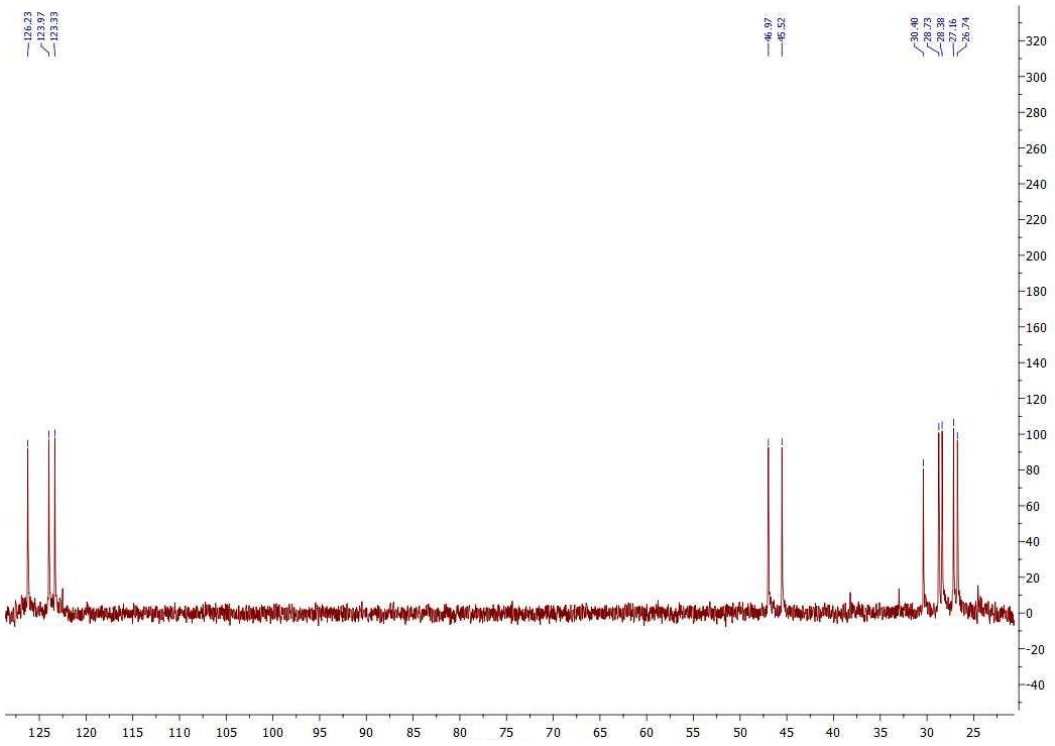

Figure 4.25: DEPT-90 NMR of **4.18** showing ten total CH and CH_3 groups ($CDCl_3$, 75 MHz).

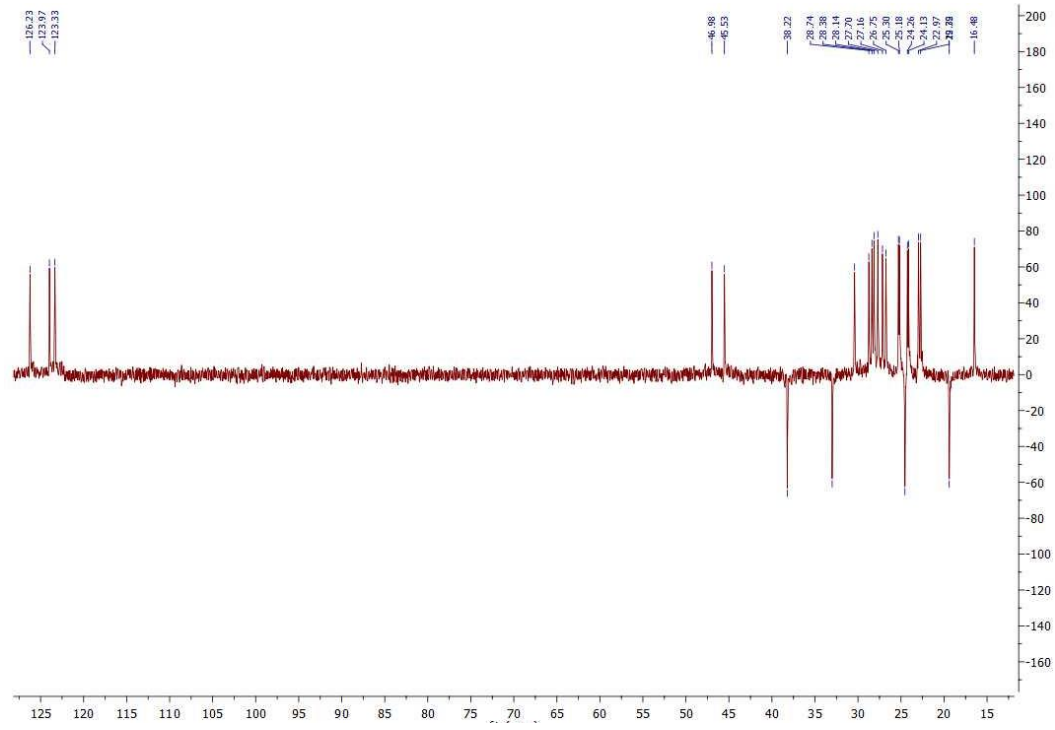

Figure 4.26: DEPT-135 NMR of **4.18** showing four CH_2 groups ($CDCl_3$, 75 MHz).

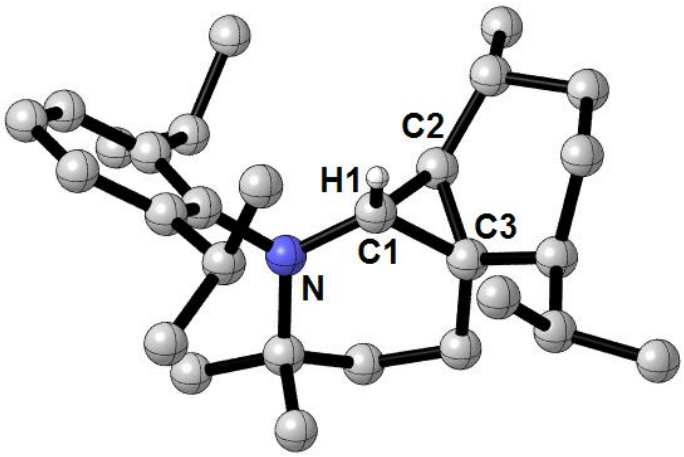

Figure 4.27: Solid-state structure of **4.18**. H-atoms except H1 were removed for clarity. Selected bond lengths (Å) and angles (°): N-C1 1.4378(18), C1-C2 1.508(2), C1-C3 1.524(2), N-C1-C2 120.85(13), N-C1-C3 121.53(13) C2-C1-C3 60.19(10).

Given the surprising ability of CAAC-6 to insert into unactivated C-H bonds, we chose to investigate the possibility of CAAC-6 activating other C-R bonds that have not been shown to be reactive towards CAAC-5 species. Unfortunately, when carbene **4.11c** was heated in the presence of either biphenylene or phenyl iodide, the respective oxidative addition products were not observed (Scheme 4.25). Additionally, subjecting the same carbene to cyclohexene did not give the corresponding cyclopropanation product. It is possible that **4.11c** is simply too bulky and inhibits potential reactivity at the carbene center. In fact, carbene **4.11c** doesn't even form the Lewis acid-base complex with tris(pentafluorophenyl)borane (BCF). Therefore, these high profile reactions might be worth revisiting with smaller CAAC-6 species **4.11a**,**b**.

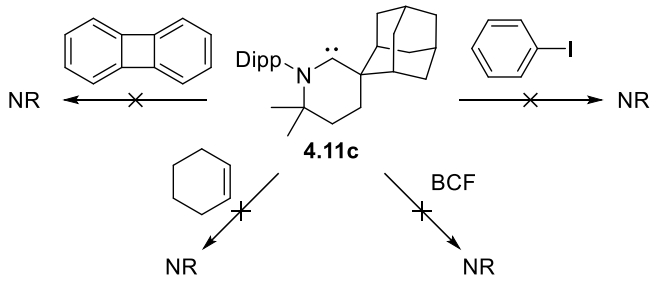

Scheme 4.25: Failed reactions with carbene **4.11c**.

Given the rich history of carbene P_4 reactivity (see section 2.1.2), we wished to investigate if the enhanced steric and electronic properties of CAAC-6 might yield new carbene stabilized allotropes of phosphorus. When **4.11a**,**c** were reacted with P_4 at -78 ºC or RT, a deep red solution was formed (Scheme 4.26). Unfortunately, no signals other than white phosphorus were visible in the ^{31}P NMR. Furthermore, if the solutions were stirred for an additional 12 h, an amorphous red solid formed. Together, these results are indicative of red phosphorus formation. It is possible that the increased steric hindrance for CAAC-6 derivatives causes the reaction of a second equivalent of CAAC-6 to be slower than the reaction of additional P_4, therefore catalyzing the formation of red phosphorus.

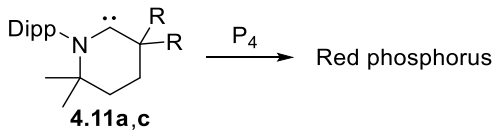

Scheme 4.26: Reactions of CAAC-6 and P_4 give red phosphorus.

In summary, when compared to CAAC-5, CAAC-6 feature increased $\%V_{bur}$ and enhanced donor and acceptor properties, as evidenced by the observed n → π^* transition trailing into the visible region. The high ambiphilic character allows for intramolecular C-H activation of an unactivated methylene group. Since such a process does not occur in the cases of **4.11a-c**, a wide variety of CAAC-6 derivatives should be synthetically available. The peculiar electronic properties of this novel family of carbenes will be useful for stabilizing electron-poor and paramagnetic species. It is also safe to predict that the corresponding metal complexes will feature very strong metal-carbene bonds, which will allow for catalysis under harsh conditions. Given the chemical potential of these species, we therefore sought to generalize the family of CAAC-6s to include species featuring an alkyl group instead of the Dipp on the nitrogen – a synthetic challenge that had not even been possible for CAAC-5.

4.3 Development of All-alkyl Substituted Six-membered Cyclic(alkyl)(amino) Carbenes

4.3.1 Synthesis

As described in the beginning of this chapter, precursors to CAACs synthesized through the hydroiminiumation method must feature an aryl group on the nitrogen. If not, the corresponding imine is too basic and inhibits proton transfer to the terminal alkene. Considering this limitation, CAAC-6 iminium precursors featuring alkyl groups required a different synthetic approach (Scheme 4.27). Imines **4.20a-d** were synthesized by condensation of isobutyraldehyde with alkyl amines **4.19a-d**, respectively. Deprotonation with LDA, alkylation with 1,3-dibromobutane, and mild heating in dry acetonitrile gave the corresponding all-alkyl CAAC-6 iminium salts. **4.21a** was left with a bromide anion, whereas **4.21b-d** required a subsequent anion exchange with $NaBF_4$ for purification. Besides the alkyl nitrogen group, **4.21a-d** also differ from iminium salts **4.4a-e** by one fewer methyl group on the backbone of the ring. Therefore, CAAC-6 precursor **4.22e** was synthesized from imine **4.2a** following an analogous method in order to have a direct comparison between the monomethyl and dimethyl backbones of CAAC-6 species. It is important to mention that this specific method does limit the size of the substituent on the quaternary carbon. For example, when bulkier imines, such as those featuring menthyl or adamantyl groups at the tertiary carbon center, were deprotonated and subjected to 1,3-dibromobutane, only the starting imine was recovered. This indicated that the bulkier nucleophiles favor an E2 mechanism over the desired S_N2 product. Nevertheless, this method allows for a wide variability of groups on the nitrogen atom.

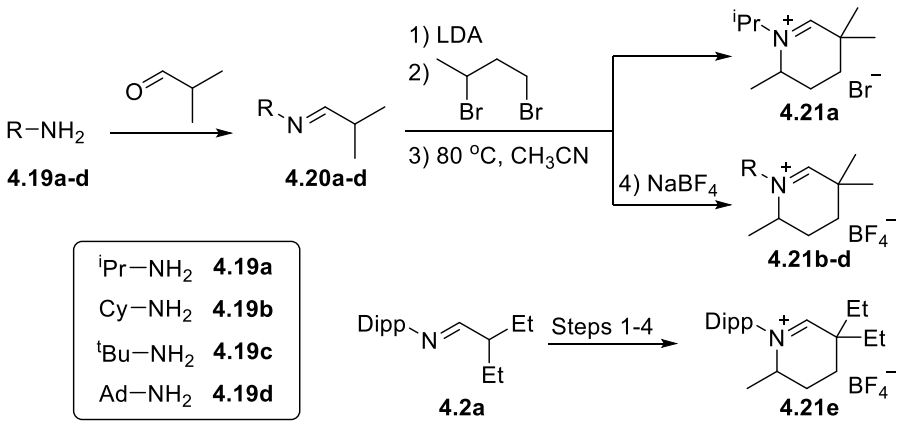

Scheme 4.27: Synthesis of CAAC-6 iminium precursors **4.21a-e** with monomethylated backbones. Isolated yields were calculated with respect to the imines **4.20a-d** or **4.2a**, respectively: **4.21a** (15%), **4.21b** (55%), **4.21c** (43%), **4.21d** (38%), **4.21e** (72%).

We next sought to test the stability of the monomethylated carbene derivatives. As a proof of principle, C_6D_6 was added to an NMR tube containing both KHMDS and **4.21e** at room temperature (Scheme 4.28). Not surprisingly, carbene **4.22e** was unstable and we instead observed a single set of ^{1}H and ^{13}C NMR signals corresponding to clean formation of enamine **4.23**.[9] However, we hypothesized that carbene **4.22e** might be persistent at low temperatures. To confirm, we performed a $^{13}C\{^{1}H\}$ VT-NMR study on a THF mixture of KHMDS and **4.21e**. To our delight, a broad carbene signal at 324 ppm could be observed at -80 ºC which remained stable below -60 ºC (Figures 4.28). We believe the 7 ppm shift between the two carbene signals of **4.22e** and its analogous dimethylated version **4.11a** was due to the formation of a KBF_4 adduct by the former at low temperatures. To check, we repeated the experiment with LiHMDS as the base. Indeed, the resulting carbene signal appeared at 327 ppm, as would be expected if the carbene was coordinated to the more electronegative lithium atom.

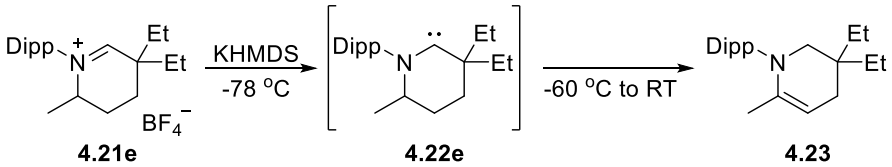

Scheme 4.28: CAAC-6 **4.22e** with a monomethylated backbone rearranges to enamine **4.23** above -60 ºC.

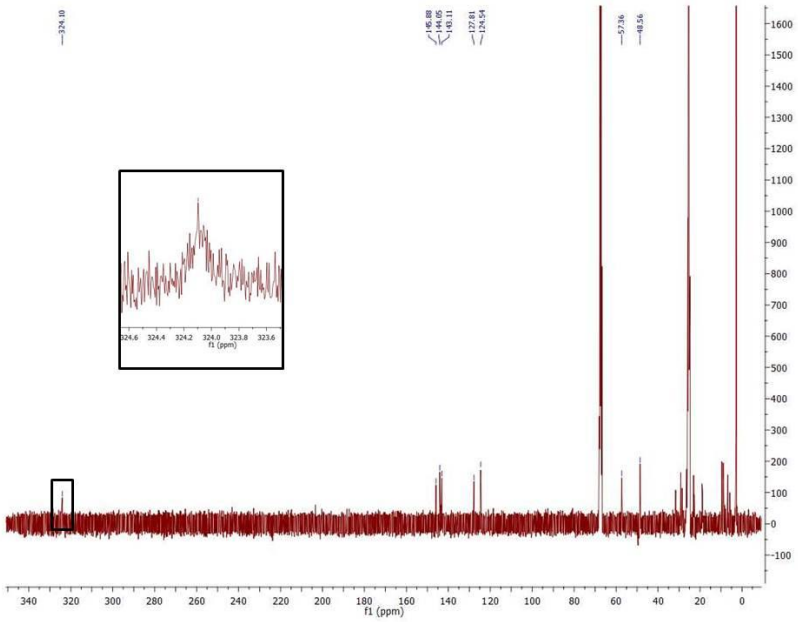

Figure 4.28: ^{13}C VT-NMR of **4.22e** at -80 ºC (75 MHz, THF).

Excited by the fact that CAACs with monomethylated backbones were persistent at laboratory accessible temperatures, we reconsidered expanding the family of CAACs to seven-membered rings. As such, we adapted the synthetic protocol and imine **4.2b** was alkylated with 1,4-dibromopentane giving the respective bromo alkyl imine (Scheme 4.29). Unfortunately, all attempts to cyclize this species led to the formation of iminium **4.24** in at most 3% overall yield**.** This remained the case even when TMSOTf was added to potentially assist bromine substitution. We therefore decided to drop this side project and proceeded exclusively with an investigation of the six-membered derivatives given the much better yield of their precursors. Nevertheless, it is still unclear why there was such a low cyclization yield for the seven-membered species, and the project deserves reinvestigation.

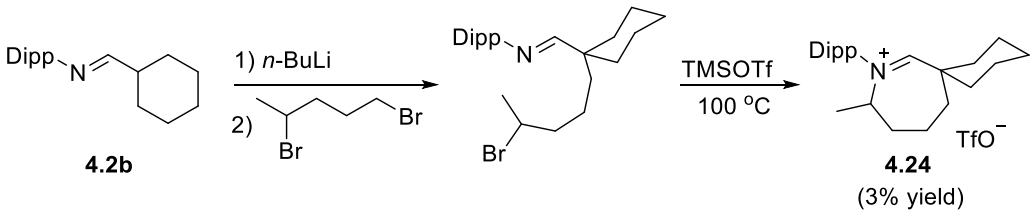

Scheme 4.29: Formation of a seven-membered CAAC iminium precursor by S_N2 is low yielding.

4.3.2 Coordination Complexes Featuring Monomethylated CAAC-6 Derivatives

Considering the low stability of CAACs with monomethylated backbones at temperatures higher than -60 ºC, we first needed to confirm that these carbenes could be coordinated to a TM. As we were also interested in the overall donor properties of these ligands, we first investigated the coordination to rhodium which gave us a general *in situ* deprotonation strategy. THF was added slowly to a precooled -78 ºC solid mixture of KHMDS, $[Rh(cod)Cl]_2$ and iminiums **4.21a-e**, respectively (Scheme 4.30). These stirred solutions were then allowed to slowly warm to room temperature overnight at the evaporation rate of the external dry ice acetone bath. Upon workup, (CAAC-6)Rh(cod)Cl complexes **4.25a-e** were isolated as mixtures of diastereomers. Due to the restricted rotation of the carbene-Rh bond, two enantiomers can form in which the chlorine atom is either *cis*- or *trans*- to the single methyl group on the backbone. Furthermore, since the cyclization step forming the iminium precursors **4.21a-e** was not stereoselective, a mixture of (*R*)- and (*S*)-enantiomers derived from the chiral backbone already existed. Unfortunately, this results in heavily complicated NMR spectra which are difficult to dissect except for certain key signals. Nevertheless, single crystals of complex **4.25d** were grown by slow evaporation of an Et_2O solution at room temperature, confirming the first example of an all-alkyl CAAC TM complex (Figure 4.29).

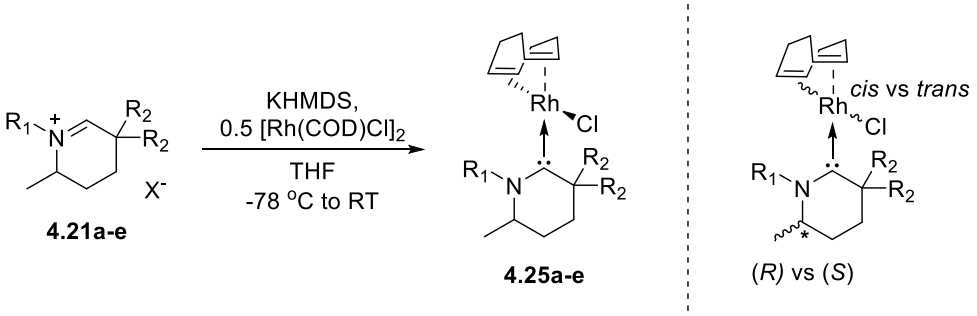

Scheme 4.30: Synthesis of (CAAC-6)Rh(cod)Cl complexes **4.25a-e** via *in situ* deprotonation (left) and representation of diastereomer mixture (right).

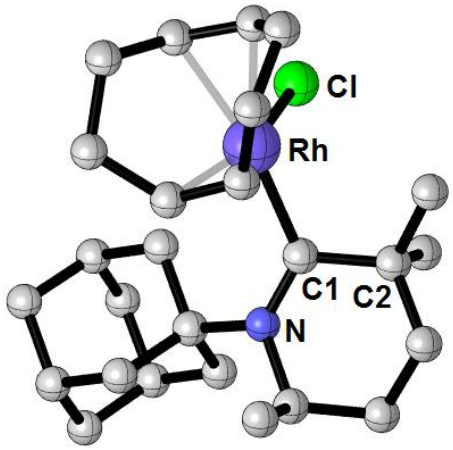

Figure 4.29: X-ray structure of **4.25d**. Only a single diastereomer is depicted and H-atoms have been removed for clarity. Selected bond lengths (Å) and angles (°): C1-Rh 2.025(3), C1-N 1.338(5), C1-C2 1.549(5), N-C1-C2 115.7(3).

With (CAAC-6)Rh(cod)Cl complexes **4.25a-e** in hand, we next set out to determine the overall donating properties of the new carbenes. Bubbling CO into DCM solutions of **4.25a-e** for 20 min gave crude mixtures which contained *cis*-[(CAAC-6)Rh$(CO)_2$Cl] complexes **4.26a-e** as the major products, respectively (Scheme 4.31). The IR spectra (KBr, DCM solution) of these compounds were then quickly measured and the CO stretching frequencies of each compound averaged (Figure 4.30). When comparing the values, it becomes evident that there is not a clear donor trend between aryl and alkyl CAAC-6 species as **4.26e** falls right at the median of this sample size. There does however appear to be a trend with respect to the size of the carbene. Indeed, the smallest CAAC-6s, featuring ^{i}Pr and Cy groups on the nitrogen, have the highest average CO stretching frequencies at 2032 cm^{-1}. **4.26d**, which featured the bulky adamantyl group on the nitrogen, appears on the other side of the spectrum at 2028 cm^{-1}. It is therefore possible that the substituents about the carbene are perturbing the CO bonds and leading to a skewed comparison (see section 1.3.2). That being said, the average CO stretching frequency of each species are all far lower than the respective (CAAC-5)Rh$(CO)_2$Cl analogues (2036 cm^{-1}). Therefore, it can be safely assumed that all-alkyl and aryl CAAC-6s are better overall donors than CAAC-5s.

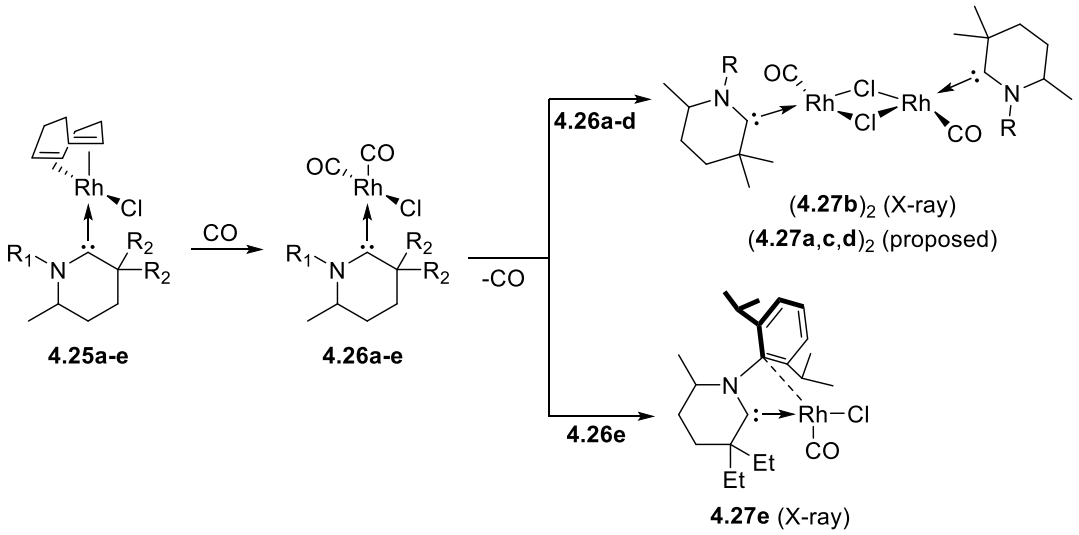

Scheme 4.31: *cis*-[(CAAC-6)Rh(CO)$_2$Cl] complexes **4.26a-e** spontaneously lose CO overtime.

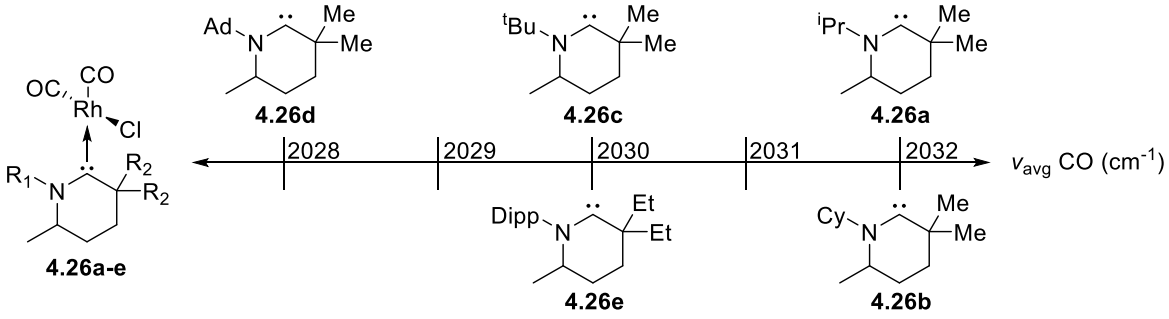

Figure 4.30: Average CO stretching frequencies of *cis*-[(CAAC-6)Rh(CO)$_2$Cl] complexes **4.26a-e**.

In order to better understand if the carbonyl groups were indeed being perturbed in these complexes, we attempted to grow single crystals of both **4.26b** and **4.26e** by slow evaporation or diffusion of pentane into DCM solutions, respectively. Surprisingly, an X-ray diffraction study revealed that both compounds spontaneously lost one equivalent of CO (Figure 4.31). In the case of **4.26b**, the loss of CO resulted in the coordinatively unsaturated rhodium center **4.27b**, which reacted with a second equivalent of itself giving the μ-Cl bridged dimer (**4.27b**)$_2$. For **4.26e** however, the monomer **4.27e** was stabilized by coordination of the Dipp C_{ipso} carbon. This kind of behavior has been observed before with the bulkiest CAAC-5 featuring a menthyl group, but in that example the resulting stabilization of the rhodium center

came from agostic interactions with the menthyl C-H bonds and not the Dipp.[33] We believe that the other all-alkyl CAAC-6 species behave in the same manner as **4.27b**, however X-ray structures and/or additional spectroscopic evidence still needs to be collected to confirm this hypothesis. It is worth noting that the *cis*-[(CAAC-6)Rh(CO)$_2$Cl] complex **4.15c** featuring the dimethyl backbone did not naturally lose CO upon crystallization. This is likely due to the fact that in this case the rigid adamantyl group inhibits the rate of chair-flipping for the six-membered ring, and therefore prevents approach of the Dipp group to the rhodium center.

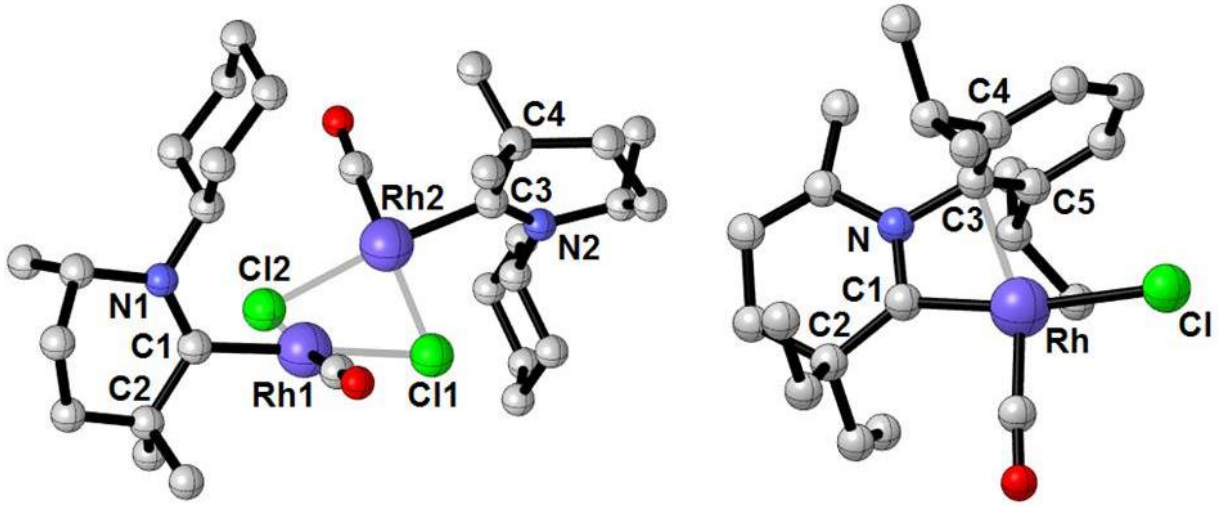

Figure 4.31: X-ray structures of (**4.27b**)$_2$ (left) and **4.27e** (right). H-atoms have been removed for clarity. Selected bond lengths (Å) and angles (°): (**4.27b**)$_2$ C1-Rh1 1.998(3), C3-Rh2 1.991(3), C1-N1 1.301(4), C3-N2 1.311(5), N1-C1-C2 120.1(3), N2-C3-C4 120.1(3); **4.27e** C1-Rh 1.957(3), C1-N1 1.317(4), C3-Rh 2.368(2), N-C1-C2 119.8(3), N-C3-Rh 82.7(2).

The Rh-C$_{ipso}$ bond in **4.27e** can be formally described as a η-1 π-interaction [C3-Rh 2.368(3) Å] as the aryl ring of the Dipp group remains completely planar and orthogonal to the nitrogen atom. Additionally, only a slight lengthening of the neighboring C$_{ipso}$-C$_{ortho}$ bonds [C3-C4 1.413(4) and C3-C5 1.417(4) Å] was observed. Other groups have reported η-1 Rh-C$_{ipso}$ π-interactions in NHC complexes with distances ranging from 2.346(2)-2.509(2) Å with an average of 2.414 Å. In all these cases however, the Rh center is locally cationic, either [L$_3$Rh(I)]$^+$X$^-$[81] or L$_3$Rh(I)[82-84] where one of the L ligands is

globally anionic. Therefore, **4.27e** represents the first example of an η-1 C_{ipso} π-interaction from a neutral carbene ligand to a locally neutral Rh center. It is worth mentioning that this C_{ipso} coordination to the rhodium is reminiscent to that commonly observed in palladium systems using the Buchwald ligands.[85]

Considering this unique result, we revisited the possibility that the Dipp C_{ipso} bond might stabilize other coordinatively unsaturated rhodium centers. In fact, a closer inspection of the crude reaction mixture which gave **4.25e** revealed such a product. Until this point, workup of the (CAAC-6)Rh(cod)Cl complexes included an Et_2O extraction to remove the KBF_4 salt byproducts generated from the *in situ* deprotonation reaction. In the case of **4.25e**, this always left a small amount of red solid (~5%) with the KBF_4 salt. Upon extraction of this unknown side product with $CHCl_3$, followed by slow diffusion of pentane into the solution, single red crystals suitable for an X-ray diffraction study revealed the structure of **4.28** as the cationic complex [(**4.22e**)Rh(cod)][BF_4] (Figure 4.32). The carbene-Rh bond in this complex [C1-Rh 2.048(4)] is slightly longer than the same bond in the analogous neutral complex **4.25d** [C1-Rh 2.025(3)]. The lengthening of the bond is most likely due to weaker Rh-carbene π-backbonding as the now cationic rhodium center better localizes its d-orbitals closer to the metal center. The cationic rhodium center also has a significant effect on the C_{ipso}-Rh interaction. Indeed, this bond is significantly shortened in the cationic complex [C3-Rh 2.316(3)] when compared to the same bond in the neutral complex **4.27e** [C3-Rh 2.368(2)].

We believe that since the complexation reaction was done *in situ* with external base, a small percentage of the resulting KBF_4 salt byproduct reacted as a halide abstracting agent towards **4.25e** which gave **4.28** (Scheme 4.32). We were therefore curious if a similar halide abstraction strategy could give a cationic rhodium center stabilized by agostic interactions instead of the C_{ipso} bond. Unfortunately, when either **4.25c** or **4.25d** were reacted with $AgBF_4$ at room temperature, an unidentifiable mixture of products was observed. Nonetheless, this reaction deserves reinvestigation at lower temperatures.

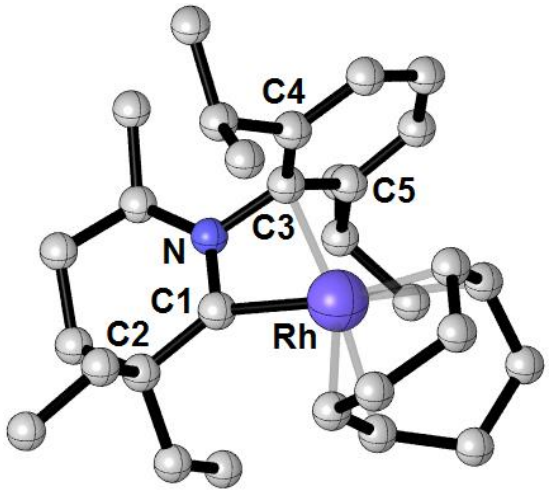

Figure 4.32: X-ray structure of **4.28**. H-atoms, solvent, and the BF_4^- anion have been removed for clarity. Selected bond lengths (Å) and angles (°): C1-Rh 2.048(4), C1-N 1.304(5), C3-Rh 2.316(3), C3-C4 1.420(5), C3-C5 1.423(6), N-C1-C2 119.2(3), N-C3-Rh 85.5(2).

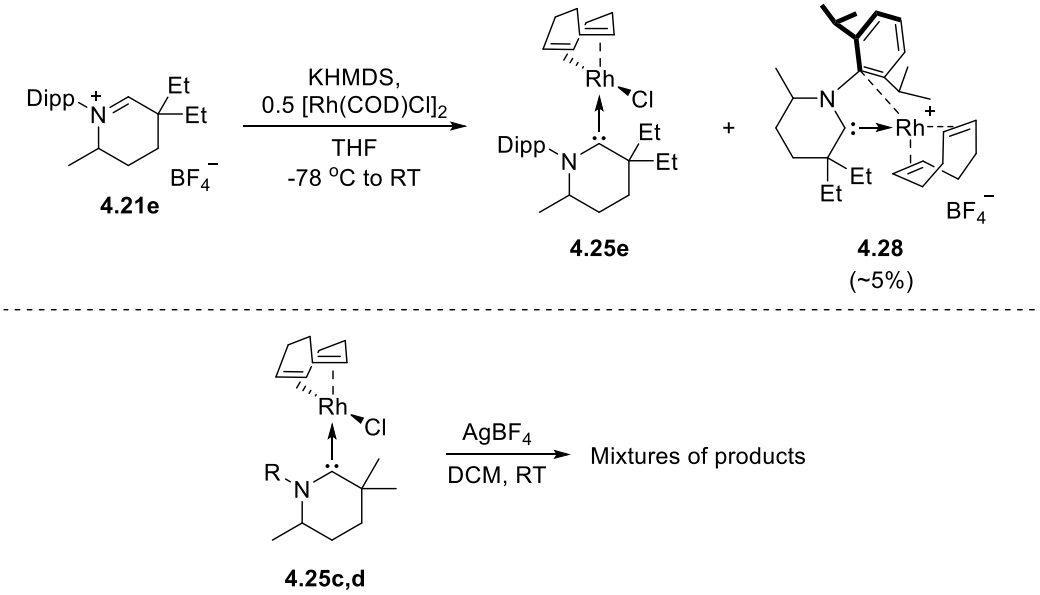

Scheme 4.32: Halide abstraction reactions yield the cationic C_{ipso} stabilized rhodium center (top) or mixtures of products for all-alkyl CAAC-6 species (bottom).

Given that the peculiar steric and donor properties of carbenes **4.22a-e** led to new CAAC-rhodium chemistry so far unreported with CAAC-5s, we wanted to investigate how these new carbenes

might behave in the sphere of coinage metal complexes. As a cheap synthetic test, we first attempted the *in situ* deprotonation procedure on a mixture of iminium salt **4.21e**, KHMDS, and CuCl (Scheme 4.33). Upon inspection of the crude $^{13}C\{^{1}H\}$ NMR, we observed two separate carbene signals at 253.5 and 254.0 ppm, likely indicating the formation of both the neutral and cationic copper complexes **4.29** and **4.30**, respectively.[35, 41] Following a workup, colorless single crystals were grown by slow diffusion of pentane into a DCM solution which indeed unambiguously confirmed the structure of **4.30** as the [(**4.22e**)$_2$Cu][$CuCl_2$] complex (Figure 4.33).

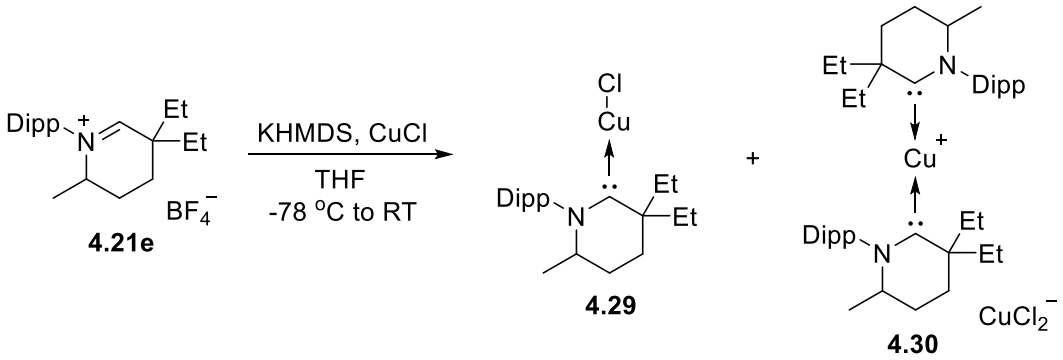

Scheme 4.33: *In situ* deprotonation yields both mono- and bis-(CAAC-6) copper complexes.

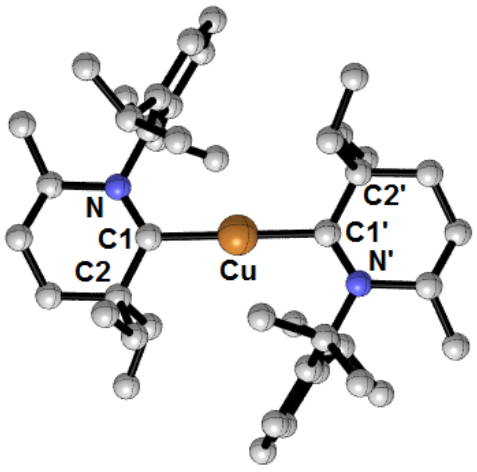

Figure 4.33: X-ray structure of **4.30**. H-atoms, solvent, and the $[CuCl_2]^-$ anion have been removed for clarity. Selected bond lengths (Å) and angles (°) are not given because of the low data quality of the structure.

Since using a simple coinage metal halide source yielded mixtures of both mono- and bis-(CAAC-6) complexes using the *in situ* deprotonation method, we couldn't use (tht)AuCl for the exclusive synthesis of the analogous (CAAC-6)AuCl species. Therefore, we adapted a method that was used to isolated (MIC)AuCl complexes.[86] Using the same deprotonation procedure as described above, except now on a mixture of iminiums **4.21a-e**, KHHMDS, and (PMe_3)AuPh, yielded (CAAC-6)AuPh complexes **4.31a-e**, respectively (Scheme 4.34). Subsequent workup and proto-demetalation with HCl gave the desired (CAAC-6)AuCl complexes **4.32a-e**, respectively. For the all-alkyl CAAC-6 derivatives **4.32a-d**, the ^{13}C carbene signals appear between 228-231 ppm. In contrast, the same signal for the aryl substituted version **4.32e** is downfield shifted from these values at 239 ppm. The stark difference in carbene signals simply highlights the changes in the carbenes' electronic properties between alkyl and aryl substituted CAAC-6s.

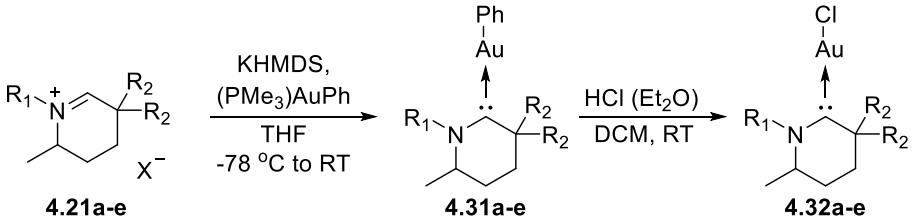

Scheme 4.34: Synthesis of (CAAC-6)AuCl complexes **4.32a-e** via a proto-demetalation procedure.

Considering the high variability in size among the substituents attached to the nitrogen atom in carbenes **4.22a-e**, we wanted to use the newly synthesized gold complexes to explore the differences in the $\%V_{bur}$ of these carbenes. Therefore, colorless single crystals of **4.32b-e** were grown by slow evaporation of DCM solutions at room temperature (Figure 4.34). Unfortunately, at the time of writing this thesis, crystals of the smallest version **4.32a** had not been grown. Additionally, there was a high level of twinning in each crystal structure below due to the racemic mixture of two enantiomers. Therefore, although they are listed as observed in the figure, it would be ill advised to make comparisons between the carbenes using bond length and angle arguments. As a result, a comparison of the respective $\%V_{bur}$

was not conducted as it is normally highly dependent on X-ray crystal quality for accuracy (see section 1.3.1).

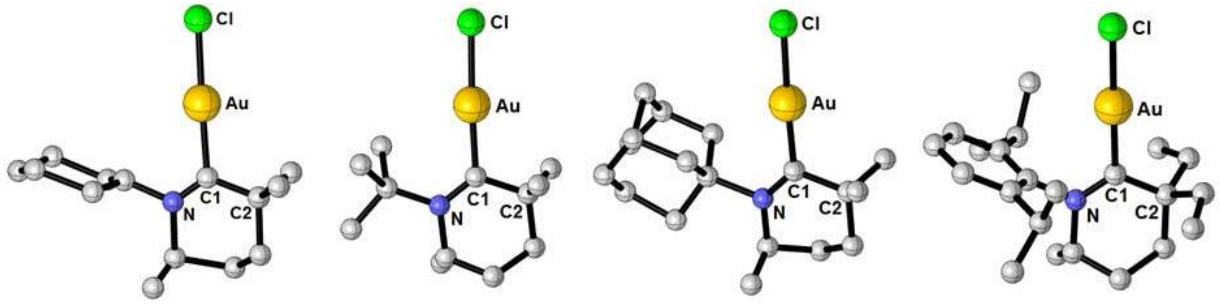

Figure 4.34: X-ray structures of **4.32b-e** (sequential left to right). H-atoms have been removed for clarity. Selected bond lengths (Å) and angles (°): **4.32b** C1-Au 2.012(1), C1-N 1.304(1), N-C1-C2 121.6(2); **4.32c** C1-Au 2.031(7), C1-N 1.296(7), N-C1-C2 123.2(9); **4.32d** C1-Au 2.01(2), C1-N 1.31(3), N-C1-C2 121(2); **4.32e** C1-Au 2.00(1), C1-N 1.280(4), N-C1-C2 120.5(4).

Echevarren et al. have recently reported that Buchwald phosphines can stabilize a "naked" gold cation through arene interactions giving highly active catalysts.[87-88] Given that carbene **4.22e** mimics the η-1 π-coordination mode of Buchwald type ligands in the sphere of rhodium, we were curious if the same effect could be translated to gold. We therefore tried reacting **4.32e** with halide abstracting agents $AgSbF_6$ and $GaCl_3$ in noncoordinating solvents (Scheme 4.35). The cleanest reaction came from the latter, and gave a new product with a carbene ^{13}C NMR signal upfield shifted from the starting material at 232 ppm. Unfortunately, an X-ray diffraction study confirmed the structure of **4.33e** as the μ-Cl bridged dimer (Figure 4.35). It is recommended that this reaction be revisited however, as it is clear the order of reagent addition, relative equivalents, and temperature could have a heavy effect on the outcome.

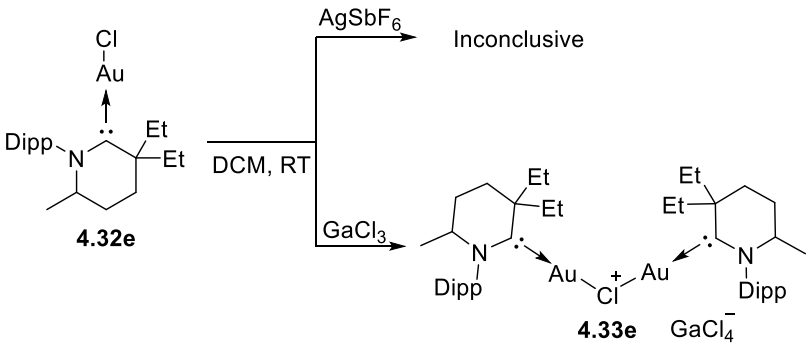

Scheme 4.35: Halide abstraction reactions on **4.32e** do not give a "naked" gold atom at room temperature.

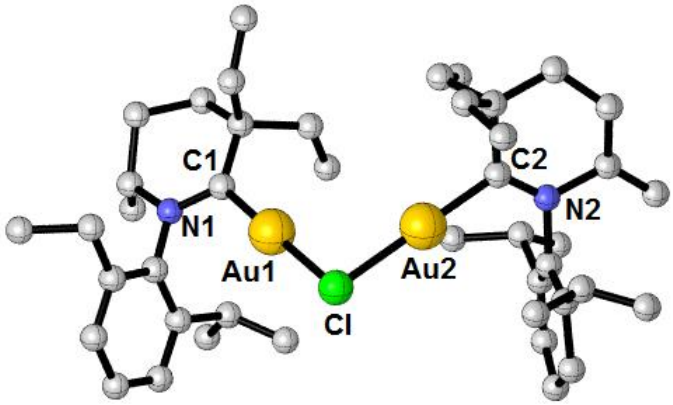

Figure 4.35: X-ray structures of **4.33e**. H-atoms and $GaCl_4^-$ anion have been removed for clarity. Selected bond lengths (Å) and angles (°) are not given as the structure could not be fully refined.

Shifting gears, instead of using the bulkier CAAC-6s to stabilize low coordinate gold species, we were curious if the least sterically hindered versions could allow access to higher nuclear CAAC gold clusters. We hypothesized that with smaller groups on nitrogen, trimeric gold species like **4.AQ** might aggregate into larger clusters, a process that was previously inhibited by the Dipp group.[45] As such, we adapted the established procedure in the hope of synthesizing $[(CAAC\text{-}6)Au]_3[BF_4]$ salts derived from the smallest (CAAC-6)AuCl complexes **4.32a** or **4.32b.**

Sequential addition of $AgBF_4$ followed by a $KOH/NaBF_4$ mixture to DCM solutions of **4.32a**,**b** gave new compounds with ^{13}C NMR carbene signals at ~216 ppm, which we propose corresponded to the oxonium complexes **4.34a**,**b**, respectively (Scheme 4.36). Unfortunately, **4.34a**,**b** were not stable in

solution over 12h as we observed complete replacement of the ^{13}C carbene signal by a new signal at ~242 ppm. At the same time, a significant amount of Au^0 precipitated from these solutions. Subsequent synthetic studies confirmed that the carbene signals at ~242 ppm corresponded to the [(CAAC-6)$_2$Au][BF_4] complexes **4.35a**,**b**. Although the oxonium salts could not be isolated, if the synthesis of **4.34a**,**b** was conducted in a solution saturated with CO, complexes **4.35a**,**b** were not observed and a new ^{13}C carbene NMR signal appeared at ~248 ppm. In the case of the cyclohexyl derivative, ESI-MS gave an *m*/*z* peak at 1212.21, which perfectly matched the mass of [(**4.22b**)Au]$_3^+$. Therefore, we are confident that reduction of oxoniums **4.34a**,**b** with CO yielded the [(CAAC-6)Au]$_3$[BF_4] complexes **4.36a**,**b**, respectively. Unluckily, all attempts at isolating X-ray quality single crystals of these species failed. Furthermore, both compounds were susceptible to disproportionation reactions as we observed total conversion of the timeric gold species to Au^0 precipitate and **4.35a**,**b** after seven days, respectively. Considering that this decomposition pathway had not been previously observed for **4.AQ**, it's likely that the bigger central void space in these species allow for undesired transmetalation and subsequent disproportionation reactions to occur.

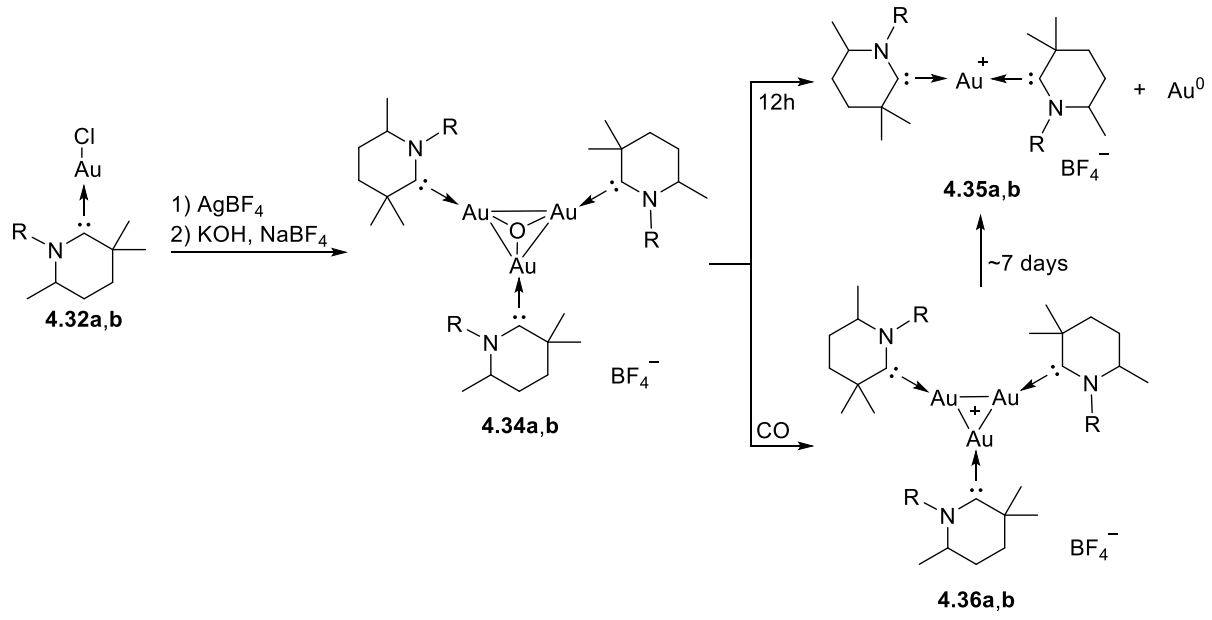

Scheme 4.36: Synthesis of [(CAAC-6)Au]$_3$[BF_4] complexes **4.36a,b** which decompose into [(CAAC-6)$_2$Au][BF_4] complexes **4.35a,b**, respectively.

4.3.3 All-alkyl CAAC-6-Selenium Adducts Reveal Novel Examples of Non-Classical Hydrogen Bonding

We lastly directed our attention to determining the π-accepting properties of all-alkyl CAAC-6 species. Unfortunately, due to the low stability of the carbenes at ambient temperatures, all attempts at synthesizing the carbene-phenylphosphinidene adducts failed. We therefore turned towards exclusively making the respective carbene-selenium adducts.[89] Using the same synthetic procedure as described before, THF was now added to a solid mixture of iminium salts **4.21a-e**, KHMDS, and Se (black) at -78 ºC. The stirred solutions were then slowly warmed to room temperature and, after workup, gave the carbene-Se adducts **4.37a-e**, respectively (Scheme 4.37). A summary of the ^{77}Se NMR signals for these species is given below (Figure 4.36). Quite confusingly, although they should be essentially identical in π-accepting strength, the all-alkyl CAAC-6 carbene-Se adducts **4.37a-d** have ^{77}Se NMR signals that span a range of 268 ppm! As a frame of reference, this range is larger than the difference in ^{77}Se NMR signals between Alder's acyclic NHC-Se adduct (593 ppm) and DAC-Se adducts (847-856 ppm), two extremely different types of carbenes.[90] Even more surprising was the fact that the ^{77}Se signal of the aryl substituted species **4.37e** (669 ppm), and by extension the ^{77}Se signal of the analogous compound **4.17a** (715 ppm), appear sandwiched between the signals for the all-alkyl CAAC-6 derivatives, when they should theoretically appear the most downfield. Finally, adding to the confusion the ^{77}Se signal of the aryl substituted CAAC-6-Se adduct **4.17c** appeared at 845 ppm, 148-176 ppm downfield of the other two aryl substituted derivatives.

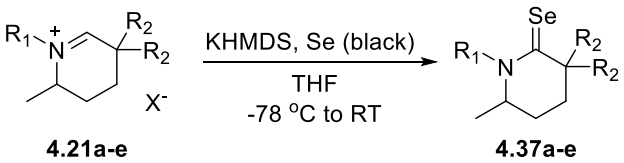

4.21a-e **4.37a-e**

Scheme 4.37: Trapping experiments giving CAAC-6 Se adducts **4.37a-e**.

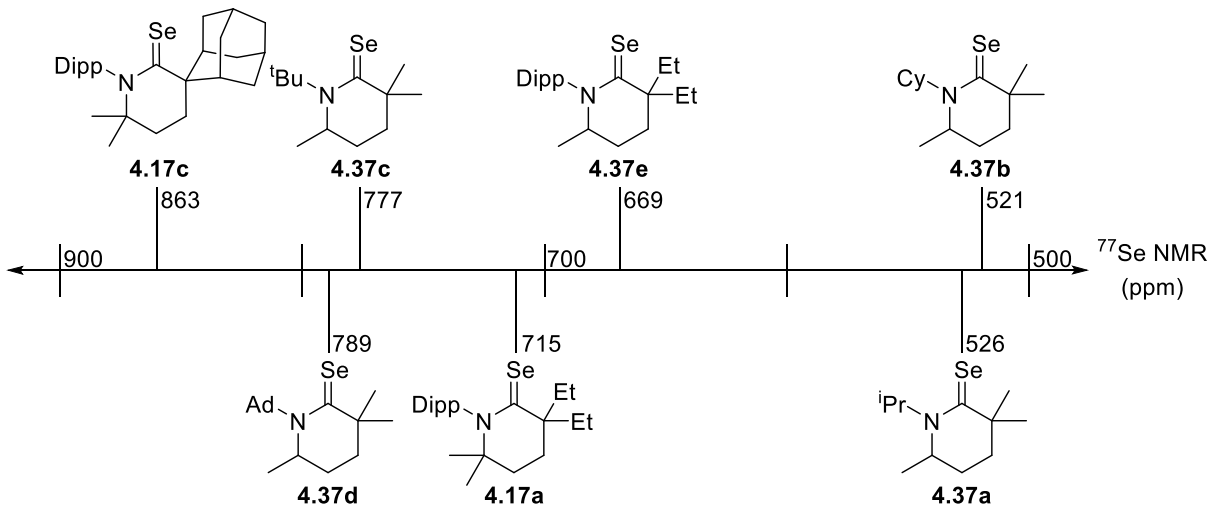

Figure 4.36: ^{77}Se NMR signals of every CAAC-6-Se adduct.

Given the high discrepancy in these signals, we wanted to investigate the bonding environment about the selenium center in order to hopefully better understand these anomalies. Therefore, single crystals of **4.37a-e** and **4.17c** suitable for X-ray diffraction studies were grown from their respective concentrated pentane solutions at -20 ºC (Figure 4.37). Most importantly for this discussion, the structures of **4.37a-d** and **4.17c** revealed rather short intramolecular distances between selenium and the closest hydrogen atoms [Se-H 2.464-2.662 Å]. All of these distances are well shorter than sum of the Van der Waals radii for Se and H (*ca*. 3.1 Å), and even within the range of reported intermolecular hydrogen bonding distances for a crystalline selenourea adduct [Se-H 2.513-2.605].[91] Furthermore, these distances are in the range of reported intramolecular Se-H distances in oxazolidine-selenium adducts with pendant carbonyls [Se-H 2.63-2.72 Å] which Silks et al. determined to be C-H···Se NCHB interactions (Figure 4.37).[92] We therefore propose that the steric effects transferred by the six-membered rings also gives rise to C-H···Se NCHB in **4.37a-d** and **4.17c**. We also propose that such a scenario does not exist in **4.37e** as the closest selenium hydrogen bond distances are all longer than 2.8 Å, and we believe a distance shorter than 2.70 Å is needed for there to be a significant interaction in these weakly acidic hydrogen bonds (*vide infra*).

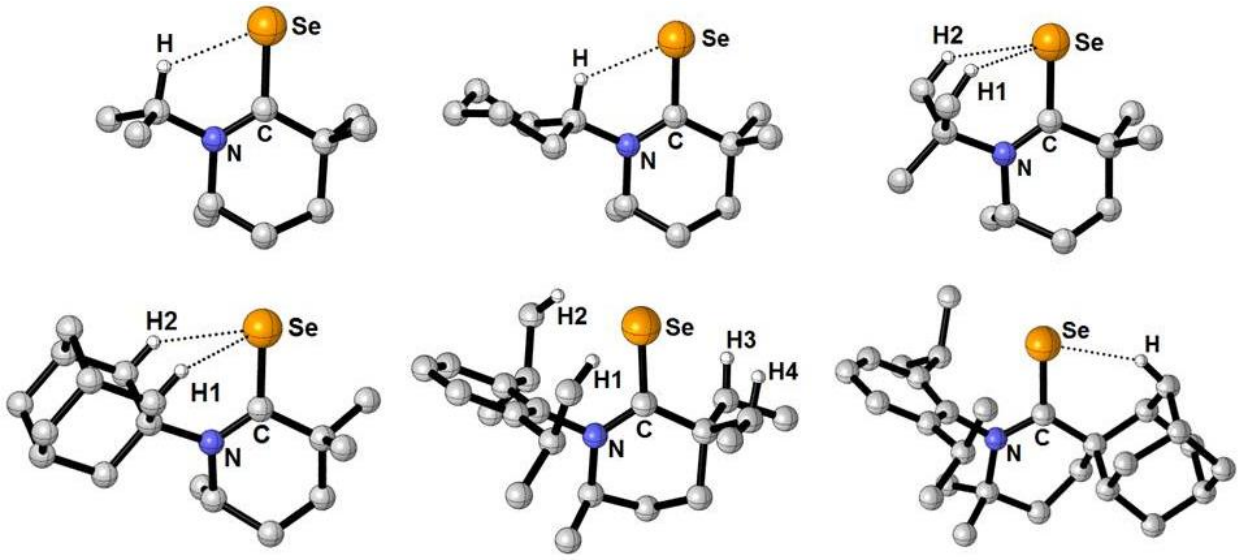

Figure 4.37 X-ray structures of **4.37a-e** and **4.17c** (top left to bottom right). H-atoms, except for those closest to Se, have been removed for clarity. Selected bond lengths (Å): **4.37a** Se-H 2.497; **4.37b** Se-H 2.464; **4.37c** Se-H1 2.548, Se-H2 2.609; **4.37d** Se-H1 2.531, Se-H2 2.662; **4.37e** Se-H1 3.070, Se-H2 3.245, Se-H3 2.850, Se-H4 2.893; **4.17c** Se-H 2.548.

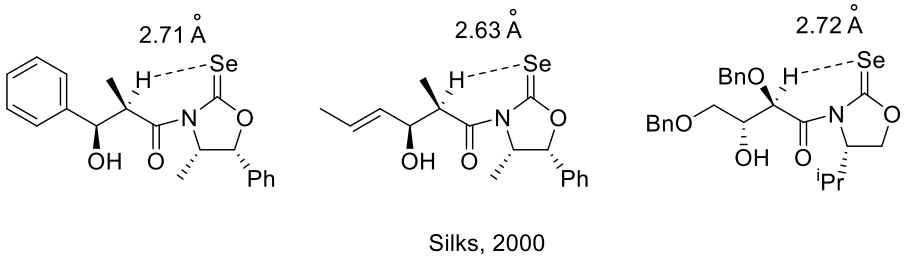

Figure 4.38: Short intramolecular Se-H distances observed in oxazolylidene-selenium adducts with carbonyls.

It is well established that C-H groups can participate as weak hydrogen bond donors,[93] however applying a NCHB description to close C-H···X (X = electronegative atom) interactions has been a heavily debated topic.[94-96] Nevertheless, weak C-H···X interactions have led to the stabilization of supramolecular complexes,[97] and have even been shown to dictate the stereochemistry of organic transformations.[98] However, all cases where C-H···X NCHB arguments were evoked involved a C-H bond in which the hydrogen was at least mildly acidic (the most extreme cases where the C-H bond came

from an aromatic system).[99] Therefore, to the best of this author's knowledge, no C-H···X NCHB has been explicitly argued to exist in systems where the C-H hydrogen bond donor is an sp^3 alkyl group which is not located β to a π-system. It is thus quite surprising that such anomalous scenarios for NCHB exist in **4.37a-d** and **4.17c**. Even more remarkable is the case of **4.17c** where the closest electronegative atom is four bonds away from the C-H hydrogen bond donor! If we do however assume this bond exists, we can explain the irregularities of the ^{77}Se NMR π-accepting scale for CAAC-6 species.

For **4.37a,b** and **4.17c**, there exists only one short Se-H distance which can translate to a NCHB. On the other hand, **4.37c,d** exhibit two such short Se-H distances, and thus the argument can be made that two cases of NCHB exist. We see that shifting from all-alkyl CAAC-6s **4.37a,b** to **4.37c,d**, which contain one and two NCHB interactions, respectively, the ^{77}Se NMR signals shift downfield an average of ~260 ppm. Furthermore, comparing aryl substituted CAAC-6s **4.37e** and **4.17a** to **4.17c,** which contain zero and one NCHB interactions, respectively, an average of ~170 ppm downfield shift was observed. Averaged, this roughly equates for each NCHB to give a ^{77}Se NMR signal which is ~220 ppm downfield shifted of the alleged signal in which no such interaction occurs. This is very much a qualitative argument and does not account for the strength of each interaction based on the relative basicity of selenium, acidity of the hydrogen, and/or the actual distances observed. Nevertheless, evidence for an identical shift can be found upon a closer inspection of previously reported NHC-selenium adducts **4.38a-e** and **4.39** (Figure 4.39).[100-102]

Five of the six carbenes are unsaturated five-membered ring NHCs with alkyl groups on the nitrogen atom. Therefore, by all measures of carbenes these five ligands should have nearly identical π-accepting properties, and by extension very similar ^{77}Se NMR signals. On the contrary, the ^{77}Se NMR signals for **4.38d,e** appear on average ~200 ppm downfield shifted from the same signals in **4.38a-c**. Indeed, X-ray structures of **4.38a,b** revealed that the closest Se-H distances were 3.25 and 2.81 Å, respectively (X-ray structure of **4.38c** was not reported). On the other hand, the X-ray structure of **4.38e** revealed one extremely close Se-H intramolecular interaction [Se-H 2.62 Å]. Although a structure for **4.38d** does not exist, the structure a *t*-Bu substituted benzimidazole-selenium adduct **4.39** (^{77}Se NMR 222

ppm) does exist. Inspection of this structure also revealed one extremely close Se-H distance [Se-H 2.66 Å], therefore we can likely assume that such a short contact also exists in **4.38d**.

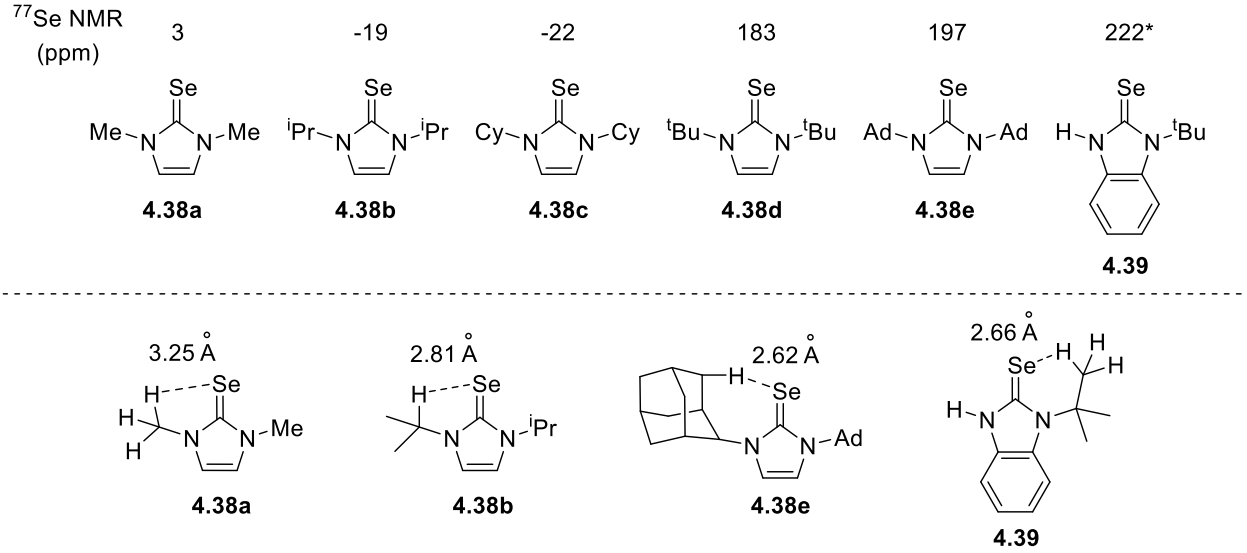

Figure 4.39: Reported ^{77}Se NMR signals of unsaturated NHC-selenium adducts showing large discrepancies in the signals (top) and shortest Se-H distances for examples with reported structures (bottom). *NMR in DMSO.

Additional evidence of NCHB in CAAC-6-Se adducts can be found upon comparing the ^{1}H NMR of **4.37a** and **4.37b** to their respective iminium precursors **4.21a** and **4.21b** (Figures 4.40 and 4.41). In the latter cases, the proton signal corresponding to the iminium exocyclic N-C-H bond can be clearly observed as a multiplet at 4.32 and 3.75 ppm, respectively. However, when the carbene is coordinated to a selenium atom, these same signals are significantly broadened and shifted downfield to 6.24 and 5.85 ppm. Considering that other N-C-H proton signals move upfield upon coordination, we can assume that the broadening and downfield shifting of the signals are due to C-H···Se NCHB. In the cases of **4.37c** and **4.37d** however, we did not observe a similar downfield shift in the ^{1}H NMR corresponding to the protons potentially involved in NCHB with selenium. In fact, the signals for these protons remained equivalent in both **4.37c** and **4.37d**, indicating that both the Ad and *t*-Bu groups maintain their free rotation even though they have protons that are interacting with the selenium center. This is best explained by considering the C_3 rotational symmetry of both groups. As the groups rotate, the selenium center is

always involved in two NCHB interactions with the Ad or *t*-Bu groups, and thus the net deshielding effect is still observed in the ^{77}Se NMR.

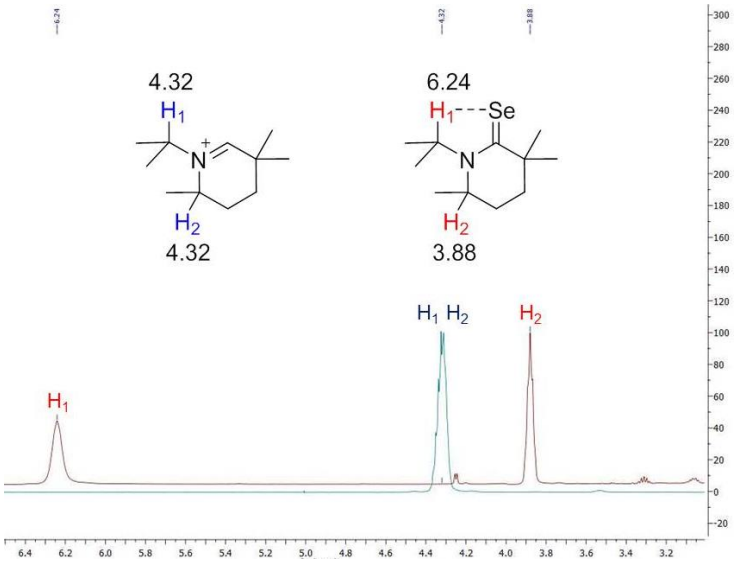

Figure 4.40: ^{1}H NMRs of **4.21a** and **4.37a** showing C-H···Se NCHB (500MHz, $CDCl_3$).

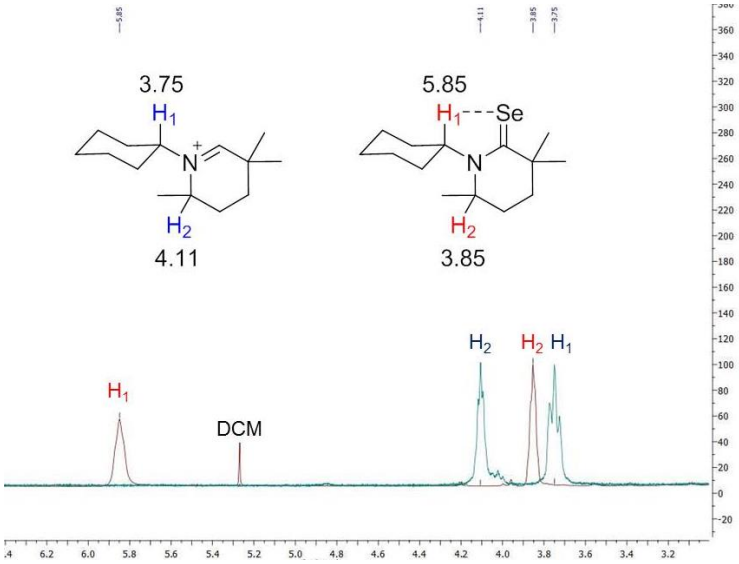

Figure 4.41: ^{1}H NMRs of **4.21b** and **4.37b** showing C-H···Se NCHB (500MHz, $CDCl_3$).

Altogether, anomalies in the ^{77}Se NMR signals of CAAC-6-Se adducts revealed the first cases of nonacidic C-H···Se NCHB. Although ^{77}Se NMR is a convenient tool to gain insight into the π-accepting

properties of carbenes, these results demonstrate that without structural information one cannot draw conclusions from the NMR signals alone if close intramolecular Se-H distances are possible. Additionally, if such an interaction does occur in a carbene-selenium adducts, a rough approximation factor should be applied to the NMR signal accordingly (Equation 4.1).

$$\delta\ ^{77}\text{Se NMR} = \delta\ ^{77}\text{Se NMR}_{\text{observed}} - 210*n \text{ where } n = \#\text{C-H}\cdots\text{Se within 2.70 Å} \quad (4.1)$$

As this equation originated from a qualitative approximation of a relatively small sample size, it should not be used to make definitive comparisons of carbenes' π-acidity if the corrected ^{77}Se NMR signals are close in value. Instead, the correction factor should only be used to gather a general idea of how the π-accepting properties of carbenes might be similar to others which fall in the same range on the ^{77}Se π-scale. For example, when this correction factor is applied to the CAAC-6-Se adducts, a new general trend can be observed (Figure 4.42). As expected, CAAC-6 species featuring alkyl substituents on the nitrogen atom are far less π-acidic than their aryl substituted analogues. Importantly though, the correction factor lets us recognize that all-alkyl CAAC-6 species are also less π-acidic than CAAC-5s (^{77}Se NMR 482 ppm)[64] and only slightly more π-acidic than a six-membered NHC (δ ^{77}Se NMR 271 ppm).[90]

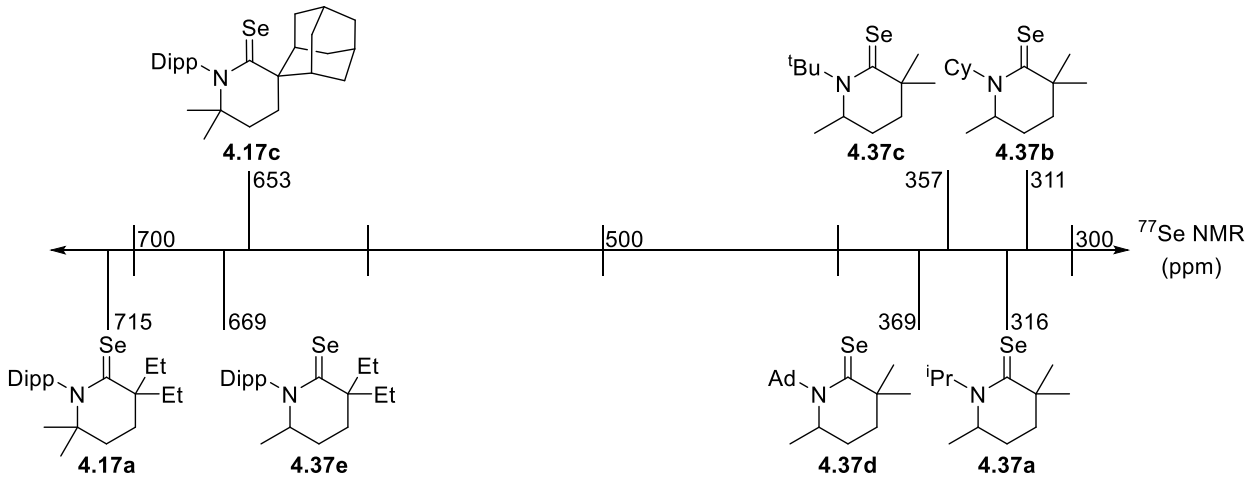

Figure 4.42: ^{77}Se NMR signals of every CAAC-6-Se adduct with correction factor applied when needed.

4.4 Conclusion

In all, we developed synthetic methods giving access to a wide range of CAAC-6 ligands. This even included all-alkyl derivatives which were previously unattainable in CAAC-5 systems. The latter carbenes are persistent, and can be coordinated *in situ* to a variety of TMs. TEP values confirmed that CAAC-6 species are indeed better overall donors than CAAC-5s. For the aryl substituted derivatives, ^{31}P and ^{77}Se NMR experiments showed that these species are also more π-accepting, therefore making them highly ambiphilic. The small HOMO-LUMO gaps and ΔE_{ST} of these carbenes allows for the stabilization of a rare amino ketene, and even for the intramolecular C-H activation of an unactivated methylene group. Finally, irregularities in ^{77}Se NMR π-scale of CAAC-6 derivatives revealed the existence of a previously undescribed C-H···Se NCHB with extremely nonacidic protons.

4.5 Experimental

4.5.1 General Considerations

All manipulations were performed under an Argon atmosphere in either an MBraun glovebox or using standard Schlenk techniques. Glassware was dried in an oven overnight at 150 ºC or flame dried

before use. Benzene, THF, Et_2O, and toluene were freshly distilled over Na metal. Hexanes, *n*-pentane, DCM, and $CHCl_3$ were freshly distilled over CaH_2. Acetonitrile was distilled over P_2O_5. Additionally, benzene (C_6D_6) and chloroform ($CDCl_3$) used for NMR spectroscopy were purchased from Cambridge Isotope Laboratories and dried according to published methods.[103]

NMR: Multinuclear NMR data were recorded on a Varian INOVA 500MHz and 400MHz, or Bruker 300 MHz spectrometers. NMR signals are listed in ppm, relative to residual solvent signals (^1H and ^{13}C), H_3PO_4 (^{31}P), and $(PhSe)_2$ (^{77}Se). Coupling constants are in Hertz (Hz). NMR multiplicities are abbreviated as follows: s = singlet, d = doublet, t = triplet, q = quartet, sext = sextet, sept = septet, m = multiplet, br = broad. All spectra were recorded at 25 ^oC unless otherwise noted.

Melting Points: Melting points were measured with an electrothermal MEL-TEMP apparatus. Pure crystals of each compound were added to a capillary tube which was then sealed from air with vacuum grease.

Mass Spectrometry: High resolution mass spectrometry data was collected on an Agilent 6230 TOF-MS at the UC San Diego Mass Spectrometry Laboratory.

X-Ray Crystallography: Single crystal X-Ray diffraction data were collected on Bruker Apex II difractometers using Mo-K_α radiation (λ = 0.71073 Å) or Cu-K_α radiation (λ = 1.54178 Å). Crystals were selected under oil, mounted on nylon loops then immediately placed in a cold stream of N_2. Structures were solved and refined using SHELXTL and Olex2 software.[104] Hydrogen atoms were included in the refinement in calculated positions depending on the connecting carbon atoms. X-ray images were generated using CYLview.

UV-Vis Spectroscopy: Compound **4.11c** was dissolved in pentane (3.4 mM) and the stock solution was transferred to an air-tight cuvette (l = 1.0 mm). The UV-Vis spectrum was recorded on a Shimadzu UV–3600 UV/vis/NIR spectrometer.

IR Spectroscopy: *cis*-[(CAAC-6)Rh(CO)$_2$Cl] species **4.15c** and **4.26a-e** were diluted in DCM and injected into a Thermo-Fischer solution cell equipped with a KBr window. The FTIR spectrum was recorded on a Thermo-Nicolet iS10 FTIR spectrometer.

4.5.2 Synthetic Procedures

4.4a: Imine **4.2a** (3.48 g) was dissolved in 24 mL Et_2O and cooled to -78 ºC. *n*-BuLi (5.6 mL, 1.05 eq) was added to the solution. The solution was stirred at -78 ºC for 15 min and then naturally warmed to RT over 3h. The yellow solution was then cooled to again to -78 ºC and a Et_2O (10 mL) solution of 4-iodo-2-methylbut-1-ene (3.1 g, 1.2 eq) was added by cannula. The resulting mixture was naturally warmed to RT over 12h resulting in a crude mixture containing alkenyl imine **4.10a**. This solution was washed with a conc. $NaHSO_3/H_2O$ solution (2 x 50 mL), followed by H_2O (3 x 50 mL), dried over $MgSO_4$, filtered, and Et_2O was removed *in vacuo*. [Note: This washing step is very important. If not washed properly, the final step will yield a mixture of 5 and 6 membered iminium salts.] The resulting oil was washed into a pre weighed/dried pressure proof Teflon sealed Schlenk with ~ 3-5 mL Et_2O. The remaining volatiles (including excess 4-iodo-2-methylbut-1-ene) were removed by high vacuum on the Schlenk line. The weight of the resulting oil was determined, and dissolved in dry Et_2O (30 mL). HCl (2.0 M in Et_2O) was added (2.0 eq with respect to oil weight). The Schlenk was sealed and heated to 90 ºC over 16h with vigorous stirring inducing the precipitation of a white ppt. (CAUTION: High pressure system! Take proper precautions assuming possible explosion might occur). After cooling to RT, the supernatant was filtered off, and the solid was washed with Et_2O (3 x 50 mL) and minimal cold THF (3 x 3 mL, 0 ºC) [Note: The THF portion can be saved and some product recovered by recrystallization in a concentrated solution at -20 ºC]. After removal of residual Et_2O *in vacuo*, the white ppt was dissolved in DCM (15 mL) and transferred to a Schlenk containing $NaBF_4$ (1.47 g, 3 eq) and the slurry was stirred over 16h. Extracting the supernatant by cannula filtration, removal of DCM *in vacuo*, subsequent washings with pentane (2 x 10 mL), and drying *in vacuo* gave pure white microcrystals of iminium **4.4a** (0.53 g, 11% yield). **MP:** 202 ºC (dec.); **^{1}H NMR** (300 MHz, $CDCl_3$) δ 8.61 (s, 1H), 7.52

(t, *J* = 7.8 Hz, 1H), 7.34 (d, *J* = 7.8 Hz, 2H), 2.61 (sept, *J* = 6.7 Hz, 2H), 2.26 – 2.19 (m, 2H), 2.09 – 2.01 (m, 2H), 2.00 – 1.84 (m, 4H), 1.65 (s, 4H), 1.46 (s, 6H), 1.39 (d, *J* = 6.7 Hz, 6H), 1.25 (s, 3H), 1.17 (d, *J* = 6.7 Hz, 6H), 1.09 (t, *J* = 7.4 Hz, 6H). **^{13}C{^{1}H} NMR** (126 MHz, $CDCl_3$) δ 192.40 (NCH), 143.49 (C_{Ar}), 135.26 (C_{Ar}), 131.94 (C_{Ar}), 125.77 (C_{Ar}), 68.68 (C_q), 46.36 (C_q), 33.88, 29.96, 29.84, 28.91, 27.39, 26.22, 22.54, 22.07, 8.88. **HRMS**: *m/z* calculated for $[C_{23}H_{38}N]^+$ $[M]^+$ 328.2999, found 328.3003.

4.4b: Prepared following a nearly identical procedure to **4.4a** except the volumes of all solvents used were doubled and more purification was needed after the final step. The final salt was dissolved in DCM, washed with H_2O (3 x 100 mL), dried over $MgSO_4$ and filtered, and the residual solvent removed *in vacuo*. The remaining ppt was then washed with Et_2O (3 x 50 mL). [Note: The final product should be white microcrystalline, but residual solvent not properly removed gives the solid a slightly yellow color. Although colored, this product is pure by NMR and safe to use for following steps]. Imine **4.2b** (9.7 g, 1 eq), *n*-BuLi (14.6 mL, 1.05 eq), 4-iodo-2-methylbut-1-ene (8.2 g, 1.2 eq), and $NaBF_4$ (7.6 g, 2 eq) gave pure slightly pale yellow microcrystals of iminium **4.4b** (2.0 g, 14% yield). **^{1}H NMR** (500 MHz, $CDCl_3$) δ 8.62 (s, 1H), 7.51 (t, *J* = 7.8 Hz, 1H), 7.32 (d, *J* = 7.8 Hz, 2H), 2.59 (sept, *J* = 6.6 Hz, 2H), 2.24 – 2.00 (m, 6H), 1.81 – 1.63 (m, 5H), 1.57 – 1.47 (m, 2H), 1.45 (s, 6H), 1.37 (d, *J* = 6.6 Hz, 6H), 1.31 – 1.20 (m, 2H), 1.16 (d, *J* = 6.6 Hz, 6H). **^{13}C{^{1}H} NMR** (126 MHz, $CDCl_3$) δ 190.56 (NCH), 143.55 (C_{Ar}), 134.99 (C_{Ar}), 131.95 (C_{Ar}), 125.62 (C_{Ar}), 68.77 (C_q), 42.64 (C_q), 33.88, 31.69, 29.95, 27.43, 26.06, 24.08, 22.37, 19.79.

4.4c: Prepared following a nearly identical procedure to **4.4a** except the volumes of all solvents used were doubled and the product was only washed with THF after the anion exchange with $NaBF_4$. [Note: The final product should be white microcrystalline, but residual solvent not properly removed gives the solid a slightly yellow color. Although colored, this product is pure by NMR and safe to use for following steps.] Imine **4.2c** (6.2 g, 1 eq), *n*-BuLi (8.0 mL, 1.05 eq), 4-iodo-2-methylbut-1-ene (4.5 g, 1.2 eq), and $NaBF_4$ (6.3 g, 3 eq) gave pure slightly pale yellow microcrystals of iminium **4.4c** (1.7 g, 19% yield). **MP**: 240 ºC (dec.): **^{1}H NMR** (500 MHz, $CDCl_3$) δ 8.87 (s, 1H), 7.54 (t, *J* = 7.8 Hz, 1H), 7.35 (d, *J* = 7.8 Hz, 2H), 2.62 (sept, *J* = 6.6 Hz, 2H), 2.33 (d, *J* = 6.6 Hz, 2H), 2.27 (d, *J* = 6.8 Hz, 2H), 2.22 (br s,

2H), 2.20 (br s, 2H), 2.06 – 2.02 (m, 2H), 2.02 – 1.97 (m, 2H), 1.93 (br s, 1H), 1.90 (br s, 1H), 1.81 (m, 4H), 1.48 (s, 6H), 1.37 (d, *J* = 6.6 Hz, 6H), 1.09 (d, *J* = 6.6 Hz, 6H). **^{13}C{^{1}H} NMR** (126 MHz, $CDCl_3$) δ 191.38 (NCH), 143.67 (C_{Ar}) , 135.57 (C_{Ar}), 132.07 (C_{Ar}), 125.78 (C_{Ar}), 69.66 (C_q), 46.56 (C_q), 38.26, 35.48, 32.99, 32.60, 31.86, 29.74, 27.50, 27.31, 26.53, 26.12, 24.62, 22.23. **HRMS**: *m/z* calculated for $[C_{28}H_{42}N]^+$ $[M]^+$ 392.3312, found 392.3311.

4.4d: Prepared following a nearly identical procedure to **4.4a** except the final product was never completely purified successfully. Imine **4.4d** (0.60 g, 1 eq), *n*-BuLi (0.90 mL, 1.05 eq), 4-iodo-2-methylbutene (0.50 g, 1.2 eq), and $NaBF_4$ (0.70 g, 3 eq) gave a crude solid which was mainly **4.4d**.

4.4e: Prepared following a nearly identical procedure to **4.4a** except the final product was not washed with THF. Imine **4.2e** (3.63 g, 1 eq), *n*-BuLi (4.7 mL, 1.05 eq), 4-iodo-2-methylbut-1-ene (2.61 g, 1.2 eq), and $NaBF_4$ (3.65 g, 3 eq) gave pure white microcrystals of iminium **4.4e** (0.81 g, 15% yield) **MP**: 218-220 ºC; **^{1}H NMR** (400 MHz, $CDCl_3$) δ 8.70 (s, 1H), 7.54 (t, *J* = 7.8 Hz, 1H), 7.37 – 7.32 (m, 2H), 2.72 – 2.42 (m, 5H), 2.36 – 2.12 (m, 4H), 1.99 – 1.92 (m, 1H), 1.84 – 1.68 (m, 3H), 1.66 (s, 3H), 1.57 – 1.45 (m, 3H), 1.40 (d, *J* = 6.6 Hz, 3H), 1.37 (d, *J* = 6.6 Hz, 3H), 1.32 (s, 3H), 1.16 (dd, *J* = 6.7, 2.9 Hz, 6H), 1.06 (d, *J* = 6.8 Hz, 3H), 0.92 (d, *J* = 5.6 Hz, 3H), 0.80 (d, *J* = 7.0 Hz, 3H). **^{13}C{^{1}H}** (126 MHz, $CDCl_3$) δ 190.83 (NCH), 144.24 (C_{Ar}), 142.85 (C_{Ar}), 135.94 (C_{Ar}), 131.83 (C_{Ar}), 126.39 (C_{Ar}), 125.96 (C_{Ar}), 69.81 (C_q), 53.95 (C_H), 50.24 (C_{H2}), 47.81 (C_q), 34.60, 33.35, 29.73, 29.69, 29.42, 28.90, 28.83, 28.04, 26.96, 26.61, 26.52, 25.82, 23.96, 23.13, 22.92, 21.96, 21.01, 18.84. **HRMS**: *m/z* calculated for $[C_{28}H_{46}N]^+$ $[M]^+$ 396.3625, found 396.3627.

4.11a (NMR Crude): C_6D_6 was added to an NMR tube containing **4.4a** (20 mg, 1 eq) and KHMDS (10 mg, 1.4 eq) giving a crude mixture of **4.11a**, KBF_4, HHMDS, and excess KHMDS, however no other organic compounds, including **4.10a,** were observed in the NMR. This carbene is stable is solution for at least 5 days at RT, however decomposition was observed starting at 50 ºC. Attempts to isolate pure crystals of the carbene failed. **^{1}H NMR** (500 MHz, C_6D_6) δ 7.19 (m, 1H), 7.11 (d, *J* = 7.7 Hz, 2H), 3.04 (sept, *J* = 6.7 Hz, 2H), 1.91 – 1.81 (m, 2H), 1.71 – 1.62 (m, 2H), 1.49 – 1.41 (m, 4H), 1.23 (d, *J* = 6.9 Hz, 6H), 1.15 (d, *J* = 6.7 Hz, 6H), 1.06 (t, *J* = 7.4 Hz, 6H), 0.98 (s, 6H). **^{13}C{^{1}H} NMR** (126 MHz,

C_6D_6) δ 330.29 ($C_{carbene}$), 144.64 (C_{Ar}), 142.34 (C_{Ar}), 127.19 (C_{Ar}), 124.03 (C_{Ar}), 59.53 (C_q), 49.04 (C_q), 35.79, 30.36, 30.08, 29.61, 28.64, 28.16, 25.85, 25.29, 24.85, 23.17, 22.14, 9.21. [Note: The fact that no imine **4.10a** was initially observed in this case is likely due to the minimal steric hindrance of the Et groups. In some of the following deprotonation reactions, a mixture which included the respective alkenyl imine was observed likely because the iminium proton was more kinetically protected by the large alkyl substituents. Although this species was stable in the NMR tube for multiple days, upon concentration of the solvent, and/or extractions with pentane, a considerable amount of **4.10a** was generated. It is therefore advised that use of **4.11a** should be limited to synthesis in which deprotonation and subsequent reactivity can be performed in the same solvent system (see synthesis of **4.14a**, **4.16a**, and **4.17a** for examples).]

4.11b (NMR Crude): C_6D_6 was added to an NMR tube containing **4.4b** (38 mg, 1 eq) and KHMDS (19 mg, 1.05 eq) giving a crude mixture of **4.11b**, KBF_4, HHMDS, and excess KHMDS. This carbene is stable is solution for at least 5 days at RT, however decomposition was observed starting at 50 ºC. Attempts to isolate pure crystals of the carbene failed. **^{1}H NMR** (500 MHz, C_6D_6) δ 7.18 (d, *J* = 7.8 Hz, 1H), 7.10 (d, *J* = 7.8 Hz, 2H), 3.02 (sept, *J* = 6.8 Hz, 2H), 2.26 – 2.09 (m, 2H), 1.94 (br s, 2H), 1.73 – 1.34 (m, 10H), 1.24 (d, *J* = 6.8 Hz, 6H), 1.12 (d, *J* = 6.8 Hz, 6H), 0.98 (s, 6H). **^{13}C{^{1}H} NMR** (126 MHz, C_6D_6) δ 330.57 ($C_{carbene}$), 144.64 (C_{Ar}), 142.14 (C_{Ar}), 127.19 (C_{Ar}), 123.90 (C_{Ar}), 60.42 (C_q), 46.07 (C_q), 35.54, 29.66, 28.25, 27.22, 27.01, 25.46, 22.04, 21.93.

4.11c: Benzene (20 mL) was added to a Schlenk containing a solid mixture of **4.4c** (0.994 g, 1 eq) and KHMDS (0.434 g, 1.05 eq). The solution immediately turned yellow and was stirred for 2h giving a ~10:2 ratio of carbene **4.11c** and imine **4.10c**. The benzene was removed *in vacuo* and the product was extracted with pentane (15 mL). Concentrating the pentane solution to half volume and storing in a -20 ºC freezer overnight yielded bright yellow crystals of **4.11c** (0.218 g, 27%). **MP**: 120 ºC (dec.); **^{1}H NMR** (500 MHz, C_6D_6) δ 7.43 – 7.39 (m, 1H), 7.33 (d, *J* = 7.8 Hz, 2H), 3.89 (d, *J* = 11.6 Hz, 2H), 3.23 (sept, *J* = 6.6 Hz, 2H), 2.45 (br s, 2H), 2.35 (d, *J* = 12.5 Hz, 2H), 2.25 – 2.04 (m, 4H), 1.90 (d, *J* = 12.2 Hz, 4H) 1.86 – 1.78 (m, 4H), 1.66 – 1.59 (m, 2H), 1.52 – 1.40 (m, 2H), 1.46 (d, *J* = 6.6 Hz, 6H), 1.29 (d, *J* = 6.6 Hz, 6H), 1.21 (s, 6H). **^{13}C{^{1}H} NMR** (126 MHz, C_6D_6) δ 345.19 ($C_{carbene}$), 144.72 (C_{Ar}), 141.86 (C_{Ar}),

126.99 (C_{Ar}), 123.95 (C_{Ar}), 60.37 (C_q), 50.23 (C_q), 40.43, 36.99, 34.84, 33.65, 33.46, 30.20, 29.57, 28.65, 28.44, 26.41, 25.83, 24.69, 24.12, 22.10. **UV-Vis**: λ_{max} (nm) = 250, 300, 396.

4.13c: THF (5 mL) was added to a vial containing **4.11c** (40 mg, 1 eq) and (tht)AuCl (32 mg, 1 eq). The mixture was stirred and a white ppt quickly crashed out of solution. After 3h of stirring, the THF was filtered off and the ppt was taken up in DCM (2 mL). Filtration through a pipette stuffed with glass filter paper removed any residual Au^0 ppt leaving a clear solution. Slow diffusion of pentane into this solution resulted in the isolation of **4.13c** as large colorless block crystals (30 mg, 47%). **MP:** 284 ºC (dec.) **^{1}H NMR** (500 MHz, $CDCl_3$) δ 7.39 (t, *J* = 7.7 Hz, 1H), 7.21 (d, *J* = 7.7 Hz, 2H), 4.00 (d, *J* = 13.2 Hz, 2H), 2.72 (sept, *J* = 6.6 Hz, 2H), 2.16 (d, *J* = 13.2 Hz, 2H), 2.13 – 2.00 (m, 4H), 2.06 (s, 3H), 1.93 (s, 1H), 1.80 (d, *J* = 13.2 Hz, 2H), 1.75 (s, 2H), 1.67 (d, *J* = 13.2 Hz, 2H), 1.50 (d, *J* = 6.6 Hz, 6H), 1.35 (s, 6H), 1.31 (d, *J* = 6.6 Hz, 6H). **^{13}C{^{1}H}** NMR (126 MHz, $CDCl_3$) δ 251.61 ($C_{carbene}$), 144.59 (C_{Ar}), 141.74 (C_{Ar}), 129.33 (C_{Ar}), 125.24 (C_{Ar}), 66.43 (C_q), 51.09 (C_q), 39.75, 35.81, 34.90, 33.50, 32.20, 31.25, 29.22, 27.99, 27.21, 27.05, 24.52, 23.54. **HRMS**: *m/z* calculated for $[C_{28}H_{40}AuN]^+$ $[M\text{-}Cl]^+$ 588.2899, found 588.2909.

4.14a: **4.4a** (48 mg, 1 eq), KHMDS (23 mg, 1.05 eq) and C_6D_6 were added to a J-Young NMR tube in the glovebox and thoroughly shaken. The solution was then degassed using the freeze-pump-thaw method and then subjected to CO giving an immediate red color. After 1 hr, the benzene was removed *in vacuo*. Pentane (~2 mL) was added to the red solid and the solution was filtered through a pipette stuffed with glass filter paper and the resulting solution was stored in a -40 ºC freezer overnight which yielded **4.14a** as red single crystals. **^{1}H NMR** (400 MHz, C_6D_6) δ 7.07 (m, 3H), 3.51 (sept, *J* = 6.6 Hz, 2H), 1.76 – 1.46 (m, 6H), 1.27 (d, *J* = 6.6 Hz, 6H), 1.22 (d, *J* = 6.6 Hz, 6H), 1.12 (s, 6H), 0.76 (t, *J* = 7.3 Hz, 6H). **^{13}C{^{1}H} NMR** (75 MHz, C_6D_6) δ 235.60 (*C*CO), 150.23 (C_{Ar}), 140.87 (C_{Ar}), 127.95 (C_{Ar}), 124.91 (C_{Ar}), 67.61 (C_q), 54.28 (C_q), 38.40, 36.37, 31.68, 29.29, 28.77, 26.13, 25.87, 25.41, 8.59.

4.15c: THF (5 mL) was added to a vial containing **4.11c** (57 mg, 1 eq) and $[Rh(cod)Cl]_2$ (30 mg, 0.4 eq). The solution was stirred for 2 hours. THF was removed *in vacuo*, and the remaining solid was washed with 3 x 5 mL pentane to give pure (**4.11c**)Rh(cod)Cl. The carbene complex was taken up in 10

mL THF and subjected to 3 successive freeze-pump-thaw cycles. CO was then bubbled into the solution for 15 min and the resulting mixture stirred at RT for 12hrs. The solution was extracted from insoluble ppt, the solvent removed *in vacuo*, and the product washed with pentane 2 x 5 mL to yield pure **4.15c** as a yellow-orange solid (42 mg, 48 % yield). **^{1}H NMR** (500 MHz, C_6D_6) δ 7.16 (t, *J* = 7.1 Hz, 2H), 6.99 (d, *J* = 7.1 Hz, 1H), 5.19 (d, *J* = 13.3 Hz, 1H), 3.96 (sept, *J* = 6.6 Hz, 1H), 3.28 (s, 1H), 3.02 (d, *J* = 12.4 Hz, 1H), 2.74 (sept, *J* = 6.6 Hz, 1H), 2.34 – 1.82 (m, 14H), 1.77 – 1.55 (m, 8H), 1.26 (m, 10H), 1.02 (d, *J* = 6.5 Hz, 3H), 0.84 (s, 3H). **^{13}C{^{1}H} NMR** (126 MHz, C_6D_6) δ 280.18 (d, *J* = 37 Hz) (C_{carb}), 188.85 (d, *J* = 52 Hz) (C_{CO}), 184.62 (d, *J* = 82 Hz) (C_{CO}), 147.20 (C_{Ar}), 146.36 (C_{Ar}), 144.21 (C_{Ar}), 129.37 (C_{Ar}), 127.24 (C_{Ar}), 125.84 (C_{Ar}), 66.47 (C_q), 57.83 (C_q), 40.07, 38.62, 37.02, 35.75, 34.05, 33.85, 33.71, 31.61, 30.24, 29.40, 29.23, 28.76, 28.29, 27.70, 27.54, 27.47, 27.31, 25.54, 25.04. **HRMS**: *m/z* calculated for $[C_{30}H_{41}NO_2Rh]^+$ $[M\text{-}Cl]^+$ 550.2187, found 550.2184. **FTIR**: (KBr, DCM solution) 2067.4 (CO), 1989.8 (CO) cm^{-1}.

4.16a: **4.4a** (37 mg, 1 eq) and KHMDS (19 mg, 1.05 eq) and C_6D_6 were added to an NMR tube in the glovebox and thoroughly shaken. To this mixture was added $(PhP)_5$ (10 mg, 0.2 eq) and the resulting solution was heated at 60 ºC for 3h. The crude mixture was analyzed by NMR which showed the presence of **4.16a**, **4.10a**, $(PhP)_5$ and other unidentified products. **4.16a** could not be separated from the other products and therefore was not isolated. **^{31}P NMR** (121 MHz, C_6D_6) δ 103.17. [Note: The crude $^{13}C\{^{1}H\}$ NMR shows a clear doublet ($^{1}J_{C\text{-}P}$ = 73 Hz) at 206.38 ppm, indicative of the formation of **4.16a**.]

4.17a: In a glovebox, **4.4a** (48 mg, 1 eq), KHMDS (24 mg, 1.05 eq), and Se (18 mg, 2 eq) and THF (3 mL) were stirred in a vial overnight. The THF was removed *in vacuo* and the product extracted with pentane (5 mL). Removal of residual pentane *in vacuo* yielded **4.17a** as a yellow microcrystalline solid (36 mg, 77%) **MP**: 134-137 ºC; **^{1}H NMR** (500 MHz, C_6D_6) δ 7.21 – 7.16 (m, 1H), 7.13 – 7.05 (m, 2H), 2.84 (sept, *J* = 6.6 Hz, 2H), 2.47 – 2.34 (m, 2H), 2.03 – 1.94 (m, 2H), 1.70 – 1.63 (m, 2H), 1.60 – 1.54 (m, 2H), 1.52 (d, *J* = 6.6 Hz, 6H), 1.24 (d, *J* = 6.6 Hz, 6H), 1.00 (t, *J* = 7.4 Hz, 6H), 0.97 (s, 6H). **^{13}C{^{1}H} NMR** (126 MHz, C_6D_6) δ 220.83 (CSe), 145.25 (C_{Ar}), 141.85 (C_{Ar}), 125.14 (C_{Ar}), 63.03 (C_q),

53.60 (C_q), 38.07, 36.05, 29.73, 29.06, 27.08, 24.38, 23.29, 9.18, 3.74, 3.48. **^{77}Se NMR** (57 MHz, $(CD_3)_2CO$) δ 714.91. **HRMS**: *m/z* calculated for $[C_{23}H_{38}NSe]^+$ $[M+H]^+$ = 408.2169, found 408.2166.

4.17c: THF (5 mL) was added to a vial in the glovebox containing **4.11c** (48 mg, 1 eq) and Se (20 mg, 2 eq) at RT and stirred for 1 hr. The THF was removed *in vacuo* and the yellow product extracted with pentane and filtered through a pipette stuffed with glass filter paper. Removal of the pentane *in vacuo* gave a crude mixture that was mainly **4.17c**. Single crystals of **4.17c** were grown in at -20 ºC in a concentrated pentane solution overnight. **^{1}H NMR** (400 MHz, $CDCl_3$) δ 7.33 (t, *J* = 7.7 Hz, 1H), 7.18 (d, *J* = 7.7 Hz, 2H), 3.66 (d, *J* = 13.3 Hz, 2H), 2.73 (sept, *J* = 6.6 Hz, 2H), 2.27 – 2.19 (br s, 4H), 2.16 (s, 4H), 2.04 – 1.38 (m, 14H), 1.30 (d, *J* = 6.6 Hz, 12H), 1.28 (s, 3H), 1.23 – 1.09 (m, 4H), 0.82 (s, 1H). **^{13}C{^{1}H} NMR** (126 MHz, $CDCl_3$) δ 221.41 (CSe), 146.06 (C_{Ar}), 140.84 (C_{Ar}), 127.82 (C_{Ar}), 124.73 (C_{Ar}), 64.70 (C_q), 53.40 (C_q), 40.05, 36.16, 34.54, 33.86, 32.99, 32.10, 29.56, 28.00, 27.53, 27.43, 26.85, 24.02. **^{77}Se NMR** (57 MHz, $CDCl_3$) δ 863.29.

4.18: Benzene (30 mL) was added to Schlenk containing a solid mixture of **4.4e** (595 mg, 1 eq) and KHMDS (258 mg, 1.05 eq). The solution was stirred for 2h. The supernatant was extracted from ppt by filter cannula and concentrated *in vacuo*. Resulting solid contained a 10:1 mixture of **4.18** and **4.10e**. To isolate, the mixture was dissolved in pentane slow evaporation of the pentane solution at RT give colorless crystals of **4.18** (244 mg, 50%). **MP**: 92-93 ºC; **^{1}H NMR** (500 MHz, $CDCl_3$) δ 7.23 – 7.06 (m, 3H), 3.53 (sept, *J* = 6.6 Hz, 1H), 3.43 (sept, *J* = 6.6 Hz, 1H), 2.45 (sept, *J* = 6.8 Hz, 1H), 2.25 – 2.16 (m, 1H), 2.22 (d, *J* = 3.4 Hz, 1H), 1.80 – 1.30 (m, 8H), 1.26 (d, *J* = 6.3 Hz, 3H), 1.23 – 1.19 (m, 8H), 1.16 (d, *J* = 6.9 Hz, 3H), 1.05 – 0.99 (m, 8H), 0.94 – 0.85 (m, 1H), 0.69 (s, 2H), 0.67 – 0.56 (m, 2H), 0.50 – 0.44 (m, 1H). **^{13}C{^{1}H} NMR** (126 MHz, $CDCl_3$) δ 152.33 (C_{Ar}), 150.80 (C_{Ar}), 142.96 (C_{Ar}), 126.23 (C_{Ar}), 124.30 (C_{Ar}), 123.60 (C_{Ar}), 52.13 (C_q), 47.19 (C_H), 45.98 (C_H), 38.78 (C_{H2}), 33.53 (C_{H2}), 30.98 (C_H), 29.21 (C_q), 28.91 (C_H), 28.80 (C_H), 28.26 (C_{H3}), 27.68 (C_H), 27.27 (C_H), 25.84 (C_{H3}), 25.80 (C_{H3}), 25.06 (C_{H3}), 24.90 (C_{H3}), 24.68 (C_{H2}), 23.68 (C_{H3}), 23.36 (C_{H3}), 19.88 (C_{H2}), 17.12 (C_{H3}). **HRMS**: *m/z* calculated for $[C_{28}H_{45}N]^+$ $[M+H]^+$ 396.3625, found 396.3628.

4.21a: In a Schlenk, imine **4.20a** (8.1 g, 1 eq) was dissolved in THF (100 mL) and cooled to -78 ºC. Freshly prepared LDA in THF (1.1 eq) was then slowly added to the imine generating a slightly yellow colored solution. The solution was stirred while gradually warmed to room temperature over 2h. The solution was then cooled back to -78 ºC and 1,3-dibromobutane (16.2 g, 1.05 eq) was added in one portion. The solution was stirred and warmed to room temperature over 12h. THF was removed *in vacuo* and the resulting slurry was dissolved in Et_2O, washed with H_2O (3 x 100 mL), dried over $MgSO_4$ and filtered. The Et_2O was removed *in vacuo* and the resulting oily solid was dissolved in dry CH_3CN (50 mL) and heated to 70 ºC under an Argon atmosphere for 12h. The CH_3CN was removed *in vacuo* and the resulting oily solid was washed with additional Et_2O (2 x 200 mL) and pentane (2 x 200 mL). Finally, residual solvent was removed *in vacuo* and **4.21a** was isolated as a white microcrystalline solid (2.60 g, 15% yield). **MP**: 211-213 ºC; **^{1}H NMR** (300 MHz, $CDCl_3$) δ 9.56 (s, 1H), 4.26 – 4.16 (m, 2H), 2.26 – 2.23 (br s, 1H), 2.22 – 2.15 (m, 1H), 2.08 – 1.98 (m, 1H), 1.87 – 1.79 (m, 1H), 1.70 – 1.55 (m, 8H), 1.46 – 1.40 (m, 6H), 1.36 (br d, 3H); **^{13}C{^{1}H} NMR** (126 MHz, $CDCl_3$) δ 183.08 (C*C*HN), 62.36 (N*C*$_{i\text{-Pr}}$), 57.13 (N*C*$_H$CH$_3$), 37.29 (C_q), 27.11, 26.31, 25.51, 25.47, 22.98, 22.33, 19.53. **HRMS:** *m/z* calculated for $[C_{11}H_{22}N]^+$ $[M]^+$ 168.1752, found 168.1748.

4.21b: Prepared following a nearly identical procedure to **4.21a** except following removal of CH_3CN *in vacuo*, the product was dissolved in H_2O and a solution of $NaBF_4$ in H_2O (1.5 eq) was added causing **4.21b** to precipitate from solution. [Note: Addition of Et_2O to the mixture and vigorous shaking can help with precipitation of the desired product]. The solvent was filtered off, and the resulting solid was washed with H_2O (3 x 100 mL), Et_2O (2 x 100 mL), and pentane (2 x 100 mL). The final product was then dried *in vacuo* at 80 ºC for 12h. Imine **4.20b** (11.7 g, 1 eq), LDA (8.6 g, 1.1 eq), 1,3-dibromobutane (16.4 g, 1.05 eq), and $NaBF_4$ (12.5 g, 1.5 eq) gave **4.21b** as a white microcrystalline solid (8.7 g, 55% yield). **MP**: 245-248 ºC; **^{1}H NMR** (500 MHz, $CDCl_3$) δ 8.59 (s, 1H), 4.14 – 4.06 (m, 1H), 3.80 – 3.70 (m, 1H), 2.25 – 1.60 (m, 14H), 1.50 (d, *J* = 7.0 Hz, 2H), 1.43 (s, 3H), 1.42 – 1.38 (m, 2H), 1.36 (s, 3H); **^{13}C{^{1}H} NMR** (126 MHz, $CDCl_3$) δ 182.80 (C*C*HN), 70.23 (N*C*$_{Cy}$), 57.25 (N*C*$_H$CH$_3$), 37.38 (C_q), 33.17,

32.05, 27.11, 26.41, 25.59, 25.45, 25.40, 24.31, 19.58. **HRMS:** *m/z* calculated for $[C_{14}H_{26}N]^+$ $[M]^+$ 208.2065, found 208.2060.

4.21c: Prepared following a nearly identical procedure to **4.21b.** Imine **4.20c** (13.6 g, 1 eq), LDA (12.0 g, 1.1 eq), 1,3-dibromobutane (23.0 g, 1.05 eq), and $NaBF_4$ (17.5 g, 1.5 eq) gave **4.21c** as a white microcrystalline solid (10.6 g, 43% yield). **MP**: 243-245 ºC; **^{1}H NMR** (500 MHz, CD_3CN) δ 8.27 (s, 1H), 4.39-4.32 (m, 1H), 1.86-1.80 (m, 3H), 1.67-1.61 (m, 1H), 1.52 (s, 9H), 1.38 (d, *J* = 6.7 Hz, 3H), 1.33 (s, 3H), 1.23 (s, 3H); **^{13}C{^{1}H} NMR** (126 MHz, CD_3CN) δ 181.82 (C*C*HN), 70.85 (N*C*$_{t\text{-Bu}}$), 54.17 (N*C*$_H$CH$_3$), 38.49 (C_q), 28.46, 28.45, 27.13, 26.92, 26.18, 21.37, 21.35. **HRMS:** *m/z* calculated for $[C_{12}H_{24}N]^+$ $[M]^+$ 182.1909, found 182.1900.

4.21d: Prepared following a nearly identical procedure to **4.21b.** Imine **4.20d** (6.5 g, 1 eq), LDA (3.6 g, 1.1 eq), 1,3-dibromobutane (6.8 g, 1.05 eq), and $NaBF_4$ (5.2 g, 1.5 eq) gave **4.21d** as a white microcrystalline solid (4.2 g, 38% yield). **MP**: 280-282 ºC; **^{1}H NMR** (500 MHz, $CDCl_3$) δ 8.47 (s, 1H), 4.51 – 4.44 (m, 1H), 2.32 – 2.28 (m, 3H), 2.22 – 2.15 (m, 3H), 2.10 – 2.04 (m, 3H), 1.96 – 1.84 (m, 3H), 1.78 – 1.66 (m, 8H), 1.46 – 1.43 (m, 6H), 1.32 (s, 3H); **^{13}C{^{1}H} NMR** (126 MHz, $CDCl_3$) δ 181.25 (C*C*HN), 71.03 (N*C*$_{Ad}$), 52.00 (N*C*$_H$CH$_3$), 40.55, 37.91 (C_q), 35.00, 29.92, 27.18, 26.79, 26.49, 26.40, 21.92. **HRMS**: *m/z* calculated for $[C_{13}H_{30}N]^+$ $[M]^+$ 260.2378, found 260.2374.

4.21e: Prepared following a nearly identical procedure to **4.21b.** Imine **4.2a** (4.3 g, 1 eq), LDA (2.0 g, 1.1 eq), 1,3-dibromobutane (3.8 g, 1.05 eq), and $NaBF_4$ (2.8 g, 1.5 eq) gave **4.21e** as a white microcrystalline solid (4.8 g, 72% yield). **MP**: 227-229 ºC; **^{1}H NMR** (500 MHz, $CDCl_3$) δ 8.57 (s, 1H), 7.50 (t, *J* = 7.6 Hz, 1H), 7.30 (dd, *J* = 7.6 Hz, 2H), 4.26 – 4.18 (m, 1H), 2.63 (sept, *J* = 7.0 Hz, 1H), 2.53 (sept, *J* = 7 Hz, 1H), 2.44 – 2.37 (m, 1H), 2.10 – 2.00 (m, 2H), 1.97 – 1.80 (m, 6H), 1.35 – 1.28 (m, 8H), 1.22 (d, *J* = 7.0 Hz, 3H), 1.20 (d, *J* = 7.0 Hz, 3H), 1.06 (t, *J* = 8.0 Hz, 3H), 1.03 (t, *J* = 8.0 Hz, 3H); **^{13}C{^{1}H} NMR** (126 MHz, $CDCl_3$) δ 190.98 (C*C*HN), 142.64 (C_{Ar}), 142.58 (C_{Ar}), 136.95 (C_{Ar}), 131.92 (C_{Ar}), 125.86 (C_{Ar}), 125.47 (C_{Ar}), 63.25 (N*C*HMe), 45.65 (C_q), 29.40, 29.33, 29.26, 28.93, 26.45, 25.70, 24.93, 23.83, 23.03, 22.53, 18.10, 8.67, 8.48. **HRMS**: *m/z* calculated for $C_{22}H_{36}N$ $(M)^+$ 314.2848, found 314.2843.

4.22e: THF (1 mL) was added to an NMR tube containing a solid mixture of iminium **4.21e** (40 mg, 1 eq) and KHMDS (21 mg, 1.05 eq) slowly at -78 ºC. The NMR tube was carefully shaken to retain cold temperature, and transferred quickly to an NMR machine precooled to -80 ºC. **^{13}C VT-NMR** (75 MHz, THF, -80 ºC) δ 324.10 (br s, C_{carb}), 145.88 (C_{Ar}), 145.05 (C_{Ar}), 143.11 (C_{Ar}), 127.81 (C_{Ar}), 124.54 (C_{Ar}), 57.36, 48.56, and other alkyl signals appearing around the THF solvent signal.

4.23: THF (5 mL) was added at RT to a vial containing a solid mixture of iminium **4.21e** (40 mg, 1 eq) and KHMDS (21 mg, 1.05 eq) in the glovebox. The solution was stirred for 1h, at which time the THF was removed *in vacuo* and the product extracted with Et_2O. Removal of the Et_2O *in vacuo* yielded **4.23** as a yellow oil (31 mg, 99% yield) **^{1}H NMR** (500 MHz, $CDCl_3$) δ 7.31 – 7.26 (m, 1H), 7.16 (d, *J* = 7.7 Hz, 2H), 4.22 (br s, 1H), 3.40 (sept, *J* = 6.8 Hz, 2H), 2.96 (br s, 2H), 1.95 (br s, 2H), 1.56 – 1.39 (m, 8H), 1.26 (d, *J* = 6.9 Hz, 6H), 1.24 (d, *J* = 6.9 Hz, 6H), 0.88 (t, *J* = 7.5 Hz, 6H). **^{13}C{^{1}H} NMR** (126 MHz, $CDCl_3$) δ 148.91, 141.38, 138.97, 127.39, 124.13, 89.57, 59.52, 34.59, 32.66, 27.63, 27.24, 25.77, 24.17, 20.48, 7.79.

4.24: In a Schlenk, imine **4.2b** (480 mg, 1 eq) was dissolved in Et_2O (24 mL) and cooled to -78 ºC. *n*-BuLi (1.1 eq) was then slowly added to the imine generating a slightly yellow colored solution. The solution was stirred while gradually warmed to room temperature over 2h. The solution was then cooled back to -78 ºC and 1,4-dibromopentane (430 mg, 1.05 eq) was added in one portion. The solution was stirred and warmed to room temperature over 12h. The Et_2O solution was then washed with H_2O (3 x 100 mL), dried over $MgSO_4$ and filtered. The Et_2O was removed *in vacuo* and the oil was subjected to new, dried Et_2O (24 mL) in an air free Schlenk. TMSOTf (0.35 mL, 1.1 eq) was then added to the Schlenk and the solution heated at 100 ºC overnight causing a tiny amount of white precipitate to appear from the solution. Removal of the supernatant and the ppt *in vacuo* yielded **4.24** as a white solid (30 mg, 3% yield). **^{1}H NMR** (500 MHz, $CDCl_3$) δ 8.01 (s, 1H), 7.45 (t, *J* = 7.8 Hz, 1H), 7.28 (d, *J* = 7.8 Hz, 2H), 4.14 (m, 1H), 2.85 (sept, *J* = 6.7 Hz, 2H), 2.13 – 2.01 (br s, 2H), 2.01 – 1.80 (m, 6H), 1.73 (d, *J* = 6.6 Hz, 3H), 1.66 – 1.46 (m, 6H), 1.25 (d, *J* = 6.7 Hz, 12H). **^{13}C{^{1}H} NMR** (126 MHz, $CDCl_3$) δ 192.44 (NCHC),

143.02 (C_{Ar}), 131.34 (C_{Ar}), 124.79 (C_{Ar}), 121.58 (C_{Ar}), 119.04 (C_{Ar}), 51.08 (NC_HCH_3), 46.76, 40.97, 35.50, 32.82, 32.65, 28.83, 26.68, 24.99, 23.76, 22.78, 22.03. **$^{19}F\{^1H\}$ NMR** (282 MHz, $CDCl_3$) δ -77.67.

4.25a: Iminium salt **4.21a** (356 mg, 1 eq), KHMDS (315 mg, 1.05 eq), and $[Rh(cod)Cl]_2$ (354 mg, 0.5 eq) were all combined in a Schlenk with a stir bar. The Schlenk was cooled to -78 ºC and THF (15 mL) was added slowly to maintain a cold temperature. The resulting slurry was slowly warmed to RT while stirring for 12h. THF was then removed *in vacuo* and the product was extracted with Et_2O. Removal of the Et_2O solvent *in vacuo* gave an orange microcrystalline solid mixture which was mainly **4.25a**. Unfortunately, total purification of this compound was never achieved. Additionally, due to the diastereotopic and impure mixture **4.25a**, the ^1H and $^{13}C\{^1H\}$ NMRs were extremely complicated, and therefore only important characteristic signals are reported herein. **$^{13}C\{^1H\}$ NMR** (126 MHz, $CDCl_3$) δ 267.15 (d, J = 40 Hz, C_{carb}).

4.25b: Iminium salt **4.21b** (185 mg, 1 eq), KHMDS (138 mg, 1.05 eq), and $[Rh(cod)Cl]_2$ (155 mg, 0.5 eq) were all combined in a Schlenk with a stir bar. The Schlenk was cooled to -78 ºC and THF (15 mL) was added slowly to maintain a cold temperature. The resulting slurry was slowly warmed to RT while stirring for 12h. THF was then removed *in vacuo* and the product was extracted with Et_2O. Removal of the Et_2O solvent *in vacuo* to half volume and storage of the solution at -20 ºC overnight gave **4.25b** as an orange microcrystalline solid. [Note: Repetitive recrystallizations seems to selectively favor only one diastereomer, however NMR reported herein still contained a mixture of diastereomers and some small percentage of residual impurities]. **$^{13}C\{^1H\}$ NMR** (126 MHz, C_6D_6) δ 267.36 (d, J = 43 Hz, C_{carb}), 263.31 (d, J = 43 Hz, C_{carb}), 98.82 (d, J = 6 Hz, C_{COD}), 98.28 (d, J = 5 Hz, C_{COD}), 96.28 (d, J = 6 Hz, C_{COD}), 95.36 (d, J = 5 Hz, C_{COD}), 70.27 (d, J = 15 Hz, C_{COD}), 68.34 (d, J = 15, C_{COD}), 65.28 (d, J = 15, C_{COD}), 64.64 (d, J = 15, C_{COD}). **HRMS**: *m/z* calculated for $[C_{22}H_{37}NRh]^-$ [M-Cl]$^-$ 418.1981, found 418.1968.

4.25c: Iminium salt **4.21c** (368 mg, 1 eq), KHMDS (273 mg, 1.05 eq), and $[Rh(cod)Cl]_2$ (337 mg, 0.5 eq) were all combined in a Schlenk with a stir bar. The Schlenk was cooled to -78 ºC and THF (15 mL) was added slowly to maintain a cold temperature. The resulting slurry was slowly warmed to RT

while stirring for 12h. THF was then removed *in vacuo* and the product was extracted with Et_2O. Removal of the Et_2O *in vacuo* to half volume and storage of the solution at -20 ºC overnight gave **4.25c** as an orange microcrystalline solid. [Note: NMRs reported herein were still not completely pure and/or very broad, therefore only important characteristic signals are reported herein.] **^{1}H NMR** (500 MHz, C_6D_6) δ 5.60 (td, *J* = 8.2, 3.8 Hz, 1H), 5.27 (q, *J* = 8.2 Hz, 1H), 3.15 – 3.09 (m, 1H), 2.63 – 2.58 (m, 1H), 2.55 (s, 3H), 2.43 – 2.31 (m, 3H), 2.23 – 2.06 (m, 4H), 1.83 – 1.69 (m, 5H), 1.63 (s, 9H), 1.36 (s, 3H), 0.46 (d, *J* = 6.6 Hz, 3H). **^{13}C{^{1}H} NMR** (126 MHz, C_6D_6) δ 279.32 (d, *J* = 43 Hz, C_{carb}), 99.44 (d, *J* = 7 Hz, C_{COD}), 95.28 (d, *J* = 6 Hz, C_{COD}), 69.77 (d, *J* = 15 Hz, C_{COD}), 67.12 (d, *J* = 16 Hz, C_{COD}), 67.19, 67.06, 66.86, 52.14, 52.13, 51.83, 33.92, 32.56, 32.39, 31.65, 31.47, 30.82, 30.26, 30.18, 29.88, 29.55, 28.11, 26.98, 25.83, 24.32, 23.17.

4.25d: Iminium salt **4.21d** (201 mg, 1 eq), KHMDS (129 mg, 1.05 eq), and $[Rh(cod)Cl]_2$ (143 mg, 0.5 eq) were all combined in a Schlenk with a stir bar. The Schlenk was cooled to -78 ºC and THF (15 mL) was added slowly to maintain a cold temperature. The resulting slurry was slowly warmed to RT while stirring for 12h. THF was then removed *in vacuo* and the product was extracted with Et_2O. Removal of the Et_2O *in vacuo* to half volume and storage of the solution at -20 ºC overnight gave **4.25d** as an orange microcrystalline solid. [Note: NMRs reported herein were still not completely pure and contained some $[Rh(cod)Cl]_2$ starting material gives incorrect integration]. **^{1}H NMR** (500 MHz, C_6D_6) δ 5.65 – 5.55 (m, 1H), 5.27 (q, 7.8 Hz, 1H), 3.34 – 3.23 (m, 1H), 2.71 – 2.66 (m, 1H), 2.60 (s, 3H), 2.47 – 2.32 (m, 4H), 2.28 – 2.18 (m, 2H), 2.16 – 2.05 (m, 4H), 1.84 – 1.75 (m, 2H), 1.72 – 1.51 (m, 10H), 1.43 – 1.12 (m, 15H), 1.03 – 0.81 (m, 6H), 0.50 (d, *J* = 6.5 Hz, 3H). **^{13}C{^{1}H} NMR** (126 MHz, C_6D_6) δ 281.38 (d, *J* = 43 Hz, C_{carb}), 99.24 (d, *J* = 7 Hz, C_{COD}), 94.69 (d, *J* = 6 Hz, C_{COD}), 69.71 (d, *J* = 15 Hz, C_{COD}), 67.15 (d, *J* = 17 Hz, C_{COD}), 68.00, 52.09, 50.56, 50.55, 42.63, 36.29, 34.11, 32.59, 32.08, 31.59, 30.50, 30.26, 29.51, 28.28, 27.28, 26.00, 24.78.

4.25e: Iminium salt **4.21e** (177 mg, 1 eq), KHMDS (97 mg, 1.05 eq), and $[Rh(cod)Cl]_2$ (109 mg, 0.5 eq) were all combined in a Schlenk with a stir bar. The Schlenk was cooled to -78 ºC and THF (15 mL) was added slowly to maintain a cold temperature. The resulting slurry was slowly warmed to RT

while stirring for 12h. THF was then removed *in vacuo* and the product was extracted with Et_2O. Removal of the Et_2O *in vacuo* to half volume and storage of the solution at -20 ºC overnight gave **4.25e** as an orange microcrystalline solid. [Note: A pure ^1H NMR of this compound could not be found and the ^{13}C NMR is from a diastereotopic mixture of **4.25e**.] **MP:** 162 ºC (dec). **$^{13}C\{^1H\}$ NMR** (126 MHz, $CDCl_3$) δ 282.45 (d, *J* = 44 Hz, C_{carb}), 277.54 (d, *J* = 44 Hz, C_{carb}), 147.14 (C_{Ar}), 146.89 (C_{Ar}), 145.69 (C_{Ar}), 144.48 (C_{Ar}), 142.35 (C_{Ar}), 141.38 (C_{Ar}), 128.78 (C_{Ar}), 126.42 (C_{Ar}), 125.67 (C_{Ar}), 123.70 (C_{Ar}), 123.45 (C_{Ar}), 100.55, 98.32, 97.44, 97.30, 69.93, 69.81, 65.75 (d, *J* = 14 Hz, C_{COD}), 63.66 (d, *J* = 14 Hz, C_{COD}), 62.16, 59.55, 49.51, 49.29, 33.89, 33.61, 33.40, 32.94, 32.37, 31.88, 29.86, 29.27, 28.95, 28.75, 27.98, 27.85, 27.53, 26.79, 26.37, 25.87, 25.39. 25.03, 23.80, 23.65, 20.87. **HRMS**: *m/z* calculated for $[C_{30}H_{47}NRh]^-$ $[M\text{-}Cl]^-$ 524.2764, found 524.2754.

4.26a: CO was bubbled into a DCM solution of **4.25a** for 1h. The crude solution was then quickly subjected to an FTIR study. **FTIR**: (KBr, DCM solution) 2071.3 (CO), 1993.2 (CO) cm^{-1}.

4.26b: CO was bubbled into a DCM solution of **4.25b** for 1h. The crude solution was then quickly subjected to an FTIR study. **FTIR**: (KBr, DCM solution) 2072.2 (CO), 1991.2 (CO) cm^{-1}.

4.26c: CO was bubbled into a DCM solution of **4.25c** for 1h. The crude solution was then quickly subjected to an FTIR study. **FTIR**: (KBr, DCM solution) 2067.4 (CO), 1992.2 (CO) cm^{-1}.

4.26d: CO was bubbled into a DCM solution of **4.25d** for 1h. The crude solution was then quickly subjected to an FTIR study. **FTIR**: (KBr, DCM solution) 2067.4 (CO), 1989.3 (CO) cm^{-1}.

4.26e: CO was bubbled into a DCM solution of **4.25e** for 1h. The crude solution was then quickly subjected to an FTIR study. **FTIR**: (KBr, DCM solution) 2070.8 (CO), 1989.3 (CO) cm^{-1}.

(**4.27b**)$_2$: Single crystals of (**4.27b**)$_2$ were grown by slow evaporation of solvent from a DCM solution of **4.26b**. No other characterization was performed on said crystals.

4.27e: Single crystals of **4.27e** were grown by slow diffusion of pentane into a DCM solution of **4.26e**. **FTIR**: (Solid) 1968 (CO) cm^{-1}. No other characterization was performed on said crystals.

4.32a: Iminium salt **4.21a** (498 mg, 1 eq), (PMe_3)AuPh (620 mg, 1 eq), and KHMDS (420 mg, 1.05 eq) were all combined in a Schlenk with a stir bar. The Schlenk was cooled to -78 ºC and THF (20

mL) was added slowly to maintain a low temperature. The slurry was let warm slowly to room temperature over 12h. THF was removed from the subsequent brown solution *in vacuo* and the product was extracted with DCM into a separate Schlenk. The extract was then treated with 2.0 M HCl in Et_2O (4.0 mL, 2 eq) and was stirred for an additional 12h. The DCM solution was then extracted from the insoluble Au^0 particles and the solvent was removed *in vacuo*. Subsequent washings with Et_2O (2 x 20 mL) and hexanes (2 x 20 mL) and removal of residual solvent *in vacuo* yielded the pure product as a white powder (445 mg, 57%). **MP**: 174 ºC (dec). **^{1}H NMR** (300 MHz, $CDCl_3$) δ 5.20 – 4.97 (br s, 1H), 3.93 – 3.72 (br s, 1H), 1.85 – 1.40 (m, 15H), 1.35 (s, 6H). **^{13}C{^{1}H} NMR** (126 MHz, $CDCl_3$) δ 228.13 (C_{Carb}), 67.28 (NC_HCH_3), 53.11 ($NC_{i\text{-}Pr}$), 43.58 (C_q), 31.34, 30.36, 27.89, 26.81, 21.89, 21.70, 21.41. **HRMS**: *m/z* calculated for $[C_{11}H_{21}AuClNNa]^+$ $[M+Na]^+$ 422.0926, found 422.0917.

4.32b: Prepared following a nearly identical procedure to **4.32a**. Iminium salt **4.21b** (960 mg, 1 eq), $(PMe_3)AuPh$ (1.0 g, 1 eq), KHMDS (680 mg, 1.05 eq), and 2.0 M HCl in Et_2O (3.3 mL, 2 eq) gave **4.32b** as a white microcrystalline solid (1.30 g, 91% yield). **MP**: 189 ºC (dec). **^{1}H NMR** (500 MHz, $CDCl_3$) δ 3.84 – 3.77 (m, 1H), 2.14 – 2.08 (br s, 1H), 1.93 – 1.59 (m, 10H), 1.50 (s, 3H), 1.47 – 1.40 (m, 2H), 1.38 (s, 3H), 1.32 (d, J = 6.0 Hz, 3H). **^{13}C{^{1}H} NMR** (126 MHz, $CDCl_3$) δ 229.11 (C_{Carb}), 43.91, 32.22, 31.67, 30.55, 28.16, 26.83, 25.94, 25.81, 25.20, 21.10, 16.43, 16.11. **HRMS**: *m/z* calculated for $[C_{14}H_{25}AuClNNa]^+$ $[M+Na]^+$ 462.1239, found 462.1232.

4.32c: Prepared following a nearly identical procedure to **4.32a**. Iminium salt **4.21c** (174 mg, 1 eq), $(PMe_3)AuPh$ (200 mg, 1 eq), KHMDS (135 mg, 1.05 eq), and 2.0 M HCl in Et_2O (1.3 mL, 2 eq) gave **4.32c** as a white microcrystalline solid (270 mg, 34% yield). **MP**: 162 ºC (dec). **^{1}H NMR** (500 MHz, $CDCl_3$) δ 4.25 – 4.17 (br s, 1H), 1.97 (s, 9H), 1.85 – 1.73 (m, 6H), 1.62 (s, 3H), 1.80 – 1.75 (m, 3H), 1.62 (s, 3H), 1.51 (br s, 1H), 1.42 (s, 3H), 1.30 (d, J = 6.4 Hz, 3H). **^{13}C{^{1}H} NMR** (126 MHz, $CDCl_3$) δ 231.75.13 (C_{Carb}), 68.26 (NC_HCH_3), 53.11 ($NC_{t\text{-}Bu}$), 45.62 (C_q), 33.09, 32.17, 31.30, 27.86, 26.66, 22.49. **HRMS:** *m/z* calculated for $[C_{12}H_{23}AuN]$ $[M-Cl]^+$ 378.1496, found 378.1487.

4.32d: Prepared following a nearly identical procedure to **4.32a**. Iminium salt **4.21d** (248 mg, 1 eq), $(PMe_3)AuPh$ (220 mg, 1 eq), KHMDS (150 mg, 1.05 eq), and 2.0 M HCl in Et_2O (1.4 mL, 2 eq) gave

4.32d as a white microcrystalline solid (84 mg, 24% yield). **MP**: 174 ºC (dec). **^{1}H NMR** (500 MHz, $CDCl_3$) δ 4.26 (m, 1H), 2.84 – 2.76 (m, 6H), 2.27 (br s, 2H), 1.85 – 1.67 (m, 8H), 1.65 (s, 3H), 1.42 (s, 3H), 1.28 (d, *J* = 6.4 Hz, 3H). **^{13}C{^{1}H} NMR** (126 MHz, $CDCl_3$) δ 230.84 (C_{Carb}), 69.82 (NC_HCH_3), 52.20 (NC_{Ad}), 43.77 (C_q), 43.22, 35.75, 33.41, 31.71, 30.90, 28.34, 26.64, 23.18.

4.32e: Prepared following a nearly identical procedure to **4.32a**. Iminium salt **4.21e** (742 mg, 1 eq), (PMe_3)AuPh (880 mg, 1 eq), KHMDS (527 mg, 1.05 eq), and 2.0 M HCl in Et_2O (5.6 mL, 2 eq) gave **4.32e** as a white microcrystalline solid (950 mg, 94% yield). **MP**: 210-213 ºC. **^{1}H NMR** (500 MHz, $CDCl_3$) δ 7.40 (t, *J* = 7.7 Hz, 1H), 7.22 (d, *J* = 7.7 Hz, 2H), 3.66 – 3.59 (m, 1H), 2.72 (sept, *J* = 6.7 Hz, 1H), 2.64 (sept, *J* = 6.7 Hz, 1H), 2.16 – 1.77 (m, 10H), 2.10 – 2.00 (m, 2H), 1.61 (d, *J* = 11.2 Hz, 1H), 1.52 (d, *J* = 6.7 Hz, 3H), 1.35 (d, *J* = 6.7 Hz, 3H), 1.29 – 1.23 (m, 10H), 1.01 – 0.95 (m, 6H). **^{13}C{^{1}H} NMR** (126 MHz, $CDCl_3$) δ 239.33 (C_{carb}), 143.69 (C_{Ar}), 143.25 (C_{Ar}), 142.31 (C_{Ar}), 129.82 (C_{Ar}), 125.43 (C_{Ar}), 125.17 (C_{Ar}), 61.19 (NC_HCH_3), 50.53 (C_q), 33.41, 33.23, 28.76, 28.74, 26.69, 26.26, 25.07, 24.11, 23.66, 9.27, 9.22. **HRMS**: *m/z* calculated for $[C_{22}H_{35}AuClNNa]^+$ $[M+Na]^+$ 568.2021, found 568.2017.

4.33e: DCM was added to a vial at RT containing **4.32e** (38 mg, 1 eq) and $GaCl_3$ (13 mg, 1.1 eq) in the glovebox and the crude mixture was analyzed by ^{13}C NMR showing only one product. The DCM was then removed *in vacuo* and the solid washed with pentane. Single crystals of **4.33e** were grown by slow evaporation of a DCM solution. **Crude ^{13}C{^{1}H] NMR** (126 MHz, DCM) δ 232.05 (C_{carb}), 143.66 (C_{Ar}), 142.98 (C_{Ar}), 142.21 (C_{Ar}), 130.26 (C_{Ar}), 125.65 (C_{Ar}), 125.37 (C_{Ar}), 62.46, 50.76, 33.23, 33.08, 28.63, 26.32, 26.22, 24.81, 23.68, 23.41, 20.56, 18.91, 8.98, 8.91.

4.35b: Iminium salt **4.21e** (214 mg, 2 eq), (tht)AuCl (116 mg, 1 eq), and KHMDS (152 mg, 2.1 eq) were all combined in a Schlenk with a stir bar. The Schlenk was cooled to -78 ºC and THF (20 mL) was added slowly to maintain a low temperature. The slurry was let warm slowly to room temperature over 12h. THF was removed from the subsequent brown solution *in vacuo* and the product was extracted with DCM into a separate Schlenk. The DCM was removed *in vacuo* and the product washed with hexanes (2 x 10 mL) giving **4.35b** as a white microcrystalline solid. [Note: Other impurities still existed in this solid mixture, however the major product was **4.35b.** This reaction was only meant to confirm the

carbene signal of this species, therefore only the crude ^{13}C NMR is reported herein.] **Crude $^{13}C\{^1H\}$ NMR** (126 MHz, $CDCl_3$) δ 241.89 (C_{carb}), 43.38, 32.05, 31.92, 31.46, 30.54, 29.59, 28.23, 26.32, 25.72, 25.60, 24.77, 24.72, 21.15.

4.36a: THF (24 mL) was added to a Schlenk containing (CAAC-6)AuCl complex **4.32a** (210 mg, 1 eq) and $AgBF_4$ (110 mg, 1.1 eq) and the mixture was stirred for 2h at RT. This solution was directly cannula transferred to a 0 ºC KOH (90 mg, 3 eq) and $NaBF_4$ (230 mg, 4 eq) MeOH solution that was also already saturated with CO. After complete addition, CO was bubbled into the solution for another 30 min then the Schlenk was capped under the CO atm and stirred for an additional 12h. The THF was removed *in vacuo* and the product extracted with DCM. Removal of the DCM *in vacuo* gave a black oily solid which contained **4.36a** as a major product. Unfortunately, all attempts to isolate **4.36a** failed and after just one week in solution this compound complete converts to **4.35a** and Au^0 ppt. **Crude $^{13}C\{^1H\}$ NMR** (126 MHz, THF) δ 247.95 (C_{carb}), 214.42 ($C_{verystrange}$), 66.02, 47.74, 43.52, 30.84, 29.96, 28.55, 26.94, 22.30, 21.96, 21.43.

4.36b: THF (15 mL) was added to a Schlenk containing (CAAC-6)AuCl complex **4.32b** (400 mg, 1 eq) and $AgBF_4$ (195 mg, 1.1 eq) and the mixture was stirred for 30 min at RT. This solution was directly cannula transferred to a 0 ºC KOH (90 mg, 3 eq) and $NaBF_4$ (230 mg, 4 eq) MeOH solution and stirred for 1h. The THF/MeOH solution was removed *in vacuo* and the product dissolved in DCM. CO was then bubbled into this solution for 20 min which gave the solution a red/orange color. DCM was removed *in vacuo* and the product extracted with Et_2O. The remaining ppt was confirmed to be **4.36a** by NMR whereas the only carbene signal of the extracted product was assigned to **4.36b**. Unfortunately, all attempts to isolate **4.36b** as single crystals failed and therefore only the crude carbene signal is reported. Nonetheless, the trimeric gold species was confirmed by an ESI-MS analysis. **Crude $^{13}C\{^1H\}$ NMR** (126 MHz, $CDCl_3$) 248.01 (C_{carb}). **ESI-MS**: *m/z* calculated for $[C_{42}H_{75}Au_3N_3]^+$ $[M\text{-}BF_4]^+$ 1212.4958, found 1212.91.

4.37a: Iminium salt **4.21a** (222mg, 1 eq), KHMDS (196 mg, 1.05 eq), and Se black (141 mg, 2 eq) were all combined in a Schlenk with a stir bar. The Schlenk was cooled to -78 ºC and THF (20 mL)

was added slowly to maintain a cold temperature. The resulting slurry was slowly warmed to room temperature while stirring for 12h. THF was then removed *in vacuo* and the product was extracted with pentane. The solution was concentrated to ¼ volume and stored at -20 ºC overnight giving **4.37a** as yellow-orange crystals (60 mg, 28% yield). **^{1}H NMR** (500 MHz, $CDCl_3$) δ 6.24 (br s, 1H), 3.88 (br s, 1H), 2.03 – 1.84 (m, 2H), 1.73 – 1.64 (m, 2H), 1.53 (s, 3H), 1.46 (s, 3H), 1.36 (d, *J* = 7.0 Hz, 3H), 1.31 (d, *J* = 6.5 Hz, 3H), 1.27 (d, *J* = 6.5 Hz, 3H). **^{13}C{^{1}H} NMR** (126 MHz, $CDCl_3$) δ 216.00 (C_{Carb}), 59.36 (NC_HCH_3), 50.72 ($NC_{i\text{-}Pr}$) , 46.59 (C_q), 34.74, 34.56, 30.73, 27.12, 21.90, 20.93, 19.58; **^{77}Se{^{1}H} NMR** (95 MHz, $(CD_3)_2CO$) δ 526.48 **HRMS**: *m/z* calculated for $[C_{11}H_{22}NSe]^+$ $[M+H]^+$ 248.0917, found 248.0911.

4.37b: Prepared following a nearly identical procedure to **4.37a**. Iminium salt **4.21b** (330 mg, 1 eq), KHMDS (245 mg, 1.05 eq), and Se black (176 mg, 2 eq) gave **4.37b** as orange crystals (78 mg, 47% yield). **MP**: 155-157 ºC. **^{1}H NMR** (500 MHz, $CDCl_3$) δ 5.90 – 5.80 (m, 1H), 3.90 – 3.80 (m, 1H), 2.20 – 2.13 (br s, 1H), 1.97 – 1.75 (m, 6H), 1.70 – 1.60 (m, 3H), 1.50 (s, 3H), 1.42 (s, 6H), 1.27 (d, *J* = 6.5 Hz, 2H), 1.18 – 0.85 (m, 3H). **^{13}C{^{1}H} NMR** (126 MHz, $CDCl_3$) δ 214.99 (C_{Carb}), 67.11, 51.18, 46.01, 34.28, 34.14, 30.63, 30.15, 29.40, 26.62, 25.56, 25.38, 25.19, 21.36. **^{77}Se{^{1}H} NMR** (95 MHz, $(CD_3)_2CO$) δ 522.64. **HRMS**: *m/z* calculated for $[C_{14}H_{26}NSe]^+$ $[M+H]^+$ 288.1230, found 288.1223.

4.37c: Prepared following a nearly identical procedure to **4.37a**. Iminium salt **4.21c** (170 mg, 1 eq), KHMDS (139 mg, 1.05 eq), and Se black (100 mg, 2 eq) gave **4.37c** as orange crystals. **^{1}H NMR** (500 MHz, $CDCl_3$) δ 4.28 – 4.21 (m, 1H), 2.14 – 2.06 (m, 1H), 1.97 – 1.91 (m, 1H), 1.89 (s, 9H), 1.64 – 1.56 (m, 2H), 1.55 (s, 3H), 1.34 (s, 3H), 1.28 (d, *J* = 6.5 Hz, 3H). **^{13}C{^{1}H} NMR** (126 MHz, $CDCl_3$) δ 219.62 (C_{Carb}), 66.66 ($NC_{t\text{-}Bu}$), 54.89 (NC_HCH_3), 49.94 (C_q), 34.91, 34.25, 31.67, 30.07, 27.55, 22.85; **^{77}Se{^{1}H} NMR** (95 MHz, $(CD_3)_2CO$) δ 779.60.

4.37d: Prepared following a nearly identical procedure to **4.37a**. Iminium salt **4.21d** (155 mg, 1 eq), KHMDS (102 mg, 1.05 eq), and Se black (73 mg, 2 eq) gave **4.37d** as orange crystals (63 mg, 42% yield). **MP**: 165-167 ºC. **^{1}H NMR** (500 MHz, $CDCl_3$) δ 4.30 (m, 1H), 2.88 (d, *J* = 11.5 Hz, 2H), 2.80 (d, *J* = 11.5 Hz, 2H), 2.18 (br s), 2.11 – 1.98 (m, 2H), 1.76 (d, *J* = 12.0 Hz, 2H), 1.63 (d, *J* = 12.0 Hz, 2H),

1.61 – 1.56 (m, 1H), 1.55 (s. 3H), 1.32 (s, 3H), 1.29 (d, *J* = 6.5 Hz, 3H). **$^{13}C\{^{1}H\}$ NMR** (126 MHz, $CDCl_3$) δ 220.48 (C_{Carb}), 68.45 (NC_{Ad}), 53.83 (NC_HCH_3), 50.81 (C_q), 39.59, 36.20, 35.10, 33.74, 32.24, 31.11, 23.69. **$^{77}Se\{^{1}H\}$ NMR** (95 MHz, $(CD_3)_2CO$) δ 792.20. **HRMS**: *m/z* calculated for $[C_{18}H_{30}NSe]^+$ $[M+H]^+$ 340.1543, found 340.1540.

4.37e: Prepared following a nearly identical procedure to **4.37a**. Iminium salt **4.21e** (240 mg, 1 eq), KHMDS (125 mg, 1.05 eq), and Se black (188 mg, 2 eq) gave **4.37e** as orange crystals (108 mg, 46% yield). **MP**: 184-186 °C. **^{1}H NMR** (500 MHz, $CDCl_3$) δ 7.39 (t, *J* = 7.5 Hz, 1H), 7.24 (d, *J* = 7.5 Hz, 1H), 7.21 (d, *J* = 7.5 Hz, 1H), 3.56 – 3.48 (m, 1H), 2.72 (sept, *J* = 6.7 Hz, 1H), 2.81 (sept, *J* = 6.5, 1H), 2.67 (sept, *J* = 6.5 Hz, 1H), 2.27 – 2.14 (m, 3H), 2.07 – 1.77 (m, 6H), 1.37 (d, *J* = 6.5 Hz, 3H), 1.31 (d, *J* = 6.5 Hz, 3H), 1.27 (d, *J* = 6.5 Hz, 3H), 1.25 (d, *J* = 6.5 Hz, 3H), 1.21 (d, *J* = 6.5 Hz, 3H), 1.01 (q, *J* = 7.5 Hz, 6H). **$^{13}C\{^{1}H\}$ NMR** (126 MHz, $CDCl_3$) δ 219.57 (C_{carb}), 143.91 (C_{Ar}), 143.41 (C_{Ar}), 143.03 (C_{Ar}), 128.42 (C_{Ar}), 125.27 (C_{Ar}), 124.52 (C_{Ar}), 60.94 (NC_HCH_3), 52.94 (C_q), 36.95, 36.84, 28.90, 28.73, 27.20, 25.75, 24.87, 24.51, 24.16, 23.01, 19.82, 9.01, 8.72. **$^{77}Se\{^{1}H\}$ NMR** (95 MHz, $(CD_3)_2CO$) δ 674.94. **HRMS**: *m/z* calculated for $[C_{22}H_{36}NSe]^+$ $[M+H]^+$ 394.2013, found 394.2011.

4.5.3 Crystallographic Data

Compound	**4.4e**
Empirical formula	$C_{28}H_{46}I_3N$
Formula weight	777.36
Temperature/K	100.0
Crystal system	orthorhombic
Space group	$P2_12_12_1$
a/Å	10.0802(7)
b/Å	15.4559(11)
c/Å	19.8248(13)
α/°	90
β/°	90
γ/°	90
Volume/Å^3	3088.7(4)
Z	4
ρ_{calc}g/cm^3	1.672
μ/mm^{-1}	3.051
F(000)	1520.0
Crystal size/mm^3	0.3 × 0.3 × 0.3

Radiation	MoKα (λ = 0.71073)
2Θ range for data collection/°	3.342 to 51.496
Index ranges	$-12 \leq h \leq 10$, $-18 \leq k \leq 18$, $-21 \leq l \leq 24$
Reflections collected	17550
Independent reflections	5892 [R_{int} = 0.0235, R_{sigma} = 0.0242]
Data/restraints/parameters	5892/0/298
Goodness-of-fit on F^2	1.084
Final R indexes [I>=2σ (I)]	R_1 = 0.0135, wR_2 = 0.0309
Final R indexes [all data]	R_1 = 0.0140, wR_2 = 0.0320
Largest diff. peak/hole / e Å^{-3}	0.27/-0.33
Flack parameter	-0.003(8)

Compound	**4.11c**
Empirical formula	$C_{28}H_{41}N$
Formula weight	391.62
Temperature/K	100.0
Crystal system	monoclinic
Space group	$P2_1/c$
a/Å	7.4475(10)
b/Å	11.6494(15)
c/Å	26.153(3)
α/°	90
β/°	90.314(7)
γ/°	90
Volume/Å^3	2269.0(5)
Z	4
ρ_{calc}g/cm^3	1.146
μ/mm^{-1}	0.065
F(000)	864.0
Crystal size/mm^3	0.6 × 0.4 × 0.2
Radiation	MoKα (λ = 0.71073)
2Θ range for data collection/°	3.114 to 54.196
Index ranges	$-9 \leq h \leq 8$, $-14 \leq k \leq 14$, $-33 \leq l \leq 33$
Reflections collected	21949
Independent reflections	4967 [R_{int} = 0.0248, R_{sigma} = 0.0209]
Data/restraints/parameters	4967/0/268
Goodness-of-fit on F^2	1.046
Final R indexes [I>=2σ (I)]	R_1 = 0.0401, wR_2 = 0.1079
Final R indexes [all data]	R_1 = 0.0462, wR_2 = 0.1135
Largest diff. peak/hole / e Å^{-3}	0.34/-0.19

Compound	**4.13c**
Empirical formula	$C_{28}H_{41}AuClN$
Formula weight	624.03

Temperature/K	100.0
Crystal system	orthorhombic
Space group	P212121
a/Å	10.6312(9)
b/Å	13.2056(10)
c/Å	17.7225(15)
α/°	90
β/°	90
γ/°	90
Volume/Å3	2488.1(4)
Z	4
ρcalcg/cm3	1.666
μ/mm-1	6.036
F(000)	1248.0
Crystal size/mm3	0.5 × 0.4 × 0.4
Radiation	MoKα (λ = 0.71073)
2Θ range for data collection/°	4.596 to 52.768
Index ranges	-12 ≤ h ≤ 12, -16 ≤ k ≤ 14, -22 ≤ l ≤ 11
Reflections collected	9264
Independent reflections	4613 [Rint = 0.0283, Rsigma = 0.0531]
Data/restraints/parameters	4613/0/286
Goodness-of-fit on F2	0.770
Final R indexes [I>=2σ (I)]	R1 = 0.0190, wR2 = 0.0406
Final R indexes [all data]	R1 = 0.0201, wR2 = 0.0410
Largest diff. peak/hole / e Å-3	0.48/-0.82

Compound	**4.14a**
Empirical formula	$C_{24}H_{37}NO$
Formula weight	355.54
Temperature/K	100.0
Crystal system	monoclinic
Space group	$P2_1/n$
a/Å	16.1893(4)
b/Å	14.4225(4)
c/Å	19.1923(5)
α/°	90
β/°	106.6520(10)
γ/°	90
Volume/Å^3	4293.3(2)
Z	8
ρ_{calc}g/cm^3	1.100
μ/mm^{-1}	0.495
F(000)	1568.0
Crystal size/mm^3	0.2 × 0.05 × 0.05

Radiation	CuKα (λ = 1.54178)
2Θ range for data collection/°	6.314 to 141.358
Index ranges	-19 ≤ h ≤ 19, -17 ≤ k ≤ 17, -23 ≤ l ≤ 23
Reflections collected	60441
Independent reflections	8214 [R_{int} = 0.0487, R_{sigma} = 0.0276]
Data/restraints/parameters	8214/0/485
Goodness-of-fit on F^2	1.027
Final R indexes [I>=2σ (I)]	R_1 = 0.0444, wR_2 = 0.1170
Final R indexes [all data]	R_1 = 0.0553, wR_2 = 0.1270
Largest diff. peak/hole / e $Å^{-3}$	0.24/-0.23

Compound	**4.15c**
Empirical formula	$C_{30}H_{41}ClNO_2Rh$
Formula weight	586.00
Temperature/K	100.0
Crystal system	monoclinic
Space group	$P2_1/n$
a/Å	9.9542(3)
b/Å	15.6195(4)
c/Å	17.9011(6)
α/°	90
β/°	103.015(2)
γ/°	90
Volume/$Å^3$	2711.76(14)
Z	4
$\rho_{calc}g/cm^3$	1.435
μ/mm^{-1}	0.756
F(000)	1224.0
Crystal size/mm^3	0.2 × 0.2 × 0.1
Radiation	MoKα (λ = 0.71073)
2Θ range for data collection/°	3.5 to 52.814
Index ranges	-11 ≤ h ≤ 12, -19 ≤ k ≤ 17, -22 ≤ l ≤ 18
Reflections collected	16964
Independent reflections	5548 [R_{int} = 0.0553, R_{sigma} = 0.0649]
Data/restraints/parameters	5548/0/322
Goodness-of-fit on F^2	1.054
Final R indexes [I>=2σ (I)]	R_1 = 0.0438, wR_2 = 0.1039
Final R indexes [all data]	R_1 = 0.0586, wR_2 = 0.1115
Largest diff. peak/hole / e $Å^{-3}$	3.89/-0.53

Compound	**4.17c**
Empirical formula	$C_{28}H_{41}NSe$
Formula weight	470.58
Temperature/K	100.0

Crystal system	monoclinic
Space group	$P2_1/n$
a/Å	11.4245(2)
b/Å	15.9264(4)
c/Å	13.2465(4)
α/°	90.00
β/°	99.4230(10)
γ/°	90.00
Volume/Å^3	2377.69(10)
Z	4
ρ_{calc}g/cm^3	1.315
μ/mm^{-1}	1.594
F(000)	1000.0
Crystal size/mm^3	0.4 × 0.2 × 0.2
Radiation	MoKα (λ = 0.71073)
2Θ range for data collection/°	4.04 to 52.74
Index ranges	$-14 \leq h \leq 14$, $-19 \leq k \leq 19$, $-16 \leq l \leq 11$
Reflections collected	14170
Independent reflections	4858 [R_{int} = 0.0241, R_{sigma} = 0.0251]
Data/restraints/parameters	4858/0/277
Goodness-of-fit on F^2	1.068
Final R indexes [I>=2σ (I)]	R_1 = 0.0314, wR_2 = 0.0922
Final R indexes [all data]	R_1 = 0.0348, wR_2 = 0.0941
Largest diff. peak/hole / e Å^{-3}	0.97/-0.42

Compound	**4.18**
Empirical formula	$C_{28}H_{45}N$
Formula weight	395.65
Temperature/K	100.0
Crystal system	triclinic
Space group	P-1
a/Å	9.9377(14)
b/Å	10.3029(15)
c/Å	13.3704(19)
α/°	104.618(3)
β/°	99.452(3)
γ/°	108.858(3)
Volume/Å^3	1207.5(3)
Z	2
ρ_{calc}g/cm^3	1.088
μ/mm^{-1}	0.061
F(000)	440.0
Crystal size/mm^3	0.6 × 0.5 × 0.3
Radiation	MoKα (λ = 0.71073)

2Θ range for data collection/°	5.8 to 51.26
Index ranges	$-12 \leq h \leq 12$, $-12 \leq k \leq 12$, $-16 \leq l \leq 16$
Reflections collected	13147
Independent reflections	4512 [R_{int} = 0.0428, R_{sigma} = 0.0556]
Data/restraints/parameters	4512/0/271
Goodness-of-fit on F^2	1.017
Final R indexes [I>=2σ (I)]	R_1 = 0.0460, wR_2 = 0.0959
Final R indexes [all data]	R_1 = 0.0741, wR_2 = 0.1072
Largest diff. peak/hole / e $Å^{-3}$	0.22/-0.22

Compound	**4.25d**
Empirical formula	$C_{26}H_{41}ClNRh$
Formula weight	505.96
Temperature/K	100.0
Crystal system	orthorhombic
Space group	$P2_12_12_1$
a/Å	10.1783(2)
b/Å	13.4549(3)
c/Å	17.2397(4)
α/°	90.00
β/°	90.00
γ/°	90.00
Volume/$Å^3$	2360.94(9)
Z	4
$\rho_{calc}g/cm^3$	1.423
μ/mm^{-1}	0.849
F(000)	1064.0
Crystal size/mm^3	0.2 × 0.1 × 0.1
Radiation	MoKα (λ = 0.71073)
2Θ range for data collection/°	3.84 to 52.76
Index ranges	$-12 \leq h \leq 12$, $-16 \leq k \leq 16$, $-21 \leq l \leq 20$
Reflections collected	20983
Independent reflections	4822 [R_{int} = 0.0567, R_{sigma} = 0.0535]
Data/restraints/parameters	4822/0/265
Goodness-of-fit on F^2	1.064
Final R indexes [I>=2σ (I)]	R_1 = 0.0341, wR_2 = 0.0724
Final R indexes [all data]	R_1 = 0.0468, wR_2 = 0.0795
Largest diff. peak/hole / e $Å^{-3}$	1.41/-0.52
Flack parameter	-0.03(4)

Compound	(**4.27b**)$_2$
Empirical formula	$C_{28}H_{50}Cl_2N_2O_2Rh_2$
Formula weight	373.77
Temperature/K	100.0

Crystal system	orthorhombic
Space group	$P2_12_12_1$
a/Å	11.6653(3)
b/Å	14.6797(4)
c/Å	18.8289(5)
α/°	90.00
β/°	90.00
γ/°	90.00
Volume/Å^3	3224.32(15)
Z	8
ρ_{calc}g/cm^3	1.540
μ/mm^{-1}	1.218
F(000)	1536.0
Crystal size/mm^3	0.1 × 0.1 × 0.05
Radiation	MoKα (λ = 0.71073)
2Θ range for data collection/°	4.32 to 51.44
Index ranges	$-11 \leq h \leq 14$, $-16 \leq k \leq 17$, $-22 \leq l \leq 22$
Reflections collected	22878
Independent reflections	6145 [R_{int} = 0.0453, R_{sigma} = 0.0441]
Data/restraints/parameters	6145/0/413
Goodness-of-fit on F^2	1.029
Final R indexes [I>=2σ (I)]	R_1 = 0.0275, wR_2 = 0.0515
Final R indexes [all data]	R_1 = 0.0332, wR_2 = 0.0535
Largest diff. peak/hole / e Å^{-3}	0.96/-0.36
Flack parameter	-0.01(3)

Compound	**4.27e**
Empirical formula	$C_{23}H_{35}ClNORh$
Formula weight	479.88
Temperature/K	100
Crystal system	monoclinic
Space group	$P2_1/n$
a/Å	15.407(3)
b/Å	9.731(2)
c/Å	16.655(3)
α/°	90
β/°	115.927(2)
γ/°	90
Volume/Å^3	2245.7(8)
Z	4
ρ_{calc}g/cm^3	1.419
μ/mm^{-1}	0.892
F(000)	1000.0
Crystal size/mm^3	0.1 × 0.1 × 0.1

Radiation	MoKα (λ = 0.71073)
2Θ range for data collection/°	4.992 to 50.772
Index ranges	$-18 \leq h \leq 17$, $-11 \leq k \leq 11$, $-20 \leq l \leq 19$
Reflections collected	14630
Independent reflections	4113 [R_{int} = 0.0522, R_{sigma} = 0.0706]
Data/restraints/parameters	4113/0/258
Goodness-of-fit on F^2	0.903
Final R indexes [I>=2σ (I)]	R_1 = 0.0293, wR_2 = 0.0478
Final R indexes [all data]	R_1 = 0.0487, wR_2 = 0.0515
Largest diff. peak/hole / e Å^{-3}	0.72/-0.38

Compound	**4.28**
Empirical formula	$C_{31}H_{48}BCl_3F_4NRh$
Formula weight	730.77
Temperature/K	100.0
Crystal system	monoclinic
Space group	$P2_1/c$
a/Å	10.6887(6)
b/Å	18.2817(11)
c/Å	17.5489(10)
α/°	90.00
β/°	105.345(2)
γ/°	90.00
Volume/Å^3	3306.9(3)
Z	4
ρ_{calc}g/cm^3	1.468
μ/mm^{-1}	0.803
F(000)	1512.0
Crystal size/mm^3	0.2 × 0.1 × 0.1
Radiation	MoKα (λ = 0.71073)
2Θ range for data collection/°	3.28 to 52.82
Index ranges	$-13 \leq h \leq 12$, $-22 \leq k \leq 22$, $-21 \leq l \leq 19$
Reflections collected	37707
Independent reflections	6722 [R_{int} = 0.0460, R_{sigma} = 0.0384]
Data/restraints/parameters	6722/0/377
Goodness-of-fit on F^2	1.071
Final R indexes [I>=2σ (I)]	R_1 = 0.0481, wR_2 = 0.1122
Final R indexes [all data]	R_1 = 0.0598, wR_2 = 0.1201
Largest diff. peak/hole / e Å^{-3}	1.73/-1.40

Compound	**4.32b**
Empirical formula	$C_{14}H_{25}AuClN$
Formula weight	422.83
Temperature/K	100.0

Crystal system	monoclinic
Space group	$P2_1/m$
a/Å	9.166(3)
b/Å	8.861(3)
c/Å	9.589(3)
α/°	90.00
β/°	107.353(7)
γ/°	90.00
Volume/Å^3	743.3(4)
Z	2
ρ_{calc}g/cm^3	1.889
μ/mm^{-1}	10.053
F(000)	396.0
Crystal size/mm^3	0.1 × 0.05 × 0.05
Radiation	MoKα (λ = 0.71073)
2Θ range for data collection/°	4.46 to 52.78
Index ranges	$-9 \leq h \leq 11$, $-11 \leq k \leq 11$, $-11 \leq l \leq 11$
Reflections collected	12325
Independent reflections	1600 [R_{int} = 0.1256, R_{sigma} = 0.0910]
Data/restraints/parameters	1600/0/110
Goodness-of-fit on F^2	0.875
Final R indexes [I>=2σ (I)]	R_1 = 0.0510, wR_2 = 0.1201
Final R indexes [all data]	R_1 = 0.0978, wR_2 = 0.1481
Largest diff. peak/hole / e Å^{-3}	1.37/-1.18

Compound	**4.32c**
Empirical formula	$C_{12}H_{23}AuClN$
Formula weight	413.73
Temperature/K	100.0
Crystal system	orthorhombic
Space group	$Cmc2_1$
a/Å	13.0763(6)
b/Å	10.7287(6)
c/Å	9.7725(5)
α/°	90
β/°	90
γ/°	90
Volume/Å^3	1371.00(12)
Z	4
ρ_{calc}g/cm^3	2.004
μ/mm^{-1}	10.897
F(000)	792.0
Crystal size/mm^3	0.275 × 0.136 × 0.117
Radiation	MoKα (λ = 0.71073)

2Θ range for data collection/°	6.442 to 52.824
Index ranges	$-16 \leq h \leq 16$, $-13 \leq k \leq 13$, $-8 \leq l \leq 12$
Reflections collected	12019
Independent reflections	1372 [R_{int} = 0.0280, R_{sigma} = 0.0143]
Data/restraints/parameters	1372/103/140
Goodness-of-fit on F^2	1.152
Final R indexes [I>=2σ (I)]	R_1 = 0.0121, wR_2 = 0.0293
Final R indexes [all data]	R_1 = 0.0146, wR_2 = 0.0307
Largest diff. peak/hole / e Å^{-3}	0.55/-0.30
Flack parameter	0.50(3)

Compound	**4.32d**
Empirical formula	$C_{18}H_{29}AuClN$
Formula weight	491.84
Temperature/K	100.0
Crystal system	monoclinic
Space group	Pc
a/Å	7.7541(4)
b/Å	17.8052(10)
c/Å	12.6183(7)
α/°	90
β/°	96.493(2)
γ/°	90
Volume/Å^3	1730.95(16)
Z	4
ρ_{calc}g/cm^3	1.887
μ/mm^{-1}	8.648
F(000)	960.0
Crystal size/mm^3	0.1 × 0.1 × 0.05
Radiation	MoKα (λ = 0.71073)
2Θ range for data collection/°	2.288 to 51.368
Index ranges	$-9 \leq h \leq 9$, $-21 \leq k \leq 21$, $-14 \leq l \leq 15$
Reflections collected	19986
Independent reflections	5560 [R_{int} = 0.0295, R_{sigma} = 0.0290]
Data/restraints/parameters	5560/2/386
Goodness-of-fit on F^2	1.031
Final R indexes [I>=2σ (I)]	R_1 = 0.0290, wR_2 = 0.0675
Final R indexes [all data]	R_1 = 0.0486, wR_2 = 0.0781
Largest diff. peak/hole / e Å^{-3}	1.35/-0.49
Flack parameter	0.50(4)

Compound	**4.32e**
Empirical formula	$C_{22}H_{35}AuClN$
Formula weight	2183.80

Temperature/K	100.0
Crystal system	monoclinic
Space group	$P2_1/c$
a/Å	15.082(2)
b/Å	8.8104(13)
c/Å	16.471(3)
α/°	90
β/°	93.711(2)
γ/°	90
Volume/Å^3	2184.1(6)
Z	4
ρ_{calc}g/cm^3	1.6602
μ/mm^{-1}	6.863
F(000)	1073.9
Crystal size/mm^3	0.2 × 0.1 × 0.1
Radiation	Mo Kα (λ = 0.71073)
2Θ range for data collection/°	4.96 to 51.44
Index ranges	-18 ≤ h ≤ 18, -10 ≤ k ≤ 10, -20 ≤ l ≤ 20
Reflections collected	46205
Independent reflections	27748 [R_{int} = N/A, R_{sigma} = N/A]
Data/restraints/parameters	27748/6/233
Goodness-of-fit on F^2	1.042
Final R indexes [I>=2σ (I)]	R_1 = 0.0510, wR_2 = 0.1269
Final R indexes [all data]	R_1 = 0.0629, wR_2 = 0.1327
Largest diff. peak/hole / e Å^{-3}	3.94/-1.67

Compound	**4.37a**
Empirical formula	$C_{11}H_{21}NSe$
Formula weight	246.05
Temperature/K	100.15
Crystal system	orthorhombic
Space group	$P2_12_12_1$
a/Å	5.9043(7)
b/Å	13.8065(15)
c/Å	14.6027(17)
α/°	90.00
β/°	90.00
γ/°	90.00
Volume/Å^3	1190.4(2)
Z	4
ρ_{calc}g/cm^3	1.373
μ/mm^{-1}	3.107
F(000)	512.0
Crystal size/mm^3	0.4 × 0.1 × 0.1

Radiation	MoKα (λ = 0.71073)
2Θ range for data collection/°	5.58 to 51.4
Index ranges	$-7 \leq h \leq 7$, $-16 \leq k \leq 16$, $-17 \leq l \leq 17$
Reflections collected	8131
Independent reflections	2262 [R_{int} = 0.0508, R_{sigma} = 0.0576]
Data/restraints/parameters	2262/0/125
Goodness-of-fit on F^2	1.016
Final R indexes [I>=2σ (I)]	R_1 = 0.0320, wR_2 = 0.0567
Final R indexes [all data]	R_1 = 0.0409, wR_2 = 0.0596
Largest diff. peak/hole / e Å^{-3}	0.39/-0.28
Flack parameter	0.00(2)

Compound	**4.37b**
Empirical formula	$C_{28}H_{50}N_2Se_2$
Formula weight	572.62
Temperature/K	100.0
Crystal system	orthorhombic
Space group	$P2_12_12_1$
a/Å	5.8542(6)
b/Å	12.9039(14)
c/Å	18.9035(18)
α/°	90.00
β/°	90.00
γ/°	90.00
Volume/Å^3	1428.0(3)
Z	2
ρ_{calc}g/cm^3	1.332
μ/mm^{-1}	2.607
F(000)	600.0
Crystal size/mm^3	0.3 × 0.1 × 0.1
Radiation	MoKα (λ = 0.71073)
2Θ range for data collection/°	3.82 to 50.84
Index ranges	$-7 \leq h \leq 7$, $-15 \leq k \leq 15$, $-22 \leq l \leq 16$
Reflections collected	8453
Independent reflections	2613 [R_{int} = 0.0556, R_{sigma} = 0.0685]
Data/restraints/parameters	2613/0/149
Goodness-of-fit on F^2	1.012
Final R indexes [I>=2σ (I)]	R_1 = 0.0403, wR_2 = 0.0718
Final R indexes [all data]	R_1 = 0.0567, wR_2 = 0.0764
Largest diff. peak/hole / e Å^{-3}	0.44/-0.42
Flack parameter	0.00(9)

Compound	**4.37c**
Empirical formula	$C_{12}H_{23}NSe$

Formula weight	260.27
Temperature/K	100.0
Crystal system	monoclinic
Space group	$P2_1/n$
a/Å	5.9560(6)
b/Å	15.3956(17)
c/Å	14.0328(14)
α/°	90.00
β/°	101.375(5)
γ/°	90.00
Volume/Å^3	1261.5(2)
Z	4
ρ_{calc}g/cm^3	1.370
μ/mm^{-1}	2.943
F(000)	544.0
Crystal size/mm^3	0.3 × 0.2 × 0.1
Radiation	MoKα (λ = 0.71073)
2Θ range for data collection/°	3.98 to 50.66
Index ranges	$-7 \leq h \leq 7$, $-12 \leq k \leq 18$, $-16 \leq l \leq 16$
Reflections collected	8197
Independent reflections	2296 [R_{int} = 0.0353, R_{sigma} = 0.0386]
Data/restraints/parameters	2296/0/133
Goodness-of-fit on F^2	1.021
Final R indexes [I>=2σ (I)]	R_1 = 0.0319, wR_2 = 0.0658
Final R indexes [all data]	R_1 = 0.0450, wR_2 = 0.0697
Largest diff. peak/hole / e Å^{-3}	0.51/-0.33

Compound	**4.37d**
Empirical formula	$C_{18}H_{29}NSe$
Formula weight	338.38
Temperature/K	100.0
Crystal system	orthorhombic
Space group	Pbca
a/Å	14.9264(9)
b/Å	10.9686(7)
c/Å	19.7127(13)
α/°	90
β/°	90
γ/°	90
Volume/Å^3	3227.4(4)
Z	8
ρ_{calc}g/cm^3	1.393
μ/mm^{-1}	2.319
F(000)	1424.0

Crystal size/mm^3	0.2 × 0.15 × 0.1
Radiation	MoKα (λ = 0.71073)
2Θ range for data collection/°	4.132 to 52.812
Index ranges	-16 ≤ h ≤ 18, -13 ≤ k ≤ 13, -21 ≤ l ≤ 24
Reflections collected	22527
Independent reflections	3307 [R_{int} = 0.0441, R_{sigma} = 0.0303]
Data/restraints/parameters	3307/0/184
Goodness-of-fit on F^2	1.022
Final R indexes [I>=2σ (I)]	R_1 = 0.0342, wR_2 = 0.0846
Final R indexes [all data]	R_1 = 0.0494, wR_2 = 0.0928
Largest diff. peak/hole / e Å^{-3}	1.06/-0.41

Compound	**4.37e**
Empirical formula	$C_{22}H_{35}NSe$
Formula weight	392.47
Temperature/K	100.0
Crystal system	monoclinic
Space group	$P2_1/n$
a/Å	10.9113(16)
b/Å	14.1348(19)
c/Å	13.955(2)
α/°	90.00
β/°	99.086(5)
γ/°	90.00
Volume/Å^3	2125.3(5)
Z	4
ρ_{calc}g/cm^3	1.227
μ/mm^{-1}	1.770
F(000)	832.0
Crystal size/mm^3	0.3 × 0.3 × 0.05
Radiation	MoKα (λ = 0.71073)
2Θ range for data collection/°	4.76 to 48.24
Index ranges	-12 ≤ h ≤ 10, -15 ≤ k ≤ 15, -15 ≤ l ≤ 12
Reflections collected	10295
Independent reflections	3220 [R_{int} = 0.0446, R_{sigma} = 0.0606]
Data/restraints/parameters	3220/0/224
Goodness-of-fit on F^2	1.042
Final R indexes [I>=2σ (I)]	R_1 = 0.0678, wR_2 = 0.1315
Final R indexes [all data]	R_1 = 0.1009, wR_2 = 0.1464
Largest diff. peak/hole / e Å^{-3}	1.12/-1.09

4.5.4 Computational Details

All calculations were performed with the Gaussian09 program package.[105] The theoretical approach is based on the framework of density functional theory (DFT).[106-107] All calculations were performed with the B3LYP functional and employing Weigend's def2-TZVPP basis set.[108-109] Ground states were fully optimized without constraints at the corresponding level of theory and uniquely characterized by occurrence of no imaginary frequencies and verified by the corresponding frequency calculation. Gibbs free reaction energies and enthalpies were calculated for standard conditions (p = 1 atm, T = 298 K) and are unscaled. For the visualization of frontier molecular orbitals and optimized structures, GaussView was used.

NHC-5 singlet

N	1.07256800	0.20730300	-0.03549100
C	0.00000200	1.01233500	-0.00006100
C	-0.76599300	-1.23284700	-0.03345500
H	-1.22900800	-1.77362700	0.79482300
H	-1.14600100	-1.66294600	-0.96530600
N	-1.07256800	0.20730100	0.03538300
C	-2.43855100	0.66335500	0.00281700
H	-2.43758100	1.74874000	0.04768500
H	-2.94430600	0.34594200	-0.91594400
H	-3.00681000	0.27077800	0.85199100
C	2.43855500	0.66335800	-0.00272800
H	2.43756400	1.74873600	-0.04775500
H	2.94412200	0.34609300	0.91618400
H	3.00696900	0.27066300	-0.85173700
C	0.76599400	-1.23287400	0.03346700
H	1.14600600	-1.66286100	0.96536100
H	1.22900100	-1.77370800	-0.79477400

NHC-5 triplet

N	1.08692900	-0.29445100	0.44910700
C	0.00000800	-1.02998100	-0.00009700
C	2.36850600	-0.48271000	-0.23090300
H	2.61278100	-1.54269800	-0.23199000
H	2.35231100	-0.13353000	-1.27329700
H	3.15194400	0.04668500	0.31206300
C	0.57604800	1.09462100	0.51711500
H	1.36988800	1.80402400	0.28830500
H	0.20175300	1.30510800	1.52114700
C	-0.57607600	1.09464900	-0.51708200

H	-1.36991900	1.80403700	-0.28823500
H	-0.20178000	1.30518300	-1.52110200
N	-1.08695200	-0.29443000	-0.44914900
C	-2.36847300	-0.48274100	0.23095800
H	-3.15195200	0.04671900	-0.31188600
H	-2.61276100	-1.54272600	0.23196000
H	-2.35218100	-0.13366600	1.27338500

NHC-6 singlet

N	1.14019700	-0.39113400	0.00089600
C	0.00001600	-1.09479400	-0.09208500
C	-1.24324200	1.05701800	0.20521700
H	-1.38168600	1.27783800	1.27073000
H	-2.13383400	1.41996800	-0.31262100
C	-2.40290000	-1.10626200	-0.02034900
H	-3.04157000	-0.75272200	-0.83620800
H	-2.19136400	-2.16202300	-0.15820900
H	-2.94899100	-0.96854400	0.91922400
C	0.00003200	1.75024900	-0.32976400
H	0.00000200	2.80324400	-0.04685900
H	0.00017900	1.70157600	-1.42071600
C	1.24315000	1.05699500	0.20553200
H	2.13391400	1.42006900	-0.31191000
H	1.38118200	1.27761400	1.27114100
N	-1.14017900	-0.39114000	0.00087400
C	2.40294200	-1.10620700	-0.02044600
H	3.04146600	-0.75275300	-0.83645800
H	2.94917800	-0.96835400	0.91901900
H	2.19141500	-2.16198800	-0.15816300

NHC-6 triplet

N	-1.15833800	-0.58323100	-0.46634200
C	0.15731200	-0.90075500	-0.61393900
C	1.02591400	1.15614400	0.17969800
H	1.39983500	1.54995900	-0.77858700
H	1.66323500	1.55202800	0.97336700
C	2.49546800	-0.79300700	-0.00603800
H	3.14328000	-0.37852800	0.76726100
H	2.51229300	-1.87883100	0.07031000
H	2.89847700	-0.50902200	-0.98867500
C	-0.42342000	1.59987800	0.38784500
H	-0.49505100	2.67992000	0.24126300
H	-0.72196900	1.39345600	1.41810800
C	-1.37033800	0.87029200	-0.57930900
H	-2.41469300	1.10310600	-0.36648400
H	-1.16033400	1.16605900	-1.60881500
C	-1.93222100	-1.26774900	0.57438900
H	-2.99605700	-1.07354400	0.43101100
H	-1.76169200	-2.33825100	0.48699000

H	-1.64747700	-0.95534800	1.58680000
N	1.13889000	-0.31674400	0.19656800

CAAC-5 singlet

N	-0.64861500	0.90511900	0.04811300
C	0.59902800	1.28088100	0.08315400
C	0.44778200	-1.12521400	-0.38583200
H	0.52303200	-1.37880400	-1.44420100
H	0.64752200	-2.03763100	0.17653000
C	1.44244900	0.02170800	-0.04238700
C	-1.74666000	1.85888100	0.17533200
H	-2.36422600	1.86487300	-0.72347900
H	-2.38031800	1.61239400	1.02837100
H	-1.31006400	2.84104700	0.32062700
C	2.49819700	0.21124100	-1.13935900
H	3.15843500	1.04291300	-0.89416800
H	3.10338000	-0.69203900	-1.25098100
H	2.03329700	0.42810100	-2.10267600
C	2.15189300	-0.20344100	1.30589300
H	2.78942900	-1.08908700	1.25344400
H	2.77337600	0.65594800	1.55666500
H	1.44144800	-0.34703100	2.12126200
C	-0.95787200	-0.57256700	-0.08449700
C	-1.94155200	-0.82732400	-1.22953300
H	-2.04243700	-1.90117200	-1.39359700
H	-2.93630400	-0.43624200	-1.01192500
H	-1.58711000	-0.37676000	-2.15736500
C	-1.53590500	-1.10599700	1.23294100
H	-2.48799900	-0.63310800	1.47683900
H	-1.71567500	-2.17887700	1.15110400
H	-0.84964200	-0.93936000	2.06248800

CAAC-5 triplet

N	-1.38847600	-0.17891100	-0.34478600
C	-0.23653300	-0.92432600	-0.15621400
C	0.45191800	1.28453100	-0.27955700
H	0.96336900	2.05130800	0.30210400
H	0.57157100	1.52002400	-1.33736700
C	1.03360900	-0.14433800	-0.00130700
C	-2.66785700	-0.70180600	0.08511500
H	-2.74821900	-0.76236600	1.18120900
H	-3.46844500	-0.06310600	-0.28918100
H	-2.80766300	-1.70147700	-0.32383500
C	1.61083300	-0.23964700	1.42611500
H	1.88120100	-1.26981600	1.66076500
H	2.50850600	0.37758200	1.52229600
H	0.88576700	0.09029100	2.17067500
C	2.11893800	-0.52609300	-1.01761300
H	2.98034500	0.14172900	-0.93668400

H	2.46926600	-1.54434900	-0.84170300
H	1.73468500	-0.47381300	-2.03617700
C	-1.04187600	1.19126000	0.05812900
H	-1.21423000	1.33130200	1.13544900
H	-1.65101600	1.91759100	-0.48206000

BICAAC singlet

C	-1.13001600	-0.67070900	1.25950500
C	0.35634000	-1.07595700	1.25019200
C	1.04517800	-0.49300300	0.00001500
C	-0.52925600	1.37164100	-0.00016100
C	-1.45775200	0.17302100	0.00000700
H	0.86925300	-0.71364100	2.14271500
H	0.47544800	-2.16114800	1.23428400
H	-1.36446900	-0.08215400	2.14756700
H	-1.78097900	-1.54769200	1.28314400
C	-2.92073100	0.60781200	-0.00001500
H	-3.14004200	1.21520800	-0.87892200
H	-3.59274100	-0.25452100	0.00008500
H	-3.14001400	1.21538900	0.87877400
C	-1.13007100	-0.67102000	-1.25930400
H	-1.78102500	-1.54801700	-1.28264700
H	-1.36459800	-0.08271900	-2.14751400
C	0.35628500	-1.07628000	-1.24997900
H	0.47539400	-2.16146500	-1.23381600
H	0.86915100	-0.71417800	-2.14261800
N	0.71956300	0.97559900	-0.00016700
C	1.79404000	1.96893500	-0.00020200
H	2.42329400	1.87092700	-0.88581800
H	1.31526300	2.94255300	-0.00031300
H	2.42318900	1.87106900	0.88551500
C	2.53683100	-0.79851700	0.00003500
H	3.03860600	-0.40709800	-0.88496800
H	3.03872500	-0.40620000	0.88458400
H	2.67352200	-1.88104300	0.00055500

BICAAC triplet

C	1.24827000	-1.26861700	-0.66764000
C	-0.27330200	-1.52728800	-0.77566400
C	-1.07685700	-0.47580200	0.01816400
C	0.53090100	1.03216200	-0.78899200
C	1.47626200	0.13939800	-0.05186600
H	-0.59760300	-1.48879600	-1.81597100
H	-0.52731700	-2.51733200	-0.39362300
H	1.71636500	-1.31668100	-1.65042300
H	1.73562000	-2.01991200	-0.03784000
C	2.93226100	0.57676500	-0.13977300
H	3.07869600	1.54862000	0.33384200
H	3.58254200	-0.14562100	0.35817500

H	3.24885100	0.65907100	-1.18033800
C	0.97435600	0.07191500	1.41787300
H	1.61933900	-0.60105100	1.98959700
H	1.06668300	1.06176800	1.86686400
C	-0.49670500	-0.41206300	1.45317400
H	-0.57232200	-1.40569400	1.90030600
H	-1.10815800	0.24783300	2.07059600
N	-0.82591500	0.84371600	-0.65120800
C	-1.61849300	1.99891300	-0.23182900
H	-1.49588500	2.24615100	0.83186300
H	-1.29365100	2.85844900	-0.81440300
H	-2.67496500	1.83339800	-0.43571800
C	-2.56094800	-0.82020700	0.01468900
H	-2.95722200	-0.81311100	-1.00161000
H	-2.70810300	-1.81793500	0.43027800
H	-3.14593500	-0.12622900	0.61803800

CAAC-6 singlet

N	-0.62495300	0.92458300	0.00862100
C	0.65297500	1.19903600	0.02707800
C	1.05203600	-1.34167100	0.27141900
H	0.92264500	-1.48636800	1.34694800
H	1.74425200	-2.12153100	-0.05758900
C	1.64708200	0.05369400	0.00978100
C	2.71522600	0.36839000	1.07177700
H	3.49062500	-0.40238500	1.06998100
C	2.31917400	0.10787300	-1.37998100
H	3.15465800	-0.59509000	-1.41573900
H	1.62514400	-0.14930600	-2.18141900
H	3.17724300	1.33520700	0.87618500
H	2.27777500	0.40414200	2.07130300
H	2.69720800	1.10987200	-1.57935400
C	-0.28518900	-1.49568200	-0.43492600
H	-0.71688600	-2.48196800	-0.25056500
H	-0.14109900	-1.41943700	-1.51549600
C	-1.54554900	2.07543300	0.02611200
H	-2.29431300	1.96809700	0.81138400
H	-0.94318400	2.95686900	0.21124300
H	-2.05802300	2.18112700	-0.92991400
C	-1.30646000	-0.43699200	-0.00054700
C	-2.46687400	-0.44561600	-1.00422500
H	-2.84921900	-1.46373200	-1.09511300
H	-3.29693300	0.18780700	-0.69497700
H	-2.13490900	-0.12513900	-1.99246900
C	-1.83922600	-0.73638100	1.40894700
H	-2.57196100	0.00383000	1.72886600
H	-2.33120200	-1.71065400	1.41960400
H	-1.03631200	-0.75192300	2.14415900

CAAC-6 triplet

N	-0.67092200	0.91508100	-0.02912300
C	0.58205700	0.92519400	0.52816900
C	1.08064200	-1.36579800	-0.00786000
H	1.04294900	-1.74291600	1.01594800
H	1.74813800	-2.03095600	-0.56462600
C	1.69520200	0.06862300	0.02704700
C	2.88783700	0.09417700	0.98942800
H	3.66370300	-0.59965600	0.65822900
C	2.16457200	0.49877400	-1.38081300
H	2.92867500	-0.18417500	-1.76162700
H	1.33659200	0.51705300	-2.08879000
H	3.32573300	1.09224400	1.03664900
H	2.58138700	-0.18608900	1.99753600
H	2.59416600	1.50061100	-1.34616400
C	-0.31854600	-1.41142900	-0.62917300
H	-0.72066700	-2.42401600	-0.54604100
H	-0.24940300	-1.19155800	-1.69713800
C	-1.47464300	2.11469600	0.15147700
H	-2.26047200	2.16987600	-0.59935400
H	-1.93552500	2.17365100	1.14561600
H	-0.82547600	2.98045200	0.03415400
C	-1.34205100	-0.42657500	-0.01373200
C	-2.58430300	-0.40043600	-0.90882200
H	-2.96270800	-1.41597100	-1.03251500
H	-3.38888900	0.19689000	-0.48016200
H	-2.34568500	-0.00554600	-1.89717500
C	-1.74029700	-0.83684200	1.41293600
H	-2.46602600	-0.13691300	1.83015600
H	-2.19814900	-1.82755700	1.41388200
H	-0.87470900	-0.85329800	2.07334000

Optimized structure of singlet **4.11c**

N	0.73111400	-0.04552400	0.60780800
C	2.54196600	1.28662000	-0.45180500
C	1.99261900	0.02925700	-0.13478200
C	2.60948900	-1.15981100	-0.57099200
C	-1.71454500	-0.22612300	0.50854400
C	3.77942100	1.32251200	-1.09461800
H	4.22072400	2.27878300	-1.34095600
C	1.92674500	-2.52116200	-0.51430600
H	1.08673200	-2.45333300	0.16987100
C	-0.34498100	-0.07296100	-0.13601000
C	3.84782500	-1.06452000	-1.20734000
H	4.34066400	-1.96670100	-1.54251200
C	0.84508600	-0.11137200	2.14796100
C	1.79303900	2.59773700	-0.24812100
H	0.93201100	2.40352400	0.38731700
C	-2.51342600	-1.29330700	-0.32242400
H	-1.99296500	-2.25213200	-0.23665700
C	-2.50567100	1.12509700	0.32685900

H	-1.98795500	1.91907600	0.87186300
C	-2.59957800	1.51846100	-1.16192400
H	-3.12737300	2.47417900	-1.24175400
H	-1.60556900	1.65357500	-1.58212500
C	4.44640100	0.16076400	-1.44469100
H	5.41079900	0.21143600	-1.93319800
C	1.80169700	0.95655600	2.68452400
H	2.82015800	0.81664400	2.32726100
H	1.81828500	0.88502500	3.77361300
H	1.47437600	1.96097400	2.42796100
C	-3.94338700	0.99419100	0.86798500
H	-3.95640500	0.78994100	1.93938600
H	-4.45327600	1.95314400	0.73582600
C	-4.77920200	0.28761400	-1.38449800
H	-5.32983500	-0.47363800	-1.94523600
H	-5.33068500	1.22632600	-1.49477100
C	2.63463900	3.69244400	0.42210300
H	3.05851800	3.35899800	1.36919100
H	2.01763900	4.57145400	0.61781100
H	3.46006200	4.01457000	-0.21427100
C	-3.35709400	0.43490000	-1.94717400
H	-3.40593000	0.71878600	-3.00188000
C	-4.69835900	-0.10417600	0.09977900
H	-5.70641800	-0.21026100	0.50998700
C	-2.60994800	-0.90077000	-1.80774500
H	-3.14617600	-1.68589100	-2.34988700
H	-1.61365200	-0.81791700	-2.23594300
C	-1.62635700	-0.65249800	1.98678400
H	-2.57285300	-0.53740000	2.51027700
H	-1.39409000	-1.72046100	2.03193600
C	-3.94360800	-1.43927600	0.23385700
H	-4.46667900	-2.21622200	-0.33121400
H	-3.93534900	-1.77042100	1.27401400
C	-0.55252400	0.13978400	2.71462800
H	-0.53837000	-0.10792400	3.77835900
H	-0.77795400	1.20725300	2.65053100
C	2.83779000	-3.65321100	-0.02048500
H	3.65068300	-3.85466800	-0.71921900
H	2.26399800	-4.57630400	0.07976100
H	3.28250500	-3.42731800	0.94916500
C	1.37185100	-1.48113700	2.59403200
H	0.71108100	-2.29693100	2.30792400
H	1.45897500	-1.48764100	3.68197900
H	2.36002900	-1.67770400	2.18385900
C	1.34239700	-2.86117900	-1.89745400
H	0.65476600	-2.08259000	-2.22515200
H	0.80019100	-3.80851700	-1.86005200
H	2.13344500	-2.95553500	-2.64381000
C	1.24292500	3.09396700	-1.59732300
H	2.05547600	3.33889300	-2.28396000
H	0.63954700	3.99309800	-1.45620300

H	0.62181600	2.33208000	-2.06594600

Optimized structure of triplet **4.11c**

N	0.78298400	-0.09390200	0.69238600
C	2.31985600	1.38161400	-0.55599700
C	1.91863000	0.07709100	-0.18520500
C	2.59921400	-1.04724400	-0.70549400
C	-1.75543200	-0.28408600	0.59366500
C	3.43053000	1.53170900	-1.38577500
H	3.74818500	2.52584500	-1.67076400
C	2.17226500	-2.48485400	-0.44159600
H	1.33898300	-2.46491600	0.25356800
C	-0.36204600	-0.66382800	0.19613900
C	3.69984300	-0.83727600	-1.53757800
H	4.22872900	-1.69170600	-1.93857700
C	0.89235600	-0.13060600	2.19908500
C	1.56054000	2.63759600	-0.14757900
H	0.80105100	2.34202900	0.57330200
C	-2.76252900	-1.38985500	0.15966200
H	-2.45687700	-2.32908100	0.62774500
C	-2.23901400	1.04921600	-0.08048400
H	-1.56594900	1.85847500	0.21005300
C	-2.21073700	0.88361900	-1.61140400
H	-2.49835700	1.82540700	-2.08805400
H	-1.19756300	0.64895200	-1.94368000
C	4.12603600	0.43655900	-1.86822600
H	4.98593000	0.57544100	-2.51079500
C	2.07085400	0.70179900	2.69931200
H	3.01780500	0.34029200	2.29951900
H	2.11767800	0.62636800	3.78650400
H	1.96641500	1.75276800	2.44479700
C	-3.67948700	1.40559500	0.33742000
H	-3.74872500	1.59049800	1.41104200
H	-3.97129200	2.33965300	-0.15267700
C	-4.60126900	0.11169500	-1.60113100
H	-5.29404500	-0.67595300	-1.91200300
H	-4.92968300	1.03515500	-2.08745500
C	2.45657100	3.69794200	0.51149800
H	3.02429900	3.29318900	1.34884500
H	1.84905200	4.52564100	0.88259700
H	3.17246500	4.11506600	-0.19859500
C	-3.17020200	-0.23854000	-2.03976800
H	-3.13576600	-0.35212500	-3.12663800
C	-4.64018100	0.27809100	-0.07328400
H	-5.65617000	0.52710900	0.24482400
C	-2.73693400	-1.55215900	-1.36926900
H	-3.40944300	-2.36327000	-1.66419500
H	-1.73256200	-1.83119800	-1.69467800
C	-1.69207500	-0.18942000	2.15324200
H	-2.56325300	0.33906900	2.53984000

H	-1.75412200	-1.20581800	2.54777100
C	-4.19599500	-1.03452500	0.59445400
H	-4.86960600	-1.84601500	0.30411000
H	-4.26637100	-0.94952600	1.68107400
C	-0.43165900	0.48959000	2.69718200
H	-0.44826600	0.45024900	3.78946000
H	-0.43411500	1.54797400	2.42492000
C	3.29582600	-3.32474000	0.18486700
H	4.13076200	-3.46270400	-0.50431100
H	2.92312200	-4.31616500	0.44936100
H	3.69057800	-2.86081200	1.08962200
C	1.05598000	-1.56484000	2.73307200
H	0.30081700	-2.23596400	2.32819200
H	0.96596300	-1.56645400	3.82094100
H	2.03806300	-1.96284000	2.48323800
C	1.65357600	-3.15012000	-1.72709700
H	0.82097600	-2.58696900	-2.14820800
H	1.30497700	-4.16303000	-1.51590000
H	2.43425400	-3.21717100	-2.48720300
C	0.83245000	3.25083100	-1.35617100
H	1.54503800	3.59184100	-2.10943900
H	0.23690700	4.11232900	-1.04683600
H	0.16743600	2.53056200	-1.82924900

To choose the appropriate functional and computation method (Tamm-Dancoff approximation or formal TD-DFT), we simulated the UV-Vis spectrum of **4.11c** with a model compound **M**. **M** was created from the optimized structure of singlet **4.11c** (B3LYP/def2-TZVPP) followed by deletion of the unnecessary atoms (Figure 4.43). The structure was not re-optimized, in order to better mimic the geometry and molecular orbital structure of **4.11c**

Model **M**

N	0.73111400	-0.04552400	0.60780800
C	1.99261900	0.02925700	-0.13478200
C	-1.71454500	-0.22612300	0.50854400
C	3.77942100	1.32251200	-1.09461800
H	4.22072400	2.27878300	-1.34095600
C	-0.34498100	-0.07296100	-0.13601000
C	3.84782500	-1.06452000	-1.20734000
H	4.34066400	-1.96670100	-1.54251200
C	0.84508600	-0.11137200	2.14796100
C	4.44640100	0.16076400	-1.44469100
H	5.41079900	0.21143600	-1.93319800
C	1.80169700	0.95655600	2.68452400
H	2.82015800	0.81664400	2.32726100
H	1.81828500	0.88502500	3.77361300
H	1.47437600	1.96097400	2.42796100

C	-1.62635700	-0.65249800	1.98678400
H	-2.57285300	-0.53740000	2.51027700
H	-1.39409000	-1.72046100	2.03193600
C	-0.55252400	0.13978400	2.71462800
H	-0.53837000	-0.10792400	3.77835900
H	-0.77795400	1.20725300	2.65053100
C	1.37185100	-1.48113700	2.59403200
H	0.71108100	-2.29693100	2.30792400
H	1.45897500	-1.48764100	3.68197900
H	2.36002900	-1.67770400	2.18385900
C	2.60948900	-1.15981100	-0.57099200
H	2.14795593	-2.11364300	-0.42235908
C	2.54196600	1.28662000	-0.45180500
H	2.03041963	2.19467376	-0.20960946
C	-2.49773188	-1.27234203	-0.30609952
H	-2.48451518	-1.00131288	-1.34112055
H	-2.04330783	-2.23322299	-0.18319077
H	-3.50953474	-1.30940831	0.03999446
C	-2.48745813	1.09398995	0.33104165
H	-2.56538032	1.32433478	-0.71096094
H	-3.46756842	0.99229864	0.74810604
H	-1.96644946	1.88255742	0.83265038

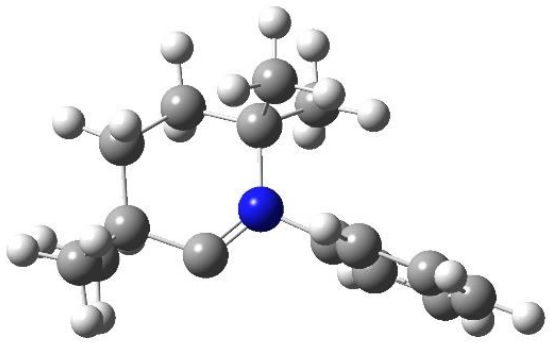

Figure 4.43: Structure of model **M**.

Despite the obvious differences in simulated UV-Vis spectra, the frontier orbitals involved in the transitions are essentially identical throughout all methods (Figure 4.44). As a result, the functional of choice becomes the one that best simulated experimental data. Since M062X functional with Tamm-Dancoff approximation most accurately predicted peak shape, position, and relative intensity of the experimental spectrum, we proceed to use the calculation on the full molecule **4.11c**.

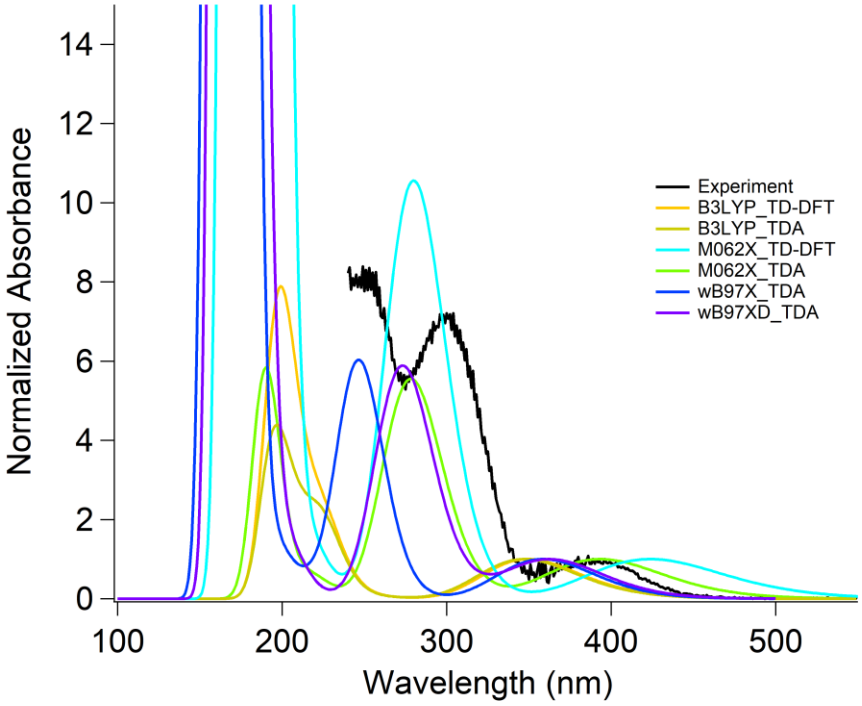

Figure 4.44: Comparison of computational methods on model compound **M** (geometry specified above).

Both DFT calculations, for optimization, frequencies, and population analysis, and TD-DFT, to simulate UV-Vis spectra, utilized the M062X functional and def2-TZVPP basis set. Pentane was used as solvent, and we used the Tamm-Dancoff approximation.

Optimized structure of singlet **4.11c** by the M062X functional with pentane

N	0.70873900	-0.15474900	0.54472800
C	2.39113700	1.42972200	-0.30515400
C	1.97869600	0.10562400	-0.11583900
C	2.73322900	-0.97059200	-0.59943900
C	-1.67945100	-0.49666100	0.36598700
C	3.64593000	1.65266800	-0.86528700
H	3.98678000	2.66911700	-1.01526600
C	2.17657800	-2.37973500	-0.67313300
H	1.30170800	-2.43852900	-0.03043500
C	-0.32235400	-0.22586800	-0.25473000
C	3.97984800	-0.69909800	-1.15691900
H	4.58209100	-1.51550400	-1.53400800
C	0.79633200	-0.32269900	2.05810900
C	1.47099700	2.61282800	-0.07083600
H	0.58511800	2.26575100	0.45866400
C	-2.52873000	-1.34261000	-0.62628800

H	-2.02784100	-2.30614700	-0.76594600
C	-2.40932500	0.87668800	0.51177100
H	-1.83166100	1.52543200	1.17526300
C	-2.54967700	1.57722700	-0.84997200
H	-3.05200200	2.53778300	-0.69955800
H	-1.56809200	1.77790400	-1.27817000
C	4.45080600	0.59856700	-1.26160600
H	5.42650100	0.78926400	-1.68886500
C	1.47662700	0.88501600	2.69778100
H	2.50728500	1.00130800	2.36392400
H	1.48426400	0.73494800	3.77851800
H	0.93046500	1.80447300	2.49459700
C	-3.81572100	0.66768600	1.08866100
H	-3.77647300	0.23119200	2.08857000
H	-4.30234800	1.64181600	1.19276800
C	-4.76765300	0.48385700	-1.21374600
H	-5.37030300	-0.12636000	-1.89233300
H	-5.28001200	1.44269900	-1.09194400
C	2.11665300	3.73340800	0.74259100
H	2.49640400	3.37304200	1.69848900
H	1.38715800	4.52102700	0.93671100
H	2.94830100	4.18619300	0.20108900
C	-3.37159700	0.70574600	-1.80500500
H	-3.45745300	1.20594700	-2.77231100
C	-4.63956100	-0.21762300	0.14291900
H	-5.63218200	-0.37963800	0.56930300
C	-2.66661200	-0.64256200	-1.98437500
H	-3.25159300	-1.27882500	-2.65514400
H	-1.68266200	-0.49449600	-2.42675500
C	-1.53028700	-1.23425300	1.70189200
H	-2.48441900	-1.40452500	2.19519100
H	-1.11149300	-2.22619400	1.49742400
C	-3.93917600	-1.56848700	-0.05816700
H	-4.51475000	-2.17305600	-0.76466100
H	-3.90940200	-2.12868400	0.87727600
C	-0.61325600	-0.46159700	2.62829900
H	-0.53237700	-0.95046200	3.60106900
H	-1.03468500	0.52786900	2.81572600
C	3.16821700	-3.45323800	-0.22960600
H	4.01307000	-3.52377100	-0.91589700
H	2.67891700	-4.42800100	-0.21745400
H	3.56152800	-3.25704300	0.76824900
C	1.61492100	-1.56963200	2.39903700
H	1.11593500	-2.48508500	2.08354100
H	1.74266400	-1.61105000	3.48115400
H	2.60440100	-1.53358200	1.94599500
C	1.69289600	-2.64402900	-2.10324400
H	0.94601900	-1.90395500	-2.39204200
H	1.25049300	-3.63895700	-2.17791500
H	2.52731100	-2.58795700	-2.80503300
C	0.99692900	3.13820100	-1.43078400

H	1.83677000	3.54561000	-1.99703400
H	0.25694100	3.92941400	-1.29894600
H	0.55007800	2.33296400	-2.01439500

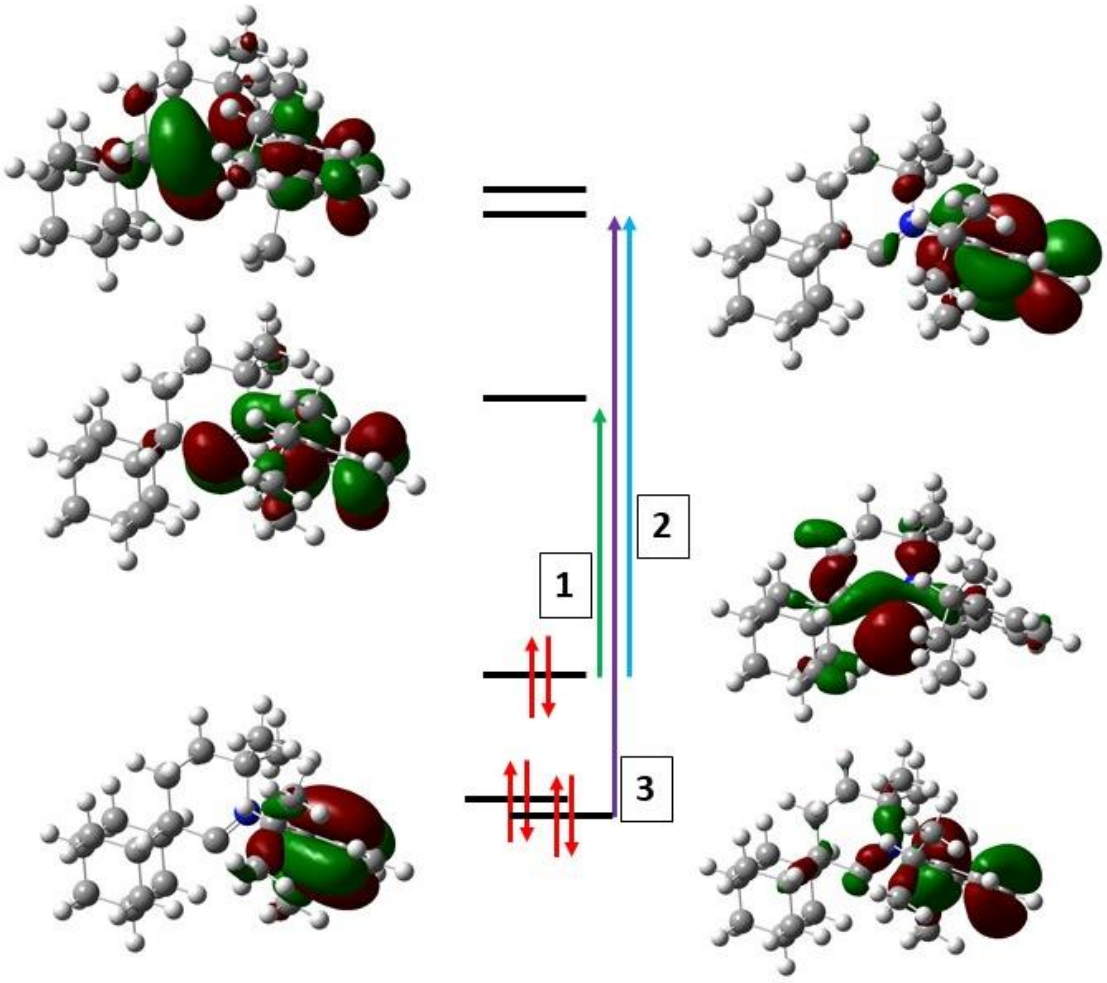

Figure 4.45: Calculated MOs and corresponding electronic transitions for **4.11c**.

Table 4.1: Calculated transitions involved in simulated spectrum with respective energies and oscillator strengths. Major Kohn-Sham orbitals involved in the transitions are noted.

	Energy (eV)	Oscillator Strength	Kohn-Sham orbitals involved
1	3.0854	0.0070	HOMO → LUMO
2	4.6662	0.0452	HOMO → LUMO+1
3	4.8003	0.0058	HOMO-1 → LUMO+1
4	5.5046	0.0069	HOMO-2 → LUMO
5	5.5450	0.0035	HOMO-1 → LUMO+1
6	5.9097	0.0021	HOMO → LUMO+2
7	6.2322	0.0221	HOMO-2 → LUMO+1
8	6.2942	0.0484	HOMO-2 → LUMO+1

4.6 Acknowledgements

Chapter 4 is adapted, in part, from Eder Tomás-Mendivil, Max M. Hansmann, Cory M. Weinstein, Rodolphe Jazzar, Mohand Melaimi and Guy Bertrand "Bicyclic (Alkyl)(amino)carbenes (BICAACs): Stable Carbenes More Ambiphilic than CAACs," *Journal of the American Chemical Society*, 2017, **139**, 7753-7756. Copyright 2017 the American Chemical Society. The dissertation author was the third author of the manuscripts.

Chapter 4 is also adapted, in part, from Cory M. Weinstein, Glen P. Junor, Daniel R. Tolentino, Rodolphe Jazzar, Mohand Melaimi and Guy Bertrand "Highly Ambilphilic Room Temperature Stable Six-Membered Cyclic (Alkyl)(amino)carbenes," which is being prepared for submission. The dissertation author will be the first author of the manuscripts.

Chapter 4 is also adapted, in part, from Cory M. Weinstein, Glen P. Junor, Rodolphe Jazzar, Mohand Melaimi and Guy Bertrand "All-alkyl Six-Membered Cyclic (Alkyl)(amino)carbenes Reveal a

New Form of Non Classical Hydrogen Bonding," which is being prepared for submission. The dissertation author will be the first author of the manuscripts.

Permission to use copyrighted images, data, and unpublished material was obtained from Eder Tomás-Mendivil, Max M. Hansmann, Rodolphe Jazzar, Mohand Melaimi, Glen P. Junor, Daniel R. Tolentino, Guy Bertrand and the American Chemical Society.

4.7 References

[1] V. Lavallo, Y. Canac, C. Präsang, B. Donnadieu and G. Bertrand, *Angew. Chem. Int. Ed.*, 2005, **44**, 5705-5709.

[2] M. Melaimi, R. Jazzar, M. Soleilhavoup and G. Bertrand, *Angew. Chem. Int. Ed.*, 2017, **56**, 10046-10068.

[3] S. Roy, K. C. Mondal and H. W. Roesky, *Acc. Chem. Res.*, 2016, **49**, 357-369.

[4] S. D. U. Paul and U. Radius, *Eur. J. Inorg. Chem.*, 2017, 3362-3375.

[5] M. Soleilhavoup and G. Bertrand, *Acc. Chem. Res.*, 2015, **48**, 256-266.

[6] R. Jazzar, J. B. Bourg, R. D. Dewhurst, B. Donnadieu and G. Bertrand, *J. Org. Chem.*, 2007, **72**, 3492-3499.

[7] R. Jazzar, R. D. Dewhurst, J. B. Bourg, B. Donnadieu, Y. Canac and G. Bertrand, *Angew. Chem. Int. Ed.*, 2007, **46**, 2899-2902.

[8] V. M. Marx, A. H. Sullivan, M. Melaimi, S. C. Virgil, B. K. Keitz, D. S. Weinberger, G. Bertrand and R. H. Grubbs, *Angew. Chem. Int. Ed.*, 2015, **54**, 1919-1923.

[9] X. Cattoen, S. Sole, C. Pradel, H. Gornitzka, K. Miqueu, D. Bourissou and G. Bertrand, *J. Org. Chem.*, 2003, **68**, 911-914.

[10] Z. R. Turner, *Chem. Eur. J.*, 2016, **22**, 11461-11468.

[11] G. D. Frey, J. D. Masuda, B. Donnadieu and G. Bertrand, *Angew. Chem. Int. Ed.*, 2010, **49**, 9444-9447.

[12] C. Mohapatra, P. P. Samuel, B. Li, B. Niepotter, C. J. Schurmann, R. Herbst-Irmer, D. Stalke, B. Maity, D. Koley and H. W. Roesky, *Inorg. Chem.*, 2016, **55**, 1953-1955.

[13] S. Wurtemberger-Pietsch, H. Schneider, T. B. Marder and U. Radius, *Chem. Eur. J.*, 2016, **22**, 13032-13036.

[14] G. D. Frey, V. Lavallo, B. Donnadieu, W. W. Schoeller and G. Bertrand, *Science*, 2007, **316**, 439-441.

[15] A. V. Zhukhoyitskiy, M. G. Mavros, K. T. Queeney, T. Wu, T. Van Voorhis and J. A. Johnson, *J. Am. Chem. Soc.*, 2016, **138**, 8639-8652.

[16] R. Kinjo, B. Donnadieu, M. A. Celik, G. Frenking and G. Bertrand, *Science*, 2011, **333**, 610-613.

[17] Y. Wang, B. Quillian, P. Wei, C. S. Wannere, Y. Xie, R. B. King, H. F. Schaefer, P. V. Schleyer and G. H. Robinson, *J. Am. Chem. Soc.*, 2007, **129**, 12412-+.

[18] M. Arrowsmith, D. Auerhammer, R. Bertermann, H. Braunschweig, G. Bringmann, M. A. Celik, R. D. Dewhurst, M. Finze, M. Grune, M. Hailmann, T. Hertle and I. Krummenacher, *Angew. Chem. Int. Ed.*, 2016, **55**, 14462-14466.

[19] M. Arrowsmith, H. Braunschweig, M. A. Celik, T. Dellermann, R. D. Dewhurst, W. C. Ewing, K. Hammond, T. Kramer, I. Krummenacher, J. Mies, K. Radacki and J. K. Schuster, *Nat. Chem.*, 2016, **8**, 890-894.

[20] C. D. Martin, M. Soleilhavoup and G. Bertrand, *Chem. Sci.*, 2013, **4**, 3020-3030.

[21] P. Bissinger, H. Braunschweig, A. Damme, I. Krummenacher, A. K. Phukan, K. Radacki and S. Sugawara, *Angew. Chem. Int. Ed.*, 2014, **53**, 7360-7363.

[22] B. Li, S. Kundu, A. C. Stuckl, H. P. Zhu, H. Keil, R. Herbst-Irmer, D. Stalke, B. Schwederski, W. Kaim, D. M. Andrada, G. Frenking and H. W. Roesky, *Angew. Chem. Int. Ed.*, 2017, **56**, 397-400.

[23] L. H. Gu, Y. Y. Zheng, E. Haldon, R. Goddard, E. Bill, W. Thiel and M. Alcarazo, *Angew. Chem. Int. Ed.*, 2017, **56**, 8790-8794.

[24] O. Back, M. A. Celik, G. Frenking, M. Melaimi, B. Donnadieu and G. Bertrand, *J. Am. Chem. Soc.*, 2010, **132**, 10262-10263.

[25] R. Kretschmer, D. A. Ruiz, C. E. Moore, A. L. Rheingold and G. Bertrand, *Angew. Chem. Int. Ed.*, 2014, **53**, 8176-8179.

[26] J. K. Mahoney, D. Martin, C. E. Moore, A. L. Rheingold and G. Bertrand, *J. Am. Chem. Soc.*, 2013, **135**, 18766-18769.

[27] J. K. Mahoney, D. Martin, F. Thomas, C. E. Moore, A. L. Rheingold and G. Bertrand, *J. Am. Chem. Soc.*, 2015, **137**, 7519-7525.

[28] L. Q. Jin, M. Melaimi, L. Liu and G. Bertrand, *Organic Chemistry Frontiers*, 2014, **1**, 351-354.

[29] Y. Li, K. C. Mondal, P. P. Samuel, H. Zhu, C. M. Orben, S. Panneerselvam, B. Dittrich, B. Schwederski, W. Kaim, T. Mondal, D. Koley and H. W. Roesky, *Angew. Chem. Int. Ed.*, 2014, **53**, 4168-4172.

[30] S. Styra, M. Melaimi, C. E. Moore, A. L. Rheingold, T. Augenstein, F. Breher and G. Bertrand, *Chem. Eur. J.*, 2015, **21**, 8441-8446.

[31] D. Munz, J. X. Chu, M. Melaimi and G. Bertrand, *Angew. Chem. Int. Ed.*, 2016, **55**, 12886-12890.

[32] M. M. Hansmann, M. Melaimi and G. Bertrand, *J. Am. Chem. Soc.*, 2017, **139**, 15620-15623.

[33] V. Lavallo, Y. Canac, A. DeHope, B. Donnadieu and G. Bertrand, *Angew. Chem. Int. Ed.*, 2005, **44**, 7236-7239.

[34] V. Lavallo, G. D. Frey, S. Kousar, B. Donnadieu and G. Bertrand, *PNAS*, 2007, **104**, 13569-13573.

[35] X. B. Hu, M. Soleilhavoup, M. Melaimi, J. X. Chu and G. Bertrand, *Angew. Chem. Int. Ed.*, 2015, **54**, 6008-6011.

[36] K. C. Mondal, P. P. Samuel, Y. Li, H. W. Roesky, S. Roy, L. Ackermann, N. S. Sidhu, G. M. Sheldrick, E. Carl, S. Demeshko, S. De, P. Parameswaran, L. Ungur, L. F. Chibotaru and D. M. Andrada, *Eur. J. Inorg. Chem.*, 2014, **2014**, 818-823.

[37] S. Roy, K. C. Mondal, J. Meyer, B. Niepotter, C. Kohler, R. Herbst-Irmer, D. Stalke, B. Dittrich, D. M. Andrada, G. Frenking and H. W. Roesky, *Chem. Eur. J.*, 2015, **21**, 9312-9318.

[38] A. P. Singh, P. P. Samuel, H. W. Roesky, M. C. Schwarzer, G. Frenking, N. S. Sidhu and B. Dittrich, *J. Am. Chem. Soc.*, 2013, **135**, 7324-7329.

[39] P. P. Samuel, K. C. Mondal, H. W. Roesky, M. Hermann, G. Frenking, S. Demeshko, F. Meyer, A. C. Stuckl, J. H. Christian, N. S. Dalal, L. Ungur, L. F. Chibotaru, K. Propper, A. Meents and B. Dittrich, *Angew. Chem. Int. Ed.*, 2013, **52**, 11817-11821.

[40] G. Ung, J. Rittle, M. Soleilhavoup, G. Bertrand and J. C. Peters, *Angew. Chem. Int. Ed.*, 2014, **53**, 8427-8431.

[41] D. S. Weinberger, N. A. Sk, K. C. Mondal, M. Melaimi, G. Bertrand, A. C. Stuckl, H. W. Roesky, B. Dittrich, S. Demeshko, B. Schwederski, W. Kaim, P. Jerabek and G. Frenking, *J. Am. Chem. Soc.*, 2014, **136**, 6235-6238.

[42] D. S. Weinberger, M. Melaimi, C. E. Moore, A. L. Rheingold, G. Frenking, P. Jerabek and G. Bertrand, *Angew. Chem. Int. Ed.*, 2013, **52**, 8964-8967.

[43] P. Jerabek, H. W. Roesky, G. Bertrand and G. Frenking, *J. Am. Chem. Soc.*, 2014, **136**, 17123-17135.

[44] P. P. Samuel, R. Neufeld, K. Chandra Mondal, H. W. Roesky, R. Herbst-Irmer, D. Stalke, S. Demeshko, F. Meyer, V. C. Rojisha, S. De, P. Parameswaran, A. C. Stuckl, W. Kaim, J. H. Christian, J. K. Bindra and N. S. Dalal, *Chem. Sci.*, 2015, **6**, 3148-3153.

[45] L. Q. Jin, D. S. Weinberger, M. Melaimi, C. E. Moore, A. L. Rheingold and G. Bertrand, *Angew. Chem. Int. Ed.*, 2014, **53**, 9059-9063.

[46] A. S. Romanov, D. W. Di, L. Yang, J. Fernandez-Cestau, C. R. Becker, C. E. James, B. N. Zhu, M. Linnolahti, D. Credgington and M. Bochmann, *Chem. Commun.*, 2016, **52**, 6379-6382.

[47] D. W. Di, A. S. Romanov, L. Yang, J. M. Richter, J. P. H. Rivett, S. Jones, T. H. Thomas, M. A. Jalebi, R. H. Friend, M. Linnolahti, M. Bochmann and D. Credgington, *Science*, 2017, **356**, 159-163.

[48] R. Hamze, R. Jazzar, M. Soleilhavoup, P. I. Djurovich, G. Bertrand and M. E. Thompson, *Chem. Commun.*, 2017, **53**, 9008-9011.

[49] V. Lavallo, G. D. Frey, B. Donnadieu, M. Soleilhavoup and G. Bertrand, *Angew. Chem. Int. Ed.*, 2008, **47**, 5224-5228.

[50] R. Kinjo, B. Donnadieu and G. Bertrand, *Angew. Chem. Int. Ed.*, 2011, **50**, 5560-5563.

[51] J. P. Chen and L. L. Lim, *Chemosphere*, 2002, **49**, 363-370.

[52] Y. Wei, B. Rao, X. Cong and X. Zeng, *J. Am. Chem. Soc.*, 2015, **137**, 9250-9253.

[53] M. P. Wiesenfeldt, Z. Nairoukh, W. Li and F. Glorius, *Science*, 2017, **357**, 908-912.

[54] D. R. Anderson, V. Lavallo, D. J. O'Leary, G. Bertrand and R. H. Grubbs, *Angew. Chem. Int. Ed.*, 2007, **46**, 7262-7265.

[55] B. Rao, H. R. Tang, X. M. Zeng, L. Liu, M. Melaimi and G. Bertrand, *Angew. Chem. Int. Ed.*, 2015, **54**, 14915-14919.

[56] T. Kosai, S. Ishida and T. Iwamoto, *Angew. Chem. Int. Ed.*, 2016, **55**, 15554-15558.

[57] L. L. Wang, Y. S. Lim, Y. X. Li, R. Ganguly and R. Kinjo, *Molecules*, 2016, **21**, 990.

[58] Y. Mizuhata, T. Sasamori and N. Tokitoh, *Chem. Rev.*, 2009, **109**, 3479-3511.

[59] D. Bourissou, O. Guerret, F. P. Gabbai and G. Bertrand, *Chem. Rev.*, 2000, **100**, 39-91.

[60] T. W. Hudnall, A. G. Tennyson and C. W. Bielawski, *Organometallics*, 2010, **29**, 4569-4578.

[61] E. O. Karaca, M. Akkoc, E. Oz, S. Altin, V. Dorcet, T. Roisnel, N. Gurbuz, O. Celik, A. Bayri, C. Bruneau, S. Yasar and I. OZdemir, *J. Coord. Chem.*, 2017, **70**, 1270-1284.

[62] N. Phillips, C. Y. Tang, R. Tirfoin, M. J. Kelly, A. L. Thompson, M. J. Gutmann and S. Aldridge, *Dalton Trans.*, 2014, **43**, 12288-12298.

[63] J. Li, W. X. Shen and X. R. Li, *Curr. Org. Chem.*, 2012, **16**, 2879-2891.

[64] E. Tomas-Mendivil, M. M. Hansmann, C. M. Weinstein, R. Jazzar, M. Melaimi and G. Bertrand, *J. Am. Chem. Soc.*, 2017, **139**, 7753-7756.

[65] L. Benhamou, E. Chardon, G. Lavigne, S. Bellemin-Laponnaz and V. Cesar, *Chem. Rev.*, 2011, **111**, 2705-2733.

[66] N. de Kimpe, M. Boelens, J. Piqueur and J. Baele, *Tetrahedron Lett.*, 1994, **35**, 1925-1928.

[67] R. M. Beesley, C. K. Ingold and J. F. Thorpe, *J. Chem. Soc.*, 1915, **107**, 1080-1106.

[68] J. X. Chu, D. Munz, R. Jazzar, M. Melaimi and G. Bertrand, *J. Am. Chem. Soc.*, 2016, **138**, 7884-7887.

[69] Z. R. McCarty, D. N. Lastovickova and C. W. Bielawski, *Chem. Commun.*, 2016.

[70] V. Lavallo, J. Mafhouz, Y. Canac, B. Donnadieu, W. W. Schoeller and G. Bertrand, *J. Am. Chem. Soc.*, 2004, **126**, 8670-8671.

[71] G. D. Frey, R. D. Dewhurst, S. Kousar, B. Donnadieu and G. Bertrand, *J. Organomet. Chem.*, 2008, **693**, 1674-1682.

[72] A. Gomez-Suarez, D. J. Nelson and S. P. Nolan, *Chem. Commun.*, 2017, **53**, 2650-2660.

[73] V. Lavallo, Y. Canac, B. Donnadieu, W. W. Schoeller and G. Bertrand, *Angew. Chem. Int. Ed.*, 2006, **45**, 3488-3491.

[74] T. W. Hudnall and C. W. Bielawski, *J. Am. Chem. Soc.*, 2009, **131**, 16039-16041.

[75] S. N. Lyashchuk and Y. G. Skrypnik, *Tetrahedron Lett.*, 1994, **35**, 5271-5274.

[76] D. A. Dixon, A. J. Arduengo, K. D. Dobbs and D. V. Khasnis, *Tetrahedron Lett.*, 1995, **36**, 645-648.

[77] C. Goedecke, M. Leibold, U. Siemeling and G. Frenking, *J. Am. Chem. Soc.*, 2011, **133**, 3557-3569.

[78] D. Martin, C. E. Moore, A. L. Rheingold and G. Bertrand, *Angew. Chem. Int. Ed.*, 2013, **52**, 7014-7017.

[79] U. Siemeling, C. Farber, C. Bruhn, M. Leibold, D. Selent, W. Baumann, M. von Hopffgarten, C. Goedecke and G. Frenking, *Chem. Sci.*, 2010, **1**, 697-704.

[80] U. S. D. Paul and U. Radius, *Organometallics*, 2017, **36**, 1398-1407.

[81] Y. Zhang, D. R. Wang, K. Wurst and M. R. Buchmeiser, *J. Organomet. Chem.*, 2005, **690**, 5728-5735.

[82] N. Phillips, R. Tirfoin and S. Aldridge, *Dalton Trans.*, 2014, **43**, 15279-15282.

[83] E. L. Kolychev, S. Kronig, K. Brandhorst, M. Freytag, P. G. Jones and M. Tamm, *J. Am. Chem. Soc.*, 2013, **135**, 12448-12459.

[84] V. Cesar, N. Lugan and G. Lavigne, *J. Am. Chem. Soc.*, 2008, **130**, 11286-11287.

[85] R. Martin and S. L. Buchwald, *Acc. Chem. Res.*, 2008, **41**, 1461-1473.

[86] D. R. Tolentino, L. Q. Jin, M. Melaimi and G. Bertrand, *Chem. Asian J.*, 2015, **10**, 2139-2142.

[87] E. Herrero-Gómez, C. Nieto-Oberhuber, S. López, J. Benet-Buchholz and A. M. Echavarren, *Angew. Chem. Int. Ed.*, 2006, **45**, 5455-5459.

[88] C. Nieto-Oberhuber, S. Lopez and A. M. Echavarren, *J. Am. Chem. Soc.*, 2005, **127**, 6178-6179.

[89] A. Liske, K. Verlinden, H. Buhl, K. Schaper and C. Ganter, *Organometallics*, 2013, **32**, 5269-5272.

[90] K. Verlinden, H. Buhl, W. Frank and C. Ganter, *Eur. J. Inorg. Chem.*, 2015, 2416-2425.

[91] V. K. Landry, M. Minoura, K. L. Pang, D. Buccella, B. V. Kelly and G. Parkin, *J. Am. Chem. Soc.*, 2006, **128**, 12490-12497.

[92] R. Michalczyk, J. G. Schmidt, E. Moody, Z. Z. Li, R. L. Wu, R. B. Dunlap, J. D. Odom and L. A. Silks, *Angew. Chem. Int. Ed.*, 2000, **39**, 3067-3070.

[93] G. R. Desiraju, *Acc. Chem. Res.*, 1991, **24**, 290-296.

[94] F. A. Cotton, L. M. Daniels, G. T. Jordan and C. A. Murillo, *Chem. Commun.*, 1997, 1673-1674.

[95] T. Steiner and G. R. Desiraju, *Chem. Commun.*, 1998, 891-892.

[96] G. R. Desiraju, *Angew. Chem. Int. Ed.*, 2011, **50**, 52-59.

[97] K. N. Houk, S. Menzer, S. P. Newton, F. M. Raymo, J. F. Stoddart and D. J. Williams, *J. Am. Chem. Soc.*, 1999, **121**, 1479-1487.

[98] R. C. Johnston and P. H. Y. Cheong, *Org. Biomol. Chem.*, 2013, **11**, 5057-5064.

[99] C. Avendano, M. Espada, B. Ocana, S. Garciagranda, M. D. Diaz, B. Tejerina, F. Gomezbeltran, A. Martinez and J. Elguero, *Journal of the Chemical Society-Perkin Transactions 2*, 1993, 1547-1555.

[100] S. V. C. Vummaleti, D. J. Nelson, A. Poater, A. Gomez-Suarez, D. B. Cordes, A. M. Z. Slawin, S. P. Nolan and L. Cavallo, *Chem. Sci.*, 2015, **6**, 1895-1904.

[101] J. H. Palmer and G. Parkin, *Polyhedron*, 2013, **52**, 658-668.

[102] D. J. Williams, M. R. Fawcettbrown, R. R. Raye, D. Vanderveer, Y. T. Pang, R. L. Jones and K. L. Bergbauer, *Heteroat. Chem.*, 1993, **4**, 409-414.

[103] W. L. F. Armarego and C. L. L. Chai, *Purification of Laboratory Chemicals: 5th Edition*, Elsevier Science, Burlington, MA, 2003.

[104] O. V. Dolomanov, L. J. Bourhis, R. J. Gildea, J. A. K. Howard and H. Puschmann, *J. Appl. Crystallogr.*, 2009, **42**, 339-341.

[105] M. J. Frisch, G. W. Trucks, H. B. Schlegel, G. E. Scuseria, M. A. Robb, J. R. Cheeseman, G. Scalmani, V. Barone, B. Mennucci, G. A. Petersson, H. Nakatsuji, M. Caricato, X. Li, H. P. Hratchian, A. F. Izmaylov, J. Bloino, G. Zheng, J. L. Sonnenberg, M. Hada, M. Ehara, K. Toyota, R. Fukuda, J. Hasegawa, M. Ishida, T. Nakajima, Y. Honda, O. Kitao, H. Nakai, T. Vreven, J. A. Montgomery, J. E. Peralta, F. Ogliaro, M. Bearpark, J. J. Heyd, E. Brothers, K. N. Kudin, V. N. Staroverov, R. Kobayashi, J. Normand, K. Raghavachari, A. Rendell, J. C. Burant, S. S. Iyengar, J. Tomasi, M. Cossi, N. Rega, J. M. Millam, M. Klene, J. E. Knox, J. B. Cross, V. Bakken, C. Adamo, J. Jaramillo, R. Gomperts, R. E. Stratmann, O. Yazyev, A. J. Austin, R. Cammi, C. Pomelli, J. W. Ochterski, R. L. Martin, K. Morokuma, V. G. Zakrzewski, G. A. Voth, P. Salvador, J. J. Dannenberg, S. Dapprich, A. D. Daniels, Farkas, J. B. Foresman, J. V. Ortiz, J. Cioslowski and D. J. Fox, Wallingford CT, 2009.

[106] W. Kohn and L. J. Sham, *Phys Rev*, 1965, **140**, A1133-1138.

[107] P. Hohenberg and W. Kohn, *Phys Rev B*, 1964, **136**, B864-871.

[108] F. Weigend, *Phys. Chem. Chem. Phys.*, 2006, **8**, 1057-1065.

[109] F. Weigend and R. Ahlrichs, *Phys. Chem. Chem. Phys.*, 2005, **7**, 3297-3305.

Chapter 5 : Investigation of $\alpha,\alpha,\gamma,\gamma$-Tetrasubstitued-2-Allenyl Ketimines as "Masked" Remote *N*-Heterocyclic Carbene Sources

5.1 Introduction

As evident from chapter 4, the inherent reduced heteroatom stabilization of CAACs gives extremely small ΔE_{ST} and HOMO-LUMO gaps which have led to exciting reactivity. Although the utilization of CAACs is still a very active field, if we are to continue pushing the limits of carbenes we must consider methods in which heteroatom stabilization can be reduced even further. As such, "remote" heteroatom stabilization, defined as cases where the carbene carbon is not α to any heteroatom,[1-2] is a potential future direction for carbene chemists. Such a description comes counter to the fundamental idea that mesomeric effects of α-substituents are required to stabilize the singlet ground state of a free carbene (see section 1.1). It is therefore of no surprise that BAC **5.A** is the only example of an isolated singlet carbene fitting the "remote" definition (Figure 5.1).[3] The remarkable stability of **5.A**, and by extension its lithium adduct,[4] is best explained by two factors. First, the 2π-electron 3-membered aromatic ring stabilizes the singlet state of the carbene by ~46 kcal mol^{-1}.[5] Second, the lone pairs of the strongly donating bis(isopropyl)amino substituents can conjugate into the LUMO of the carbene giving its two major zwitterionic resonance forms. Although "remote" from the carbene center, this mesomeric effect adds more than 14 kcal mol^{-1} stabilization energy to the singlet state.

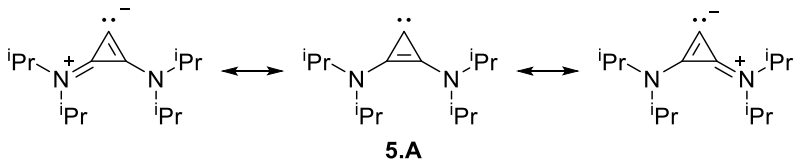

Figure 5.1: The only example of a stable singlet carbene in which no heteroatoms are α to the carbene center.

As BAC **5.A** does not technically qualify, the field of *r*NHCs has been completely limited to the coordination sphere of TMs. To the best of this author's knowledge, the first unambiguous example of an *r*NHC TM complex comes from a report by Tanaka et al. of the (N,N,N)-tridentate-(N,N,C)-tridentate hexakispyridine ruthenium(III) complex **5.B** (Figure 5.2).[6] In this detailed study, ^{13}C NMR, X-ray, and CV data all corroborated the hypothesis that the Ru-C bond in **5.B** best fit the description of a Ru-pyridinylidene bond as opposed to the Ru-pyridinium bond in **5.C**. Subsequent studies by Tanaka et al. on a similar systems added evidence for this bonding description.[7] Therefore following Tanaka's observation, *r*NHC TM complexes featuring a pyridinylidene ligand only have carbeneic character if the nitrogen is 2n+1 bonds from the TM center. With this restriction, TM complexes featuring a pyridinylidene ligand (and their annulated analogues) have been expanded to the coordination spheres of Mn,[8] Cr,[9] W,[9]Au,[9] Rh,[9-10] Ir,[11-12] and group X metals[8, 13-18] including one example where the nitrogen was located in a different ring five bonds away.[19]

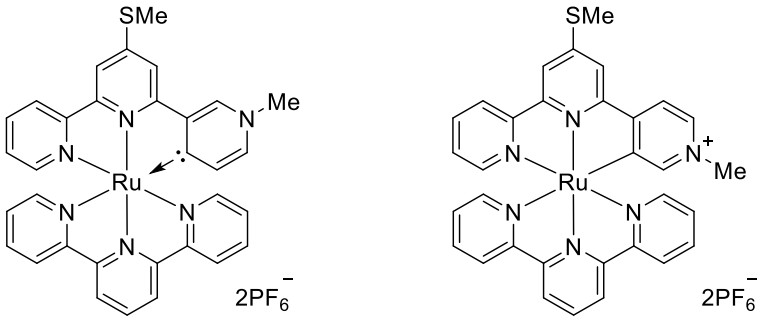

Figure 5.2: Carbeneic character in pyridinylidene *r*NHCs requires the heteroatom to be 2n+1 bonds from the carbene.

Another subset of *r*NHCs TM complexes can be found in carbenes derived from pyrazoles. In several reports, Han et al. demonstrated that the neutral or cationic monomer or dimer pyrazolylidene TM complexes **5.E-I** were synthesized by oxidative addition with $Pd_2(dba)_3$ of their respective iodo pyrazolium salts **5.D** (Scheme 5.1).[20-23] Unlike the pyridinylidenes, canonical resonance structures of pyrazolylidenes cannot be drawn completely charged balanced, and thus they also qualify as MICs. As such, pyrazolylidenes have been calculated to be very strong donors with negligible π-accepting ability.[24-25] In general, the ^{13}C NMR signal for the C4 palladium bound carbon atoms in **5.E-I** appear ~50-60 ppm downfield shifted of the same carbon resonance in the pyrazolium precursors. Although usually good indication of carbene character, the observed ^{13}C downfield shift might also be a side effect of the unusually high field signal caused by the shielding of iodine in the precursor.

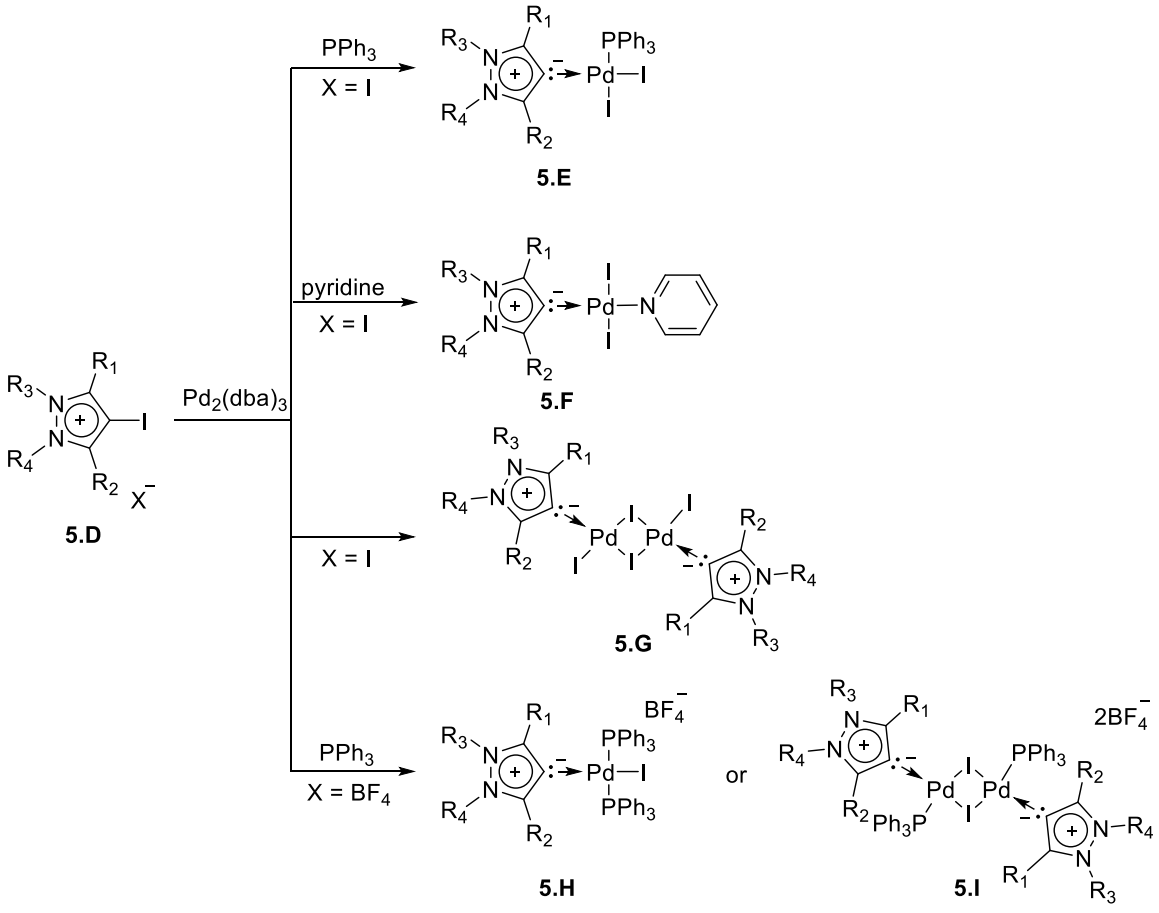

Scheme 5.1: Oxidative addition to palladium is the only known synthetic route for pyrazolylidene complexes.

Although strictly speaking not *r*NHCs, Furstner et al. used a similar oxidative addition strategy to access to cyclic carbene TM complexes **5.J-M** (Figure 5.3).[26] Here however, the carbenes' singlet states are stabilized remotely through extended π-systems of enamines. The structural scope for these types of carbenes could even be expanded to acyclic versions **5.N-P**. Carbene character of these ligands was proposed due to significant downfield shifting of the ^{13}C NMR C-M signal (202-230 ppm) as compared to the respective C-X signal in the halo vinamidinium precursors (147-157 ppm).

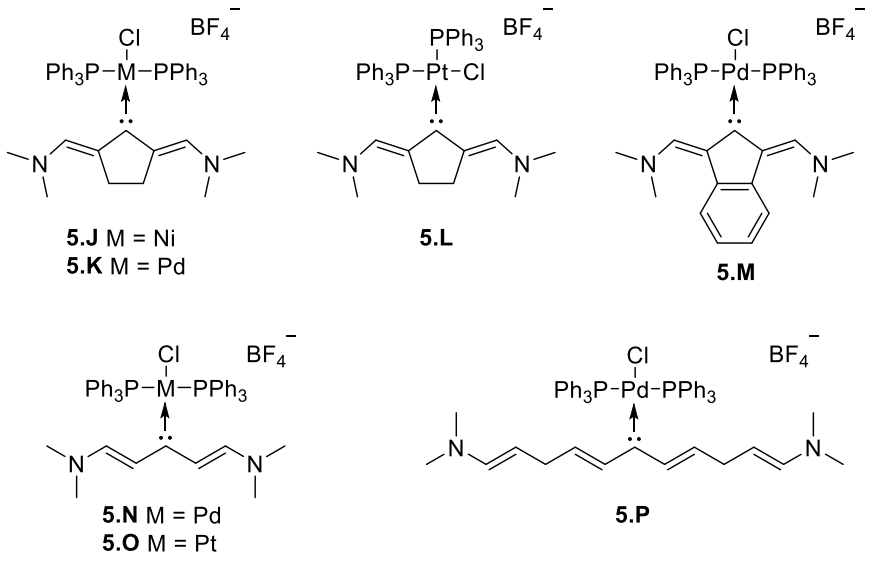

Figure 5.3: Remote carbenes stabilized by extended enamine π-systems.

Given their synthetic accessibility, detailed catalytic studies of *r*NHC-Pd complexes have also been reported. Raubenheimer et al. directly compared the catalytic activity of *r*NHC-Pd complex **5.Q** with the "normal" NHC-Pd complex **5.R** (Figure 5.4).[27] Note that **5.R** features small methyl groups on the nitrogen atoms as to best compare how purely electronic differences between "normal" and *r*NHCs affect catalytic performance. Remarkably, for both the Mizoroki-Heck and Suzuki-Miyaura coupling reactions, the *r*NHC catalyst gave higher yields with lower catalyst loadings than **5.R**. Furthermore, time-conversion curves of both coupling reactions demonstrated that catalyst **5.Q** required essentially zero inductive period. Calculations on model systems also found the metal carbene bond in the *r*NHC complex to be 22.1 kcal mol^{-1} stronger than the analogous bond in the "normal" system. The increased bond

strength is due to the higher π-accepting character of *r*NHCs, which will likely lead to more robust catalysts.

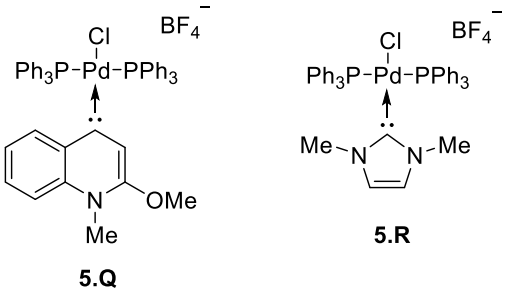

Figure 5.4: Comparing *r*NHC and "normal" NHC catalysts.

Lastly, *r*NHC-TM complexes have been synthesized by TM induced cyclization reactions. Indeed, Fensterback et al. recently demonstrated that the tetrasubstituted allene with a pendent pyridine moiety **5.S** reacted with Me_2SAuCl, closing the ring and giving the respective gold carbene complex **5.T** (Scheme 5.2).[28] This result was highly reminiscent of work published by Bertrand et al. in which an acyclic ethynylcarbamodithioate cyclized in the presence of Pd(II), Au(I), or Rh(I) sources giving the respective 1,3-dithiol-5-ylidene TM complexes.[29] Subsequent studies by Bertrand et al. on a similar system showed that when the alkynyl benzothioamide **5.U** was subjected to a Au(III) source, the thiopyran derived six-membered *r*NHC Au(III) complex **5.U** could be generated. Finally, although never isolated, Gevorgyan et al. questioned the possibility that a *r*NHC TM complex might be an intermediate in the catalytic formation of furans and pyrroles from 2-alkynyl ketones and ketimines, respectively.[30]

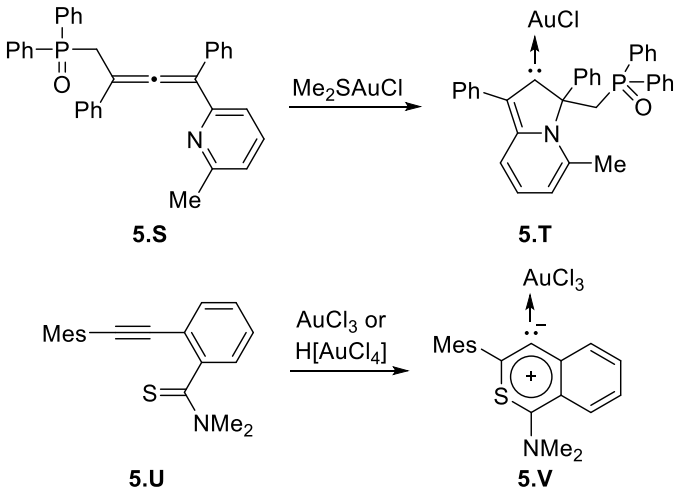

Scheme 5.2: Synthesis of *r*NHC TM complexes via Au induced cyclization.

Considering the rather unexplored nature of the field, we sought to investigate the synthesis of new *r*NHCs. Given that both pyridinylidenes and pyrazolylidenes are derived from aromatic systems, we focused our attention on designing a *r*NHC which does not feature an aromatic ring. As such, five-membered *r*NHC model compound **5.W** was proposed and compared to model CAACs discussed in chapter 4 (Figure 5.5). Calculations at the B3LYP/def2-TZVPP level of theory showed that moving to remote heteroatom stabilization in **5.W** lowered the LUMO energy by 1.33 eV compared to CAAC-6. Furthermore, due to the nearest electronegative atom being two bonds away from the carbene center, **5.W** has the highest the highest HOMO of the series at -4.65 eV. Finally, the effect of a single conjugated enamine stabilization on the carbene can be clearly seen by looking at the ΔE_{ST} of **5.W**. Indeed, the *r*NHC has the lowest ΔE_{ST} of the series at 23.0 kcal mol^{-1} which is less than half the ΔE_{ST} of CAAC-5. It should be noted that although **5.W** appears closely related to the *r*NHC in complex **5.T**, the removal of the pyridine backbone should give the resulting complexes higher carbene character as they will no longer need to be dearomatized in their carbene resonance form.

A simple retrosynthetic analysis of **5.W** revealed that this *r*NHC might be easy to make (Scheme 5.3). As most of the known *r*NHC TM complexes are derived from the oxidative addition of their respective $[C\text{-}X]^+$ salts, the most logical precursor to **5.W** would be the chloro pyrrolidinium salt **5.X**.

Given the high basicity of the tertiary amine in **5.Y**, chlorination to yield **5.X** should be easily achieved with oxalyl chloride. Finally and quite spectacularly, molecules like **5.Y** have been reported to be easily synthesized by the reaction of 1,2-diphenylcyclopropenone with a variety of different ketimines.[31-34] In conclusion, a wide range of *r*NHCs like **5.W** are theoretically synthetically possible.

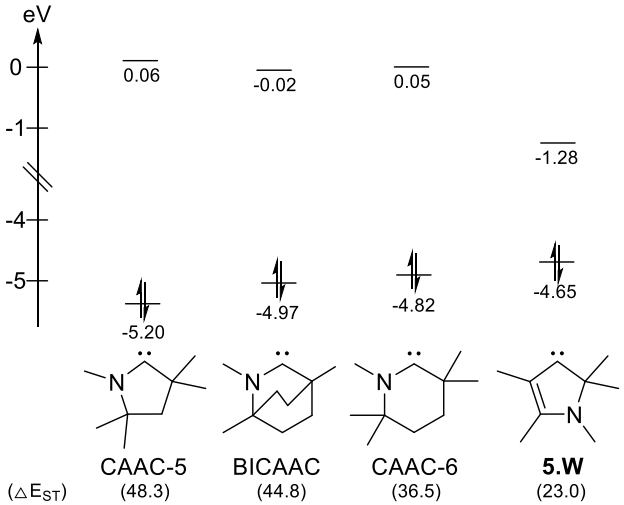

Figure 5.5: Calculated HOMO-LUMO gaps (eV) and ΔE_{ST} (kcal mol^{-1}) of CAAC derivatives and *r*NHC **5.W**.

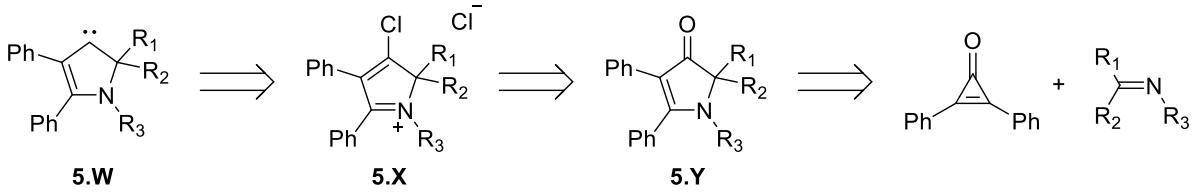

Scheme 5.3: Retrosynthetic analysis for *r*NHC **5.W**.

5.2 Pursuit of a Pyrrolidinylidene *r*NHC

Ketimines **5.1a**,**b** were synthesized by condensation reactions in a Dean-Stark apparatus from aniline and cyclohexanone or 2-adamantanone, respectively (Scheme 5.4). Once isolated, either **5.1a**,**b** were combined to a Schlenk with 1,2-diphenylcyclopropenone and heated for several days. For the reaction involving **5.1a**, full consumption of the starting material was observed after 3 days of heating at 70 ºC, with **5.2a** formed as the major product of the reaction. Although this reaction does not yield a

single clean product, key ^{13}C NMR signals characteristic of **5.2a** can be observed at 202.6, 70.5, and 170.6 ppm belonging to C_1-C_3, respectively. One the other hand, the analogous reaction with **5.1b** had to be heated for 22 days at 100 ºC before NMR signals of the starting materials completely disappeared. We are confident that the major product of the reaction was indeed **5.2b**, as we observed similar C_1-C_3 ^{13}C NMR signals at 202.4, 75.8, and 172.5 ppm. However considering the time required making starting material **5.2b**, we proceeded purely with subsequent synthetic investigations on **5.2a**.

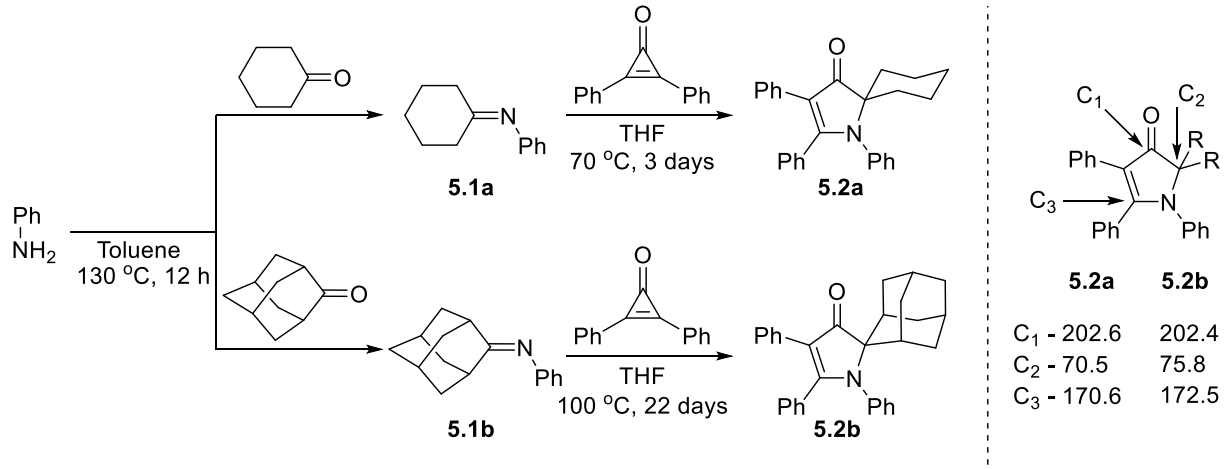

Scheme 5.4: Synthesis of five-membered rings **5.2a**,**b** (left) with diagnostic ^{13}C NMR signals in ppm (right).

We then probed reactions of **5.2a** that might yield easily reducible precursors of the desired *r*NHC. Heating solutions of **5.2a** at 100 ºC for 12 h in the presence of with Lawesson's or Woollins' reagent did not yield the respective sulfonated or selonated compounds (Scheme 5.5). Fortunately however, we observed immediate effervesce upon addition of oxalyl chloride to a DCM solution of **5.2a** at RT. Stirring the solution for 12 h yielded, after workup, chloro pyrrolidinium salt **5.3a** as a pure white microcrystalline solid. Interestingly, when the analogous reaction was attempted with oxalyl bromide, the oxygen was instead protonated by adventitious HBr, yielding the pyrrolidinium alcohol **5.4a**. A single crystal X-ray diffraction study confirmed the structure of this species (Figure 5.6). Although both oxalyl halide solutions contain respective HX acids, only HBr was strong enough to protonate the carbonyl.

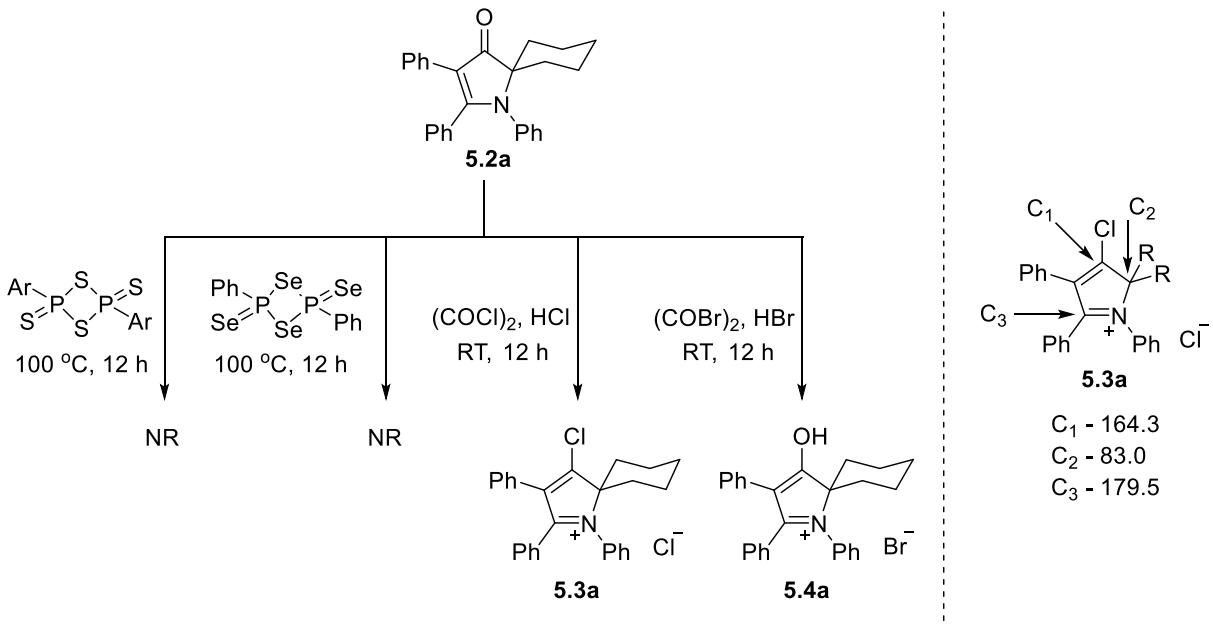

Scheme 5.5: Attempted deoxygenation reactions of **5.2a** (left) and diagnostic ^{13}C NMR signals in ppm of chloro pyrrolidinium salt **5.3a** (right). Ar = *p*-OMe(C_6H_5).

Analysis of the ^{13}C NMR of **5.3a** revealed three signals in the alkyl region for the cyclohexyl methylene groups and at least 14 closely grouped signals from 124-137 ppm. This left only three remaining signals. The lowest field signal appears at 179.5 ppm, which fits for the tertiary iminium carbon C_3. Next, we assigned the signal at 164.3 ppm to the chloro alkene C_1. Finally, the remaining carbon signal appears at 83.0 ppm and corresponds to the quaternary carbon C_2. This signal is downfield shifted from the same signal in the neutral precursor by 12.5 ppm, as would be expected for a species with a more cationic nitrogen.

With **5.3a** in hand, we next probed the reduction potential electrochemically. A CV study of **5.3a** revealed at least three independent reduction waves at -1.02, -1.27, and -1.61 V vs Fc/Fc^+ (Figure 5.7). Additionally, two oxidation waves appeared at -0.912 and 0.190 V. From these data, it's tough to know if the first reduction wave is a multi- or single-electron process. If it is the latter however, then in order to access the carbene through chemical reduction a species more reducing than -1.27 V was needed. Note

that a third reduction appeared at -1.61 V, indicating that over reduction of the desired carbene might be possible.

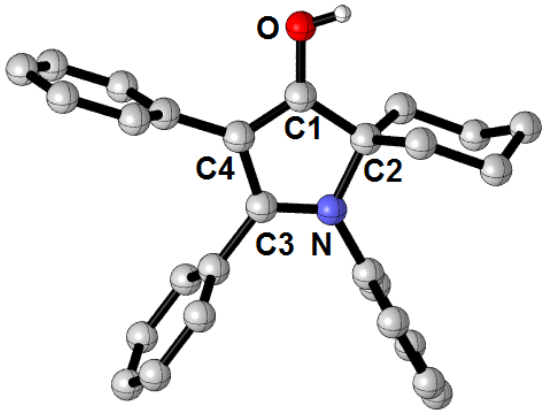

Figure 5.6: Solid state structure of **5.4a**. H-atoms, except on oxygen, and the Br^- anion have been omitted for clarity. Selected bond lengths (Å) and angles (º): C1-O 1.329(1), C1-C2 1.505(1), C1-C4 1.373(1), C2-N 1.496(1), C3-N 1.318(1), C3-C4 1.430(1), C4-C1-C2 112.2(1).

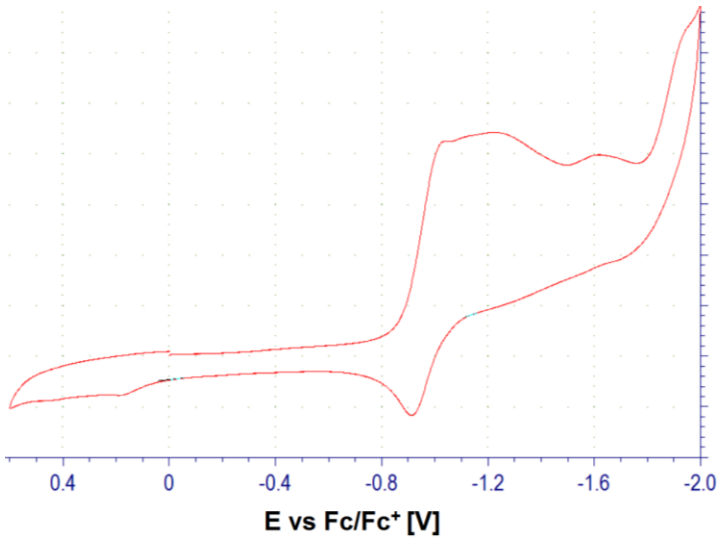

Figure 5.7: Cyclic voltammogram of chloro pyrrolidinium salt **5.3a**. ($n$$Bu_4NPF_6$ 0.1 M in THF vs Fc/Fc^+).

Given the small reduction potential window, we first explored the reaction of **5.3a** with two equivalents of cobaltocene (-1.33 V vs Fc/Fc^+) (Scheme 5.6).[35] Inspection of the ^{13}C NMR revealed the consumption of all starting materials. Unfortunately, no signal downfield of 150 ppm was observed. We

did however observe a single signal corresponding to C_2 at 73.4 ppm, leading us to believe the organic pyrrolidinium was indeed reduced. Additionally, a new aliphatic C-H signal (d, $^1J_{C\text{-}H}$ = 141 Hz) appeared at 47 ppm indicative of a potential C-H insertion product. Although all attempts to grow single crystals failed, an ESI-MS study gave an *m*/*z* peak at 552.30 which matched perfectly for the *r*NHC cobaltocenium C-H insertion product **5.5**. Although more experimental data is needed to confirm the structure of **5.5**, it was clear from this experiment that we needed to move towards investigating different reducing agents.

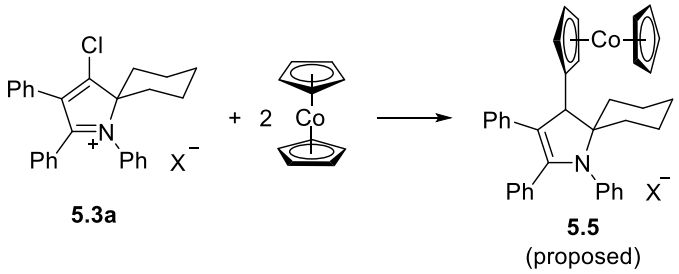

5.3a **5.5** (proposed)

Scheme 5.6: Reduction of **5.3a** with cobaltocene gives proposed C-H insertion product **5.5**.

Subsequent reduction reactions of **5.3a** were attempted with KC_8, K (mirror), Zn, Mg, and Mg-anthracene (MgA). In each case, the reducing agent was added to a THF slurry of **5.3a** and a deep purple solution appeared. For the reaction with KC_8, the purple solution was found to be completely NMR silent after 1h of stirring. An EPR study of the purple solution gave a broad signal confirming the radical character of this species (Figure 5.8). The closely matching simulated EPR spectra yielded hyperfine couplings to one S = 3/2 (a = 1.1 G) and S = 1 (a = 2.8 G) nuclei, which was indicative of coupling to chlorine and nitrogen atom, respectively. Given closely matched spectra, we propose that the first reduction of **5.3a** gives the 5π-electron conjugated species shown below, however computational data of the SOMO is needed to better support this hypothesis. The paramagnetic species was fairly stable in solution, although we did observe slow decomposition after two days as new signals began to appear in the ^{13}C NMR. Unfortunately, all attempts to grow crystals of this species failed and its absolute structure still remains unconfirmed.

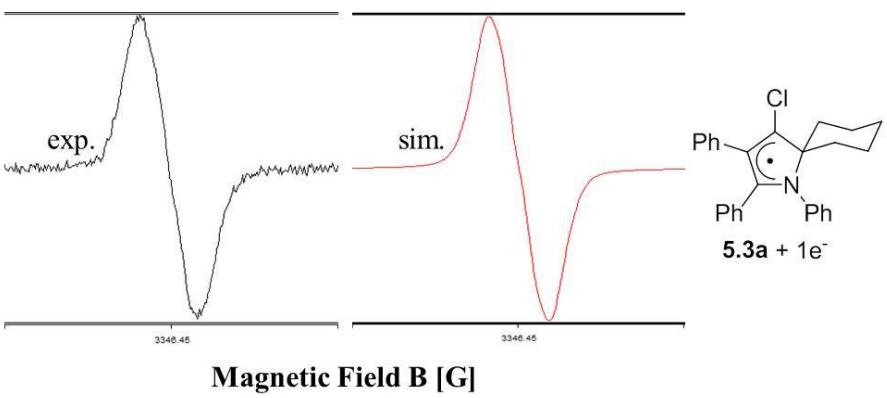

Figure 5.8: Experimental and simulated EPR spectra of the neutral product from a one electron reduction of **5.3a**

Although every reducing agent gave some percentage of the proposed radical species, the reduction with MgA yielded the cleanest formation of a diamagnetic compound. This new species was highly soluble in Et_2O and benzene which was indicative of a neutral organic molecule. The most downfield signal in the crude $^{13}C\{^1H\}$ NMR of this reaction appeared at 198.6 ppm (Figure 5.9). Surprisingly, only three carbon signals (other than residual THF) appeared upfield of 100 ppm, with no signal in the range normally observed for the quaternary carbon α to the nitrogen atom. Furthermore, two distinct alkene signals could be observed at 102.1 and 107.8 ppm. From the combined NMR evidence, it was clear that the product of this reaction was the *α,α,γ,γ*-tetrasubstitued-2-allenyl ketimines **5.6a**.

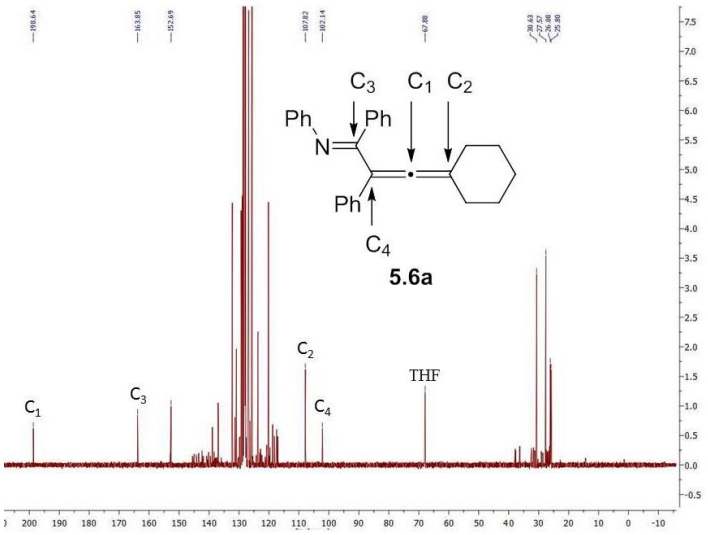

Figure 5.9 Crude $^{13}C\{^{1}H\}$ of the reduction of **5.3a** with Mg-anthracene giving allene **5.6a** as the major product.

The ring opening formation of **5.6a** was intriguing but in retrospect not surprising. If we assume that MgA first reduces **5.3a** by two electrons, then we hypothetically generate the intermediate *r*NHC **5.6a'** (Scheme 5.7). The *r*NHC can then either be drawn as a carbene or as its zwitterionic resonance form. In the latter case, the formal anionic charge is now β to an iminium leaving group. We can therefore imagine that **5.6'** quickly proceeded through a β-elimination to give allene **5.6a**. A similar ring opening reaction has been observed before on NHCs derived from pyrazoles.[36] In this case however, the carbene **5.8'** was generated in the "normal" position upon loss of CO_2 from the parent carbonate compound **5.7**. Nevertheless, this species was also susceptible to ring opening. Calculations of the mechanism showed that the cleavage of the N-N bond was only endergonic by 14.8 kcal mol^{-1}. Furthermore, although unstable and continues through subsequent rearrangement reactions, the respective ketenimine **5.8** was found to 20.5 kcal mol^{-1} energetically more favorable than the carbene. It should be noted that alternative synthetic routes giving *α,α,γ,γ*-tetrasubstitued-2-allenyl ketimines like **5.6a** are not currently known. As such, this reduction method from the corresponding pyrrolidinium salt might be useful for the derivatization of this type of organic functionality.

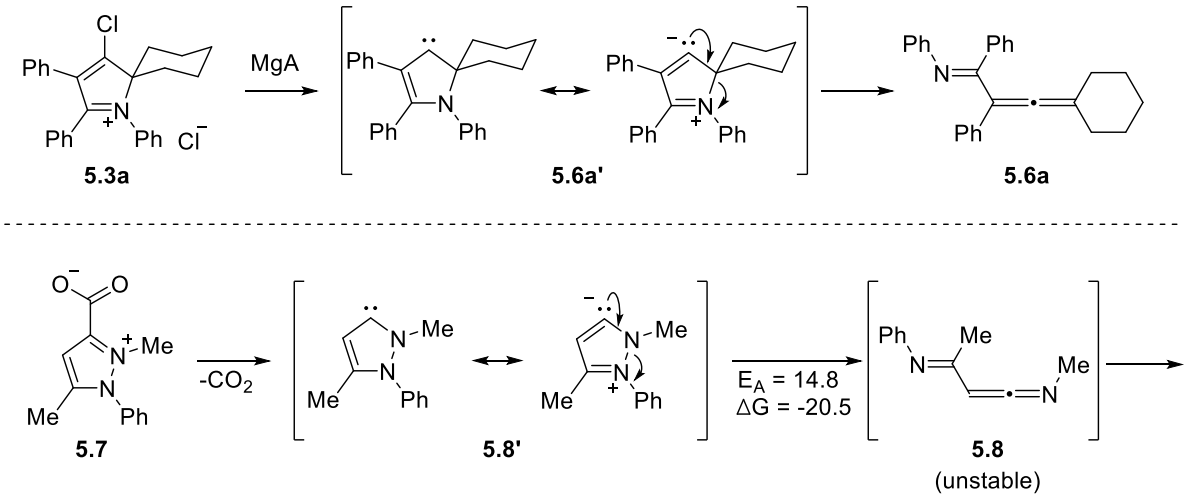

Scheme 5.7: Mechanism of allene **5.6a** formation (top) and analogous ring opening mechanism of a "normal" pyrazolylidene (bottom). Energies are given in kcal mol^{-1}.

Given the observed ring opening decomposition pathway, we were curious if the stability of **5.6'** cold be increased if the N-C bond prone to breaking was tethered by a rigid exocyclic system. Therefore, the tricyclic ketimine was first synthesized in four steps from 2-adamantanone (Scheme 5.8). Encouragingly, the five-membered ring formation with 1,2-diphenylcyclopropenone yielded **5.2c** in just 12 h as the only product evident by ^{1}H and ^{13}C NMR. As in the previous systems, **5.2c** shares highly similar characteristic ^{13}C NMR signals at 201.5, 74.6, and 172.8 ppm for C_1-C_3, respectively. The shorter reaction time and cleaner product formation was likely due to the increased basicity of the alkyl substituted ketimine compared to the aryl substituted ketimine in the previous cases. Although the formation of **5.2c** proved easier, deoxygenation with oxalyl chloride required a DMF catalyst in addition to three days of heating. The higher heating and longer reaction time was likely due to the nitrogen atom's resistance towards accepting a planar geometry, given the high rigidity of the tethered tricyclic group. Characteristic ^{13}C NMR signals for **5.3c** carbons C_1-C_3 were observed at 166.1, 88.1, and 180.4 ppm, respectively, which matched very well with both **5.3a**,**b**. Note that the chloro pyrrolidinium salt **5.3c** is balanced by an HCl_2^- anion which was likely formed from HCl that contaminated the oxalyl chloride

solution. Single crystals suitable for X-ray diffraction grown in a THF solution at -20 ºC confirmed the structure of **5.3c** (Figure 5.10).

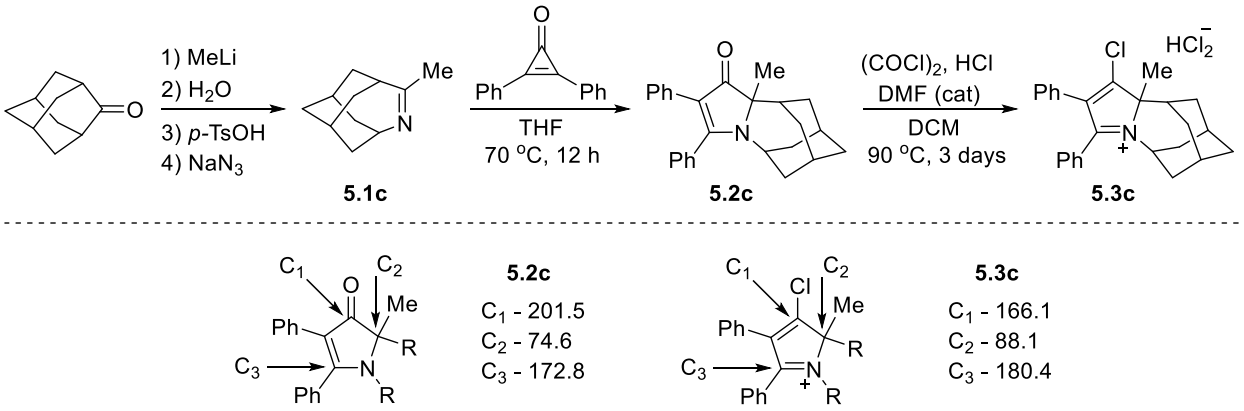

Scheme 5.8 Synthesis of tethered compounds **5.2c** and **5.3c** (top) with diagnostic ^{13}C NMR signals (ppm) on the left and right, respectively (bottom).

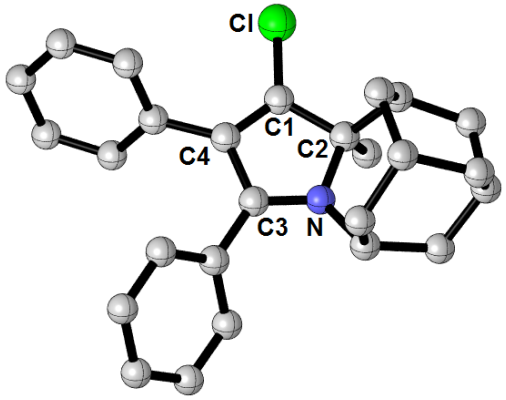

Figure 5.10: Solid state structure of **5.3c**. H-atoms, HCl_2^- anion, and residual solvent have been omitted for clarity. Selected bond lengths (Å) and angles (º): C1-Cl 1.707(2), C1-C2 1.503(2), C1-C4 1.348(2), C2-N 1.486(2), C3-N 1.317(2), C3-C4 1.461(2), C4-C1-C2 112.7(1).

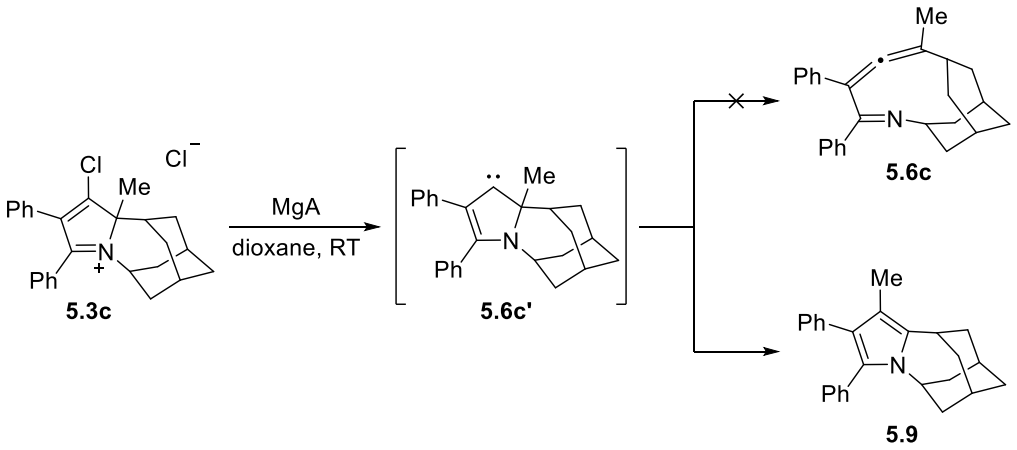

Scheme 5.9: Reduction of tethered system **5.3c** at RT gives the 1,2-methyl migration pyrrole product **5.9**.

Considering the fact that *r*NHC **5.6c'** decomposed into a relatively stable aromatic compound, we redirected our attention to the chemistry of allene **5.6a**. We first tested if a TM could induce cyclization giving the respective *r*NHC TM complex. Gratifyingly, addition of (tht)AuCl to a solution of the allene in C_6D_6 quickly gave a new set of ^{13}C NMR signals which included a carbene signal at 217.0 ppm (Scheme 5.10). The signal is downfield shifted by 26 ppm of the carbene signal in the analogous *r*NHC complex **5.T**.[28] The more deshielded signal is indicative of the higher carbeneic character of the *r*NHC in complex **5.10**, likely due to the fact that unlike **5.T**, dearomatization is not needed for the carbene resonance form. A similar cyclization reaction occurred when a solution of **5.6a** and $[Rh(cod)Cl]_2$ were stirred in THF. A carbene signal was clearly observed as a doublet at 267.1 ppm ($^1J_{Rh\text{-}C}$ = 39 Hz) in the ^{13}C NMR indicative of the formation of **5.11**. This species is the first example of a nonaromatic *r*NHC coordinated to rhodium. Moving beyond TM mediated cyclization, the formation of a five-membered ring was also observed when **5.6a** was subjected to HCl. Indeed, a new singlet was observed in the ^1H NMR at 3.94 ppm in addition to the ^{13}C NMR displaying a new doublet at 51.8 ppm ($^1J_{C\text{-}H}$ = 132 Hz). Combined, these signals point to the formation of the *r*NHC-HCl adduct **5.12**. It should be noted that this neutral adduct is reminiscent of those seen for DAC-HCl precursors.[37] For these species, the carbenes' conjugate acids are highly electrophilic due to amide resonance forms (see section 1.2). As an effect, the protonated carbenes are susceptible to nucleophilic attack by the chlorine anion, therefore giving the neutral precursors. The fact that **5.12**

behaves in a similar manor is good indication that *r*NHCs like **5.6a'** might be extremely π-acidic. Finally, we attempted to cyclize **5.6a** with main-group and organic species. Unfortunately, no change was observed when the allene was subjected to Se, CO, or adamantyl isocyanide. Although this is only a small sample size, the lack of a reaction in these examples indicated that ring closure of the allene might require strong electrophiles.

Given the unique formation of the neutral HCl adduct **5.12**, we wanted to explore the π-accepting abilities of this *r*NHC.[38-39] Considering that the carbene-phenylphosphinidene adduct of **5.6a'** cannot be made through normal routes, we instead thought about accessing this species from the chloro pyrrolidinium salt **5.3a**. Satisfactorily, total consumption of the starting material was observed upon heating a DCM solution of $PhPH_2$, NEt_3, and **5.3a** at 45 ºC for 12 h (Scheme 5.11). Analysis of the ^{13}C NMR revealed two doublets at 196.9 ($^1J_{C\text{-}P}$ = 60 Hz) and 79.2 ($^2J_{C\text{-}P}$ = 19 Hz) ppm, and a singlet at 167.6 ppm, which were indicative of the carbons C_1-C_3 in the phenylphosphinidene adduct **5.13**, respectively. Amazingly, the ^{31}P NMR signal for **5.13** appears at 150 ppm, downfield shifted compared to those of BICAAC, CAAC-6, and even AAAC by 60, 47 and 24 ppm, respectively (Figure 5.11). From these results, we can conclude that *r*NHC **5.6a'** is by far the most π-accepting singlet carbene ever recorded.

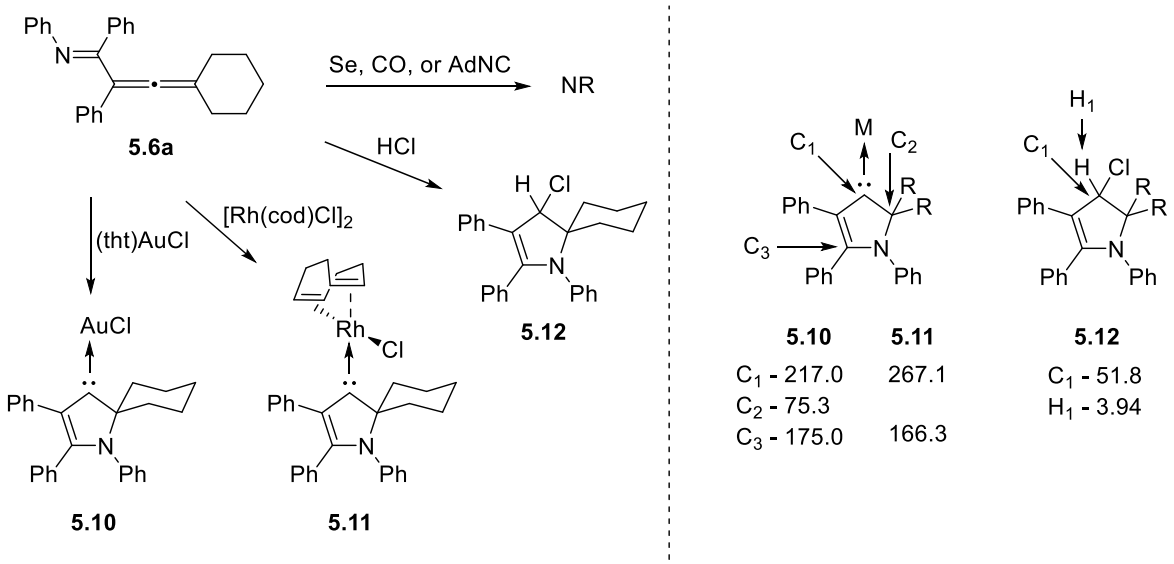

Scheme 5.10: Electrophiles induce the cyclization of allene **5.6a** giving *r*NHC TM complexes or an HCl adduct (left) with their respective characteristic ^{13}C and ^{1}H NMR signals (right). Ad = adamantyl, tht = tetrahydrothiopene.

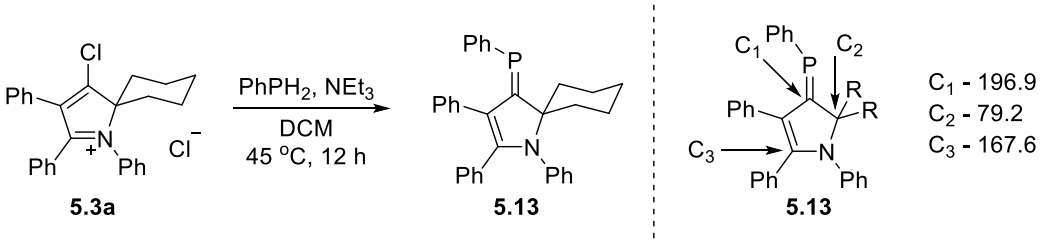

Scheme 5.11: Synthesis of the *r*NHC-phenylphosphinidene adduct **5.13** (left) with diagnostic ^{13}C NMR signals in ppm (right).

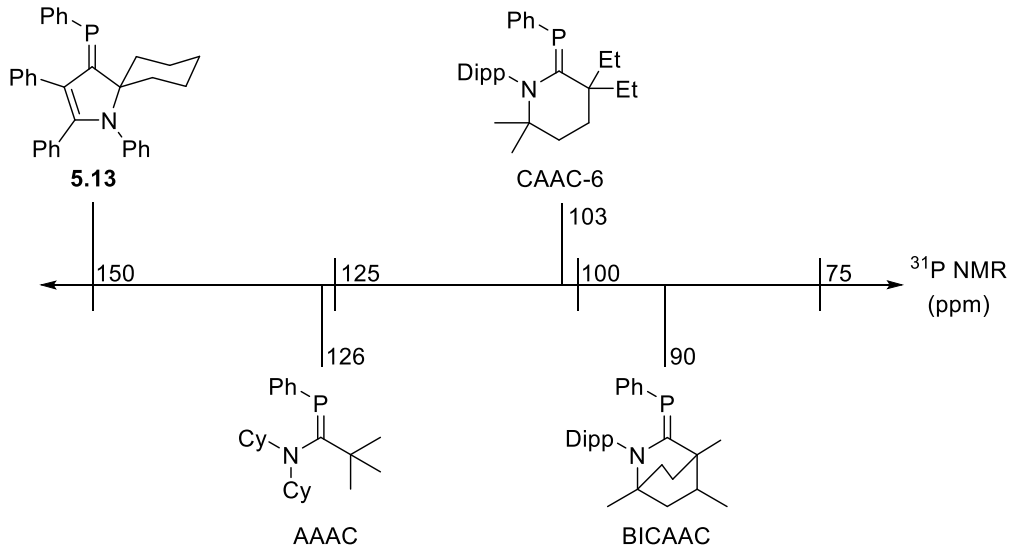

Figure 5.11: ^{31}P NMR π-accepting scale demonstrating that pyrrolidinylidene *r*NHCs are highly electrophilic.

5.3 Conclusion

In summary, we developed a three step synthesis for five-membered remote chloro pyrrolidinium salts from common starting materials. EPR experiments provided evidence that the single electron reduction of these species yields a neutral radical which is stabilized by a relatively small π-system. On the other hand, a second chemical reduction induces a ring opening giving a stable *α*,*α*,*γ*,*γ*-tetrasubstitued-2-allenyl ketimine. This allene was shown ring close and react like a "masked" *r*NHC in the presence of electrophiles giving the first example of a nonaromatic *r*NHC-Rh complex. Finally, ^{31}P NMR experiments showed that pyrrolidinylidene derived *r*NHCs are indeed the most π-accepting singlet carbenes ever recorded. It is quite likely that a wide range of *r*NHC-TM complexes can be generated using this strategy; however experiments are currently ongoing testing the limits of reactive for these "masked' *r*NHCs.

5.4 Experimental

5.4.1 General Considerations

All manipulations were performed under an Argon atmosphere in either an MBraun glovebox or using standard Schlenk techniques. Glassware was dried in an oven overnight at 150 ºC or flame dried before use. Benzene, THF, Et_2O, and dioxane were freshly distilled over Na metal. Hexanes, *n*-pentane, DCM, and $CHCl_3$ were freshly distilled over CaH_2. Additionally, benzene (C_6D_6) and chloroform ($CDCl_3$) used for NMR spectroscopy were purchased from Cambridge Isotope Laboratories and dried according to published methods.[40]

NMR: Multinuclear NMR data were recorded on a Varian INOVA 500MHz or Bruker 300 MHz spectrometers. NMR signals are listed in ppm, relative to residual solvent signals (^1H and ^{13}C) or H_3PO_4 (^{31}P). Coupling constants are in Hertz (Hz). NMR multiplicities are abbreviated as follows: s = singlet, d = doublet, t = triplet, q = quartet, sext = sextet, sept = septet, m = multiplet, br = broad. All spectra were recorded at 25 ºC.

Mass Spectrometry: Electrospray ionization mass spectrometry data was collected on an Agilent 6230 TOF-MS at the UC San Diego Mass Spectrometry Laboratory.

X-Ray Crystallography: Single crystal X-Ray diffraction data were collected on Bruker Apex II difractometers using Mo-K_α radiation (λ = 0.71073 Å) or Cu-K_α radiation (λ = 1.54178 Å). Crystals were selected under oil, mounted on nylon loops then immediately placed in a cold stream of N_2. Structures were solved and refined using SHELXTL and Olex2 software.[41] Hydrogen atoms were included in the refinement in calculated positions depending on the connecting carbon atoms. X-ray images were generated using CYLview.

CV: Electrochemical experiments were performed with an analyzer from CH Instruments (Model 620E) with platinum working and auxiliary electrodes. The reference electrode was built from a silver wire inserted in a small glass tube fitted with a porous Vycor frit and filled with a $AgNO_3$ solution in THF

(0.1 M). Ferrocene was used as a standard, and all reduction potentials are reported with respect to the $E_{1/2}$ of the Fc/Fc^+ redox couple.

EPR: EPR spectra were obtained using an X-band Bruker E500 spectrometer. Field calibration was accomplished by using a standard of solid 2,2-diphenyl-1-picrylhydrazyl, g = 2.0036.

5.4.2 Synthetic Procedure

5.2a: Ketimine **5.1a** (2.57 g, 1 eq) and 1,2-diphenylcyclopropeneone (3.06g, 1 eq) were added to a Schlenk flask. THF (40 mL) was added and the mixture was stirred at 60 ºC for 3 days. The solvent was removed *in vacuo* leaving a pale yellow solid which was composed of two products in which the major was **5.2a**. The mixture was used without further any further purification and therefore **only key signals of the crude NMR are reported**. **$^{13}C\{^1H\}$ NMR** (126 MHz, $CDCl_3$) δ 203.12 (CO), 171.03 (CN), 156.47, 148.89, 147.20, 139.41, 118.86, 115.65, 111.97, 70.97 (C_q), 33.09, 25.52, 20.70.

5.2b: Ketimine **5.1b** (2.54 g, 1 eq) and 1,2-diphenylcyclopropeneone (2.30g, 1 eq) were added to a Schlenk flask. THF (40 mL) was added and the mixture was stirred at 100 ºC for 22 days. The solvent was removed *in vacuo* and the product was washed with Et_2O at -78 ºC giving a pure beige solid. **^1H NMR** (500 MHz, $CDCl_3$) δ 7.30 – 7.04 (m, 15H), 3.12 (d, J = 12.5 Hz, 2H), 2.57 (s, 1H), 2.20 – 1.97 (m, 6H), 1.92 (t, J = 12.5 Hz, 4H), 1.80 – 1.68 (m, 3H), 1.59 – 1.48 (m, 4H). **$^{13}C\{^1H\}$ NMR** (126 MHz, $CDCl_3$) δ 203.89 (CO), 173.47 (CN), 143.74, 132.57, 132.19, 131.67, 129.71, 129.49, 129.10, 128.88, 128.46, 127.96, 127.71, 127.52, 125.60, 117.04, 76.04 (C_q), 39.14, 35.24, 34.59, 32.04, 27.08, 26.66.

5.2c: Ketimine **5.1c** (0.83 g, 1 eq) and 1,2-diphenylcyclopropeneone (1.04g, 1 eq) were added to a Schlenk flask. THF (30 mL) was added and the mixture was stirred at 60 ºC for 12 h. The solvent was removed *in vacuo* leaving a pale yellow solid which was exclusively **5.2c** (1.84 g, 99% yield). **^1H NMR** (500 MHz, $CDCl_3$) δ 7.58 – 7.37 (m, 3H), 7.29 – 7.22 (m, 1H), 7.15 – 6.98 (m, 5H), 4.20 (br s, 1H), 2.67 (m, 1H), 2.23 (d, J = 14 Hz, 1H), 2.13 (d, J = 14 Hz, 1H), 2.07 (br s, 1H), 1.94-1.75 (m, 4H), 1.69 – 1.57 (m, 1H), 1.49 – 1.31(m, 7H); **$^{13}C\{^1H\}$ NMR** (126 MHz, $CDCl_3$) δ 203.55 (CO), 174.17 (CN), 132.47,

132.06, 129.80, 128.84, 128.31, 127.73, 125.14, 115.30, 75.87 (C_q), 52.02, 39.35, 36.36, 35.64, 32.15, 32.05, 31.87, 27.32, 25.94, 25.90.

5.3a: DCM (20 mL) was added to **5.2a** (1.1 g, 1 eq) in a Schlenk. Oxalyl chloride (0.50 mL, 2 eq) was added to the solution slowly causing bubbles to form. The mixture was stirred for 16 h at RT. DCM was removed *in vacuo* leaving an orange solid. The solid was washed with Et_2O (3 x 15 mL) leaving **5.3a** as a white microcrystalline solid (0.750 g, 60% yield). **^{1}H NMR** (300 MHz, $CDCl_3$) δ 7.88 (br s, 2H), 7.58 – 7.42 (m, 7H), 7.34 – 7.26 (m, 3H), 7.24 – 7.18 (m, 1H), 7.13 – 7.05 (m, 2H), 2.75 – 2.62 (m, 2H), 2.44 – 2.33 (m, 2H), 2.20 – 2.04 (m, 2H), 1.73 – 1.59 (m, 3H), 1.35 – 1.20 (m, 1H). **^{13}C{^{1}H} NMR** (126 MHz, $CDCl_3$) *δ* 179.41 (CN), 164.24 (CCl), 136.65, 134.21, 131.90, 130.84, 130.77, 130.13, 129.60, 129.27, 129.11, 128.21, 127.78, 127.67, 127.37, 125.74, 82.97 (C_q), 30.76, 23.29, 19.97.

5.3c: DCM (20 mL) was added to **5.2c** (0.855 g, 1 eq) in a pressure Schlenk. To this solution was added oxalyl chloride (0.99 mL, 5 eq) followed by a catalytic amount (~2 drops) of dry DMF. After the passing of initial effervescence, the Schlenk was closed and heated at 80 ºC for 3 days. The DCM was then removed *in vacuo* and the remaining brown oily solid was vigorously stirred and washed with Et_2O (4 x 20 mL) leaving a microcrystalline brown solid. Washing this solid with 0 ºC THF (3 x 5 mL) leaves a fine white powder of **5.3c**. The washings were saved, concentrated to half volume, and stored at -20 ºC overnight giving colorless X-ray quality crystals (445 mg combined, 42% yield). **^{1}H NMR** (500 MHz, $CDCl_3$) δ 11.01 (br s, 1H), 7.70 (br s, 1H), 7.53 – 7.40 (m, 3H), 7.32 – 7.23 (m, 3H), 7.11 – 7.03 (m, 2H), 5.44 (br s, 1H), 3.00 (d, *J* = 15 Hz, 1H), 2.73 (t, *J* = 6 Hz, 1H), 2.37 (d, *J* = 15 Hz, 1H), 2.21 (br s, 1H), 2.10 (s, 3H), 2.10 – 2.00 (m, 2H), 1.97 – 1.90 (m, 2H), 1.69 (d, *J* = 15 Hz, 1H), 1.55 (t, *J* = 15 Hz, 2H), 1.30 (d, *J* = 15 Hz, 1H), 1.18 (d, *J* = 15 Hz, 1H) **^{13}C{^{1}H] NMR** (126 MHz, $CDCl_3$) *δ* 180.41 (CN), 166.11 (CCl), 136.98, 133.45, 129.80, 129.48, 129.38, 128.73, 126.89, 126.89, 125.94, 88.11 (C_q), 59.90, 40.29, 35.78, 33.82, 31.88, 29.90, 29.69, 26.28, 25.80, 24.91.

5.6a: THF (3 mL) was added at RT to a vial containing **5.3a** (68 mg, 1 eq) and magnesium anthracene (72 mg, 1.1 eq) in the glovebox. The solution turns purple immediately and was stirred for an additional hour. The THF was removed *in vacuo* and the product extracted with Et_2O. Subsequent

removal of Et_2O *in vacuo* gave a mixture which contained **5.6a** and anthracene as the major products. [Note: This step needs optimizing. All attempts at reducing **5.3a** give a mixture of products in which the allene **5.6a** has thus far not been isolated. For the following reactions, the crude product from this reduction method was used. As such, **only key signals of the crude NMR are reported.**] **Crude $^{13}C\{^1H\}$NMR** (126 MHz, C_6D_6) δ 198.63 (C*C*C), 163.84 (CN), 152.67 ($C_{Ph}N$), 107.80 (CC*C*), 102.13 (*C*CC), 30.62, 27.56, 26.06.

5.9: Dioxane (3 mL) was added to a vial containing **5.3c** (40 mg, 1 eq) and Mg (10 mg, 5 eq) at RT and the solution was stirred for 12 h. The supernatant was extracted from the ppt and the solvent removed *in vacuo*. NMR of remaining crude gave a product which was 95% one species tentatively assigned to **5.9**. **Crude ^1H NMR** (500 MHz, $CDCl_3$) δ 7.31 – 7.04 (m, 10H), 4.32 (t, J = 5.3 Hz, 1H), 3.33 (t, J = 5.7 Hz, 1H), 2.24 (s, 1H), 2.12 (br s, 2H), 2.07 (s, 3H), 2.10 – 2.02 (m, 2H), 2.01 – 1.70 (m, 10H). **Crude $^{13}C\{^1H\}$ NMR** (126 MHz, $CDCl_3$) δ 136.98, 136.79, 133.63, 133.43, 131.36, 130.52, 129.95, 129.58, 128.89, 128.57, 128.29, 128.07, 127.61, 126.48, 124.76, 121.20, 110.91, 49.32 (CH), 36.22, 35.69, 35.50, 28.93, 27.35, 10.49 (CH_3).

5.10: A crude mixture of C_6D_6 containing allene **5.6a** (57 mg, 1 eq) was combined with (tht)AuCl (50 mg, 1 eq) in a J-Young NMR tube. The solution turns dark brown immediately with a lot of ppt crashing out of solution. NMR of the crude after 10 min reaction time displayed signals for both **5.6a** and a new compound assigned to **5.10**. Therefore, **only key signals of the crude ^{13}C NMR are reported. Crude $^{13}C\{^1H\}$ NMR** (126 MHz, C_6D_6) δ 216.93 (C_{carb}), 175.02 (CN), 92.28, 75.30 (C_q).

5.11: A crude mixture of THF containing allene **5.6a** (20 mg, 1 eq) was combined with $[Rh(cod)Cl]_2$ (17 mg, 0.5 eq) in a vial in the glovebox. The solution immediately turned a dark orange color and was stirred for an additional 12 h. NMR of the crude mixture displayed signals that included a new compound assigined to **5.11**. Therefore, **only key signals of the crude ^{13}C NMR are reported. Crude $^{13}C\{^1H\}$ NMR** (126 MHz, $CDCl_3$) δ 267.10 (C_{carb}, d, $^1J_{C\text{-}Rh}$ = 39 Hz), 166.65 (CN), 97.57 (d, $^1J_{C\text{-}Rh}$ = 35 Hz), 92.40.

5.12: A crude mixture of Et_2O containing allene **5.6a** (50 mg, 1 eq) was combined with 2.0 M HCl in Et_2O (0.17 mL, 2 eq) in an NMR tube. The solution was shaken for 10 min and an NMR of the crude solution was taken. Only the characteristic NMR signals that were not buried by the aryl or alkyl regions or residual solvent can be clearly given. **Crude $^{13}C\{^1H\}$ NMR** (126 MHz, $CDCl_3$) δ 51.81 (C_H). **Crude ^{13}C NMR** (126 MHz, $CDCl_3$) δ 51.81 (d, $^1J_{C\text{-}H}$ = 132 Hz). **Crude ^1H NMR** (500 MHz, $CDCl_3$) 3.94 (s).

5.13: DCM (12 mL) was added to a Schlenk containing **5.3a** (190 mg, 1 eq). To this solution was added NEt_3 (0.27 mL, 4 eq) followed by $PhPH_2$ (0.09 mL, 1.5 eq) and the mixture turned a deep red-orange color. The solution was stirred at 45 ºC for 12 h. The DCM was removed *in vacuo*, the product extracted with pentane which was then also removed *in vacuo* giving a crude red solid which was mainly **5.13,** therefore **only key signals of the crude NMRs are given**. **Crude $^{13}C\{^1H\}$ NMR** (126 MHz, C_6D_6) δ 196.90 (CP, d, $^1J_{C\text{-}P}$ = 60 Hz), 167.57 (CN), 79.21 (C_q, d, $^2J_{C\text{-}P}$ = 23 Hz). **$^{31}P\{^1H\}$ NMR** (121 MHz, C_6D_6) δ 149.80.

5.4.3 Crystallographic Data

Compound	**5.3c**
Empirical formula	$C_{30}H_{36}Cl_3NO$
Formula weight	532.95
Temperature/K	100.0
Crystal system	triclinic
Space group	P-1
a/Å	9.074(3)
b/Å	10.979(3)
c/Å	14.168(4)
α/°	74.242(9)
β/°	81.414(9)
γ/°	86.542(9)
Volume/Å^3	1342.9(6)
Z	2
ρ_{calc}g/cm^3	1.318
μ/mm^{-1}	0.365
F(000)	564.0
Crystal size/mm^3	0.4 × 0.5 × 0.7
Radiation	MoKα (λ = 0.71073)

2Θ range for data collection/°	3.02 to 51.52
Index ranges	$-10 \leq h \leq 11$, $-13 \leq k \leq 13$, $-17 \leq l \leq 17$
Reflections collected	19912
Independent reflections	5107 [R_{int} = 0.0270, R_{sigma} = 0.0256]
Data/restraints/parameters	5107/0/329
Goodness-of-fit on F^2	1.044
Final R indexes [I>=2σ (I)]	R_1 = 0.0334, wR_2 = 0.0794
Final R indexes [all data]	R_1 = 0.0417, wR_2 = 0.0862
Largest diff. peak/hole / e Å^{-3}	0.34/-0.19

Compound	**5.4a**
Empirical formula	$C_{13.5}H_{13}Br_{0.5}N_{0.5}O_{0.5}$
Formula weight	230.20
Temperature/K	100.0
Crystal system	monoclinic
Space group	$P2_1/m$
a/Å	11.3733(9)
b/Å	8.7385(7)
c/Å	12.1146(11)
α/°	90.00
β/°	106.549(3)
γ/°	90.00
Volume/Å^3	1154.14(17)
Z	4
ρ_{calc}g/cm^3	1.325
μ/mm^{-1}	1.799
F(000)	476.0
Crystal size/mm^3	0.3 × 0.3 × 0.5
Radiation	MoKα (λ = 0.71073)
2Θ range for data collection/°	3.5 to 51.32
Index ranges	$-13 \leq h \leq 13$, $-10 \leq k \leq 10$, $-8 \leq l \leq 14$
Reflections collected	7096
Independent reflections	2336 [R_{int} = 0.0615, R_{sigma} = 0.0751]
Data/restraints/parameters	2336/0/158
Goodness-of-fit on F^2	1.083
Final R indexes [I>=2σ (I)]	R_1 = 0.0458, wR_2 = 0.1122
Final R indexes [all data]	R_1 = 0.0730, wR_2 = 0.1572
Largest diff. peak/hole / e Å^{-3}	1.75/-0.77

5.4.4 Computational Details

All calculations were performed with the Gaussian09 program package.[42] The theoretical approach is based on the framework of density functional theory (DFT).[43-44] All calculations were performed with the B3LYP functional and employing Weigend's def2-TZVPP basis set.[45-46]

5.W singlet

C	0.90521100	0.57085900	0.00002300
C	1.21495600	-0.81933000	0.00009400
C	0.06160700	-1.58536600	0.00013800
N	-0.40472100	0.76542100	0.00002900
C	-1.10681600	2.02825800	0.00001200
H	-1.74287300	2.11665900	-0.88322100
H	-1.74238100	2.11700500	0.88356800
H	-0.40603400	2.85965100	-0.00035300
C	1.87794000	1.70552700	-0.00005300
H	1.74689500	2.33819900	-0.88057300
H	1.74666800	2.33854600	0.88018000
H	2.89710500	1.33022200	0.00014200
C	2.62226300	-1.35357300	0.00006200
H	3.19269200	-1.04294500	-0.88066500
H	3.19285100	-1.04263900	0.88057600
H	2.57769500	-2.44074100	0.00024800
C	-1.06400300	-0.59685300	0.00003100
C	-1.91308100	-0.74108300	-1.26910400
H	-2.34865600	-1.73729500	-1.29069500
H	-2.72207700	-0.00676300	-1.29834100
H	-1.29726200	-0.62462700	-2.16111600
C	-1.91344500	-0.74094600	1.26890400
H	-2.72244900	-0.00662500	1.29782600
H	-2.34901800	-1.73716100	1.29047100
H	-1.29790300	-0.62439400	2.16109800

5.5 Acknowledgements

Chapter 5, in part, is currently being prepared for submission for publication of the material. Cory M. Weinstein, Mohand Melaimi, and Guy Bertrand "Allenyl Ketimines are Masked Remote *N*-Heterocyclic Carbenes," The dissertation author was the primary investigator and author of this material.

5.6 References

[1] R. H. Crabtree, *Coord. Chem. Rev.*, 2013, **257**, 755-766.

[2] O. Schuster, L. Yang, H. G. Raubenheimer and M. Albrecht, *Chem. Rev.*, 2009, **109**, 3445-3478.

[3] V. Lavallo, Y. Canac, B. Donnadieu, W. W. Schoeller and G. Bertrand, *Science*, 2006, **312**, 722-724.

[4] V. Lavallo, Y. Ishida, B. Donnadieu and G. Bertrand, *Angew. Chem. Int. Ed.*, 2006, **45**, 6652-6655.

[5] W. W. Schoeller, G. D. Frey and G. Bertrand, *Chem. Eur. J.*, 2008, **14**, 4711-4718.

[6] T. Koizumi, T. Tomon and K. Tanaka, *Organometallics*, 2003, **22**, 970-975.

[7] T. Koizumi, T. Tomon and K. Tanaka, *J. Organomet. Chem.*, 2005, **690**, 1258-1264.

[8] W. H. Meyer, M. Deetlefs, M. Pohlmann, R. Scholz, M. W. Esterhuysen, G. R. Julius and H. G. Raubenheimer, *Dalton Trans.*, 2004, 413-420.

[9] C. E. Strasser, E. Stander-Grobler, O. Schuster, S. Cronje and H. G. Raubenheimer, *Eur. J. Inorg. Chem.*, 2009, 1905-1912.

[10] C. Segarra, E. Mas-Marza, M. Benitez, J. A. Mata and E. Peris, *Angew. Chem. Int. Ed.*, 2012, **51**, 10841-10845.

[11] C. Segarra, E. Mas-Marza, J. A. Mata and E. Peris, *Organometallics*, 2012, **31**, 5169-5176.

[12] G. Y. Song, Y. Zhang, Y. Su, W. Q. Deng, K. L. Han and X. W. Li, *Organometallics*, 2008, **27**, 6193-6201.

[13] E. Stander-Grobler, O. Schuster, G. Heydenrych, S. Cronje, E. Tosh, M. Albrecht, G. Frenking and H. G. Raubenheimer, *Organometallics*, 2010, **29**, 5821-5833.

[14] S. K. Schneider, P. Roembke, G. R. Julius, H. G. Raubenheimer and W. A. Herrmann, *Adv. Synth. Catal.*, 2006, **348**, 1862-1873.

[15] M. Albrecht and H. Stoeckli-Evans, *Chem. Commun.*, 2005, 4705-4707.

[16] H. Meguro, T. A. Koizumi, T. Yamamoto and T. Kanbara, *J. Organomet. Chem.*, 2008, **693**, 1109-1116.

[17] E. Stander-Grobler, C. E. Strasser, O. Schuster, S. Cronje and H. Raubenheimer, *Inorg. Chim. Acta*, 2011, **376**, 87-94.

[18] S. K. Schneider, G. R. Julius, C. Loschen, H. G. Raubenheimer, G. Frenking and W. A. Herrmann, *Dalton Trans.*, 2006, 1226-1233.

[19] O. Schuster and H. G. Raubenheimer, *Inorg. Chem.*, 2006, **45**, 7997-7999.

[20] Y. A. Han, D. Yuan, Q. Q. Teng and V. H. Han, *Organometallics*, 2011, **30**, 1224-1230.

[21] Y. Han and H. V. Huynh, *Chem. Commun.*, 2007, 1089-1091.

[22] Y. Han, L. J. Lee and H. V. Huynh, *Organometallics*, 2009, **28**, 2778-2786.

[23] Y. Han, H. V. Huynh and G. K. Tan, *Organometallics*, 2007, **26**, 6581-6585.

[24] B. Borthakur, B. Silvi, R. D. Dewhurst and A. K. Phukan, *J. Comput. Chem.*, 2016, **37**, 1484-1490.

[25] R. Sevincek, H. Karabiyik and H. Karabiyik, *J. Mol. Model.*, 2013, **19**, 5327-5341.

[26] M. Alcarazo, K. Radkowski, R. Goddard and A. Furstner, *Chem. Commun.*, 2011, **47**, 776-778.

[27] S. K. Schneider, P. Roembke, G. R. Julius, C. Loschen, H. G. Raubenheimer, G. Frenking and W. A. Herrmann, *Eur. J. Inorg. Chem.*, 2005, 2973-2977.

[28] A. Vanitcha, G. Gontard, N. Vanthuyne, E. Derat, V. Mouriès-Mansuy and L. Fensterbank, *Adv. Synth. Catal.*, 2015, **357**, 2213-2218.

[29] G. Ung, D. Mendoza-Espinosa, J. Bouffard and G. Bertrand, *Angew. Chem. Int. Ed.*, 2011, **50**, 4215-4218.

[30] A. S. Dudnik, A. W. Sromek, M. Rubina, J. T. Kim, A. V. Kel'i and V. Gevorgyan, *J. Am. Chem. Soc.*, 2008, **130**, 1440-1452.

[31] T. Eicher and D. Krause, *Synthesis-Stuttgart*, 1986, 899-907.

[32] T. Eicher, H. Pielartzik and P. Zacheus, *Tetrahedron Lett.*, 1984, **25**, 4495-4498.

[33] T. Eicher and D. Krause, *Tetrahedron Lett.*, 1979, 1213-1216.

[34] T. Eicher, J. L. Weber and G. Chatila, *Liebigs Ann. Chem.*, 1978, 1203-1221.

[35] N. G. Connelly and W. E. Geiger, *Chem. Rev.*, 1996, **96**, 877-910.

[36] A. Dreger, R. Cisneros Camuña, N. Münster, T. A. Rokob, I. Pápai and A. Schmidt, *Eur. J. Org. Chem.*, 2010, **2010**, 4296-4305.

[37] J. P. Moerdyk, D. Schilter and C. W. Bielawski, *Acc. Chem. Res.*, 2016, **49**, 1458-1468.

[38] O. Back, M. Henry-Ellinger, C. D. Martin, D. Martin and G. Bertrand, *Angew. Chem. Int. Ed.*, 2013, **52**, 2939-2943.

[39] R. R. Rodrigues, C. L. Dorsey, C. A. Arceneaux and T. W. Hudnall, *Chem. Commun.*, 2014, **50**, 162-164.

[40] W. L. F. Armarego and C. L. L. Chai, *Purification of Laboratory Chemicals: 5th Edition*, Elsevier Science, Burlington, MA, 2003.

[41] O. V. Dolomanov, L. J. Bourhis, R. J. Gildea, J. A. K. Howard and H. Puschmann, *J. Appl. Crystallogr.*, 2009, **42**, 339-341.

[42] M. J. Frisch, G. W. Trucks, H. B. Schlegel, G. E. Scuseria, M. A. Robb, J. R. Cheeseman, G. Scalmani, V. Barone, B. Mennucci, G. A. Petersson, H. Nakatsuji, M. Caricato, X. Li, H. P. Hratchian, A. F. Izmaylov, J. Bloino, G. Zheng, J. L. Sonnenberg, M. Hada, M. Ehara, K. Toyota, R. Fukuda, J. Hasegawa, M. Ishida, T. Nakajima, Y. Honda, O. Kitao, H. Nakai, T. Vreven, J. A. Montgomery, J. E. Peralta, F. Ogliaro, M. Bearpark, J. J. Heyd, E. Brothers, K. N. Kudin, V. N. Staroverov, R. Kobayashi, J. Normand, K. Raghavachari, A. Rendell, J. C. Burant, S. S. Iyengar, J. Tomasi, M. Cossi, N. Rega, J. M. Millam, M. Klene, J. E. Knox, J. B. Cross, V. Bakken, C. Adamo, J. Jaramillo, R. Gomperts, R. E. Stratmann, O. Yazyev, A. J. Austin, R. Cammi, C. Pomelli, J. W. Ochterski, R. L. Martin, K. Morokuma, V. G. Zakrzewski, G. A. Voth, P. Salvador, J. J. Dannenberg, S. Dapprich, A. D. Daniels, Farkas, J. B. Foresman, J. V. Ortiz, J. Cioslowski and D. J. Fox, Wallingford CT, 2009.

[43] W. Kohn and L. J. Sham, *Physical Review*, 1965, **140**, A1133-1138.

[44] P. Hohenberg and W. Kohn, *Physical Review B*, 1964, **136**, B864-871.

[45] F. Weigend, *Phys. Chem. Chem. Phys.*, 2006, **8**, 1057-1065.

[46] F. Weigend and R. Ahlrichs, *Phys. Chem. Chem. Phys.*, 2005, **7**, 3297-3305.